On the accuracy of radiowave propagation measurements : Olympus propagation experiment

Research Report
ISSN 0167-9708
Coden: TEUEDE

Eindhoven
University of Technology
Netherlands

Faculty of Electrical Engineering

On the Accuracy of Radiowave Propagation Measurements: Olympus Propagation Experiment

by
P.H.G. van de Berg

EUT Report 90-E-245
ISBN 90-6144-245-1
November 1990

Eindhoven University of Technology Research Reports
EINDHOVEN UNIVERSITY OF TECHNOLOGY

Faculty of Electrical Engineering
Eindhoven The Netherlands

ISSN 0167- 9708 Coden: TEUEDE

ON THE ACCURACY OF RADIOWAVE PROPAGATION MEASUREMENTS:
Olympus propagation experiment

by

P.H.G. van de Berg

EUT Report 90-E-245
ISBN 90-6144-245-1

Eindhoven
November 1990

This report is submitted in partial fulfillment of the requirements for the degree of electrical engineer (M.Sc.) at the Eindhoven University of Technology.

The work was carried out from December 1989 untill July 1990 in charge of Professor Dr.Ir. G. Brussaard under supervision of Ir. J. Dijk in the Telecommunications Division of the Faculty of Electrical Engineering.

CIP-GEGEVENS KONINKLIJKE BIBLIOTHEEK, DEN HAAG

Berg, P.H.G. van de

On the accuracy of radiowave propagation measurements: Olympus propagation experiment / by P.H.G. van de Berg. - Eindhoven: Eindhoven University of Technology, Faculty of Electrical Engineering. - Fig., tab. - (EUT report, ISSN 0167-9708; 90-E-245)
Met lit. opg., reg.
ISBN 90-6144-245-1
SISO 376 UDC 621.396.946 NUGI 832
Trefw.: satellietcommunicatie.

OLYMPUS PROPAGATION EXPERIMENT

ON THE ACCURACY OF RADIOWAVE PROPAGATION MEASUREMENTS

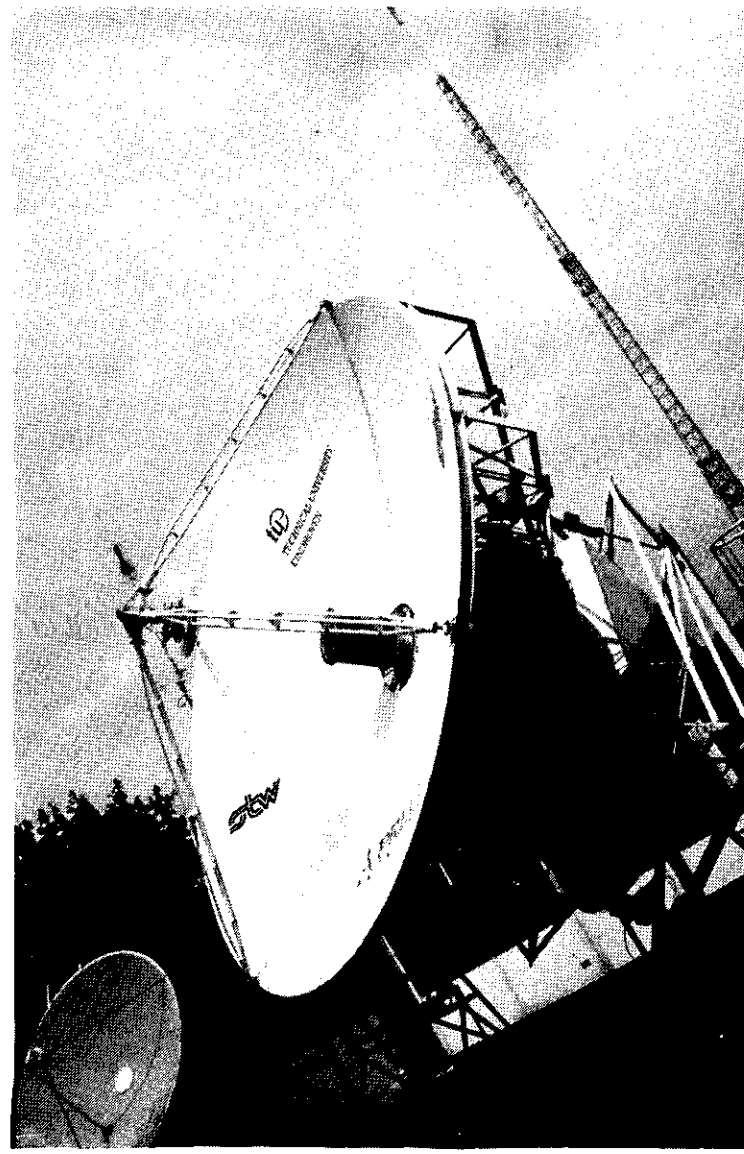

ABSTRACT

The Olympus Propagation Experiment (OPEX) has been set up to collect accurate data on propagation properties for the 10 - 30 GHz range. July 1989 the Olympus satellite was launched and October 1989 the measurement campaign was started. At the groundstation of the Eindhoven University of Technology (EUT), 12.5, 20 and 30 GHz beacons are received to investigate attenuation, depolarization and scintillation properties of the propagation medium. Obtaining accurate data is complicated by influences of the satellite and the groundstation. Biases introduced by this measurement system have to be removed from the acquired data. It is the design goal of a preprocessing system to obtain 'clean' data suitable for analysis of propagation parameters.

This report deals with the design and analysis of a preprocessing system. Methods to perform bias removal are discussed and analyzed. EUT measurements have been used to evaluate the effectiveness of these bias removal methods. It may be concluded that for attenuation measurements, radiometer measurements are necessary to obtain copolar reference levels. For crosspolar measurements at 12.5 and 30 GHz, adaptive cancellation is recommended. A method has been developed to estimate the uncertainty of propagation data in practice.

Subsequently algorithms have been developed for the EUT preprocessing system, that will be part of the EUT processing system for event analysis. For statistical analysis, a standard processing system, 'DAPPER', will be used. A prototype of DAPPER preprocessing was supplied to the EUT and has been tested. This system is under development by SIEMENS for the European Space Agency (ESA) and will be submitted to all OPEX members. Tests with real propagation data show several errors and practical problems in the software system. Some examples of the output of the preprocessing system are discussed.

ACKNOWLEDGEMENTS

This graduation work has given me the opportunity to be involved in an interesting international project. Visits to the OPEX conference, PTT Research, ESTEC and Siemens have been very valuable to get a feeling of the problems that need to be solved. Working at the EUT groundstation was an interesting experience and I want to thank the members of the radio department for their assistance. I would also like to thank A. Mawira (PTT Research), B. Arbesser-Rastburg (ESA), J. Belshaw (ESA), DAPPER software developers (Siemens AG, Austria) and F.Murr (IAS, Austria) for the pleasant cooperation. I wish all OPEX members good luck with their experiments.

P.H.G. van de Berg

CONTENTS:

PART II: SOFTWARE SET-UP FOR DATA PREPROCESSING OF SATELLITE BEACON MEASUREMENTS

PART III: SET-UP AND TESTS OF DAPPER PREPROCESSING

GENERAL INTRODUCTION

Future satellite communication systems require exploration of new frequency areas. For the design of these systems accurate data about the propagation medium must be obtained. It is the goal of the Olympus Propagation Experiment (OPEX) to collect accurate data on slant path propagation properties for frequencies between 10 and 30 GHz. The Olympus satellite transmits beacons at 12.5 (B0), 20 (B1) and 30 (B2) GHz, that are received by a number of groundstations throughout Europe and even by some on other continents.

At these groundstations, measurements are processed to investigate attenuation, depolarization, scintillation and noise properties of the propagation medium. The interpretation of these measurements is complicated by the influence of the complex measurement system. Obtaining accurate data requires careful processing to minimize the influence of the measurement system. The conversion of the raw measurement data to 'clean' data ready for analysis, is called preprocessing.

The Olympus satellite was launched in July 1989 and by October 1989 the in orbit testing was completed. At Eindhoven University of Technology (EUT) a groundstation is set up to receive all the Olympus beacons and measure copolar and crosspolar signals. This groundstation is one of the first in Europe to be almost fully operational. Presently the EUT preprocessing system is under development. OPEX initiated the development of a standard system for preprocessing and analysis. This system is under development by Siemens for ESA and will be submitted to all OPEX members.

This report concerns with the accuracy of satellite beacon measurements. It is divided into three parts. In part I a theoretical analysis is presented of the measurement system and preprocessing procedures. For typical measurements the accuracy is evaluated. Part II considers the development of preprocessing algorithms to be used at the EUT groundstation. In Part III a prototype of the standard preprocessing package 'DAPPER' is investigated and tested with EUT measurements.

LIST OF ABBREVIATIONS AND SYMBOLS

Abbreviations

B0	:	12.5 GHz beacon
B1	:	20 GHz beacon
B2	:	30 GHz beacon
DACS	:	Data Acquisition System
DANS	:	Data Analysis System
DAPPER	:	Data Analysis and Preprocessing for Propagation Effects Research
DAPS	:	Data Preprocessing System
DDD	:	Detailed Design Document
ESA	:	European Space Agency
EUT	:	Eindhoven University of Technology
EUTEC	:	Eindhoven University of Technology, Telecommunications Division
H	:	Horizontal polarization (used in channel names)
ICRT	:	Input Channel Reference Table
OCRT	:	Output Channel Reference Table
OMT	:	Orthomode Transducer
OPEX	:	Olympus Propagation Experiment
OTS	:	Orbital Test Satellite
PLL	:	Phase Locked Loop
SCO	:	Santa Cruz Operation
SWRT	:	Status Word Reference Table
V	:	Vertical polarization (used in channel names)
X/Y	:	Referring to the polarization at the transmitter side, the corresponding polarization at the receiver side after accounting for the polarization tilt angle.

Symbols and units

γ_l	:	specific attenuation of water droplets (dB/km)
γ_o	:	specific attenuation of oxygen (dB/km)
γ_r	:	specific attenuation of rain (dB/km)
γ_v	:	specific attenuation of water vapour (dB/km)
δ	:	crosspolar phasor
Δ	:	anisotropy
$\Delta\delta$	:	uncertainty in crosspolar phasor
$\Delta\delta_c$	:	uncertainty in crosspolar phasor due to correction limits
$\Delta\delta_t$	:	uncertainty in template crosspolar phasor
$\Delta\delta_u$	:	uncertainty in crosspolar phasor due to unpredictable errors
$\Delta\phi$	:	differential phase-shift (°)
$\Delta\phi_c$	:	uncertainty in corrected phase-shift (°)
$\Delta\phi_m$	:	uncertainty in measured phase-shift (°)

$\Delta\phi_t$	:	uncertainty in phase-shift template (°)
ΔA	:	differential attenuation along principal planes (dB or Np)
ΔA_c	:	uncertainty in corrected attenuation (dB)
ΔA_t	:	differential attenuation (dB)
ΔB	:	differential phase-shift (°)
δ_c	:	corrected crosspolar phasor
ΔDPH	:	uncertainty in differential phase (°)
Δf	:	frequency shift (GHz)
δ_m	:	measured crosspolar phasor
ΔR_t	:	uncertainty in copolar level template (dB)
ΔS	:	uncertainty in measured signal level (dB)
δ_x	:	atmospheric crosspolar phasor (X-polarization)
δ_x^a	:	crosspolar phasor of groundstation (X-polarization)
δ_{xL}	:	crosspolar phasor with left matrix cancellation (X-polarization)
ΔXPD	:	uncertainty in XPD (dB)
δ_{x0}	:	clear-sky crosspolar phasor
δ_{xR}	:	crosspolar phasor with right matrix cancellation (X-polarization)
δ_{xu}	:	crosspolar phasor without cancellation
δ_x^s, δ_y^s	:	crosspolar phasor of the satellite (X, Y-polarization)
δ_x^u, δ_y^u	:	crosspolar phasor of voltage matrix (X, Y-polarization)
δ_{xv}	:	crosspolar phasor with vector cancellation
ϵ	:	elevation angle (°)
η	:	part of the antenna pattern (main beam) pointed to the sky
θ	:	pointing error (°)
Θ_{3dB}	:	3 dB beam width of antenna (°)
θ_m	:	mean pointing error (°)
θ_v	:	amplitude of varying pointing error (°)
λ	:	wavelength (m)
ρ_l	:	liquid water content (g/m^3)
ρ_v	:	water vapour density (g/m^3)
σ_Φ	:	effective standard deviation of raindrop canting angle distribution (°)
ϕ	:	inclination angle (°)
Φ	:	canting angle
ϕ', ϕ''	:	real, imaginary part of inclination angle
ϕ'_t	:	estimated phase-shift template (°)
Φ_0	:	polarization tilt angle (°)
ϕ_c	:	corrected phase-shift (°)
ϕ_{cox}, ϕ_{coy}	:	copolar phase (X, Y-polarization) (°)
ϕ_{crx}, ϕ_{cry}	:	phase difference between cross- and copolar signal (X, Y-polarization) (°)
ϕ_t	:	template copolar phase-shift (°)
ω	:	angle frequency (rad/s)
A	:	receive matrix
A', A''	:	attenuation along principal planes (Np)
A_{av}	:	average attenuation (dB)

a_B	:	attenuation coefficient for water vapour at beacon frequency (dB/(kg/m^2))
A_B	:	attenuation at beacon frequency (dB)
A_c	:	atmospheric attenuation after bias removal (dB)
A_{cs}	:	clear-sky attenuation (dB)
A_f	:	feed loss (linear)
A_g, B_g	:	model constant for estimation of ground temperature
A_l	:	attenuation of liquid water (dB)
A_o	:	attenuation of oxygen (dB)
a_r	:	attenuation coefficient for water vapour at radiometer frequency (dB/(kg/m^2)
A_r	:	attenuation at radiometer frequency (dB)
A_t	:	total attenuation (dB)
A_{tx}, A_{ty}	:	total attenuation (X, Y-polarization) (dB)
E	:	transmitted electric field tensor
A_v	:	attenuation of water vapour (dB)
A_{xx}, A_{xy}, A_{yx}, A_{yy}	:	elements of receive matrix
B', B''	:	phase-shift along principal planes (rad)
b_B	:	attenuation coefficient for liquid water at beacon frequency (dB/(kg/m^2)
b_r	:	attenuation coefficient for liquid water at radiometer frequency (dB/(kg/m^2)
c_B	:	attenuation coefficient for oxygen at beacon frequency (dB)
c_o	:	velocity of light (m/s)
CPA	:	copolar attenuation (dB)
CPH	:	copolar phase (°)
CPL	:	copolar level (dB)
CPMV	:	mean copolar level (dB)
c_r	:	attenuation coefficient for oxygen at radiometer frequency (dB)
CU	:	crosspolar unbalance (dB)
d	:	distance satellite groundstation (km)
D	:	diameter antenna (m)
DPH	:	phase difference between cross- and copolar signal (°)
e	:	water vapour pressure (Pa)
EIRP	:	Effective Isotropic Radiated Power (dB)
E'	:	electric field tensor at receiver side
e_s	:	saturated water vapour pressure (Pa)
$\bar{E}_x$	:	electric field vector (X-polarization)
E_{xx}, E_{xy}, E_{yx}, E_{yy}	:	elements of electric field tensor
f	:	frequency (GHz)
h	:	part of the antenna pattern pointed to the sky
h_l	:	effective length of path through clouds (km)
h_o	:	equivalent height of oxygen (km)
H_p	:	psychrometer constant (Pa^{-1}K^{-1})
h_s	:	height above sea level (m)
h_v	:	equivalent height of water vapour (km)

h_{vo}	:	minimum equivalent height of water vapour (km)
I_δ	:	inphase component of crosspolar phasor
I_{xx}, I_{xy}, I_{yx}, I_{yy}	:	inphase components of voltage matrix
k	:	relative error crosspolar phasor
K	:	cancellation matrix
K_l	:	specific attenuation coefficient for water droplets (dB/(g/m^3))
L	:	integrated liquid water content (kg/m^2)
L_{bf}	:	basic free space transmission loss (dB)
l_{eff}	:	effective path length through rain (km)
M	:	number of seconds to calculate raw template (s)
N	:	number of days for averaging raw templates (days)
p	:	propagation parameter
P	:	atmospheric pressure (Pa)
Q_δ	:	quadrature component of crosspolar phasor
Q_{xx}, Q_{xy}, Q_{yx}, Q_{yy}	:	quadrature components of voltage matrix
R	:	rain rate (mm/h)
R_t	:	clear-sky copolar reference level (dB)
R_t'	:	estimated copolar level template (dB)
RH	:	relative humidity (%)
s	:	scale length of water vapour (km)
S	:	copolar signal level (dB)
S_{err}	:	error in received signal level (dB)
t	:	time (s)
T	:	transmission matrix
T', T''	:	integral propagation constants
T_a	:	antenna noise temperature (K)
T_c	:	cosmic noise temperature (K)
t_{cir}	:	normalized transmission matrix in circular polarization
T_{def}	:	maximum time gap for interpolation (s)
T_{dry}	:	dry bulb temperature (K)
T_g	:	ground temperature (K)
T_l	:	effective temperature of cloud (K)
T_L	:	transmission matrix after left cancellation
t_{lin}	:	normalized transmission matrix for linear polarization
T_m	:	effective medium temperature (K)
T_R	:	transmission matrix after right cancellation
t_{rr}, t_{rl}, t_{lr}, t_{ll}	:	elements of t_{cir}
T_s	:	sky noise temperature (K)
T_{wet}	:	wet bulb temperature (K)
t_{xx}, t_{xy}, t_{yx}, t_{yy}	:	elements of t_{lin}
T_{xx}, T_{xy}, T_{yx}, T_{yy}	:	elements of transmission matrix
U	:	voltage matrix
U_0	:	clear-sky voltage matrix
U_{xx}, U_{xy}, U_{yx}, U_{yy}	:	elements of voltage matrix
V	:	integrated water vapour content (kg/m^2)

VHPH	:	differential copolar phase-shift (°)
v_p	:	velocity in the direction of the groundstation (m/s)
XPD	:	crosspolarization discrimination (dB)
XPH	:	crosspolar phase (°)
XPI	:	crosspolarization isolation (dB)
XPL	:	crosspolar level (dB)
z	:	template parameter
z_{atempl}	:	average template
z_{rtempl}	:	raw template

1

THE ACCURACY OF SATELLITE BEACON MEASUREMENTS

1. INTRODUCTION

The OLYMPUS propagation experiment (OPEX) has been set up to collect accurate data on slant path propagation properties of the atmosphere in the 10 to 30 GHz range. To acquire this information, measurements at the groundstation have to be transferred to relevant propagation parameters. This is not a simple and straightforward process, as the measurement system (satellite and groundstation) introduces errors in the obtained parameters. Predictable errors (biases) may be removed from the raw data. Clear-sky measurements can be used to predict the influence during propagation events. Bias removal is a complex process and the accuracy of the obtained data has to be evaluated to determine the effectiveness. The removal of biases requires intensive processing of raw data with the use of auxiliary measurements.

Part I of this report considers one of the main objectives of the OLYMPUS experiment: collecting accurate data on propagation properties. First propagation properties of the atmosphere between 10 and 50 GHz are introduced, together with a suitable model of the experiment. Then an analysis is presented of the influence of the measurement system and of methods to perform bias removal. The uncertainties of the measurement system and bias removal process are discussed. Subsequently a method is presented to evaluate the accuracy of copolar and crosspolar data in practice. Bias removal performance and propagation data accuracy are evaluated for EUT measurements.

In the text all variables are assumed to have complex values. All signals are assumed to have a harmonic behaviour with the use of complex phasor notation.

2. PROPAGATION THEORY FOR SATELLITE BEACON MEASUREMENTS

2.1 Introduction

Beacon signals from a satellite are used to investigate propagation properties of the medium. Figure 2.1 shows the basic configuration of the Olympus experiment. The satellite propagation package consists of three horn antennas transmitting linearly polarized carrier waves. Radio waves experience attenuation, phase-shift, depolarization, scintillation and noise effects of the propagation medium. Attenuation is the loss of power due to scattering and absorption in the atmosphere. Depolarization is the crosstalk between polarizations, caused by an anisotropic medium. Scintillation is the rapid fluctuation of amplitude and phase of the received signal caused by refraction index variations. At the receiver side, the deteriorated beacon signals are demodulated. Amplitude and phase provide the information about the influence of the medium.

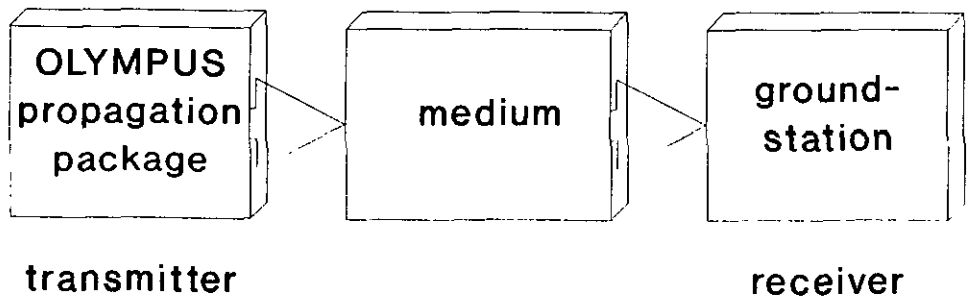

Figure 2.1: The Olympus propagation experiment

The next paragraphs discuss the basic properties of a satellite propagation link through the atmosphere for frequencies between 10 and 50 GHz. A two port model of the experiment is presented that is sutable for evaluating the effects of the medium and the equipment. The medium is represented by the transmission matrix. Evaluation of the transmission matrix provides the opportunity to derive physical medium properties such as anisotropy and canting angle.

Formulae are given in case they are relevant in this research project.

2.2 Two port model of beacon measurements

This paragraph deals with the matrix model of the medium and the measurement system. This model is suitable to describe the complete propagation experiment. Figure 2.2 shows the two port model of a satellite beacon experiment.

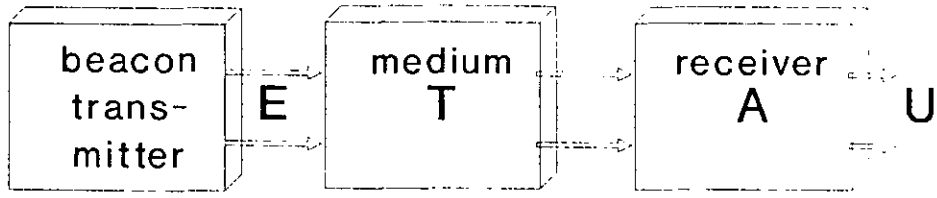

Figure 2.2: Two port model of the beacon experiment

A two port model is represented by a transmission matrix. The input signals of the system are the electric fields transmitted by the satellite. The output signals are the voltages measured in the groundstation.

Consider $\vec{E}_x$ to be the vector of the linearly polarized electric field at transmission side.

$$\vec{E}_x = \begin{pmatrix} E_{xx} \\ E_{yx} \end{pmatrix} \tag{2.1}$$

The 20 GHz beacon (B1) switches between two polarizations. One polarization is horizontal ($\vec{e}_x$) with respect to the earth equatorial plane, the other one is vertical ($\vec{e}_y$). The two polarizations are shown in figure 2.3 and can be represented by two electric field vectors $\vec{E}_x$ and $\vec{E}_y$. The transmitted fields can be described by an electric field tensor E, given by:

$$E = (\vec{E}_x \;\; \vec{E}_y) = \begin{pmatrix} E_{xx} & E_{xy} \\ E_{yx} & E_{yy} \end{pmatrix} \tag{2.2}$$

For a perfect transmission system $E_{xx} = E_{yy}$ and $E_{xy} = E_{yx} = 0$. Polarizations are linear, orthogonal, inphase and equally balanced. A combination of the two polarizations would still be linear in this case. In practice crosspolarization is not zero. The crosspolar phasor is defined by the ratio of the received signal in the crosspolar channel and the signal in the copolar channel. For the satellite this becomes:

$$\delta_x^S = E_{yx}/E_{xx} \qquad \text{(X-polarization)} \tag{2.3}$$

$$\delta_y^S = E_{xy}/E_{yy} \qquad \text{(Y-polarization)} \tag{2.4}$$

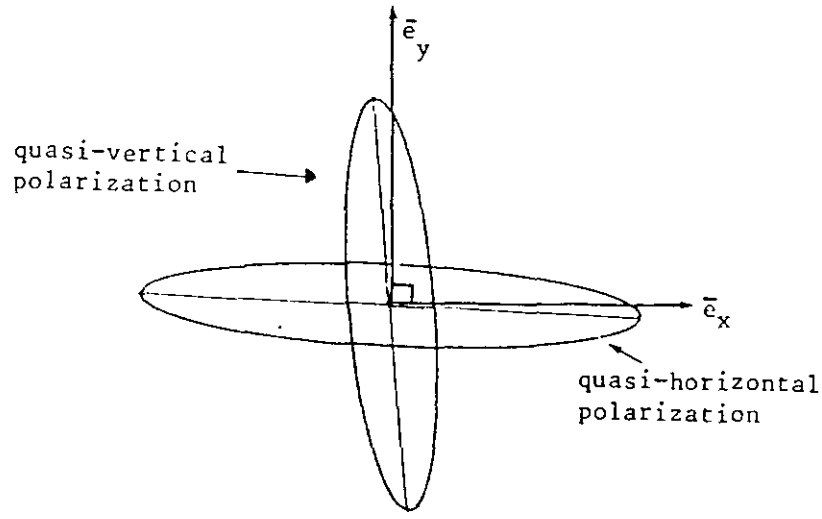

Figure 2.3: Electrical fields transmitted by the satellite

The magnitude of these phasors is usually very small. The resulting two transmitted polarizations are elliptical in general. The received electric field tensor E^r at the ground station antenna can be found by the multiplication of the transmission matrix and the transmitted electric field tensor.

$$E^r = T\,E \tag{2.5}$$

The propagation characteristics of the medium are represented in the transmission matrix T. The transmission matrix is defined with respect to two orthogonal base vectors $\bar{e}_x$ and $\bar{e}_y$ (see figure 2.4) [1].

$$T = \begin{pmatrix} T_{xx} & T_{xy} \\ T_{yx} & T_{yy} \end{pmatrix} \tag{2.6}$$

The elevation angle ϵ and polarization tilt angle Φ_0 depend on the location of the groundstation.

The 20 GHz OLYMPUS switched beacon experiments (B1) will be used to determine all the parameters of the transmission matrix (8 degrees of freedom). In contrast fixed polarization experiments provide information about only half of these parameters (4 degrees of freedom). T is also given by:

$$T = \begin{pmatrix} |T_{xx}|e^{-j\phi_{cox}} & |T_{xy}|e^{-j(\phi_{coy}-\phi_{cry})} \\ |T_{yx}|e^{-j(\phi_{cox}-\phi_{crx})} & |T_{yy}|e^{-j\phi_{coy}} \end{pmatrix} \tag{2.7}$$

This representation shows all the properties of medium.

Attenuation:

$A_{tx} = -20\log |T_{xx}|$ (dB) for X-polarization

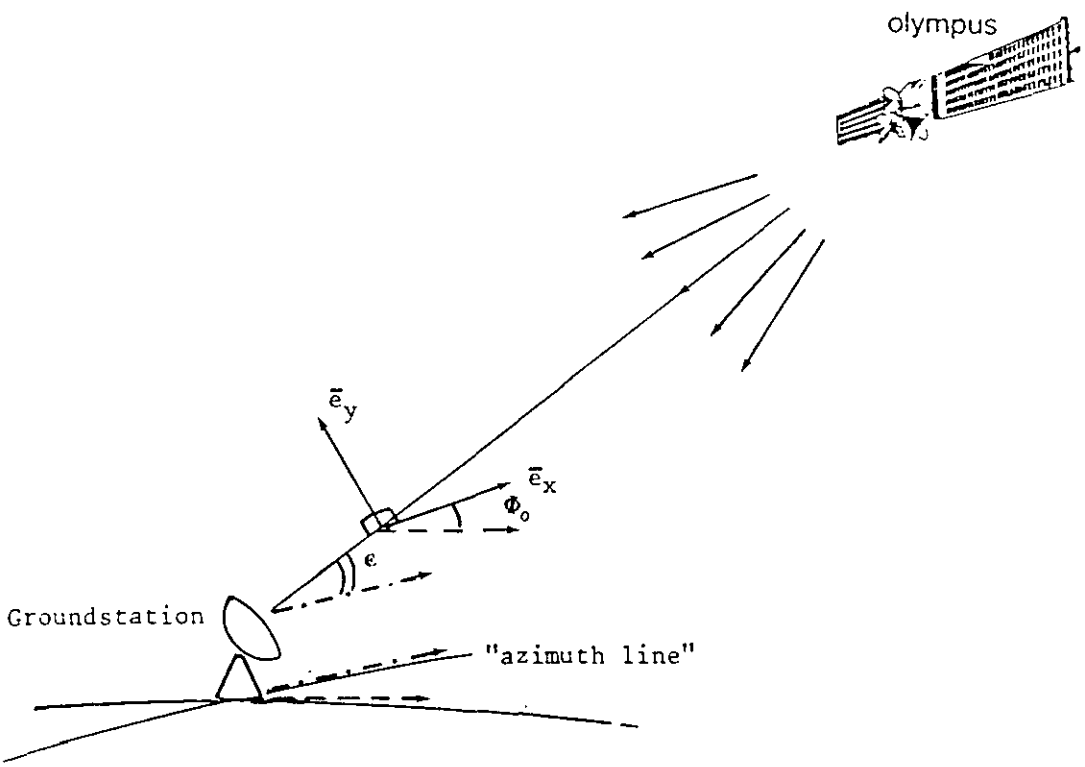

Figure 2.4: Geometry of the beacon measurement system

$A_{ty} = -20\log |T_{yy}|$ (dB) for Y-polarization

Differential attenuation between the two polarizations:

$A_{tx} - A_{ty} = 20\log |T_{yy}/T_{xx}|$ (dB)

Differential phase-shift = $\Phi_{cox} - \Phi_{coy}$

Crosspolar signals:

$20\log |T_{yx}|$ power crosstalk of X-polarization to Y-polarization
$20\log |T_{xy}|$ power crosstalk of Y-polarization to X-polarization

Phase difference between crosspolar and copolar signal:

Φ_{crx} for the X-polarization
Φ_{cry} for the Y-polarization

The transmission matrix parameters are defined relative to free space transmission. Thus for a fully transparent medium $T_{xx} = T_{yy} = 1$ and $T_{xy} = T_{yx} = 0$.

The antenna and receiver convert the beacon signals to signals representing amplitude and phase of the electric fields. The properties of the antenna receiving system are expressed in the groundstation matrix A. This matrix is given with reference to the orthogonal base vectors $\bar{e}_x$ and $\bar{e}_y$ by [1]:

$$\mathbf{A} = \begin{pmatrix} A_{xx} & A_{xy} \\ A_{yx} & A_{yy} \end{pmatrix} \tag{2.8}$$

where A_{ij} (i,j = x or y) represent attenuation, phase-shift and depolarization introduced by the groundstation. For an ideal receiving system, $A_{xx} = A_{yy}$ and $A_{yx} = A_{xy} = 0$. The measured voltage matrix U is thus related to the transmitted field tensor by [1]:

$$U = A\,T\,E \tag{2.9}$$

where:

$$\mathbf{U} = \begin{pmatrix} U_{xx} & U_{xy} \\ U_{yx} & U_{yy} \end{pmatrix} \tag{2.10}$$

The measured crosspolar phasors are expressed by the following equations.

$$\delta_x^{\,u} = U_{yx}/U_{xx} \tag{2.11}$$
$$\delta_y^{\,u} = U_{xy}/U_{yy} \tag{2.12}$$

Usually the absolute values of these parameters are given in dB's and called the XPD values. Crosspolarization discrimination (XPD) is the ratio of the received signal level in the copolar channel and the signal level in the crosspolar channel. Crosspolarization isolation (XPI) is the ratio of the wanted signal level to the unwanted signal level in the same receiver channel when two orthogonal polarizations are transmitted at the same level, simultaneously. For the X-polarization this becomes:

$$XPD_x = 20\log|U_{xx}/U_{yx}| \quad \text{(dB)} \tag{2.13}$$
$$XPI_x = 20\log|U_{xx}/U_{xy}| \quad \text{(dB)} \tag{2.14}$$

2.3 Attenuation and phase-shift

Beacon signals experience attenuation and phase-shift. In space beacon signals experience free space attenuation. Gases and clouds in the atmosphere cause little attenuation, but especially rain can cause considerable attenuation and phase-shift.

• Free space Attenuation

Free space attenuation is fundamental for point-to-point links, also known as basic free space transmission loss. This attenuation is given by:

$$L_{bf} = 20\log(4\pi d/\lambda) \quad \text{(dB)} \tag{2.15}$$

In which:

L_{bf} = basic free space transmission loss (dB)
d = distance satellite - groundstation (m)
λ = wavelength (m)

• Attenuation by atmospheric gases

Electromagnetic waves interact with gases in the atmosphere, but only oxygen and water vapour cause significant attenuation for radio frequencies between 10 to 50 GHz. The attenuation is caused by absorption of wave power by the gas molecules. The total attenuation A_t (dB) by gases is calculated by integrating the specific attenuation for the propagation path [2]:

$$A_t = \int_0^d (\gamma_o(r) + \gamma_v(r))\, dr \quad \text{(dB)} \tag{2.16}$$

where γ_o en γ_v are the specific attenuation coefficients (dB/km) for oxygen and water vapour respectively. Figure 2.5 shows the attenuation coefficients as a function of the frequency for both gases, at 20 °C and a water vapour density of 7.5 g/m^3. The peaks in figure 2.5 are the absorption bands of oxygen and water vapour.

A first order approximation of equation (2.16) is calculated by using equivalent heights. For elevation angles greater than 10°, attenuation is given by [2]:

$$A_g = A_o + A_v = \frac{h_o\gamma_o e^{-h_s/h_o} + h_v\gamma_v}{\sin(\epsilon)} \quad \text{(dB)} \tag{2.17}$$

where A_o and A_v are the attenuation caused by oxygen and water vapour respectively. h_o and h_v are the equivalent heights (km) for oxygen and water vapour respectively, ϵ is the elevation angle and h_s is the height above sea level.

The specific attenuation coefficients are assumed to be place independent in practical applications. In that case the following approximation formulae may be used (1013 mb, 15 °C) [2]:

$$\gamma_o = \left(7.19.10^{-3} + \frac{6.09}{f^2 - 0.227} + \frac{4.81}{(f-57)^2 + 1.50}\right) f^2.10^{-3} \quad (f<57\text{GHz}) \tag{2.18}$$

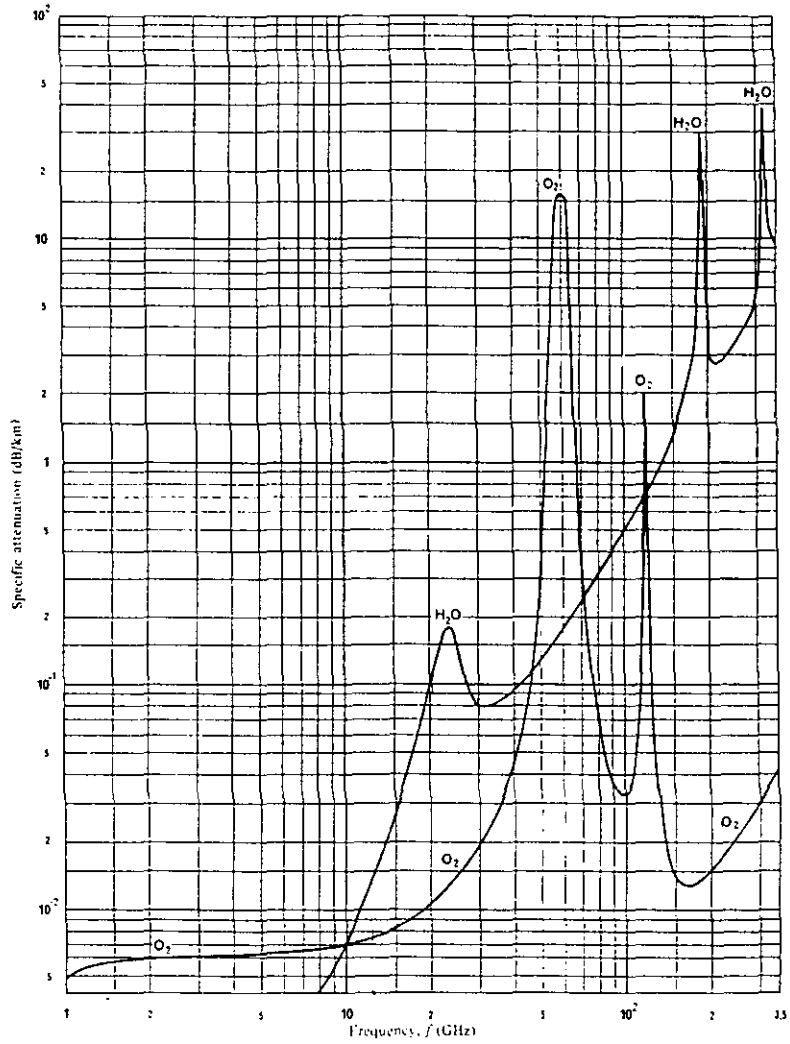

Figure 2.5: Attenuation coefficients for oxygen and water vapour [2]

$$\gamma_v = \left(0.067 + \frac{3}{(f-22.3)^2 + 7.3} + \frac{9}{(f-183.3)^2 + 6} + \frac{4.3}{(f-323.8)^2 + 10}\right) f^2 \rho_v \cdot 10^{-4} \quad (2.19)$$

for $f < 350$ GHz and $\rho_v < 12$ g/m^3

In which f is the frequency (GHz) and ρ_v is the water vapour density (g/m^3).

The coefficients can be compensated for temperature dependence by changing the calculated values -1.0% per °C for oxygen and -0.6% per °C for water vapour [2].
h_o and h_v can be found using the following formulae [2]:

$h_o = 6$ (km) for $f < 57$ GHz

$$h_v = 2.2 + \frac{3}{(f-22.3)^2 + 3} + \frac{1}{(f-183.3)^2 + 1} + \frac{1}{(f-323.8)^2 + 1} \quad \text{(km)} \qquad (2.20)$$

for $f < 350$ GHz and $\rho_v < 12$ g/m^3

For higher water vapour densities ($\rho_v > 12$g/m^3) it is better to use a second order approximation for the coefficient of water vapour attenuation [2]:

$$\gamma_v = \left(0.050 + 0.0021\rho + \frac{3.6}{(f-22.2)^2 + 8.6}\right) f^2 \rho_v .10^{-4} \qquad (2.21)$$

for $f < 100$ GHz

In this case the equivalent height is given by:

$$h_v = 1.6\left(1 + \frac{3}{(f-22.2)^2 + 5}\right) \quad \text{(km)} \qquad (2.22)$$

for $f < 100$ GHz

• Attenuation by clouds and fog

Attenuation caused by clouds or fog usually has small values, but can occur during a high percentage of time. For frequencies smaller than 100 GHz attenuation by fog is insignificant. Water droplets that constitute clouds and fog are generally less than 0.01 cm in diameter. This allows a Rayleigh approximation to calculate the attenuation for frequencies up to 100 GHz [3]. The attenuation by clouds is given by:

$$A_l = \int_0^l \gamma_l(r)\, dr = h_l \gamma_l \quad \text{(dB)} \qquad (2.23)$$

where l is the length of the path through clouds, h_l is the effective length of the path through clouds and γ_l is the specific attenuation for water droplets. The specific attenuation is a function of the liquid water content ρ_l and can be expressed by [4]:

$$\gamma_l = K_l \rho_l \qquad \text{(dB/km)} \qquad (2.24)$$

where K_l is the specific attenuation coefficient (dB/(kg/m^2)) and ρ_l is the liquid water content of the cloud (g/m^3). K_l is a function of frequency and temperature and is given in figure 2.6. An approximation formula for K_l is given by Slobin [3]:

$$K_l = 5.60.10^{-4} f^2\, 10^{0.0122(291-Tl)} \qquad \text{(dB/km)/(g/m}^3\text{)} \qquad (2.25)$$

where T_l (K) is the effective temperature of the water droplets. This formula approximates the attenuation values by Liebe [30] to within 5% for $f < 50$ GHz. Prediction of attenuation requires additional statistics of cloud density and sizes.

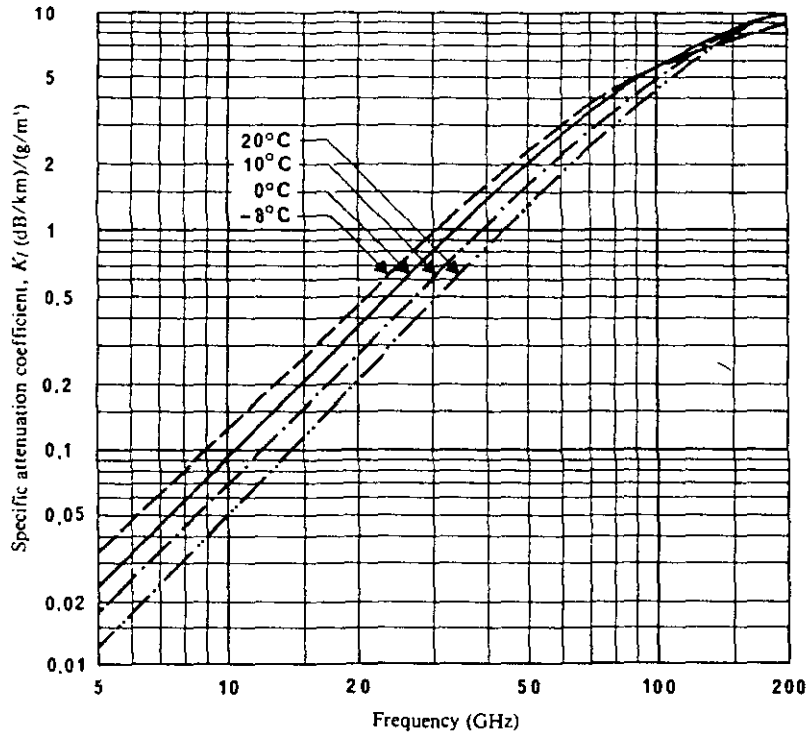

Figure 2.6: Attenuation coefficient due to water vapour droplets [4].

• Olympus low attenuation measurements

During clear-sky conditions attenuation is mainly caused by oxygen, water vapour and clouds. Thus the total attenuation is given by (2.17) and (2.23):

$$A_t = A_o + A_v + A_l = \frac{h_o \gamma_o e^{-h_s/h_o} + h_v \gamma_v}{\sin(\epsilon)} + h_l \gamma_l \quad \text{(dB)} \tag{2.26}$$

The water vapour density will usually be smaller than 12 g/m^3 (15° C) and the absorption bands above 100 GHz contribute less than 1% for Olympus frequencies. In that case equations (2.19) and (2.20) can be approximated by:

$$\gamma_v = \left(0.067 + \frac{3}{(f-22.3)^2 + 7.3}\right) f^2 \rho . 10^{-4} \tag{2.27}$$

$$h_v = 2.2 + \frac{3}{(f-22.3)^2 + 3} \quad \text{(km)} \tag{2.28}$$

• Attenuation induced by rain and snow

Rain causes severe absorption and scattering of centimetre/millimetre waves. For practical applications the specific attenuation (dB/km) is related to the rain rate R (mm/h) by [4]:

$$\gamma_r = kR^{\alpha} \tag{2.29}$$

This relationship is shown in figure 2.7.

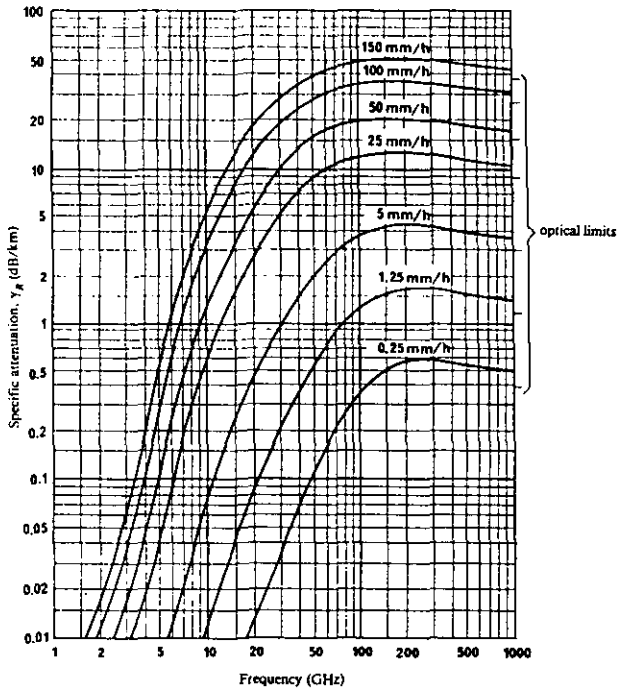

Figure 2.7: Specific attenuation due to rain [4].

k and α depend on the microstructure of rainfall (drop-size distribution, temperature, terminal velocity, shape).

Dry snow causes insignificant attenuation for frequencies below 50 GHz, but wet snow causes larger attenuation than equivalent rainfall. Hail also introduces attenuation as low as 2 GHz, but has very little effect on statistics. Accumulation of snow and melting snow on the antenna will influence the measurements more than snowfall.

• Copolar phase-shift

Phase is a relative parameter and in propagation measurements phase differences between co- and crosspolar signals and between different copolar signals may be determined. The phase-shift is introduced by hydrometeors and depends on the frequency, the precipitation medium and the rain drop-size distribution [5].

2.4 Depolarization, differential attenuation and phase-shift

Frequency-reuse systems are used to improve the efficiency of radio channels. These systems are limited by depolarization, some of the power transmitted in one polarization is transferred to the orthogonal polarization. Depolarization can be explained either by differential attenuation or differential phase-shift of the medium [6]. This causes crosstalk between orthogonally polarized channels. This phenomenon, also referred to as cross-polarization, may be caused by hydrometeors and multipath propagation. Multipath propagation is only relevant for terrestrial systems and will not be considered here.

Depolarization on the propagation path is mainly caused by hydrometeors such as rain drops and ice crystals. Projected onto the plane perpendicular to the propagation path, the medium may, for all practical purposes, be considered to have two orthogonal axis of symmetry. In these two directions of symmetry, the medium causes different attenuation and phase-shift. For waves polarized in any other direction this differential attenuation and phase-shift causes depolarization.

- Depolarization by rain

Rain introduces depolarization, which is always accompanied by attenuation. The depolarization may be explained by differential attenuation and phase-shift, due to the not spherical size of the raindrops. Figure 2.8 shows a raindrop canted due to the vertical windgradient. The angle between the symmetry axis of the raindrop and the local vertical is called the canting angle.

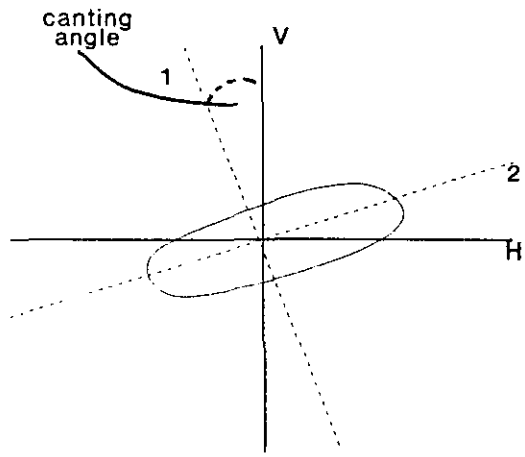

Figure 2.8: Canting angle of a rain drop

Experiments have shown a relationship between rain-induced depolarization (XPD) and attenuation (CPA). For many purposes the average XPD versus CPA relationship is sufficient [6][7]:

$$XPD = U' - V'\log(CPA) \quad (dB) \tag{2.30}$$

Several theoretical methods have been developed to predict values all fitting the general expression. U' is a function of the frequency, elevation angle, polarization tilt angle and the raindrop canting angle. V' is a function of the frequency. Using curve fitting procedures U' as a function of the frequency was found to be:

$$U' = S' + C'\log(f) \qquad (dB) \tag{2.31}$$

where S', C' are constants. Figure 2.9 shows the relationship for the Chu model for all beacons at the EUT groundstation (see appendix D).

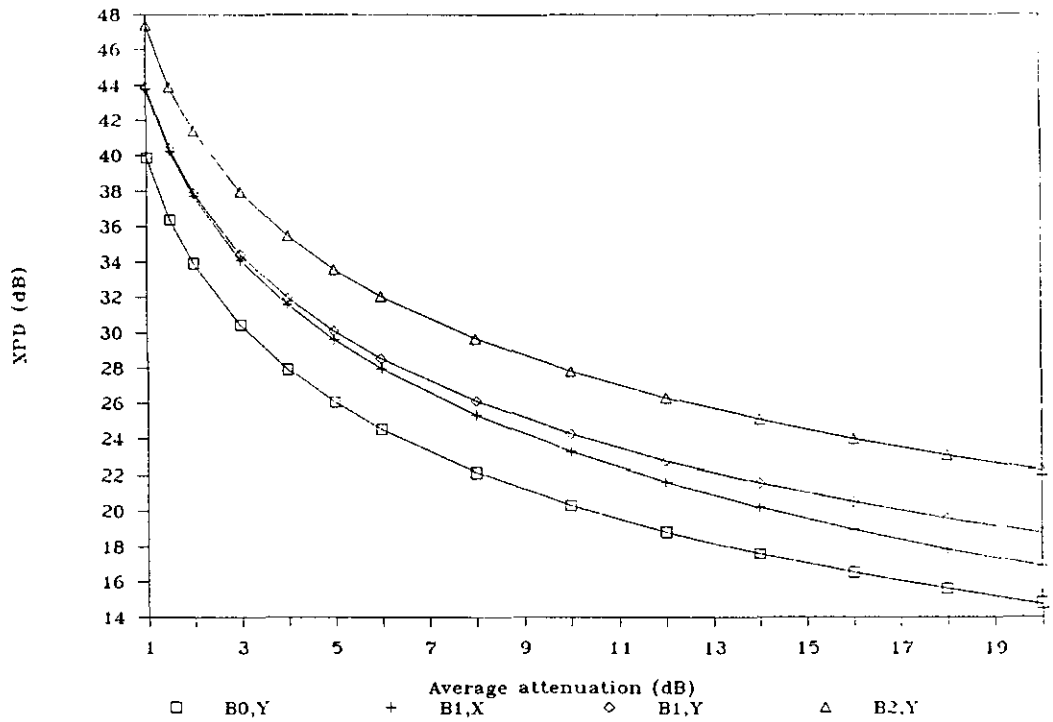

Figure 2.9: Crosspolar discrimination due to rain

- Depolarization by ice particles

High altitude ice crystals above the melting layer cause considerable depolarization on slant paths even in absence of significant attenuation. This effect is caused by differential phase shift due to the alignment of the major axis of the ice-crystals. This alignment can be explained both by aerodynamic-gravitational & electrostatic forces. This last force can be recognized for instance during lightning [8]. Abrupt phase changes of the crosspolar signal of the order of 180° can occur in association with lightning. A rayleigh scattering model of various crystal shapes is applicable up to about 20 or 30 GHz, having a frequency dependence identical to rain. In practice the effects of ice-crystal depolarization on overall XPD as a function of the attenuation can thus be accounted for by subtracting a constant value of the measured XPD [7].

Rain and ice depolarization can be separated in the measurements, by using a threshold based on the attenuation. Substantial depolarization below the attenuation threshold is considered to be caused by ice.

- Depolarization by other hydrometeors

Also snow has a depolarizing effect. This effect depends on the water content of the snow. Dry snow causes depolarization by differential phase-shift, but causes insignificant attenuation. Wet snow causes smaller depolarization than rain, with equal attenuation values. This depolarization is mainly due to differential attenuation.

- Differential attenuation and phase-shift

The difference in attenuation and phase-shift between two orthogonal linear polarizations is almost linear with total attenuation. Differential attenuation and phase-shift depend on the frequency, effective path length of rain, canting angle of the raindrops, elevation angle and rain drop size distributions. Figure 2.10 and 2.11 show the expected differential attenuation and phase-shift for the Marshall and Palmer drop-size distribution at EUT groundstation (See appendix D).

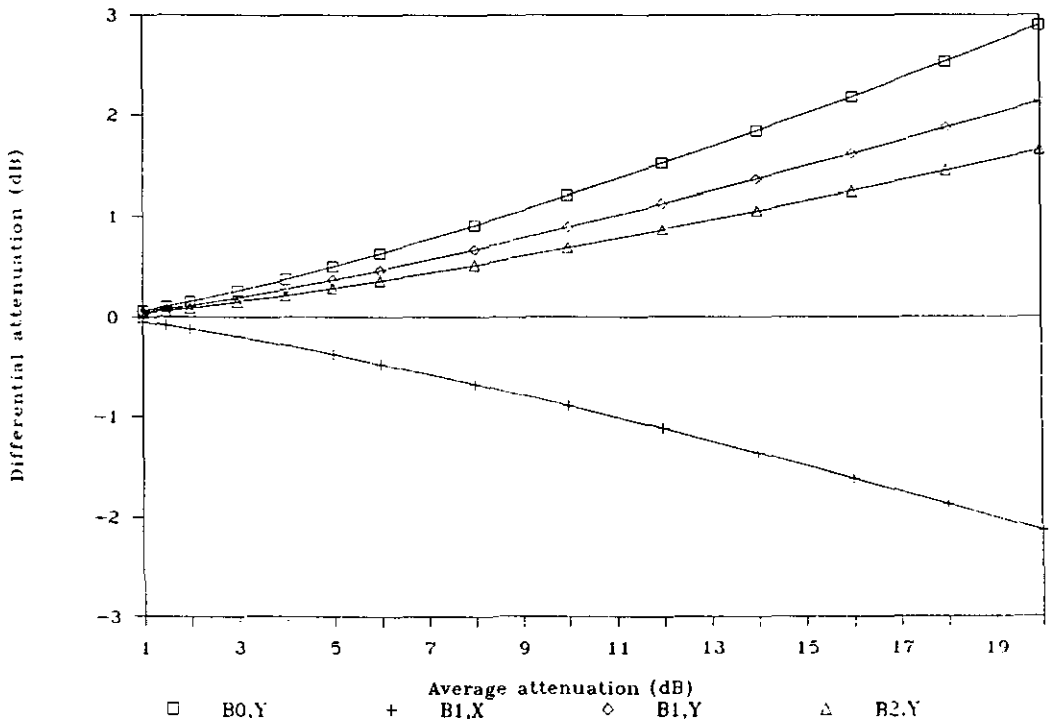

Figure 2.10: Differential attenuation due to rain

2.5 Medium models

Medium models have been developed to relate the transmission matrix parameters to quasi physical parameters such as anisotropy, canting angle and longitudinal inhomogeneity.

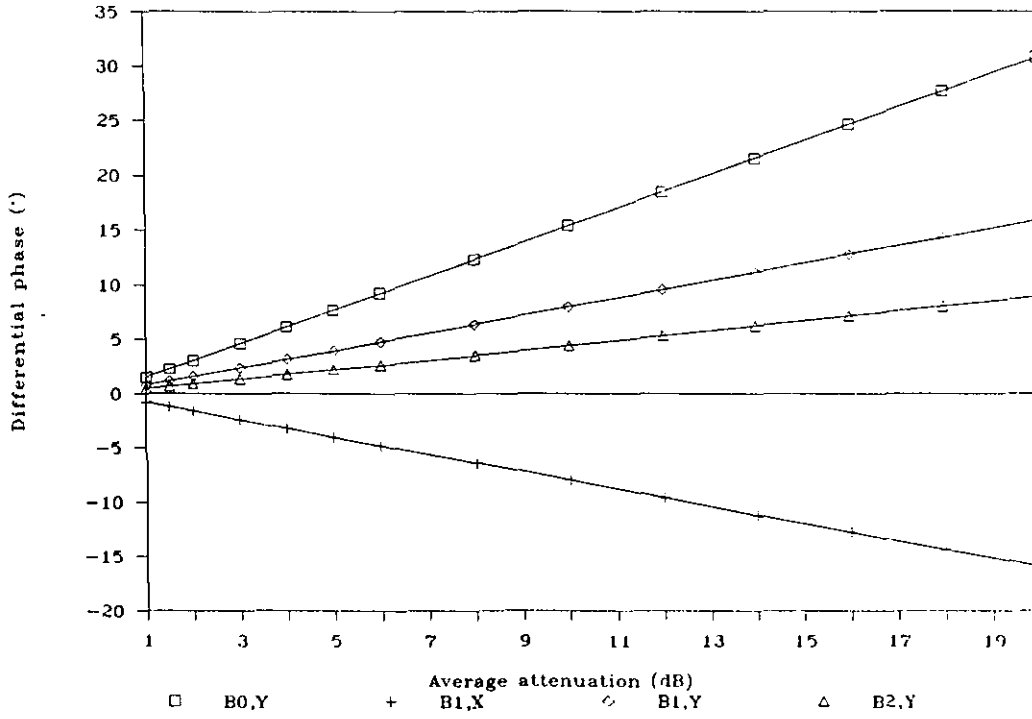

Figure 2.11: Differential phase-shift due to rain

Consider the medium in figure 2.12. xz and yz are the two polarization planes. z is the propagation direction. H and V are the local horizontal and vertical. The xy and HV plan are perpendicular to the propagation direction. This medium has two axis of symmetry. The planes through the axis of symmetry and the propagation direction are called the principal planes (1 and 2). T' and T'' are the integral propagation constants along the two principal planes.

$$T' = A' + jB' \qquad (2.34)$$
$$T'' = A'' + jB''$$

where A',A'' is the attenuation in Neper and B',B'' is the phase-shift in degrees (A''>A'). The anisotropy of the medium is defined by the differential attenuation and phase-shift between the principal planes [9]:

$$\Delta = T'' - T' = \Delta A + j\Delta B \qquad (2.35)$$

The canting angle Φ of the medium is the angle the local vertical makes with the first principal plane. This angle will be between -90° and +90°. The angle between the first principal plane and yz polarization plane is called the inclination angle ϕ. The angle between the polarization plane yz and the local vertical is the polarization tilt angle Φ_0. Thus the effective canting angle of the medium is given by [9]:

$$\Phi = \Phi_0 + \phi \qquad (2.36)$$

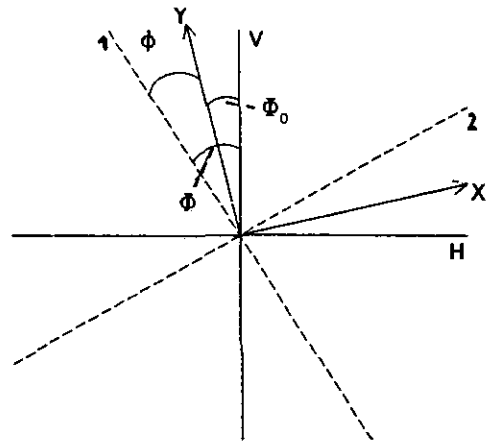

Figure 2.12: Medium model with principal planes

Longitudinal inhomogeneity can be used to describe a medium with two distinct regions of hydrometeors with different characteristics along the path.

The physical parameters are derived from the transmission matrix. In polarization oriented problems the normalized transmission matrix is used, which is defined by [9]:

$$t_{lin} = \frac{1}{T_{xx}} T = \begin{pmatrix} 1 & t_{xy} \\ t_{yx} & t_{yy} \end{pmatrix} \tag{2.37}$$

In the normalized transmission matrix the information about average attenuation and phase-shift of the propagation path is removed. This matrix has thus 6 degrees of freedom as all parameters are complex. Medium models can be subdivided according to two criteria:
- existence of principal planes.
- longitudinal homogeneity

Combining these two criteria, 3 broad families of models may be distinguished [9]:
1. 'principal planes' model with 3 degrees of freedom.
This model applies to a medium constituted by one type of particles with symmetrically distributed axial orientations. Anisotropy and canting angle describe this medium.
2. 'homogeneous without principal planes' model with 4 degrees of freedom.
This model applies to a medium consisting of two types of hydrometeors well mixed up. This model represents a general medium fairly well. Anisotropy and complex canting angle describe this medium.

3. 'inhomogeneous without principal planes' model with 6 degrees of freedom.
This model applies to a medium consisting of two distinct regions of hydrometeors with different characteristics, one succeeding the other along the path. Anisotropy, canting angle and longitudinal inhomogeneity describe this medium.

Table 2.1 summarizes the possible medium models.

For the Olympus data evaluation the second model with four degrees of freedom is chosen. The characteristic condition of this model is $t_{xy} = t_{yx}$ [9]. This assumption may improve measurement accuracy for the other parameters.

Table 2.1: Medium models

Medium	principal planes	longitudinal homogeneity	anisotropy	canting angle	degrees of freedom
transparent	any direction	yes	0	-	0
one type of particles	two	yes	complex value	real value	3
two types of particles well mixed up	no	yes	complex value	complex value	4
general	no	no	complex value	complex value	6

Paraboni [9] proposed to evaluate anisotropy and canting angle from the transmission matrix in circular polarization for uniformity. Anisotropy is given by:

$$\Delta = \Delta A + j\Delta B = 2.\mathrm{arctanh}\sqrt{\frac{t_{rl}.t_{lr}}{t_{ll}.t_{rr}}} \tag{2.38}$$

and the inclination angle is given by:

$$\phi = \phi' + j\phi'' = \frac{j}{4}\ln\left(\frac{t_{lr}.t_{ll}}{t_{rr}.t_{rl}}\right) \tag{2.39}$$

where t_{rr}, t_{rl}, t_{lr}, t_{ll} are parameters of the normalized transmission matrix in circular polarization. For the homogeneous medium model, the characteristic condition is $t_{ll} = t_{rr}$. The procedure for deriving (2.38) and (2.39) from the normalized transmission matrix in linear polarization is given in appendix A.

As can be seen from the formulae, the inclination angle and thus the canting angle can have a complex value. In fact the absence of symmetry axes results in the canting angle becoming complex. This complex canting angle can be approximated by a real value, derived from the real part of the inclination angle:

$$\Phi = \phi' + \Phi_0 \tag{2.40}$$

The imaginary part of the inclination angle is expressed in the crosspolar unbalance [9]:

$$CU = 20\log\left|\frac{t_{lr}\cdot t_{ll}}{t_{rr}\cdot t_{rl}}\right| \quad (dB) \tag{2.41}$$

Anisotropy, general canting angle and crosspolar unbalance are parameters suitable for exchange among researchers who see the satellite under different tilt angles.

2.6 Scintillation

Scintillation is the fast fluctuation of the signal level around a mean value and is caused by interference of the direct wave and the incoherent scattered wave. Both amplitude and phase scintillation exist sometimes during clear-sky or raining periods. Clear-sky scintillation may be caused by perturbations in the refractive index of the medium during air turbulence or by heavy cumulous clouds passing through the propagation path. Rain scintillation may be caused by moving raindrops, introducing a doppler shift depending on wind velocity and raindrop fall velocity. These phenomena are still under investigation. Scintillation is worse for lower elevation angles and higher frequencies. During clear air conditions, scintillation is bandlimited to about 20 Hz. During rain multiple scattering by raindrops causes scintillation effects up to 100 Hz [1].

2.7 Sky noise and sky noise measurements

Antenna measurements are also affected by sky noise. Natural sky noise is radiated due to the absorption of power by gases and hydrometeors, or is generated by lightning, the sun, radio stars and other cosmic bodies. Another part is due to reflections, for instance by the moon. An earth station observing a satellite at a large elevation angle may be considered to be receiving sky noise from the antenna boresight direction. For lower elevation angles thermal noise emission from the earth's surface will increasingly be observed in the antenna's side lobes.

Absorption of power by gases causes thermal emission of noise. The sky noise temperature T_s caused by gases is given by [10]:

$$T_s = T_m(1-10^{-At/10}) \quad (K) \tag{2.42}$$

where Tm is effective medium temperature and A_t the total attenuation (dB). During rain, the absorption component of rain introduces noise. Also clouds, fog, sand and dust contribute to sky noise, more for higher attenuation values. For the effective medium temperature the value:

$$T_m = 1.12(\text{surface temperature}) - 50 \quad (K) \tag{2.43}$$

has been derived empirically [27].

If the sun, the moon or the stars are present in the receiving beam of the antenna, noise levels will increase. This usually happens for geostationary satellites for a short period twice a year.

●Sky noise measurements
Radiometers are designed to measure sky noise for calculating low attenuation values of the atmosphere. Consider the radiometer model of figure 2.13 [11].

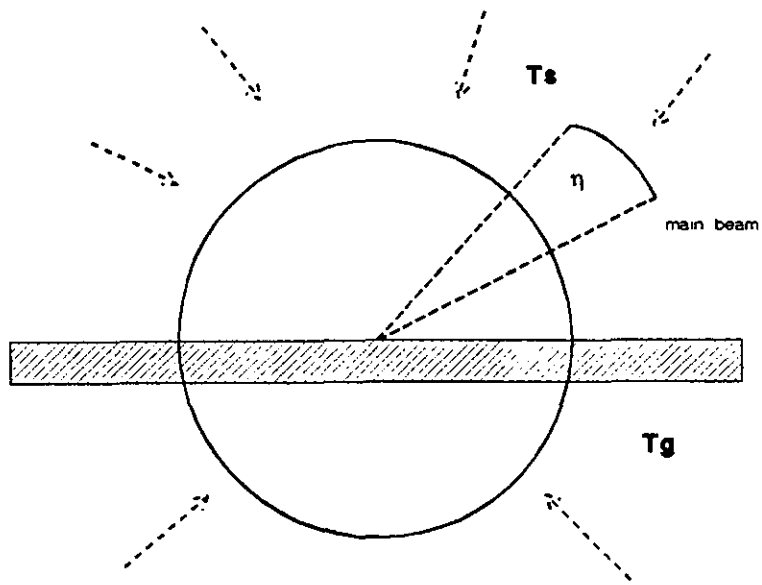

Figure 2.13: Antenna pattern of a radiometer

In this model it is assumed that the sky noise and the sidelobe diagram of the antenna are isotropic. The antenna is pointed to the sky. If η is the part of the antenna diagram of the main beam pointed to the sky, then $(1-\eta)$ is the part in the sidelobes, looking for $\frac{1}{2}(1-\eta)$ to the sky and for $\frac{1}{2}(1-\eta)$ to the ground. Thus $h = \eta + \frac{1}{2}(1-\eta) = \frac{1}{2}(1+\eta)$ is the part of the antenna pattern pointed to the sky and (1-h) is the part pointed to the ground. At the output of the antenna feed, the measured antenna noise temperature T_a is given by:

$$T_a = T_s h/A_f + (1-h)T_g/A_f + (1-1/A_f)T_g \quad (K) \tag{2.44}$$

From this equation Ts can be solved:

$$T_s = T_a A_f/h + (1 - A_f/h)T_g \qquad (K) \tag{2.45}$$

where

T_s = sky noise temperature (K)
T_a = antenna noise temperature (K)
T_g = ground temperature (K)
A_f = feed loss (linear)
h = part of the antenna pattern pointed to the sky

The atmospheric attenuation A_t (dB) can now be calculated by using (2.42) and accounting for cosmic noise:

$$A_t = 10\log\left(\frac{T_m - T_c}{T_m - T_s}\right) \quad (dB) \tag{2.46}$$

where:

T_m = effective medium temperature (K)
T_c = cosmic noise temperature (K)
A_t = total attenuation (dB)

3. ERRORS IN SATELLITE BEACON MEASUREMENTS

3.1 Introduction

The measurement system introduces errors in propagation experiments. These errors have to be recognized to estimate the quality of the measurements. Otherwise the interpretation of the measurements can lead to false predictions of the propagation properties of the atmosphere.

Errors in satellite beacon measurements are roughly divided into two groups: predictable and unpredictable errors. Predictable errors add a bias to the measurements and change slowly in time with a diurnal or seasonal characteristic. Unpredictable errors have a higher frequency content and are usually stochastic. The slow variations depend mainly on the temperature or weather conditions of the equipment.

Figure 3.1 shows the effects involved in satellite beacon measurements.

In the receiver, copolar and crosspolar signals are measured. Every block in this diagram causes gain reduction, phase-shift (vertical arrows) and cross-polarization (diagonal arrows). The line thickness of the arrows in figure 3.1 indicates the amount of influence. In figure 3.1 vertical arrows indicate attenuation and phase-shift, diagonal arrows indicate depolarization. The following paragraphs will discuss the errors in beacon measurements in detail.

3.2 Satellite

3.2.1 The Olympus propagation package

The Olympus satellite has three beacon horns transmitting linear polarized waves at three different frequencies. The quality of the propagation package is essential to obtain good measurement results. In the design of the satellite, transmitter and horn antennas the following important properties were considered [12]:
- EIRP stability
- crosspolar level
- frequency stability
- polarization stability
- phase stability and phase noise
- station keeping

The position of the Olympus satellite is 341.0° E, 0.0° N. Station keeping is within a 0.07° box seen from the centre of the Earth.

Table 3.1 shows the in orbit performance of the propagation package measured from Redu [13].

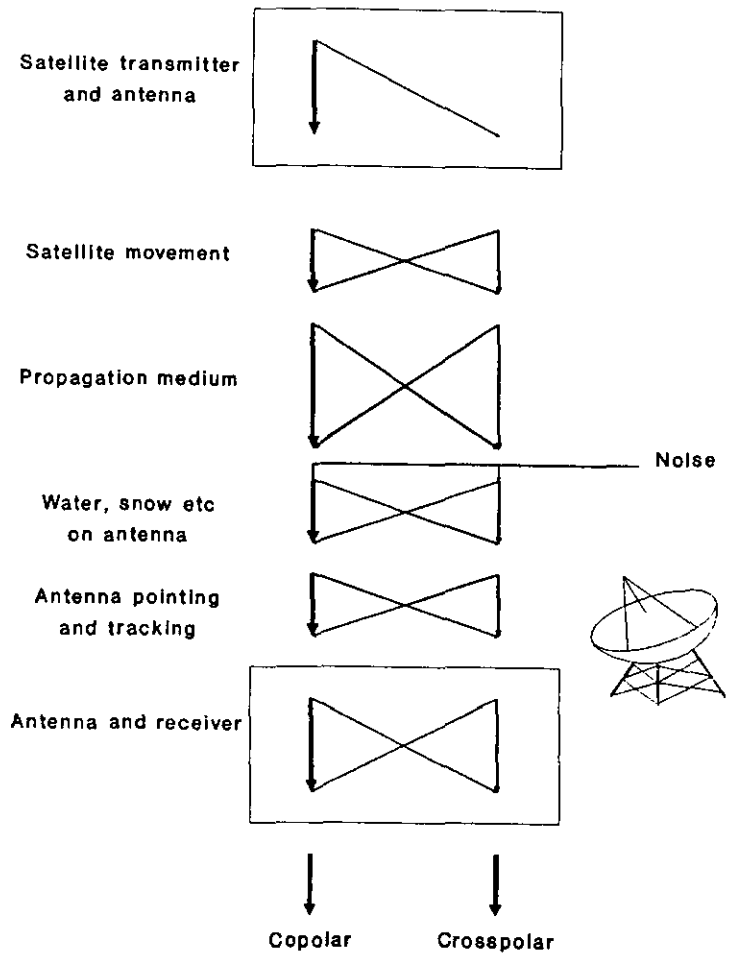

Figure 3.1: The satellite beacon measurement system

The XPD of B2 has not yet been successfully measured. The design goal of the horn antennas for the XPD was 36 dB [12]. Phase variation between the two polarizations of B1 will be smaller than 2 degrees in 24 hours.

Table 3.2 shows the specifications for the polarizations of the beacons [12]. The B1-beacon switches between two orthogonal linear polarizations with a cycle frequency of 933 Hz.

The 24 hours variations are mainly caused by the thermal cycle or motion of the spacecraft. Longer term variations will be caused by aging of the equipment. The next paragraph discusses variations due to motion of the spacecraft.

Table 3.1: In orbit performance of the Olympus propagation package [13]

	B0	B1(X)	B1(Y)	B2	
EIRP (average 24 hrs)	13.1	31.7	31.7	27 4	dBW
EIRP Variation (peak/peak 24 hrs)	0.25	0.4 (1)	0.4 (1).	0.86	dB
POLARISATION ORIENTATION (2)	Y	X	Y	Y	-
XPI (incl. earth station contribution)	35	> 43	> 43		dB
NOMINAL FREQUENCY	12501.866	19770.393	19770.393	29655.589	MHz
FREQUENCY OFF-SET (average 24 hrs)	-1.77	-2.80 note 3)	-2.80 note 3)	-4.20 note 3)	kHz
FREQUENCY VARIATION (peak/peak 24 hrs)	0.31 (3)	0.49 (3)	0.49 (3)	0.74 (3)	kHz
B1 POLARISATION TOGGLING		933.000525			kHz

Notes 1) Inclusive propagation variations.
2) X = horizontal and Y = vertical polarisation when seen from the equator. At Redu, nominal X polarisation is 19.1 degree relative to horizontal which was confirmed by measurements.
3) All frequencies are derived from one master oscillator. Values for B1 and B2 are derived from B0.
Results include negligible ground equipment contributions and Doppler effect. The Doppler shift is typically ± 60 Hz when referred to 12.5 GHz.

Table 3.2: Polarization orientation specifications [12]

Signal	Polarisation	Orientation/Accuracy
B_1	Y	(90 ±2) degrees with respect to Earth equatorial plane.
	X	90 degrees with respect to B_1 - Y.
B_2, B_0	Y	(0 ± 0.5) degrees with respect to B_1 - Y.

3.2.2 Movement of the satellite

The Olympus satellite is a geostationary satellite. For an orbit to be geostationary it must be circular, it must lie in the equatorial plane and it must have a period exactly equal to the Earth's rotation period [14]. The orbit geometry is shown in figure 3.2.

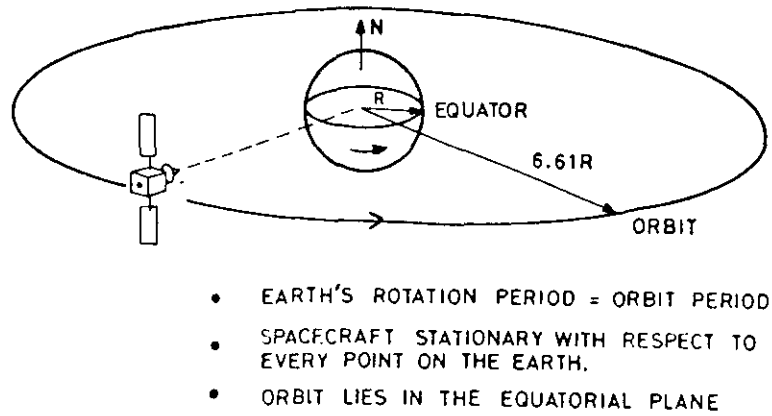

Figure 3.2: Characteristics of a geostationary orbit

A satellite has to be maintained at the required position within specific limits. The manoeuvres required to achieve this are called station-keeping. A geostationary satellite drifts in longitude mainly due to the non-sphericity of the Earth and solar radiation pressure on the satellite's sun-facing surfaces (mainly large solar arrays). Thus the orbit will be slightly elliptical resulting in a movement of the satellite relative to an Earth-fixed observer. The satellite drifts in latitude due to the influence of gravitational attraction of the sun and the moon. Station-keeping manoeuvres must be carried out through the lifetime of the satellite, at approximately weekly intervals, to keep the movements within limits.

Movements of the satellite cause pointing errors of a groundstation antenna, that is fixed pointed. Pointing errors of the groundstation antenna will result in gain loss and more equipment crosspolarization. The effects depend on the size of the groundstation antenna used. Beside pointing errors, movements cause a frequency doppler shift.

• Errors in received signal level

Consider a groundstation antenna fixed in pointing, having an aperture with uniform amplitude and phase. This is the worst case situation in terms of pointing errors. Table 3.3 shows the expected errors in measured copolar signal level for several antenna diameters for a pointing error of 0.07° (see appendix B). This shows that unacceptable errors occur in the received signal level for antennas with large diameter. In that case antenna pointing should be corrected with regular intervals (tracking).

Table 3.3: Maximum error (dB) due to satellite station keeping

Diameter (m)	3	4.5	6
B0	0.25	0.57	1.02
B1	0.63	1.43	2.62
B2	1.44	3.35	6.16

In practice the antenna diagram may be approximated by a second order polynomial function [12]. This is shown in figure 3.3

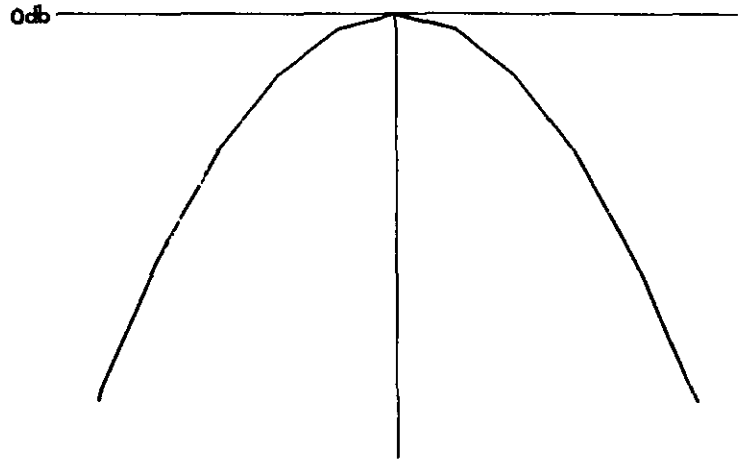

Figure 3.3: Antenna diagram

If the 3 dB beamwidth (Θ_{3dB}) is known, the error (S_{err}) in the signal level is given by (see appendix B):

$$S_{err} = \frac{12\theta^2}{\Theta_{3dB}^2} \quad (dB) \tag{3.1}$$

where θ is the actual pointing error resulting from the difference of the initial antenna pointing and the actual satellite direction.

Usually the movements will have a quasi harmonic character around a mean value. Assume θ is given by:

$$\theta = \theta_m + \theta_v \cos(\omega t) \tag{3.2}$$

where θ_m, θ_v are the mean and varying pointing errors, and ω is the angle frequency with a period of one day. For the antenna diagram of figure 3.3 the error (S_{err}) is given by:

$$S_{err} = \frac{12}{\theta_{3dB}^2}\left(\theta_m^2 + \frac{1}{2}\theta_v^2 + 2\theta_m\theta_v \sin(\omega t) + \frac{1}{2}\theta_v^2 \cos(2\omega t)\right) \quad \text{(dB)} \tag{3.3}$$

This shows that the signal level has has mean and varying errors. If the mean pointing error is very small, the signal level error will have a period of a half day. This would be the optimal for antenna systems without tracking.

- Doppler effect

The movement in the direction of the antenna boresight causes doppler frequency shifting. The frequency shift is given by:

$$\Delta f = f_0\left(\frac{v_p}{c_o - v_p}\right) \quad \text{(GHz)} \tag{3.4}$$

In which v_p is the velocity (m/s) in the direction of the groundstation, f_0 is the frequency (GHz) of the beacon and c_o is the velocity of light (m/s). This frequency shift causes phase variations and is important for the development of the receiver. The receiver should stay in lock during this frequency shift. Table 3.1 shows the frequency variation for the Olympus satellite beacons inclusive the doppler effect.

3.3 Ground station

3.3.1 Introduction

A groundstation for the Olympus satellite has to be designed to achieve good measurements of beacon signals for various atmospheric conditions. A typical groundstation measures copolar and crosspolar amplitude and phase-shift of all beacons.

The groundstation introduces extra deterioration of the beacon signals, typically caused by [12]:
- snow, ice and water on antenna and feed
- antenna pointing and tracking
- antenna impairments
- receiver crosstalk
- additive noise
- scintillation noise
- calibration
- interference
- errors due to maintenance activities

The groundstation may be equipped with radiometers for reference measurements. These measurements are also affected by errors. In the following paragraphs the groundstation errors will be discussed in more detail.

3.3.2 Snow, ice and water on antenna and feed

Antenna and feed are usually positioned in open air and thus their condition depends on the environmental circumstances. Snow and ice can accumulate on the antenna surface and rain drops or a water film can cover the antenna reflector or feed. This introduces additional attenuation, phase-shift, depolarization and noise in the measurements. Precautions should be taken to prevent these effects as much as possible.

If the antenna reflector is covered with water, wet snow or ice, the antenna pattern changes. Three effects are possible [15]:
- attenuation of the signal (gain reduction)
- difference in maximum of the beam and minimum of the tracking beam direction (beam squinting)
- possible change in sharp minimum of the tracking beam

The aperture field changes owing to variations of the reflection coefficients of the reflector. An example of the influence of a waterfilm on the antenna reflector is shown in figure 3.4 [15].

For a waterfilm all the distortions were found to increase with frequency (up to that at which the water layer is about a quarter wavelength thick). The minimum of the tracking beam was relatively high and it was found to increase with frequency. Wet snow, ice or supercooled rain on the antenna reflector can cause gain reduction up to 10 dB due to attenuation and defocussing [12] To remove snow or hail, a blower with dry hot air is used. Adequate heating is necessary to melt snow and ice first. Dry snow has insignificant effect and must not be heated to produce wet snow.

Liquid water on the antenna reflector will usually have little effect. Water drops or a water film on the feed though can introduce considerable attenuation. The magnitude of influence depends on the way water is distributed on the feed. Water on the feed can be removed by a blower or a rotating membrane. The use of water-repellent materials is recommended, but their properties will degrade in time due to the accumulation of dirt and dust.

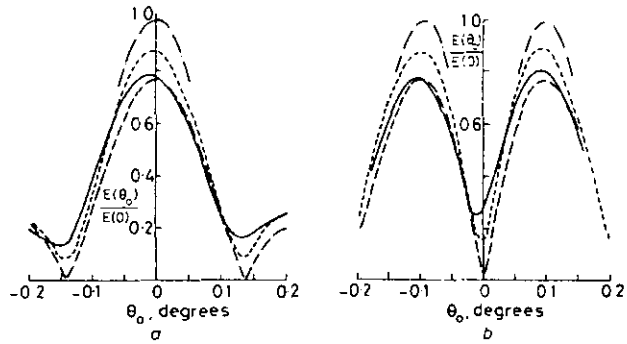

f = 15 GHz.
(a) Main mode
(b) Tracking mode
– · – · – dry antenna
– – – lower half of reflector and upper half of subreflector wet
– – – – lower half of reflector wet
– – – – lower halves of both reflectors wet

Figure 3.4: Normalized radiation pattern of a cylindrical Cassesgrain antenna

Antenna systems can be protected for weather influences by radomes [16]. Radomes on the feed introduce a small extra attenuation, noise and depolarization but this is constant for a specific frequency. The attenuation by rain on the surface of a radome is undesirable and 'hydrophobic' and 'non-filming' are often used terms to indicate water-repellent properties. The attenuation of a radome increases in time due to aging by sun light and dirt.

The mentioned effects have to be recognized in propagation measurements and removed from data. This causes a problem as these effects usually occur during events. Effects of water on the antenna system can be recognized by comparing the attenuation measurement with radiometer measurements. Accumulation of snow and ice will usually also occur on the radiometer, but during these periods atmospheric attenuation should be very small. Modelling of these effects in general is difficult, thus prevention is essential to be able to produce accurate event data.

3.3.3 Antenna pointing and tracking

- Pointing

The pointing error is the angle between the antenna beam axis and the desired direction [12]. The pointing accuracy is limited by mechanical axis and feed alignment errors, angular read-out errors, deformation of the antenna structure by wind ,gravity, thermal effects and servo-system errors. Accurate pointing is very important for crosspolar measurements. Otherwise the measured crosspolarization is mainly due to the depolarization of the antenna instead of the atmosphere.

The pointing accuracy of an antenna is usually given as a fraction of the 3dB beamwidth. Antennas with larger diameters have a greater gain and smaller beamwidth, thus a greater pointing error. The antenna is initially set by maximizing the received beacon amplitude in clear sky.

Pointing errors arise from:
- changes in the satellite position (see 3.2.2)
- bending of rays on the signal path, especially for lower elevation angles
- changes in antenna pointing

• Tracking

The tracking system is designed to decrease pointing errors. The pointing of the antenna is changed with regular intervals or continually. The tracking accuracy is the residual error angle between the antenna beam axis and the direction of arrival of the satellite received signal under auto-tracking operation [17]. This accuracy is limited by the step size of the antenna steering, the receiver thermal noise and errors due to the effect of wind. Table 3.4 shows the maximum error in received signal level as a function of the tracking accuracy for an antenna with a diameter of 5.5 m (EUT antenna) and an antenna efficiency of 55% (see appendix B).

Table 3.4: Maximum amplitude error (dB) due to tracking

tracking accuracy (°)	0.005	0.01	0.025
B0	0.003	0.012	0.076
B1	0.008	0.030	0.19
B2	0.018	0.068	0.43

Several tracking methods have been introduced, to point the antenna in the desired direction. The main automatic methods are step-track, monopulse and program-track. In step-track the pointing error is corrected with regular intervals by maximizing the received signal level. Monopulse systems make use of a special microwave coupler inserted in the antenna feed, picking up higher mode signals. These higher mode signals have a null in the beam-axis direction. Information on the pointing error is directly fed into the servo-system. With program-track, the position of the satellite is predicted from earlier measurements and pointing is corrected.

3.3.4 Antenna and receiver

• Antenna impairments

The antenna introduces uncertainties in attenuation and depolarization measurements due to its practical characteristics [12]:
- polarization purity
- sidelobe suppression
- crosspolarization of the antenna
- Surface errors
- Mechanical rigidity, stability.

Mechanical deformations due to wind and temperature changes will occur.
- Temperature stability

Heating of the surface to melt snow or ice can cause some deformations of the reflector.

• Receiver impairments

On a multichannel receiving station there is usually some residual crosstalk between different channels, affecting measurement accuracy during some circumstances. This may occur at the input frequency or any intermediate frequency. The source of this crosstalk may be:

- Signal leakage from the copolar to the crosspolar channel due to imperfect isolation between mixers and the local oscillator.
- In Olympus a reference channel is used for synchronization, so leakage is possible between all channels.

In addition non-linearities and instabilities of the receiver introduce additional errors.

• Additive noise

To analyze the influence of noise on the measurements, the receiver has to be modeled. The receiving system for one beacon consists basically of a reference channel and a test channel. The set-up (figure 3.5) provides the opportunity to measure copolar and crosspolar amplitude and phase-differences between crosspolar and copolar signals.

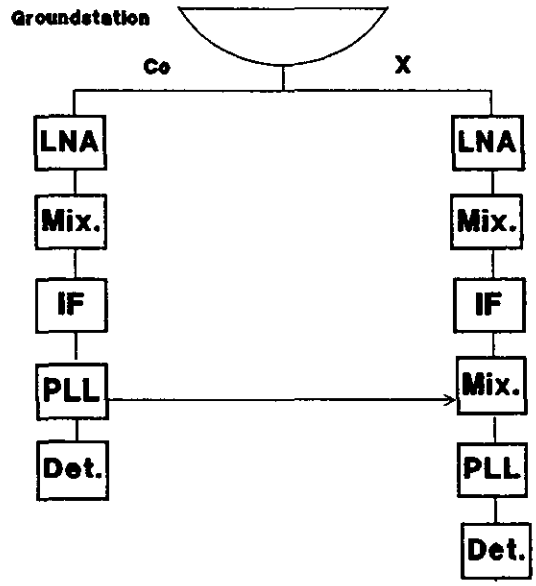

Figure 3.5: Basic blockdiagram of the beacon receiver

The reference channel in the Olympus beacon experiment is used as a phase reference for the test channel. Three sources of noise contribute to bias errors and random fluctuations in amplitude and phase measurements [12]:

- additive white gaussian noise in the reference channel
- additive white gaussian noise in the test channel
- local oscillator phase noise.

Thermal noise thus causes errors in attenuation, depolarization and phase measurements. Table 3.5 shows a summary of typical error specifications to be expected for the EUT receiving system due to additive noise (post-detection bandwidth 0.5 Hz) [5]. For copolar signals, error specifications are given for typical attenuation values. For smaller attenuation, the standard

deviation of the errors decreases. The standard deviation of the errors for crosspolar measurements depends on the crosspolar level.

Table 3.5: Standard deviation of errors due to additive noise [5]

signal	B0	B1	B2
copolar level (dB)	0.021	0.084	0.10
crosspolar level (dB) maximum for XPL= -45 dB	0.18 ... 1.2	0.21 ... 0.9	0.19 ... 0.6
phase-difference (°) maximum for XPL= -45 dB	1.7 ... 11	2.0 ... 9	1.8 ... 6
differential phase (°)		0.92	

Additive noise may deteriorate the crosspolar measurements considerably. If one is only interested in determining the mean values, the observed data errors in the receiver will be much smaller when averaging is applied to a total data base of several years of data.

- Radiometers

Radiometer measurements are important for obtaining low attenuation values. In deriving the sky noise, there are some complicating factors [1]:

- Although atmospheric attenuation is dominated by absorption, scattering plays a role especially during precipitation. In this case it is more difficult to obtain the effective medium temperature
- The antenna averages the noise coming from all directions
- For large attenuation values (>7dB) the radiometer reaches an asymptotic level, introducing large errors in measurements.

Considering these factors, the radiometer provides reasonable attenuation values up to 7dB. Thus especially for clear-sky measurements radiometers are a good reference for beacon experiments.

- Scintillation effects

Copolar and crosspolar signals will exhibit scintillation effects. Amplitude scintillation is always associated with phase scintillation, but differential phase measurements are hardly affected due to the correlation of phase scintillation on different channels. As thermal noise, scintillation causes random fluctuations of the signal and may even dominate thermal noise.

- Calibration

Calibration of the receiver is necessary to verify proper performance of the receiver. The overall accuracy is strongly affected by the calibration routine and the number of calibrations. In practice, calibration is possible within ±0.2 dB for amplitude and within ±2 degrees for phase due to instabilities and non-linearities.

- Detection and A/D conversion

To collect data into a database, the analog signals are converted to digital signals. This process consists of analog filtering, sampling, quantizing, digital filtering and again sampling. At EUT the

resulting bandwidth for the beacon channels is ±1.5 Hz (3 Hz sampling) or ±0.5 Hz (1Hz sampling). The quantization introduces an extra error.

- Interference

High power radio sources, TV transmitters and radars may cause breakthrough at any intermediate frequency of the receiver, and interfere with the wanted signal. This effect depends on the location of the receiver and the groundstation [12]. Interfering signals may also arrive within the main lobe from other payloads of Olympus or other satellites within the beamwidth.

3.4 Conclusions

The measurement system causes errors in the assessment of amplitude and phase of copolar and crosspolar signals. Errors due to noise and equipment instability are inevitable and limit the overall accuracy. Errors that have a predictable behaviour (for instance due to the thermal cycle and satellite movement) should be removed from the measurements. Table 3.6 shows a rough estimation of the total rms error of the predictable (P) and unpredictable errors (U) in co- and crosspolar measurements and the expected system depolarization (In-orbit specifications Olympus, groundstation XPD of 40 dB, 5.5 m antenna, tracking accuracy 0.01°, no snow, ice or water on antenna, A/D conversion with accuracy of 10 bits). It is assumed that all errors are not correlated and have the same statistical characteristics. For the stochastic errors, the standard deviation of the errors is given.

Table 3.6: Estimation of errors in satellite beacon measurements

Beacon		B0			B1				B2	
Source	CPL (dB)	XPD (dB)	DPH (deg)	CPL (dB)	XPD (dB)	DPH (deg)	VHPH (deg)	CPL (dB)	XPD (dB)	DPH (deg)
Satellite (P)	0.13	35		0.20	> 43		2.0	0.43	36	
Tracking (U)	0.012			0.030				0.068		
Antenna XPD (P)		40			40				40	
Stability (U)	0.20	0.20	2.0	0.20	0.20	2.0	2.0	0.20	0.20	2.0
Noise (U) maximum	0.021	0.18 1.2	1.7 11	0.084	0.21 0.9	2.0 9	0.92	0.098	0.19 0.6	1.8 6
A/D conversion (U)	0.015	0.015	0.18	0.015	0.015	0.18	0.18	0.015	0.015	0.18
total error (P)	0.13			0.20			2.0	0.43		
system XPD		31			< 40				32	
total error (U) maximum	0.20	0.27 1.2	2.6 11	0.22	0.29 0.92	2.9 9.2	2.2	0.23	0.28 0.63	2.7 6.3

The satellite and groundstation introduce considerable depolarization. cancellation of equipment-induced depolarization is necessary. Note that errors due to tracking in the crosspolar measurements cannot easily be predicted and have to be obtained in practice. Other errors due

to system outage, tracking malfunction or water and snow on the antenna have to be recognized in measurement data.

Errors that have a predictable behaviour can be compensated for during propagation events. The next chapter discusses methods to remove these errors in copolar and crosspolar data.

4 CORRECTION OF SATELLITE BEACON MEASUREMENTS

4.1 Introduction

In propagation measurements, errors are introduced by the measurement system. Several techniques have been developed to remove predictable errors. This correction is performed to gain more accurate data about the propagation phenomena. For crosspolar measurements, correction is essential, because crosspolarization by the propagation medium is usually very small and the measurements may be dominated by equipment-induced crosspolarization.

In propagation measurements two typical time periods are considered: the clear-sky and event period [1]. These two periods are shown in figure 4.1.

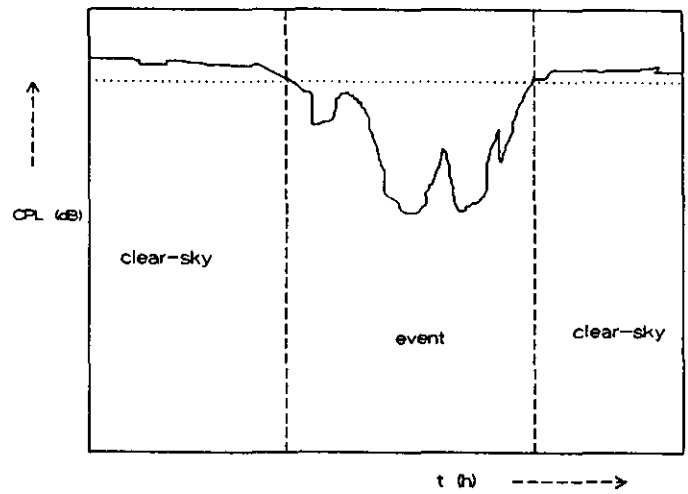

Figure 4.1: Typical periods in propagation measurements

During the clear-sky period, attenuation on the propagation path is only caused by gases and clouds in the atmosphere. No rain, snow or hail is detected on the propagation path. During the event period, severe attenuation, depolarization or phase-shift is measured due to rain, snow or hail somewhere on the propagation path. Before and after an event period the water vapour content is usually higher than during clear-sky conditions, causing higher attenuation values. This period may be distinguished as non-raining.

For data processing purposes, events are determined with an event level. Events should be selected from calibrated and edited data, typically after establishing copolar and crosspolar correction. The selection is performed according to a set of thresholds for different propagation parameters. A propagation period will be called an event if attenuation, crosspolar level, crosspolar phase or rain-rate exceeds its threshold level. The event level for attenuation is shown in figure 4.1.

The next paragraphs discuss methods to remove predictable errors from copolar and crosspolar measurements.

4.2. Copolar bias removal

4.2.1 Methods for copolar bias removal

Copolar beacon measurements are copolar amplitude and phase. These measurements are corrected for predictable system errors by bias removal of clear-sky levels (templates). A template is the measured copolar level or phase during clear-sky periods and has a diurnal and seasonal repetition characteristic due to the equipment conditions. In OTS attenuation measurements, the system bias was called the 0-dB reference level [18]. This 0-dB level changed 1 to 2 dB diurnal, mainly due to changes in EIRP of the satellite beacon. The bias removal technique is shown in figure 4.2.

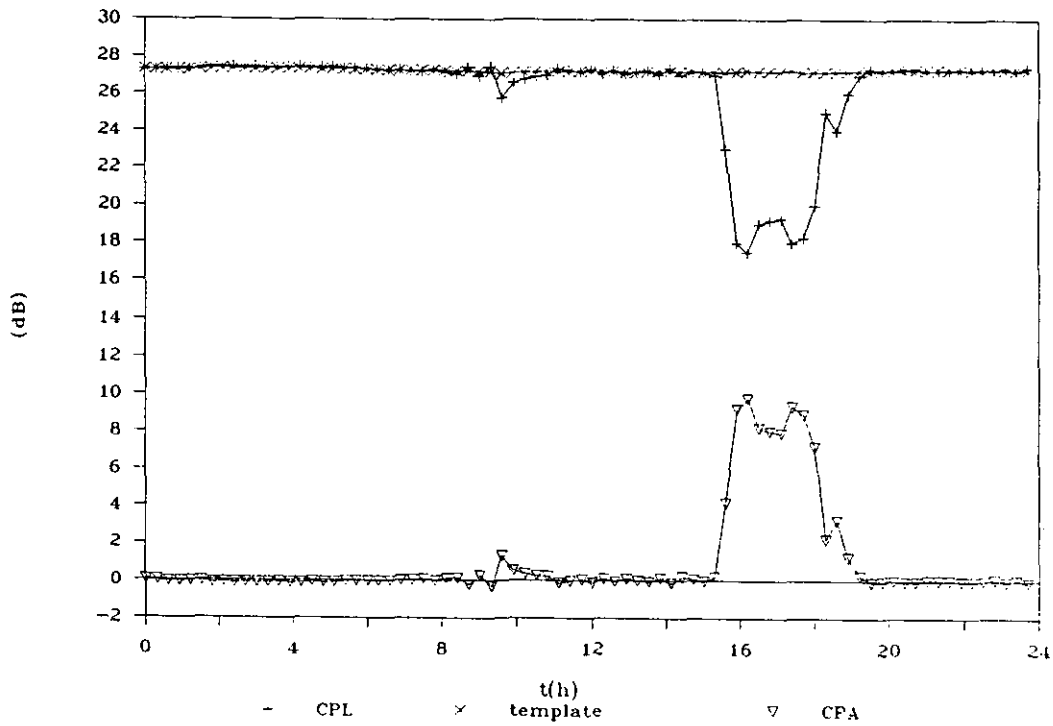

Figure 4.2: Copolar bias removal

The clear-sky copolar level still exhibits scintillation variations. Scintillation is usually a rapid fluctuation (>0.05 Hz) of the measured level with a negligible average component. By "low pass filtering" of the measured signal, this variation can be reduced in the data. Also some uncertainties in receiver and satellite EIRP variations and in rain attenuation are thus removed from the signal.

- Correction for clear-sky attenuation [19]

The template still has an attenuation component introduced by gases. Using radiometer measurements, it is possible under certain conditions to measure antenna-noise and calculate the atmospheric attenuation. During clear-sky conditions this attenuation is due to atmospheric gases

and clouds on the propagation path. The radiometer should perform noise measurements in preferably the same frequency area, at the same spot, pointed in the same direction. Radiometer measurements are not affected by diurnal variations of satellite signals. For small attenuation values, the radiometer gives good results, but for high attenuation values, especially during events, the radiometer will go into saturation. For these periods the radiometer cannot be used to estimate attenuation. In part II a procedure is derived to estimate clear-sky beacon attenuation with radiometer measurements.

- Determination of copolar templates.

During clear-sky periods a copolar level template can be derived by correcting the copolar level measurements with the radiometer derived attenuation (see figure 4.3). The template is a reference for beacon attenuation measurements. .

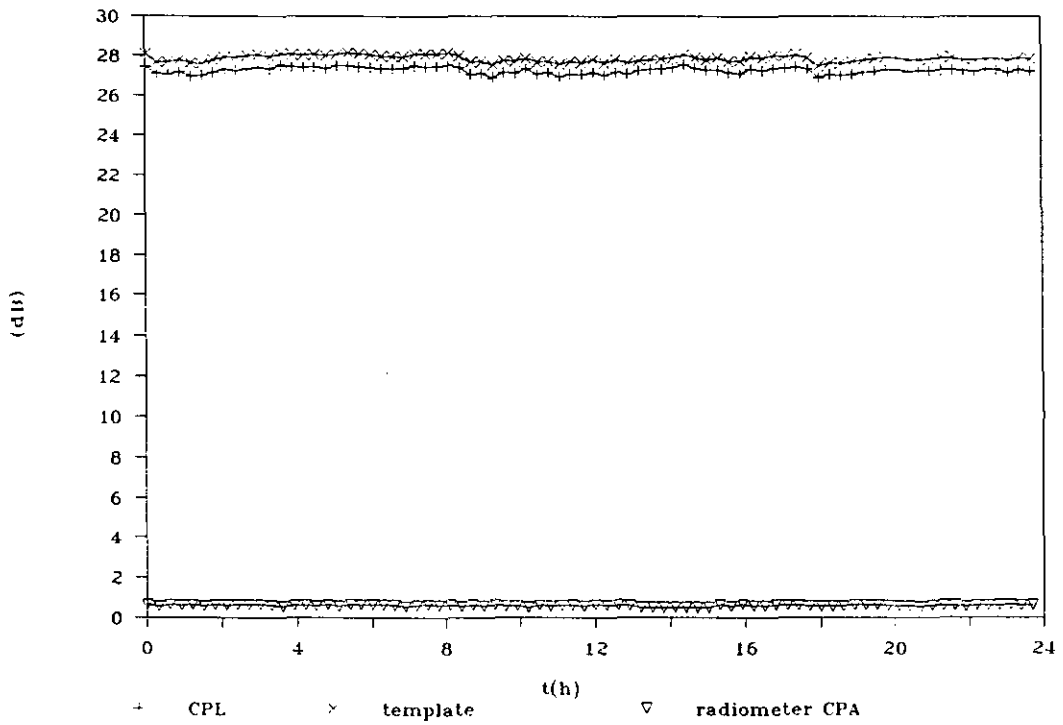

Figure 4.3: Copolar level templates

The template now only exhibits variations due to the measurement system. Note that radiometer measurements can only be used up to its saturation level. During events, the most interesting periods, the template has to be estimated. Two methods can be used to estimate the template of the system [1].

1. A typical reference template is derived by averaging clear-sky periods of several days. Averaging is only allowed for measurements at the same time of day. This template should regularly be adapted for changes in season or equipment.
2. Interpolation between template levels. During the event period the reference level can be estimated by interpolation between the values of the template before and after the event. The easiest way is linear interpolation. Improved accuracy may be obtained through

analysis of the diurnal behaviour of the template to find a suitable interpolation for the event period. This technique is called template matching.

Especially during longer lasting events in OTS measurements [18] the old 0-dB day-level was considered to be better than interpolation between levels during the day. For short events the reference level was calculated as the linear interpolation of levels at both sides of the event. These two levels should be called non-raining, as these periods exhibit high humidity levels just before and after a raining-event.

- Phase shift template

The phase shift introduced during clear-sky conditions is considered to be only due to the equipment. The phase-shift template is measured during clear-sky conditions and the mentioned approximation methods are applied to estimate the template.

- Test signal

In the beacon receiving system a test signal can be introduced, that has the same signal path as the beacon signal. By measuring the attenuation and phase shift of the test signal, thermal and linearity errors introduced by the receiver can be recognized and compensated for.

- Summary

In copolar measurements the following techniques can be used to remove predictable errors:

- Derive beacon attenuation during clear-sky conditions from radiometer measurements to correct copolar reference levels.
- Derive atmospheric attenuation and phase by correcting the copolar measurements with the system template.
- Introduce a test-signal in the receiver.

4.2.2 Analysis of copolar bias removal

As discussed in section 2, the transmission matrix represents the propagation properties on the propagation path. T_{xx} and T_{yy} are the copolar parameters and have to be determined from attenuation measurements. The voltage matrix is given by (2.9):

$$U = A\,T\,E \tag{4.1}$$

$$\mathbf{U} = \begin{pmatrix} U_{xx} & U_{xy} \\ U_{yx} & U_{yy} \end{pmatrix} = \begin{pmatrix} A_{xx} & A_{xy} \\ A_{yx} & A_{yy} \end{pmatrix} \begin{pmatrix} T_{xx} & T_{xy} \\ T_{yx} & T_{yy} \end{pmatrix} \begin{pmatrix} E_{xx} & E_{xy} \\ E_{yx} & E_{yy} \end{pmatrix} \tag{4.2}$$

In practice the ratio of crosspolar to copolar parts (4.2) is smaller than 1/10. In that case the contribution of products of crosspolar components in the measured voltages is negligible: the errors in the approximated voltages will be smaller than 1%. (4.2) may be approximated by:

$$U = \begin{pmatrix} A_{xx}T_{xx}E_{xx} & A_{xx}T_{xy}E_{yy}+A_{xx}T_{xx}E_{xy}+A_{xy}T_{yy}E_{yy} \\ A_{yx}T_{xx}E_{xx}+A_{yy}T_{yx}E_{xx}+A_{yy}T_{yy}E_{yx} & A_{yy}T_{yy}E_{yy} \end{pmatrix} \quad (4.3)$$

For the copolar components (4.3) results in:

$$U_{mm} = A_{mm}T_{mm}E_{mm} \quad (m = x,y) \quad (4.4)$$

T_{xx} and T_{yy} represent the propagation properties. For corrections of U_{mm} only the product $A_{mm}E_{mm}$ is relevant so it is not necessary to separate parameters of the satellite and groundstation. The following parameters are desired:

$$\text{Attenuation} = -20\log|T_{mm}| \quad (4.5)$$

$$\text{Phase-shift} = \text{Phase}(T_{mm}) \quad (4.6)$$

Phase-shift is only relevant if a reference beacon channel is present.
For a dual channel system the next parameters are also derived:

$$\text{Differential attenuation (X-Y)} = -20\log|T_{xx}/T_{yy}| \quad (4.7)$$

$$\text{Differential phase-shift} = \text{Phase}(T_{xx}/T_{yy}) \quad (4.8)$$

Using (4.4) the following expressions can be derived:

$$-20\log|T_{mm}| = -20\log|U_{mm}| + 20\log|A_{mm}E_{mm}| \quad (4.9)$$

$$\text{Phase}(T_{mm}) = \text{Phase}(U_{mm}) - \text{Phase}(A_{mm}E_{mm}) \quad (4.10)$$

$$20\log|T_{yy}/T_{xx}| = 20\log|U_{yy}/U_{xx}| - 20\log|A_{yy}E_{yy}/A_{xx}E_{xx}| \quad (4.11)$$

$$\text{Phase}(T_{xx}/T_{yy}) = \text{Phase}(U_{xx}/U_{yy}) - \text{Phase}(A_{xx}E_{xx}/A_{yy}E_{yy}) \quad (4.12)$$

All equations have the following form:

$$p(t) = S(t) - R_t(t) \quad (4.13)$$

p(t) is the propagation parameter, S(t) the measured signal and $R_t(t)$ the template (without radiometer correction) introduced by the measuring system. All parameters are time-dependent. During clear-sky conditions, when S(t) is very small, $R_t(t)$ can be measured. Small values of atmospheric attenuation can be derived from the radiometer measurements. The corrected $R_t(t)$ exhibits the system variations in time. Estimated values of $R_t(t)$, a template ($R_t'(t)$), are used during propagation events to calculate p(t).

$$p(t) = S(t) - R_t'(t) \quad (4.14)$$

The estimation of R_t' can be done using the techniques mentioned in 4.2.1. Equations (4.9) to (4.12) show that predictable errors are completely removed after correction.

4.3 Crosspolar bias removal

4.3.1 Cancellation systems

Performing accurate crosspolar measurements is very complex. Cancellation of equipment-induced depolarization is necessary to obtain correct atmospheric depolarization data. First of all the design of a groundstation has to be done with delicacy. Only then errors introduced by the system are recognizable and cancellation results in a better performance. This paragraphs discusses methods to cancel equipment-induced depolarization.

- Fixed cancellation in hardware

The first application of a system to compensate for equipment-induced cross polarization was due to Evans and Thompson [20][21] in 1973, which consisted of a waveguide system that coupled a phase-shifted and attenuated portion of a copolar signal into the cross-polar channel of a propagation experiment (figure 4.4).

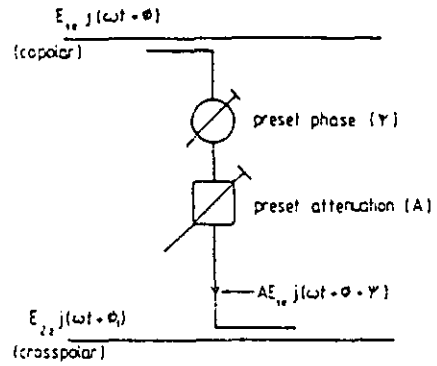

Figure 4.4: Fixed cancellation of equipment-induced depolarization [20]

The phase-shift and attenuation was set to cancel all crosspolarization during clear-sky conditions. The purpose of this static system was to improve measurement accuracy by cancelling out the residual cross polarization from the transmitter and receiver antenna and feed systems. This technique has become a standard tool for the improvement of equipment-induced crosstalk. It is called fixed or static cancellation and was used in the ATS-6 20/30 GHz propagation experiment. The typical crosspolar performance of the system with and without static cancellation is shown in figure 4.5 [20].

Essentially the equipment-induced depolarization is not constant and has a dynamic behaviour. Therefore to automatically cancel dynamic effects, an adaptive system is required. Average levels of the amplitude and phase of depolarization may be used to control the attenuation and phase

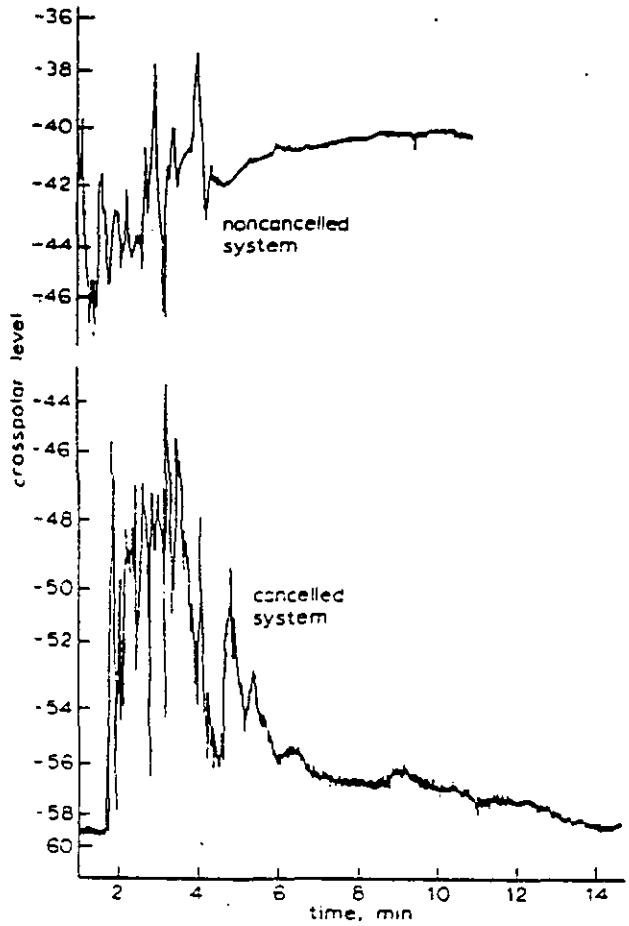

Figure 4.5: Crosspolar performance with and without static cancellation [20]

shift of the cancelling components. Three methods are available for introducing these components (See figure 4.6) [22]:

- Cross coupling arrangements.
- Orthogonality restoration by means of a differential phase and amplitude shifter in the antenna feed.
- Combination of the two systems mentioned.

These methods were used in communication links to cancel crosspolar components of the equipment and propagation path. Adaptive systems usually have a better performance than static systems. In propagation experiments, these hardware methods are not suitable to implement, because depolarization of the atmosphere has to be protected in measurements.

• Adaptive cancellation in software

The above systems are realized in hardware, but it is attractive to realize cancellation in software for narrow band propagation measurements [21]. Such an approach could not only readily carry out static cancellation but could permit variation of the cancellation to correct for known variations in the background crosspolar levels. Thus effects such as diurnal variations can be compensated

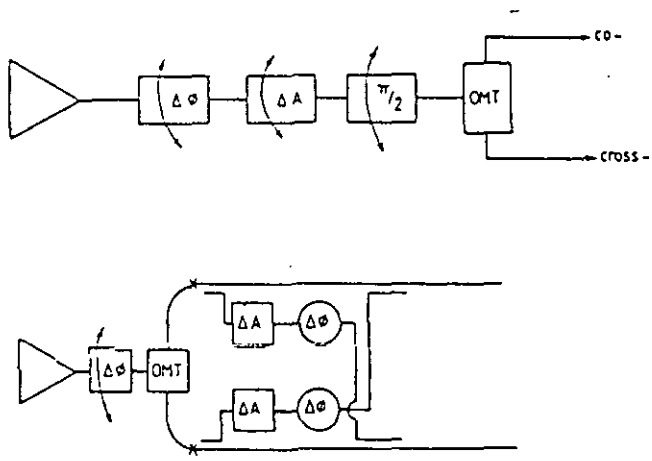

Figure 4.6: Methods for adaptive hardware cancellation [22]

for. A long time constant on the cancellation values is needed to protect the rainfall effects to be measured. An additional advantage of software cancellation is that it does not destroy the raw data and various degrees of cancellation can be experimented with. These techniques were used in depolarization measurements with OTS and SIRIO [18].

- vector cancellation

All the above systems consider the crosspolar phasor to be a vector in the complex plane (see figure 4.7). For adaptive cancellation this vector varies in amplitude and phase due to diurnal variations of the equipment-induced depolarization. Cancellation is done by carrying out a vector subtraction of the measured crosspolar phasor during an event and the reference phasor (or template phasor) [1]. This method will be called vector cancellation and can be used for all single polarized beacons. The template phasor is measured during clear-sky conditions. By 'low-pass filtering' of the measurements, scintillation and other uncertainties are removed from the template.

In COMSTAR experiments [24] in the USA, vector subtraction of the clear-sky crosspolar channel residuals suppressed the residual to -45 to -50 dB below copolar levels. The accuracy degraded with the intensity of the propagation event, because of the uncertainty in assigning residual contribution to transmitting and receiving antenna.

In the Japanese CS (20/30 GHz) and BSE (12/14 GHz) [25][26] experiments the variation of the clear-sky crosspolar components, arising from the thermal characteristics of the antenna feed assembly outside the observation room, were corrected assuming a linear relationship between outdoor ground temperature and the measured crosspolar phasor.

- Test signal

A test signal can be introduced in the receiver crosspolar channel to determine amplitude and phase-shift errors of the receiver.

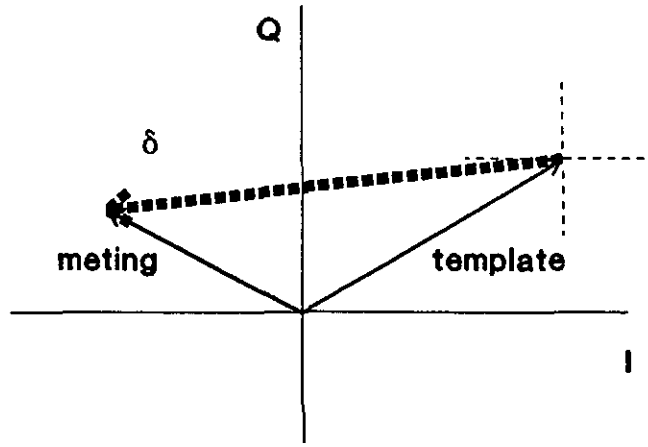

Figure 4.7: Principle of vector cancellation

• Reference horn method

In the reference horn method [1] another antenna with much better crosspolar discrimination is used as a reference. This is usually a horn antenna with a very good crosspolar performance. With this antenna it is possible to calculate the depolarization matrix of the satellite antenna during clear-sky conditions. Once the properties of the satellite antenna are known, it is possible to calculate the receive matrix of the ground station system by using the ground station antenna during clear-sky conditions. Now all the properties of the satellite and groundstation are separated and matrix calculations provide the depolarization properties of the atmosphere during events This method has not yet be put into practice. The disadvantage is the need for a complex antenna system and very sensitive antenna receivers.

• Ellipse-crossing method

In the ellipse crossing method [1], the polarization of the ground-station antenna is matched to that of the incident wave. A polarizer should be attached to the ground station antenna in such a manner that both can be rotated independently around their electrical axes. An antenna receiving the two orthogonal components is said to be perfectly matched if the polarization ellipse of the antenna has the same axial ratio, the same direction and the same sense of rotation as the incoming wave. By measuring the maximum and zero signal output, the perfectly matched and decoupled position can be found. Thus the polarization ellipse of the incoming wave is determined without influence from the groundstation. In principle this method can also be applied to a dual-polarized antenna by measuring the elipticity of the two ports separately.

• Matrix cancellation [1]

OPEX discussions have lead to develop a new method for bias removal for dual-polarized beacons. This technique is called matrix cancellation. The switched beacon experiment can be used to experiment with matrix cancellation to improve crosspolar performance. During clear-sky

conditions a cancellation matrix is derived from the measured voltage matrix. This matrix is used to compensate for equipment-induced depolarization during atmospheric depolarization periods.

Summary:
The following techniques can be used to correct crosspolar measurements for equipment influences:
- Fixed or adaptive vector cancellation
- Determine depolarization of the satellite by using the reference horn method
- Eliminate crosspolar effects of the groundstation using the ellipse crossing method
- Matrix cancellation for dual polarized beacons

Vector and matrix cancellation will be mathematically evaluated next, as these can be implemented in software to be part of a preprocessing system.

4.3.2 Analysis of crosspolar bias removal

In chapter 2 the crosspolar phasors were defined for X/Y-polarizations:

$$\delta_x^u = U_{yx}/U_{xx} \tag{4.15}$$

$$\delta_y^u = U_{xy}/U_{yy} \tag{4.16}$$

These phasors have to be corrected for system influence. Below expressions are derived for the horizontal polarization. The equations for vertical polarization are found by exchanging indices in the results. Using (4.3) δ_x^u is given by:

$$\delta_x^u = \frac{A_{yx}T_{xx}E_{xx}+A_{yy}T_{yx}E_{xx}+A_{yy}T_{yy}E_{yx}}{A_{xx}T_{xx}E_{xx}} \tag{4.17}$$

$$\delta_x^u = \frac{A_{yy}}{A_{xx}}\left(\frac{T_{yx}}{T_{xx}}+\frac{T_{yy}}{T_{xx}}\frac{E_{yx}}{E_{xx}}\right)+\frac{A_{yx}}{A_{xx}} \tag{4.18}$$

(1) (2) (3)(4) (5)

5 components can be distinguished in this equation:
(1) Groundstation unbalance (receiver channels and antenna)
(2) Crosspolar phasor of the propagation path δ_x
(3) Ratio of the copolar propagation parameters
(4) Crosspolar phasor of the satellite δ_x^s
(5) Crosspolar phasor of the groundstation δ_x^a

(4.18) is equivalent to:

$$\delta_x^u = \frac{A_{yy}}{A_{xx}}\left(\delta_x + \frac{T_{yy}}{T_{xx}}\delta_x^s\right) + \delta_x^e \qquad (4.19)$$

Now δ_y^u can easily be obtained by exchanging indices:

$$\delta_y^u = \frac{A_{xx}}{A_{yy}}\left(\delta_y + \frac{T_{xx}}{T_{yy}}\delta_y^s\right) + \delta_y^e \qquad (4.20)$$

The equations show the influence of equipment-induced depolarization. In some cases the measured phasor can even be dominated by depolarization due to the satellite or groundstation. If depolarization of the satellite and groundstation are known, the accuracy of the measured phasor can be calculated for various propagation conditions.

The problem in crosspolar bias removal is to eliminate the effects of satellite and groundstation. In beacon measurements these effects can not be separated. If the depolarization properties of the satellite and groundstation are known separately, the transmission matrix could be calculated by:

$$T = E^{-1} U A^{-1} \qquad (4.21)$$

In reality complete cancellation of satellite and groundstation predictable crosspolar influence is not possible, but better performance may be achieved.

- Vector cancellation.

This method can be applied in hard- or software for single polarized beacons. In hardware the reference phasor is fixed in the complex plane. In software the phasor changes according to the diurnal behaviour the system. During clear-sky conditions there is no depolarization on the propagation path: $T_{xy} = T_{yx} = 0$ and $T_{xx} = T_{yy}$. The measured depolarization phasor δ_{xo} reduces to:

$$\delta_{xo} = \frac{A_{yy}}{A_{xx}}\delta_x^s + \delta_x^e \qquad (4.22)$$

By subtracting this template phasor from the measured phasor during an event a better estimation of the atmospheric depolarization is obtained.

$$\delta_{xv} = \delta_x^u - \delta_{xo} = \frac{A_{yy}}{A_{xx}}\left(\frac{T_{yx}}{T_{xx}} + \left(\frac{T_{yy}}{T_{xx}} - 1\right)\delta_x^s\right) \qquad (4.23)$$

Note that this equation is only valid if the template phasor predicts the system behaviour perfectly. For a well balanced receiver, the influence of the groundstation is cancelled and the depolarization

influence of the satellite will usually be smaller. Thus the corrected phasor gives a better estimate of the atmospheric phasor than the measured phasor. With (4.23) the cancellation quality can be estimated for a specific system behaviour under different propagation conditions.

• Matrix cancellation

For dual polarized beacons it is possible to cancel either all receive or transmit crosspolar components using matrix cancellation [1]. Matrix cancellation can only be realized in software. Clear-sky measurements are used to construct the cancellation matrix (T = I):

$$K = U_o^{-1} = (AE)^{-1} = E^{-1}A^{-1} \tag{4.24}$$

This cancellation matrix is calculated by taking the inverse of the measured matrix U_o (template matrix). K is used to perform either left or right cancellation [1]:
Left cancellation:

$$T_L = K\,U \tag{4.25}$$

Right cancellation:

$$T_R = U\,K \tag{4.26}$$

T_L and T_R are new estimates of the transmission matrix T. Left cancellation corrects for groundstation influence.

$$T_L = E^{-1}\,T\,E \tag{4.27}$$

Right cancellation corrects for satellite influence.

$$T_R = A\,T\,A^{-1} \tag{4.28}$$

Note that these equations are only valid if the template matrix is a good prediction of the system influence during an event. The corrected crosspolar phasors are given by (see appendix B):
Left cancellation:

$$\delta_{xL} = \frac{E_{xx}}{E_{yy}}\left(\delta_x + \left(\frac{T_{yy}}{T_{xx}} - 1\right)\delta_x^s\right) \tag{4.29}$$

Right cancellation:

$$\delta_{xR} = \frac{A_{yy}}{A_{xx}}\delta_x + \left(1 - \frac{T_{yy}}{T_{xx}}\right)\delta_x^a \tag{4.30}$$

In δ_{xL} the ground station influence is cancelled. In δ_{xR} the satellite influence is cancelled. A choice must be made to eliminate crosspolar effects of the satellite or groundstation. The next chapter discusses the quality of propagation data using bias removal methods.

5. ACCURACY OF SATELLITE BEACON MEASUREMENTS

5.1 Introduction

In this chapter the accuracy in beacon propagation measurements is evaluated. Methods are developed to determine the accuracy for copolar and crosspolar measurements in practice. These methods are applied to the measurements of the EUT groundstation to obtain an estimate of the typical accuracy.

• The measurement system

First the measurement system has to be defined. Figure 5.1 shows the system consisting of the satellite propagation package, groundstation antenna, receiver and acquisition and the data preprocessing system. The accuracy will be determined at reference plane C (ref.C).

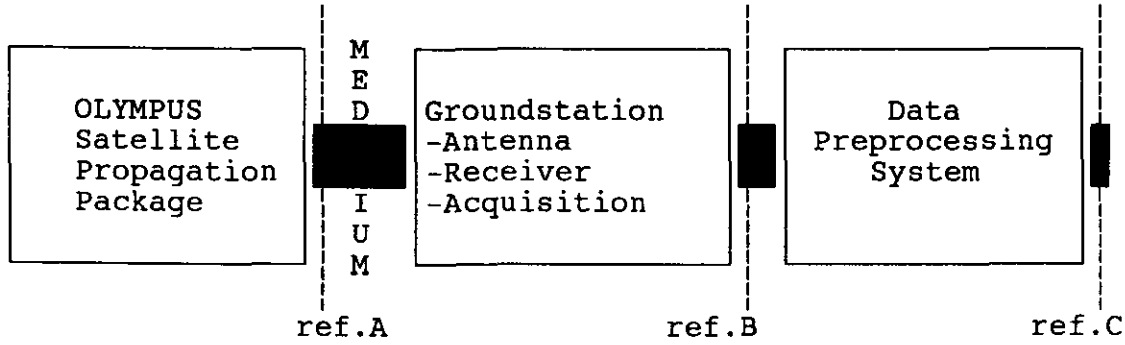

Figure 5.1: The measurement system

The Olympus satellite transmits 3 beacon signals (B0, B1, B2) at reference plane A (ref.A). The groundstation is capable of receiving all beacon signals and measures copolar and crosspolar amplitude and phase-shift. In the acquisition unit of the groundstation the analog signals are converted to a datastream. The datastream at reference plane B (ref.B) consists of copolar, crosspolar and supporting channels (radiometer and meteorologic data). Here only signal behaviour with predominantly low frequency components (< 1Hz) is considered. At reference plane C (ref.C) the datastream consists of attenuation (CPA), phase-shift (copolar phase CPH, differential phase DPH), crosspolar discrimination (XPD) and supporting channels. The satellite and groundstation unit contribute to errors in the input signals at ref.B. The preprocessing system corrects for predictable errors of the measurement system.

• Classification of errors

Errors and uncertainties may be classified into four categories:

- unpredictable, stochastic errors caused for instance by system noise (at ref.B and ref.C).
- predictable errors for which correction may be possible (at ref.B).
- errors due to correction limitations (at ref.C).
- errors due to template prediction (at ref.C).

Predictable errors (biases) may be removed from the data. Removal of biases is based on clear-sky measurements. These measurements are used to predict the system influence during an event. Predicted levels are called templates and are assumed to have a very low frequency content. To limit the frequency content of a template, typically the template changes only every 15 minutes. A template usually covers a period of one day. Bias removal is effective if this template changes only slightly from one day to the other.

Copolar measurements:
Clear-sky beacon signals experience attenuation by gases and clouds. To derive a reference pattern for attenuation, the clear-sky copolar level has to be corrected with the atmospheric attenuation derived from radiometer measurements. Ortgies [19] discussed the uncertainties of this process. Under the assumption that the reference pattern changes only slightly form one day to another, the pattern of the day preceding the event may be used as a 0-dB reference level for that day. The template for attenuation R_t (copolar level) is given by:

$$R_t = S + A_{cs} \quad \text{(dB)} \tag{5.1}$$

where S is the received copolar signal level and A_{cs} is the clear-sky atmospheric attenuation. The template for copolar phase-shift ϕ_t is directly derived from clear-sky phase-shift measurements.

The templates are used to determine the atmospheric attenuation and phase-shift during a certain period (typically during an event):
Attenuation:

$$A_c = R'_t - S \quad \text{(dB)} \tag{5.2}$$

where A_c is the attenuation after correction and R'_t is the system template for that period.
Phase-shift:

$$\phi_c = \phi_m - \phi'_t \tag{5.3}$$

where ϕ_c is the corrected phase-shift, ϕ_m is the measured copolar phase-shift and ϕ'_t is the system template for that period.

Uncertainties in A_c and ϕ_c are now due to uncertainties in the prediction of the template for a certain period and due to unpredictable errors in measured signal. The total uncertainty in A_c, ΔA_c is given by:

$$\Delta A_c = \Delta R_t + \Delta S \quad \text{(dB)} \tag{5.4}$$

where ΔR_t is the uncertainty in the template for that day and ΔS is the uncertainty in the received copolar signal level due to unpredictable errors.

The total uncertainty in ϕ_c is given by:

$$\Delta\phi_c = \Delta\phi_m + \Delta\phi_t \tag{5.5}$$

where $\Delta\phi_c$ is the uncertainty in the template for that day and $\Delta\phi_m$ is the uncertainty in the measured phase-shift due to unpredictable errors.

Crosspolar measurements:
In crosspolarization measurements the amplitude and phase of the crosspolar phasor δ is considered (for X- or Y-polarization). Crosspolar discrimination (XPD) and differential phase (DPH) are derived from this phasor:

$$XPD = -20\log|\delta| \tag{5.6}$$

$$DPH = \arg(\delta) \tag{5.7}$$

Vector and matrix cancellation can be used to correct predictable errors in crosspolar measurements. However it is not possible to remove all predictable influence during event measurements. The total uncertainty in the obtained atmospheric crosspolar phasor $\Delta\delta$ after correction is thus given by:

$$\Delta\delta = \Delta\delta_c + \Delta\delta_u + \Delta\delta_t \tag{5.8}$$

where $\Delta\delta_c$ is the error due to limitations of correction, $\Delta\delta_u$ is the uncertainty due to unpredictable errors and $\Delta\delta_t$ is the uncertainty due to template prediction

- Method to determine total accuracy

For total accuracy evaluation it will be assumed that all the errors mentioned above are not correlated. In that case the individual errors can be treated separately. The total rms error is calculated. Table 3.6 shows an estimate of the unpredictable errors and predictable errors at reference plane B. For determining the total accuracy at ref.C, errors due correction limitations and template prediction have to be evaluated. Bias removal of data only makes sense if these errors are smaller than the predictable errors.

- Preprocessing system

The preprocessing system consists of three basic modules, shown in figure 5.2. In radiometer data processing, radiometer measurements are used to estimate attenuation at beacon frequencies. In template extraction, reference levels (templates) are determined, which incorporate the predictable influence of the measurement system. In bias removal, event measurements are corrected by templates to cancel the predictable errors. Table 5.1 shows the beacon data that is considered at ref.C.

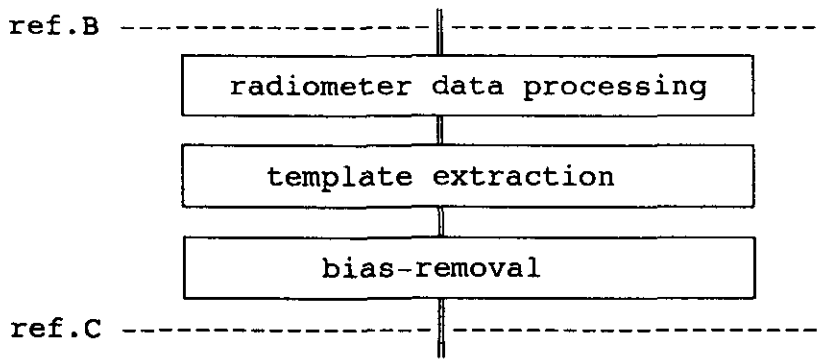

Figure 5.2: Basic modules of the preprocessing system

Table 5.1: Beacon data at reference plane C

Abbreviation	Unit	Explanation
B0VCPA_	dB	copolar attenuation B0
B2VCPA_	dB	copolar attenuation B2
B1HCPA_	dB	copolar attenuation B1,H
B1VCPA_	dB	copolar attenuation B1,V
B0VXPD_	dB	crosspolar discrimination B0
B2VXPD_	dB	crosspolar discrimination B2
B1HXPD_	dB	crosspolar discrimination B1,H
B1VXPD_	dB	crosspolar discrimination B1,V
B0VDPH_	deg	differential phase B0
B2VDPH_	deg	differential phase B2
B1HDPH_	deg	differential phase B1,H
B1VDPH_	deg	differential phase B1,V
B1VHPH_	deg	differential phase V-H copolar B1

The next paragraph considers the correction limitations for crosspolar measurements. Then the uncertainty in templates is discussed and the effect on the uncertainty in the obtained data after bias removal. Subsequently templates derived from EUT measurements are discussed and the accuracy is evaluated in practice.

5.2 Limitations of crosspolar bias removal

Depolarization of the measurement system is comparable with atmospheric depolarization. Thus crosspolar cancellation is essential to obtain accurate crosspolarization data about the propagation path. In this paragraph an estimate is made of the maximum errors in the obtained

crosspolarization discrimination (XPD) and differential phase (DPH) at ref.C with and without cancellation during rain. Four situations are considered:
- no cancellation (all beacons)
- vector cancellation (all beacons)
- left matrix cancellation (beacon B1)
- right matrix cancellation (beacon B1)

The equations for these four situations are derived in chapter 4.

Assumptions have to be made about the measurement system and the models to use for the propagation path. Table 5.2 gives an overview of the parameters and models used in the calculations.

Table 5.2: Description of measurement system and propagation path

	System I	System II
Satellite XPD	35 dB	40 dB
Groundstation XPD	40 dB	35 dB
Satellite unbalance (E_{xx}/E_{yy})	0.1 dB 0 °	0.1 dB 0 °
Groundstation unbalance (A_{xx}/A_{yy})	0.2 dB 2 °	0.2 dB 2 °
Raindrop size distribution	Marshall & Palmer	Marshall & Palmer
Depolarization model	Chu	Chu
Configuration	EUT (ϵ=26.7°, Φ_0 = -18.4°)	EUT (ϵ=26.7°, Φ_0 = -18.4°)

The described system parameters are typical for the Olympus propagation experiment. In the first system the satellite has a worse crosspolarization performance than the groundstation, in the second system it is the other way around. Other propagation models may be used to evaluate errors but this will only have minor effects on the results obtained.

The principle in calculating the maximum error in the obtained XPD and DPH is to derive the bounds of the relative error signal (k): crosspolar phasor error due to the measurement system relative to the atmospheric crosspolar phasor. If δ_m is the measured crosspolar phasor and δ is the real atmospheric crosspolar phasor, k is given by:

$$k = \frac{\delta_m - \delta}{\delta} \tag{5.9}$$

The error ΔXPD in the atmospheric crosspolarization discrimination is given by:

$$\Delta XPD = -20\log\left|\frac{\delta_m}{\delta}\right| = -20\log\left|1+\frac{\delta_m-\delta}{\delta}\right| \tag{5.10}$$

Using (5.9):

$$\Delta XPD = -20\log|1+k| \quad (dB) \tag{5.11}$$

The error bounds of ΔXPD can be determined:

$$\begin{aligned} &-20\log(1+|k|) < \Delta XPD < -20\log(1-|k|) \qquad (|k|<1) \\ &-20\log(1+|k|) < \Delta XPD < \infty \qquad\qquad (|k|\geq 1) \end{aligned} \tag{5.12}$$

The error ΔDPH in the atmospheric differential phase is given by:

$$\Delta DPH = \arg\left(\frac{\delta_m}{\delta}\right) = \arg\left(1+\frac{\delta_m-\delta}{\delta}\right) \tag{5.13}$$

Using (5.9):

$$\Delta DPH = \arg(1+k) \tag{5.14}$$

The error bounds of ΔDPH are given by:

$$-\arctan|k| < \Delta DPH < \arctan|k| \tag{5.15}$$

The error bounds as a function of the error distance (-20log|k|) are shown in figure 5.3 and 5.4.

The graphs show that the error signal always has to be 20 dB below the desired signal to achieve a result with a maximum error bound of ±1 dB. In that case the error in the phase will be limited to ±6 degrees. For Olympus it was the goal to measure XPD up to 35 dB with an accuracy of ±1dB.

To derive the errors as a function of the attenuation or crosspolar discrimination due to rain, k has to be expressed in terms that are functions of the CPA or XPD. For the four situations the ratio δ_m/δ is given by (using chapter 4 for X-polarization):

Uncancelled:

$$\frac{\delta_{xu}}{\delta_x} = \frac{A_{yy}}{A_{xx}}\left(1 + \frac{T_{yy}}{T_{xx}}\frac{\delta_x^s}{\delta_x}+\frac{A_{xx}}{A_{yy}}\frac{\delta_x^a}{\delta_x}\right) \tag{5.16}$$

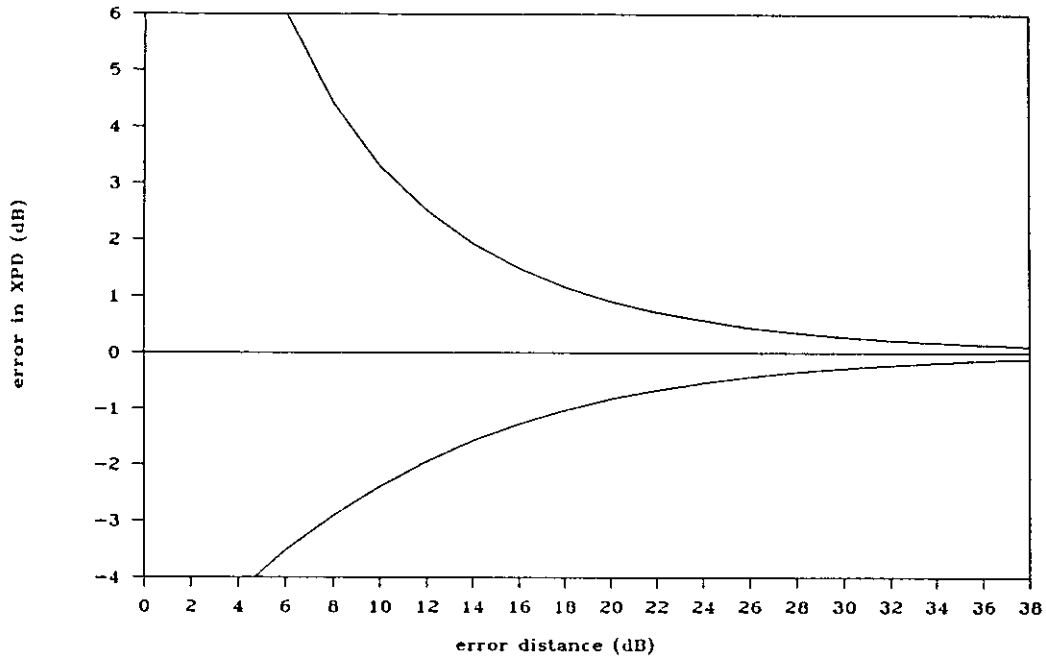

Figure 5.3: Error in XPD

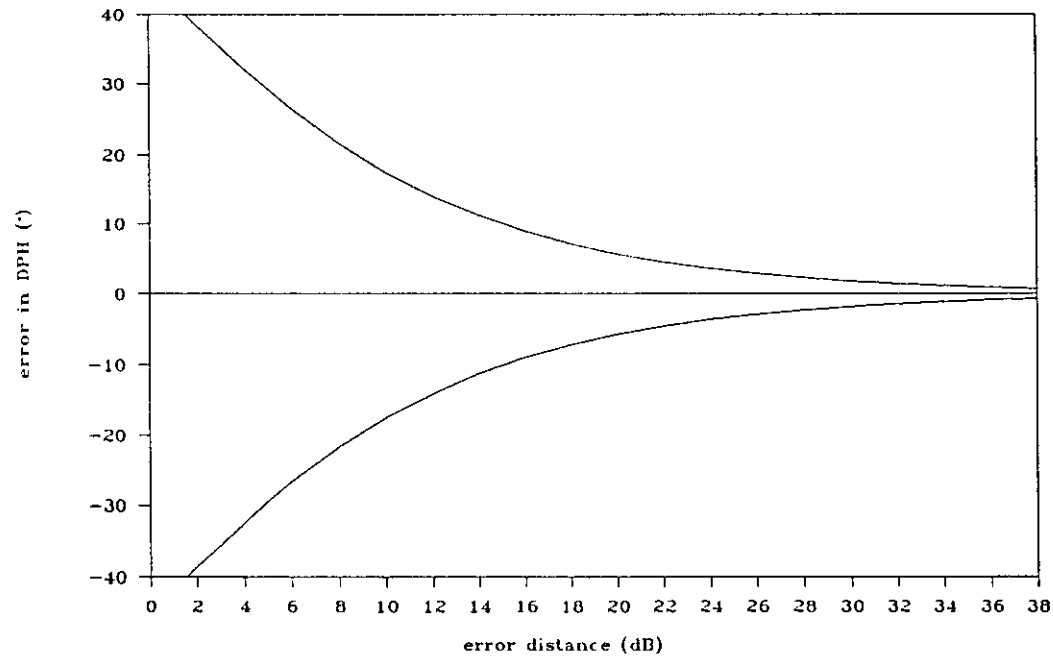

Figure 5.4: Error in DPH

Vector cancellation:

$$\frac{\delta_{xv}}{\delta_x} = \frac{A_{yy}}{A_{xx}}\left(1 + \left(\frac{T_{yy}}{T_{xx}} - 1\right)\frac{\delta_x^s}{\delta_x}\right) \tag{5.17}$$

Left matrix cancellation:

$$\frac{\delta_{xL}}{\delta_x} = \frac{E_{xx}}{E_{yy}}\left(1 + \left(\frac{T_{yy}}{T_{xx}} - 1\right)\frac{\delta_x^s}{\delta_x}\right) \tag{5.18}$$

Right matrix cancellation:

$$\frac{\delta_{xR}}{\delta_x} = \frac{A_{yy}}{A_{xx}}\left(1 + \frac{A_{xx}}{A_{yy}}\left(1 - \frac{T_{yy}}{T_{xx}}\right)\frac{\delta_x^s}{\delta_x}\right) \tag{5.19}$$

In appendix D all the formulae are derived to express the parameters of these equations in terms of average attenuation due to rain on the propagation path.

Figure 5.5 to 5.6 and E.1 to E.6 show the results of the calculations for the first two situations (system I). Figure 5.5 and 5.6 show the maximum error bounds in XPD and DPH for beacon B2 as a function of the average rain attenuation with (smaller error bounds) and without vector cancellation. Cancellation improves crosspolar data quality significantly. The maximum error with cancellation is quite constant for a large attenuation range. Without cancellation the atmospheric depolarization will increase with attenuation so the relative error decreases. With vector cancellation, the error in the XPD is smaller than ± 1 dB and the error in DPH is smaller than $\pm 6°$.

All the graphs show that the error bounds are not symmetric around the x-axis, due to the unbalance in the satellite or groundstation. Unbalance in the system gives the errors a vertical offset. Comparison of the results should be made considering:
-distance between error bounds (mainly related to system depolarization)
-error offset (related to system unbalance)
Note that the sign of the unbalance is arbitrary in practice, so the vertical shift can be positive or negative. To compare the total performance of the methods, the error bound with the largest distance to the x-axis should be evaluated.
Comparing the results of all the vertical polarized beacons shows that errors in uncancelled situation increase with frequency, but that errors with vector cancellation are almost independent of the frequency. For the horizontal polarization the maximum errors are smaller than for the vertical polarization because attenuation and phase-shift of the vertical polarization are smaller than attenuation and phase-shift of the horizontal polarization.

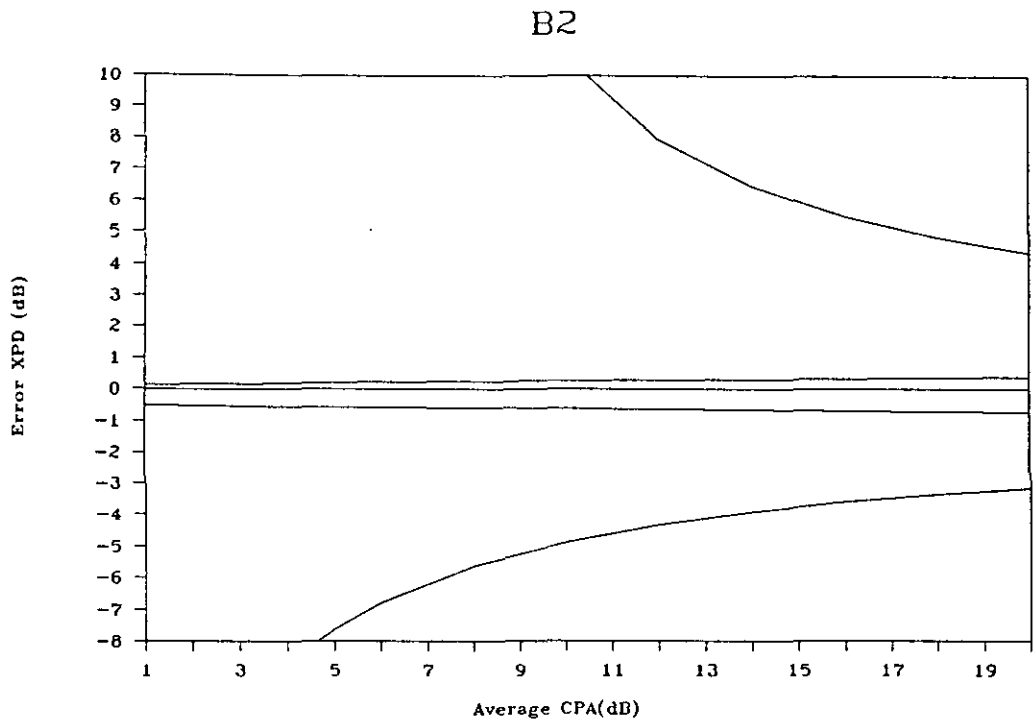

Figure 5.5: Error in XPD with and without cancellation (B2)

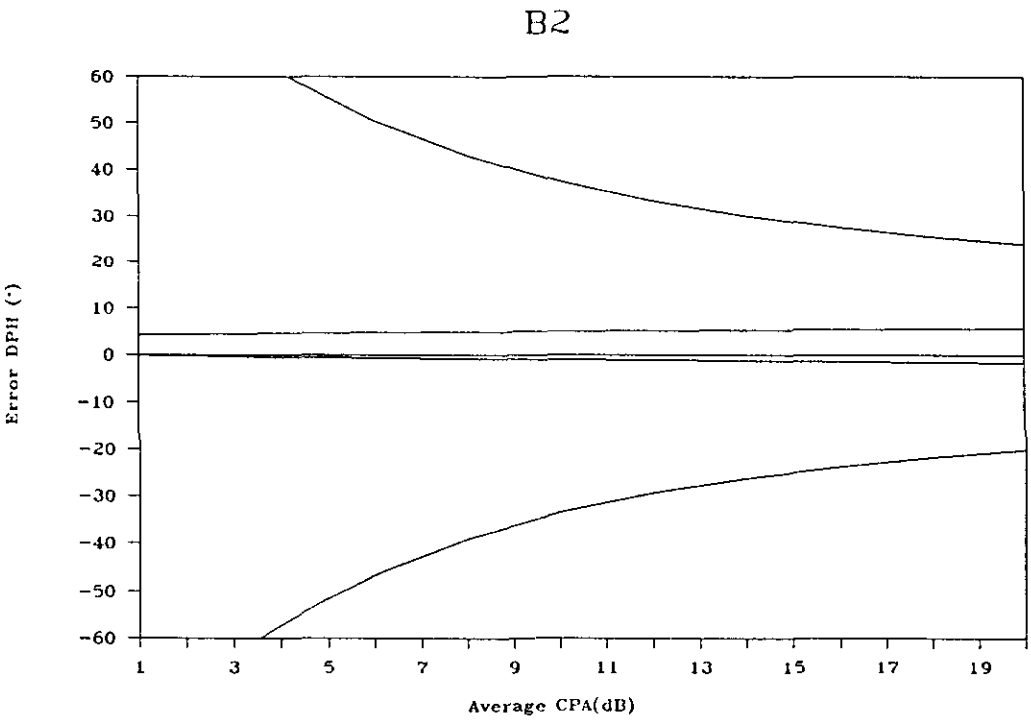

Figure 5.6: Error in DPH with and without cancellation (B2)

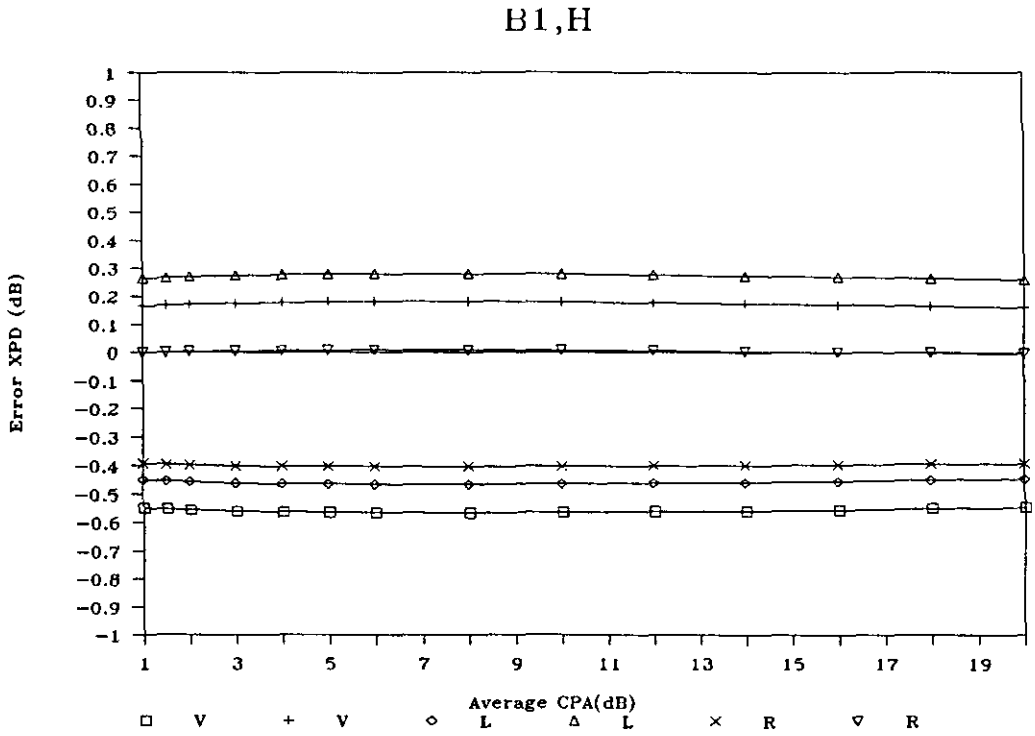

Figure 5.7: Error in XPD with various cancellation methods (B1,H)

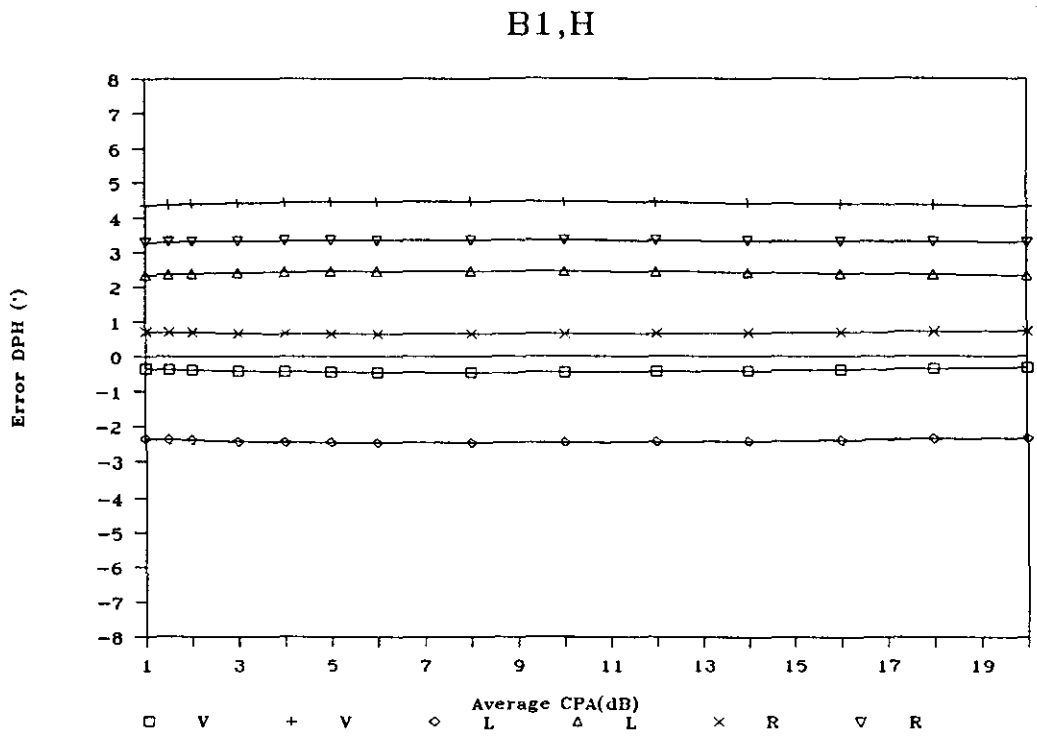

Figure 5.8: Error in DPH with various cancellation methods (B1,H)

Figure 5.7 and 5.8 show the error bounds of the various cancellation methods for beacon B1 (B1 horizontal polarization). Right cancellation gives a smaller error bound in the XPD (R) than left cancellation (L) or vector cancellation (V), because the depolarization of the satellite is worse than

that of the groundstation. The error in DPH is smaller for left cancellation due to the sensitivity of right cancellation to the phase unbalance in the groundstation. In appendix E the results are given for the vertical polarization. It is not obvious what method gives the best performance for system I, because system depolarization requires satellite correction, but unbalance requires groundstation correction. The user has to choose for better XPD (right cancellation) or better DPH (left cancellation) performance. Matrix cancellation is better than vector cancellation for XPD and DPH.

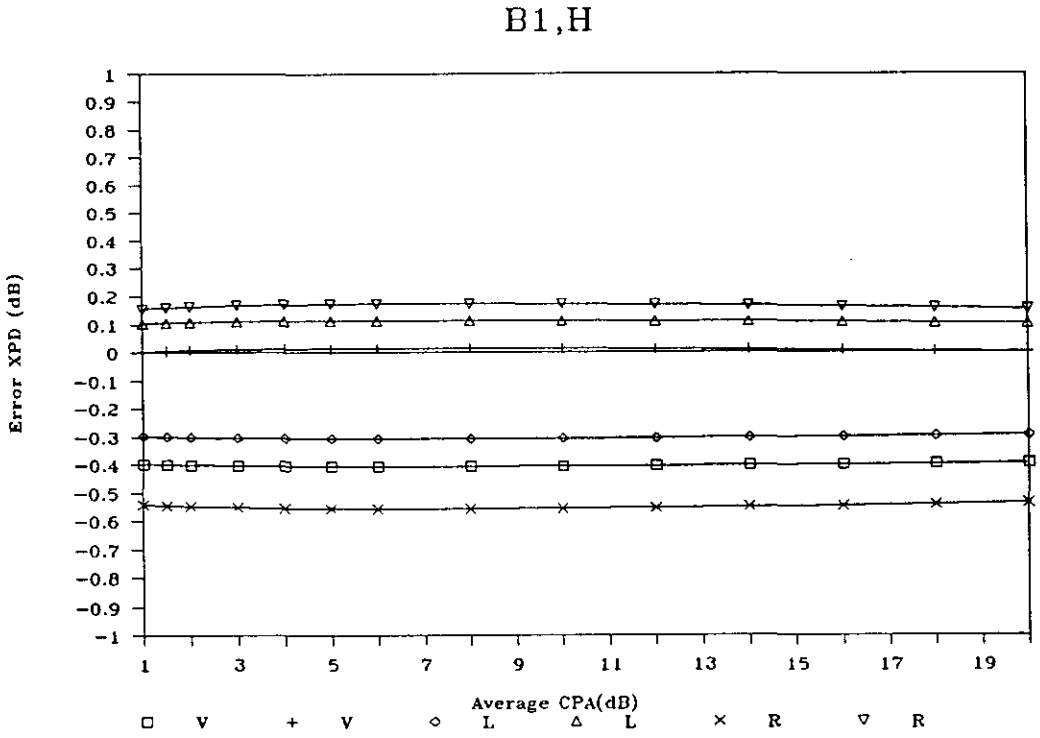

Figure 5.9: Error in XPD for various cancellation methods (B1,X system II).

Figure 5.9 and 5.10 show the error bounds for various cancellation methods for beacon B1 (horizontal polarization) for system II. For system II, left matrix cancellation shows better performance than the other methods for XPD and DPH. Unbalance and depolarization of the groundstation are worse than of the satellite, so complete groundstation correction (left cancellation) will give the best performance.

Comparing system I and II shows, that better performance may be achieved for system II. In system II, unbalance and depolarization of the groundstation is worse than that of the satellite, so left cancellation is optimal. However in system I, groundstation unbalance is worse than that of the satellite, but satellite depolarization is worse than that of the groundstation, so all methods are sub-optimal and results of the comparison depend on the values of unbalance and depolarization. Vector cancellation is both sensitive to groundstation unbalance and satellite depolarization, so this will be the worst cancellation method for system I. All methods show the same dependence of the error on the satellite or groundstation depolarization. Figure 5.11 shows the error bound of XPD as a function of the system depolarization by the groundstation or satellite for EUT conditions. This figure gives an indication of the maximum system depolarization to achieve a certain accuracy. For an accuracy of ±1 dB in XPD, the system XPD has to be better than 30 dB.

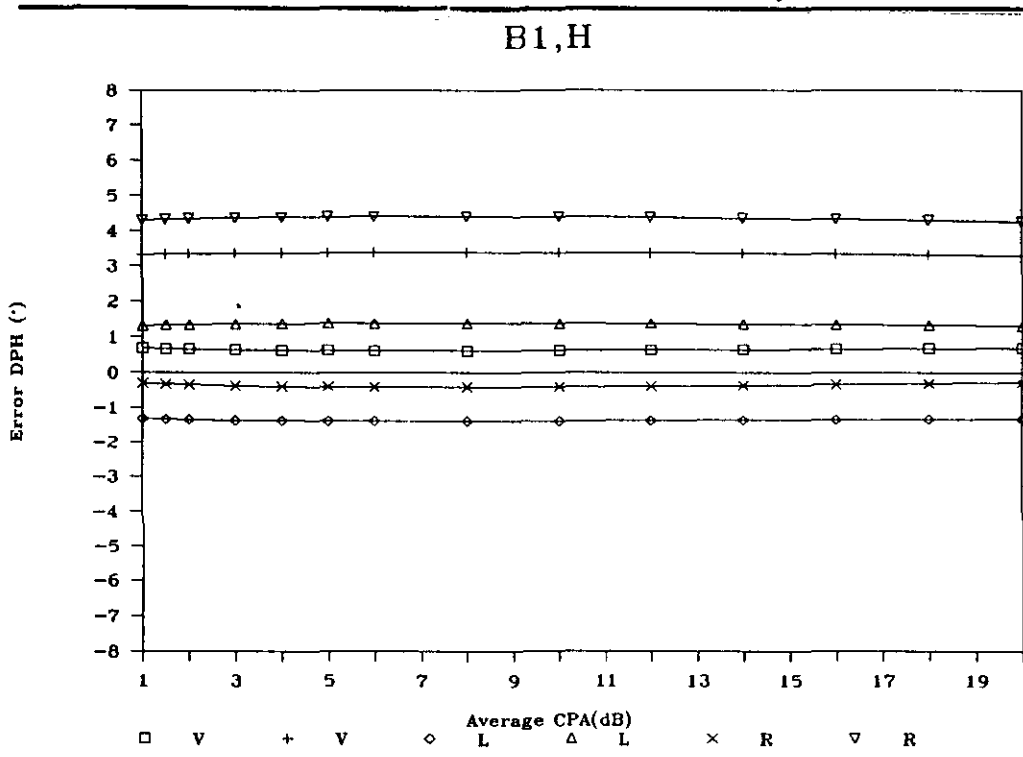

Figure 5.10: Error in DPH for various cancellation methods (B1,X system II).

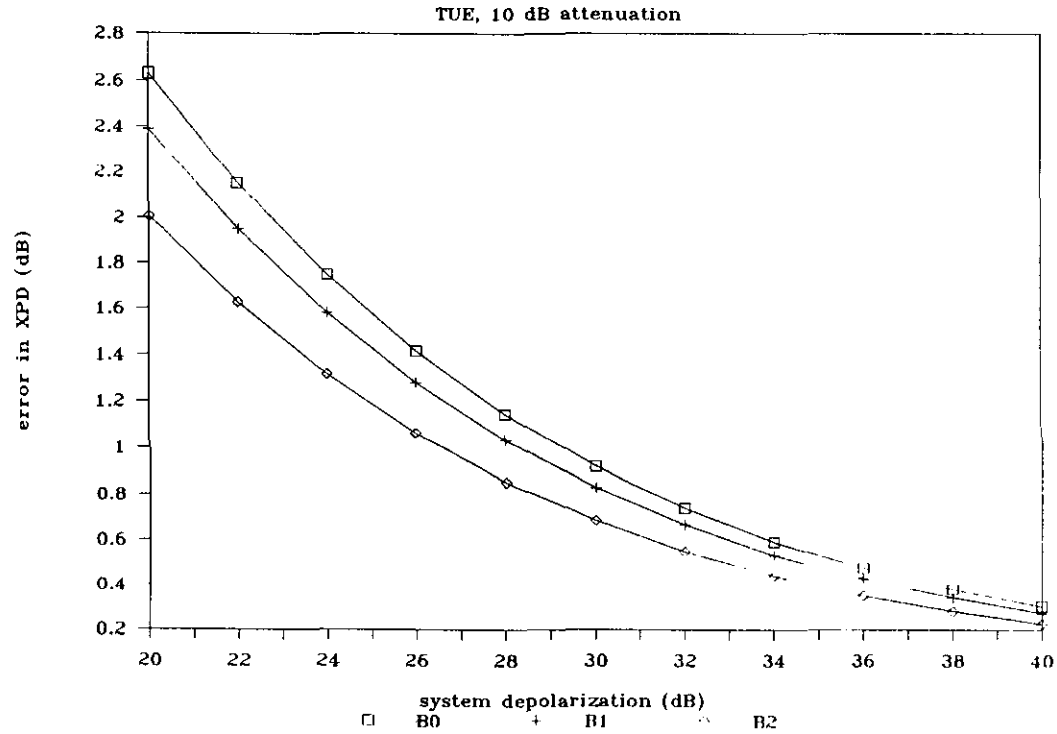

Figure 5.11: Error in XPD as a function of system depolarization with cancellation.

• Summary

The crosspolar cancellation methods have all different characteristics:

- Vector cancellation is sensitive to satellite depolarization and groundstation unbalance.
- Left matrix cancellation is sensitive to satellite depolarization and satellite unbalance.
- Right matrix cancellation is sensitive to groundstation depolarization and groundstation unbalance.

The unbalance in transmitter and receiver channels gives offset errors in XPD and DPH. In practice the best method can be chosen, depending on the depolarization and unbalance specifications of the satellite and groundstation.

For the OLYMPUS beacon B1, satellite XPD is greater than 43 dB. Groundstation XPD will be about 40 dB. The unbalance of the satellite is smaller than of the groundstation, so left cancellation seems to be the best method to choose. Data of the XPD and DPH will have a system error smaller than 0.3 dB and 1.5° respectively.

5.3 Accuracy of templates

For evaluating the accuracy of data in practice, the uncertainties in the templates for bias removal have to be considered. A template is typically a reference pattern for a whole clear-sky day. Therefore the uncertainty in the template prediction may be determined by deriving the standard deviation of raw template points for several days. Assuming this uncertainty is equal to the uncertainty in predicting the template for that day, it is possible to derive uncertainties in the propagation parameters due to the template prediction, providing objective means to evaluate bias removal.

• Copolar templates

The template for attenuation is the clear-sky copolar level. The uncertainty in the predicted template will be due to the uncertainty of the clear-sky attenuation and the uncertainty in the received signal level due to unpredictable errors.

$$\Delta R_t = \Delta S + \Delta A_{cs} \tag{5.20}$$

The accuracy of the clear-sky attenuation depends on the radiometer procedure used. Here radiometer frequencies are assumed to be close to the beacon frequencies. The uncertainty of the attenuation at the radiometer frequency is smaller than 0.1 dB during clear-sky conditions [11]. Table 5.3 gives the expected maximum uncertainties (for 99% of the time) of the clear-sky beacon attenuation for the various radiometer methods, derived from Ortgies [19].

Typical clear-sky attenuation ranges from 0.2 dB (at 12 GHz), 0.5 dB (at 20 GHz) up to 0.6 dB (at 30 GHz) without clouds. Radiometer measurements at 20 or 30 GHz seem to be desirable to get enough accuracy in the radiometer procedure for all beacon frequencies. The uncertainty in ΔS is smaller than 0.2 dB (Table 3.6), because some uncertainties are removed by the template extraction procedure.

• Crosspolar templates

In crosspolar measurements different cancellation methods use different templates:

Table 5.3: Uncertainties in attenuation at the beacon frequency

	Radiometer measurements				
beacon	Humidity detector	20 GHz	30 GHz	20, 30 GHz	12, 20 and 30 GHz
B0	0.20	0.20	0.15	0.1	< 0.1
B1	0.50	< 0.1	0.20	< 0.1	< 0.1
B2	1.0	0.50	< 0.1	< 0.1	< 0.1

- vector cancellation with a template crosspolar phasor
- matrix cancellation with a template matrix

The corrected phasor is given by:

$$\delta_c = \delta + \Delta\delta_c + \Delta\delta_u + \Delta\delta_t \tag{5.21}$$

where δ is the atmospheric crosspolar phasor. The error in XPD due to template errors is given by:

$$\Delta XPD = -20\log\left|\frac{\delta+\Delta\delta_t}{\delta}\right| = 20\log\left|1-\frac{\Delta\delta_t}{\delta_c}\right| \quad (dB) \tag{5.22}$$

The error in DPH due to template errors is given by:

$$\Delta DPH = Phase\left(\frac{\delta+\Delta\delta_t}{\delta}\right) = -Phase\left(1-\frac{\Delta\delta_t}{\delta_c}\right) \quad (°) \tag{5.23}$$

$\Delta\delta_t/\delta$ is the ratio of the absolute template phasor error and the obtained phasor after bias removal. This ratio can easily be calculated in practice. To determine the uncertainty in the crosspolar phasor due to template prediction, formulae will be derived to relate this ratio to the template uncertainties.

Template crosspolar phasor:

The template for vector cancellation is a crosspolar phasor and the bias removal is a vector subtraction in the complex plane. The uncertainty in the crosspolar phasor is thus directly related to the template uncertainty. Vector cancellation can be applied in two ways: fixed (or static) and adaptive cancellation. For fixed cancellation (usually realized in hardware), the template phasor is fixed in the complex plane. For adaptive cancellation (realized in software), the template phasor changes according to the diurnal behaviour of the clear-sky phasor. When the diurnal behaviour is not recognizable, the template phasor of adaptive cancellation will almost be fixed, due to the averaging process of template extraction, resulting in the same performance as fixed cancellation. In general adaptive cancellation is expected to be better than fixed cancellation.

Template matrix:
In appendix C the procedure is given for matrix cancellation. The crosspolar phasor is determined from the corrected transmission matrix. When uncertainties in the template matrix parameters are uncorrelated, table 5.4 gives the relation of the matrix template uncertainty and the uncertainty in the crosspolar phasor for the x-polarization. The uncertainty for the y-polarization can be found by exchanging indices.

Table 5.4: Relation between crosspolar error ratio and template errors

	vector cancellation	left matrix cancellation	right matrix cancellation
$\Delta\delta_t/\delta_c$	$\Delta\delta_t/\delta_c$	$\Delta U_{xx0}/U_{xx0} + \Delta U_{yy0}/U_{yy0} + \Delta U_{yx0}/U_{yx0}$	$\Delta U_{yy0}/U_{yy0} + \Delta U_{yx0}/U_{yx0}$

In practice table 5.4 and (5.22), (5.23) can be used to evaluate the accuracy in the obtained XPD and DPH due to template prediction.

In the next paragraph, the uncertainty of templates will be determined from clear-sky measurements.

5.4 Measurements

To make an estimate of the quality of the templates in practice, measurements of the EUT groundstation are used. At EUT beacon data at ref.B is represented by copolar level (CPL), crosspolar discrimination (XPD) and cross-copolar phase difference (DPH). An operational preprocessing system is not yet available, so template extraction and bias removal are performed with the help of a spreadsheet. Two raw templates of successive clear-sky days are used to build average templates. A template point is derived every 15 minutes by averaging over 60 seconds. The uncertainty in the templates is determined by taking the average for 24 hours (rms value) of the standard deviation of the raw template points.

- copolar measurements

Two raw templates for beacon levels of B0 and B1 are given in appendix E. Figure 5.12 shows the two raw templates for beacon B2. The uncertainties in the template seem to be mainly due to the tracking process. The uncertainties in the average templates and the expected uncertainties in attenuation (for typical attenuation values) after correction with the templates are given in table 5.5. The templates are not corrected for clear-sky attenuation, so they have an absolute error of about 0.2 dB (at 12 GHz) up to 0.6 dB at 30 GHz (no clouds).

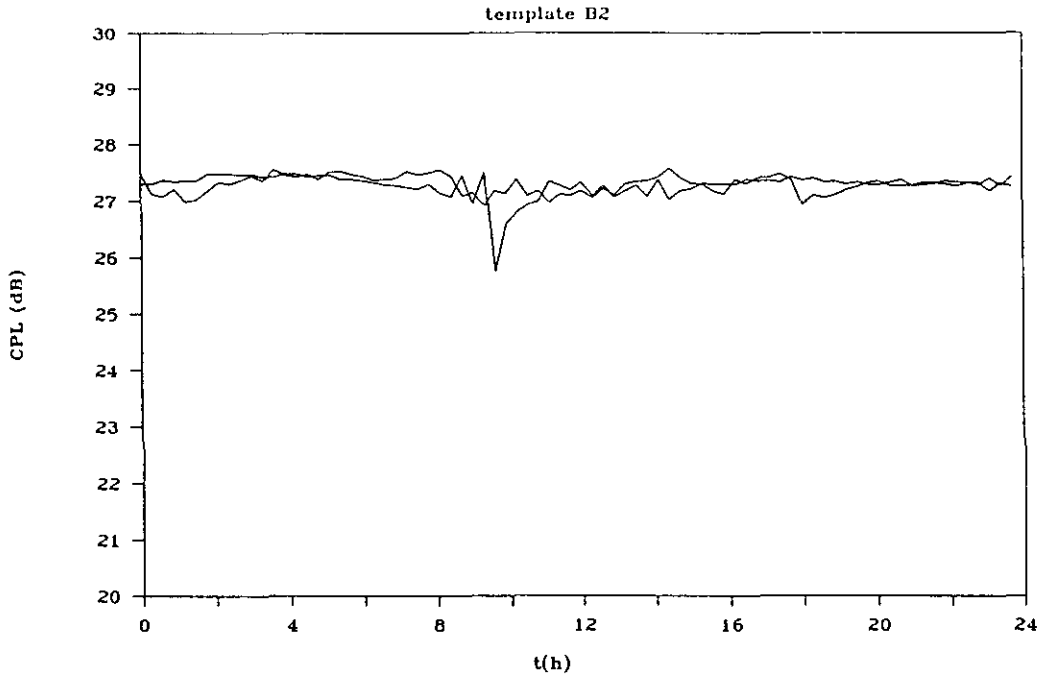

Figure 5.12: Copolar level templates for B2 (6/13/90 - 6/14/90)

Table 5.5: Uncertainty in attenuation after bias removal

uncertainty	B0	B1,H	B1,V	B2
template	0.034	0.070	0.073	0.13
system	0.20	0.22	0.22	0.23
total	0.20	0.23	0.23	0.26

Results:

The uncertainty in attenuation measurements after bias removal is mainly determined by unpredictable errors. The accuracy of attenuation measurements is improved by the bias removal procedure for all beacons. Template uncertainties seem to be smaller than predictable system variations (Table 3.6), so bias removal is effective. However template uncertainties will increase during cloudy and humid days if no radiometer measurements are used.

- crosspolar measurements

Raw templates of two successive days of the crosspolar phasor are given in appendix E for the B0. The B1 beacon receiver shows problems in crosspolar measurements, so it is not sensible to build a template matrix yet. Figure 5.13 and 5.14 show the raw templates of two days for beacon B2. A diurnal pattern is recognizable so adaptive cancellation can be used to obtain better crosspolar performance. It seems that small variations between successive template points are due to the tracking process. The template uncertainty is derived for fixed and adaptive cancellation (both in software). The fixed template phasor is chosen to minimize errors in the XPD during clear-

sky conditions. Figure 5.15 shows the XPD before and after fixed cancellation for a clear-sky day. For fixed cancellation some periods of the day give better performance than other.

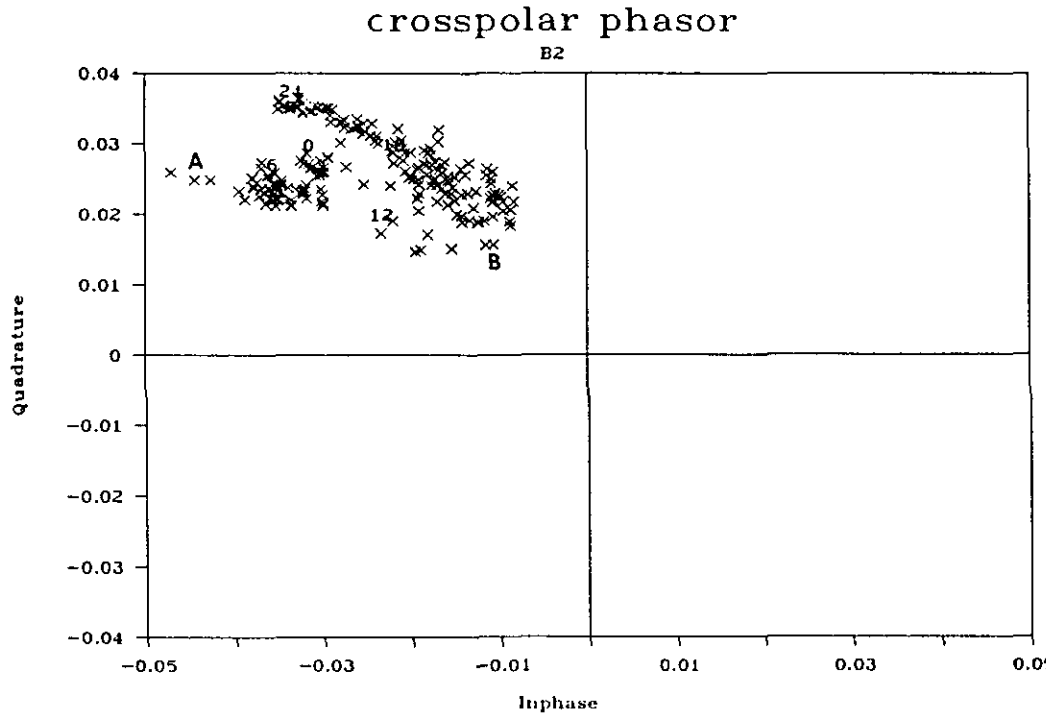

Figure 5.13: Raw template of crosspolar phasor (06/13/90)

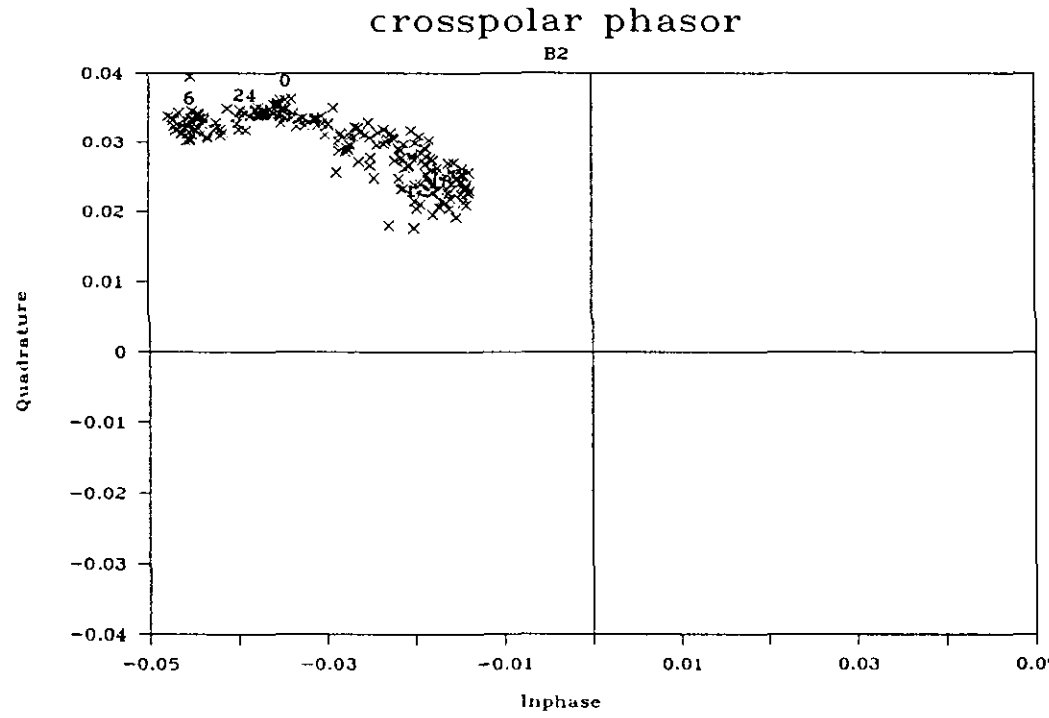

Figure 5.14: Raw template of crosspolar phasor (06/14/90)

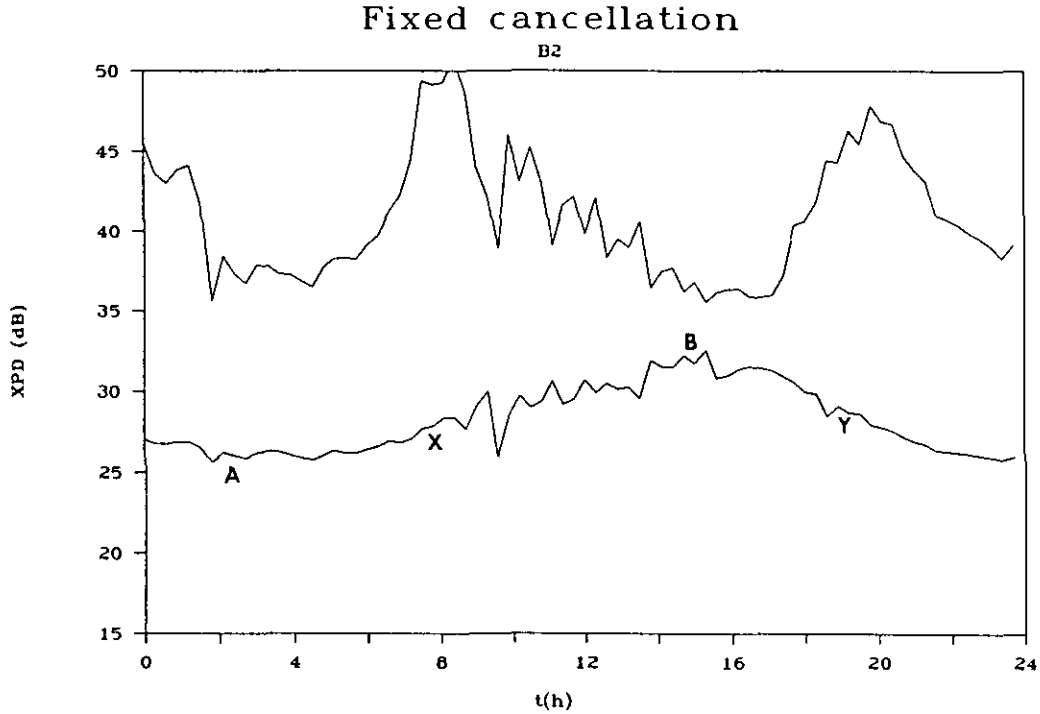

Figure 5.15: XPD improvement with fixed cancellation (06/13/90)

Table 5.6 gives the uncertainty in the average templates for inphase and quadrature components. These uncertainties are used to estimate the error bounds in the XPD and DPH due to template prediction as a function of the obtained XPD after correction (equations (5.22) and (5.23)). Figure 5.16 and 5.17 show that adaptive cancellation will give better performance than fixed cancellation. For little depolarization the maximum errors due to template uncertainty are greater than errors due to limitations of bias removal but smaller than errors due to predictable system influence (fig 5.5 and 5.6). Thus cancellation gives better performance here. For little depolarization overall accuracy seems to be limited by the template uncertainty and unpredictable errors. For severe depolarization, the accuracy is mainly limited by unpredictable errors. Table 5.7 gives the expected total uncertainty in depolarization measurements (adaptive cancellation) for B0 and B2 up to crosspolar discrimination measurements of 35 dB and 40 dB. Note that the uncertainty in XPD and DPH due to tracking errors has not yet been accounted for.

Table 5.6: Absolute uncertainty in crosspolar phasor templates

	Adaptive cancellation		Fixed cancellation	
δ	Inphase	Quadrature	Inphase	Quadrature
B0	0.0013	0.0013	0.0022	0.0023
B2	0.0020	0.0024	0.0044	0.0045

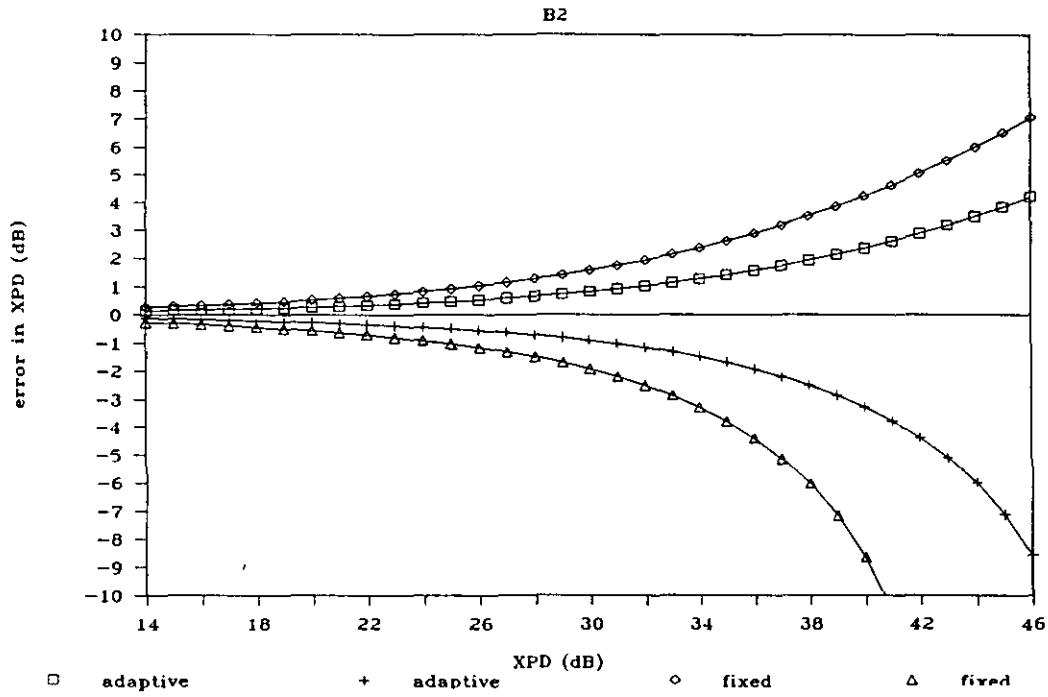

Figure 5.16: Error in XPD due to template uncertainty

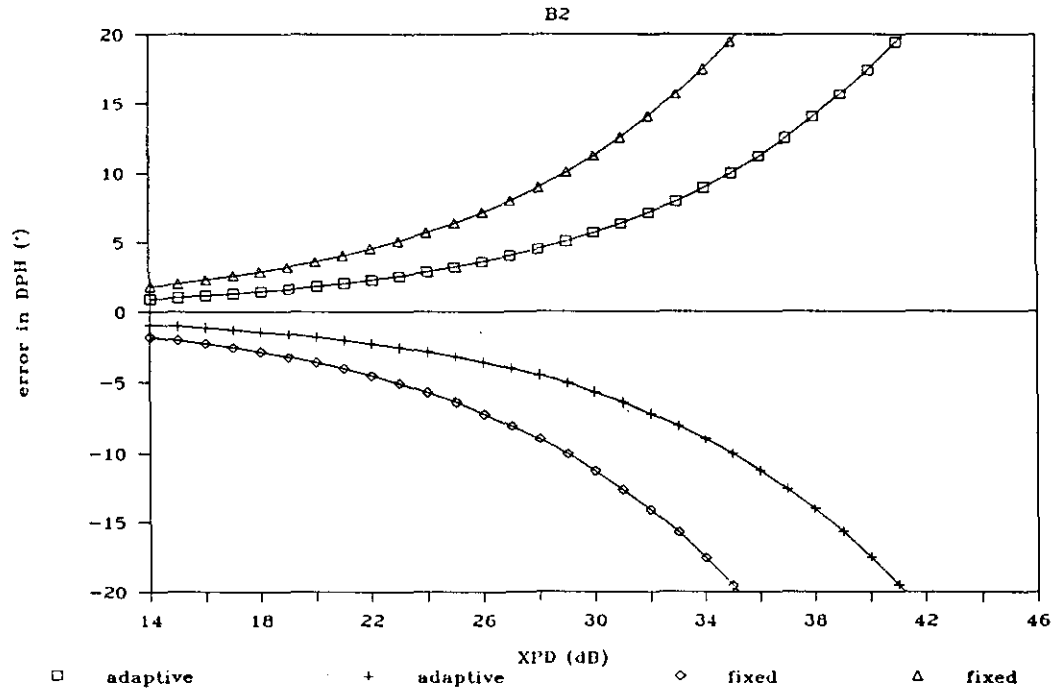

Figure 5.17: Error in DPH due to template uncertainty

Table 5.7: Maximum uncertainty of depolarization measurements for a certain measurement range

Maximum XPD measurement range	B0 ΔXPD (dB)	B2 ΔXPD (dB)	B0 ΔDPH (°)	B2 ΔDPH (°)
40 dB	2.0	3.0	10	17
35 dB	1.0	1.3	6	8

• Problems in crosspolar measurements.

Figure 5.17 shows the crosspolar phasor of the B1 beacon (horizontal polarization). At EUT groundstation XPD and differential phase values are produced in hardware. Phase measurements are not stable during clear-sky and the changes in XPD and DPH seem to be correlated. In the receiving system of the B1 beacon, the crosspolar level (XPL) seems to be limited to -38 dB below clear-sky copolar level. When the crosspolar level reaches this limit the phase will become arbitrary. System depolarization during clear-sky is expected to be higher than this limit, so during clear-sky, the XPD will almost always be limited. Consequently the measured XPD and DPH do not give any information on the crosspolar system behaviour. The same problem arises sometimes when hardware cancellation is used for the B0 or B2 crosspolar measurements. The maximum range of the XPD measurement for B0 and B2 is 45 dB. When this level is reached during clear-sky, rapid phase changes occur and information about the crosspolar system behaviour is lost. For these cases template extraction does not produce any useful templates. As B1 crosspolar measurements experience this problem for most of the time, no valid vector or matrix templates can be derived from the measurements at the time and cancellation (vector or matrix) makes no sense.

In practice it should be recommended to keep the XPD and XPL within the limits of the hardware system also during clear-sky. If hardware cancellation is used, this should be recognized. Only then adaptive cancellation (in software) can be used to achieve more accuracy. In general it would be better to produce inphase and quadrature components of crosspolar signals in hardware. These components are more independent in hardware than amplitude and phase.

• Crosspolar event measurements

Figure 5.18 shows the crosspolar phasor for the B2 beacon of a day with events. Comparing the phasor during the clear-sky period with the phasor of the other days shows that the diurnal pattern has shifted somewhat during a week time. Using the raw template of the day with interpolation during the event, it is possible perform simple adaptive cancellation for the event. Figures 5.19 and 5.20 show the XPD before and after cancellation during the event. The improvement is significant. During clear-sky the XPD goes up to 60 dB. In Appendix E, graphs are shown for the whole day.

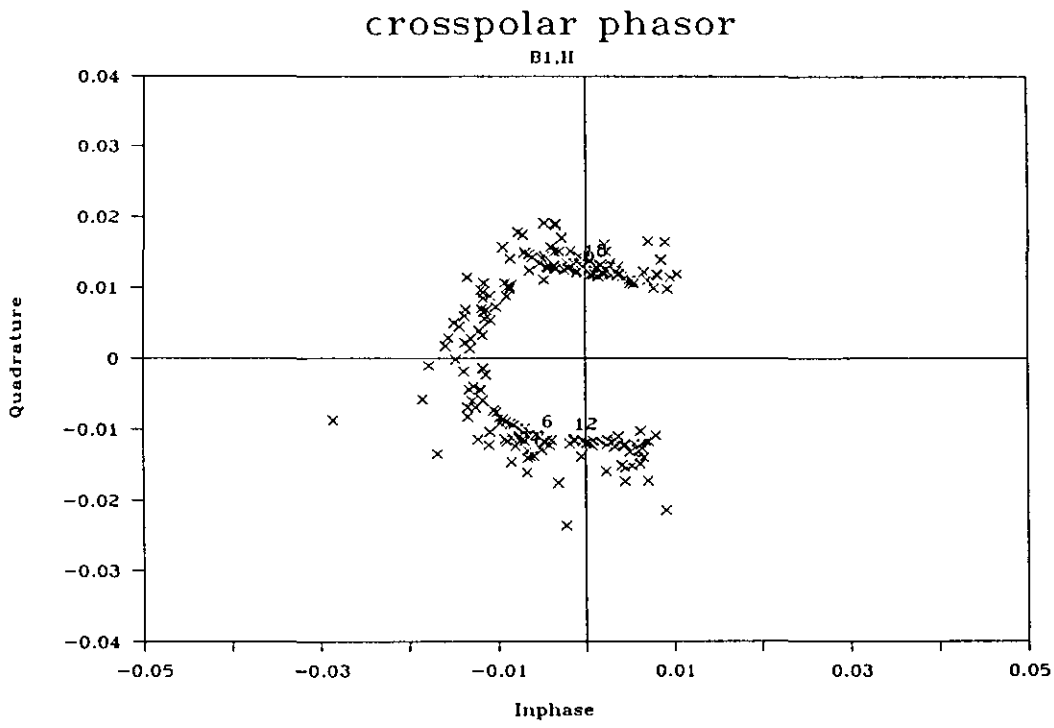

Figure 5.18: Crosspolar phasor of B1 (horizontal polarization, 06/17/90)

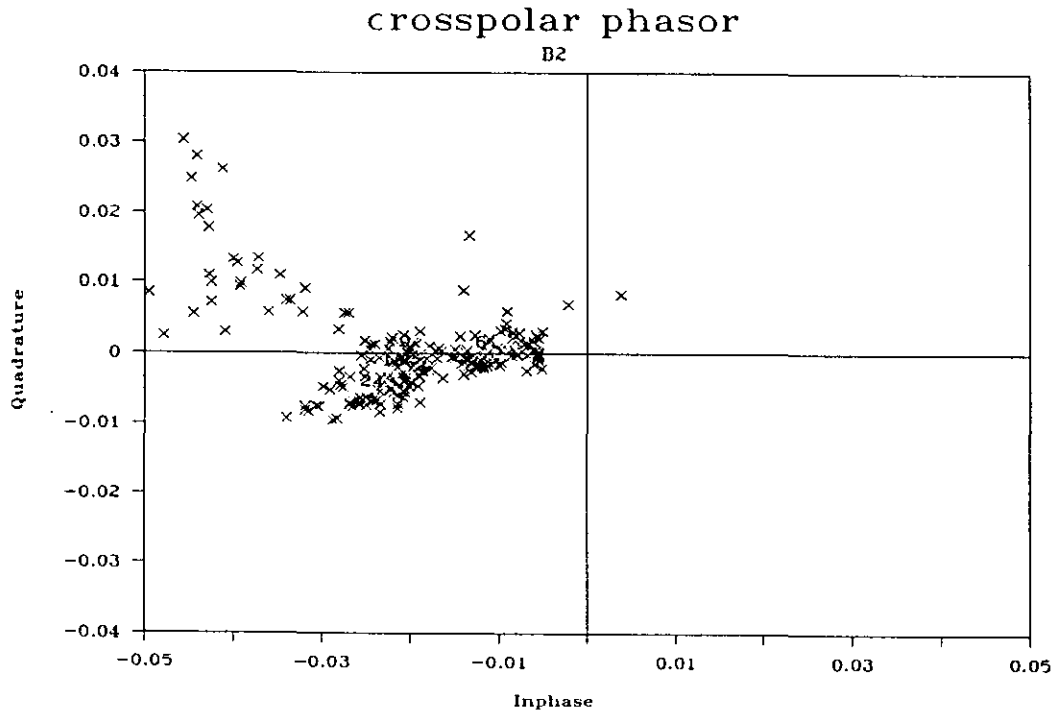

Figure 5.19: Crosspolar phasor of B2 (06/23/90)

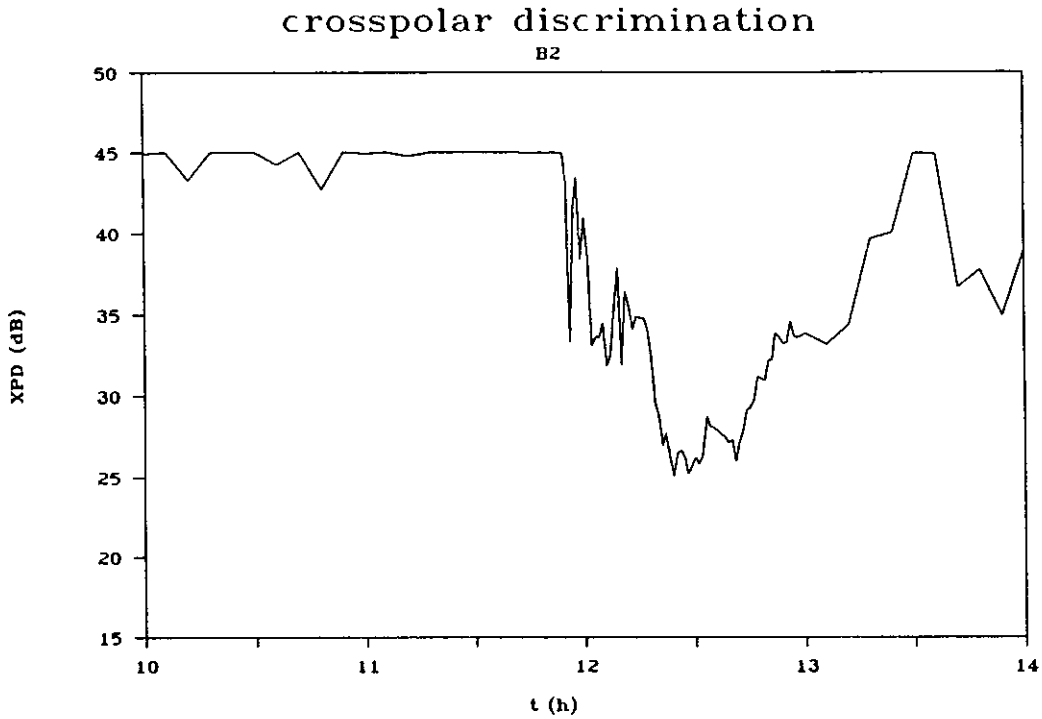

Figure 5.20: XPD during event (B2, 06/23/90)

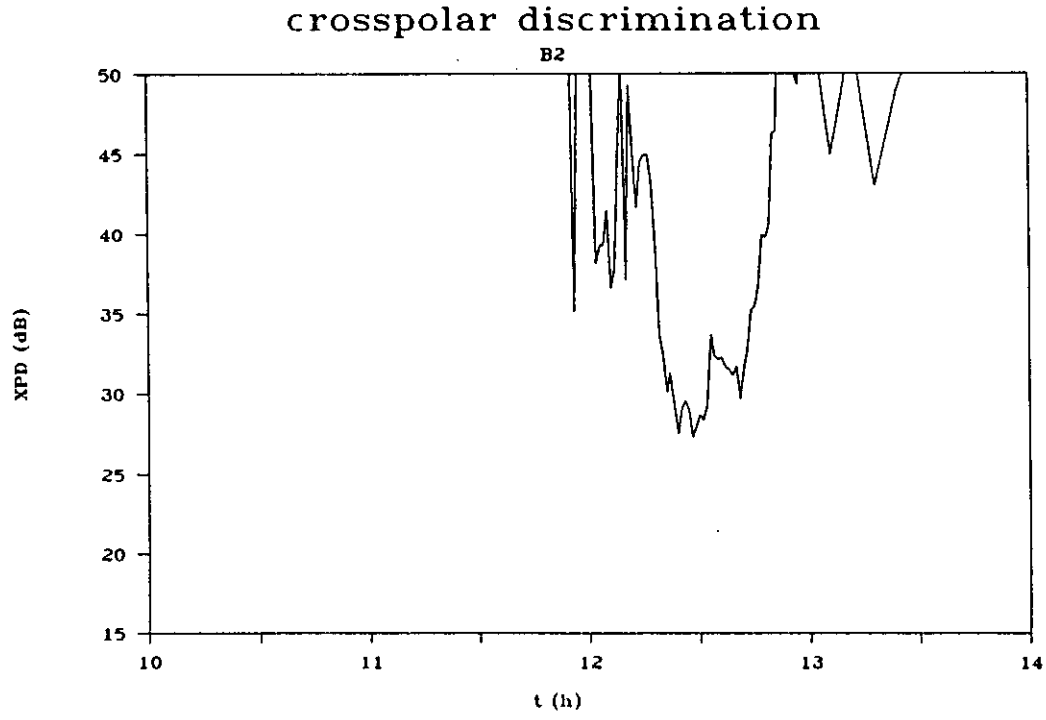

Figure 5.21: XPD during event with adaptive cancellation (B2, 06/23/90)

- Adjusting fixed cancellation in hardware.

If software cancellation is not available, it is recommended to use hardware cancellation. Fixed cancellation realized in hardware must be adjusted manually for optimal performance. Considering the diurnal behaviour of the crosspolar phasor, a procedure can be developed to adjust the fixed cancellation during clear-sky. Note that system depolarization changes somewhat from day to day and the settings should be adapted with regular intervals for good performance.

Consider the crosspolar phasor to have a kind of diurnal behaviour shown in figure 5.13. The XPD is related to the distance to the origin of the complex plane. To maximize the XPD during a clear-sky day, the diurnal pattern has to be shifted to the origin, so that all template points lie within a circle with minimum diameter. Thus a point has to be found in the complex plane with minimum distance to all the template points. In this case this is the mean of the points A and B. For this adjustment, figure 5.15 shows the resulting XPD diurnal pattern.

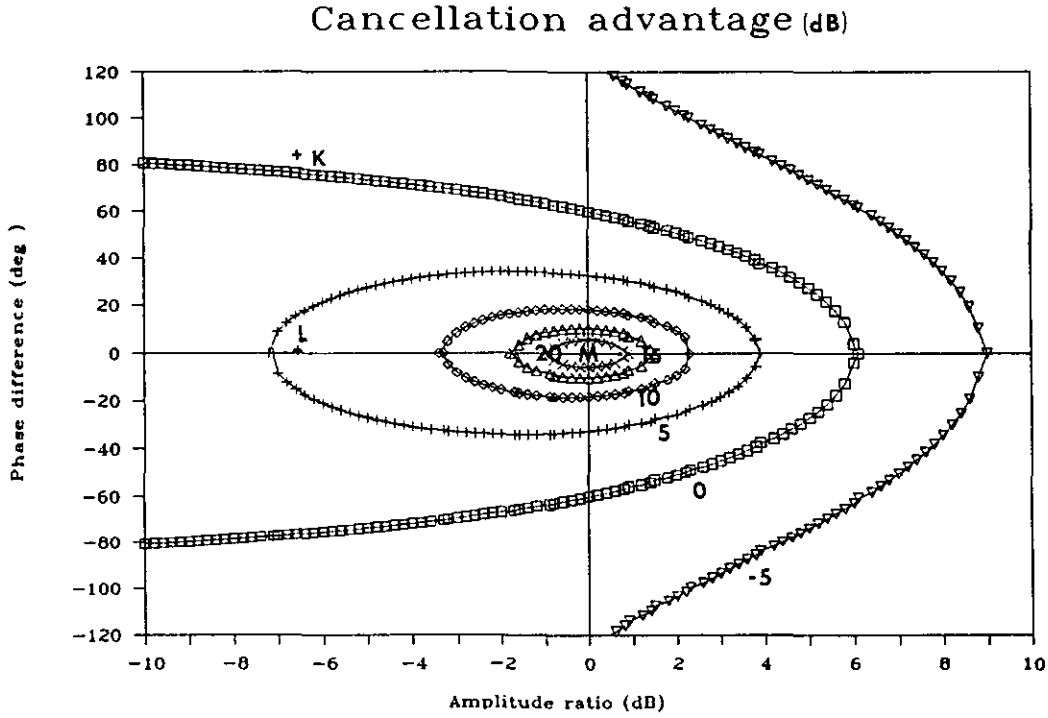

Figure 5.22: Adjustment of hardware cancellation

In practice fixed cancellation is set-up by adjusting the gain and phase-shift and optimizing the measured XPD. The adjustment can be done in several steps, as shown in figure 5.22 (K -> M). This figure shows the loci for equal cancellation advantage during clear-sky conditions as a function of the amplitude ratio and differential phase-shift of the cancellation signal and the system signal. If amplitude and phase are equal, cancellation is optimal for this time point and the XPD will be infinity (R). The diurnal pattern of the system XPD causes the working point to wander in the graph. If the amplitude of the cancellation signal is too big and the time-point for adjusting is chosen unfavourably, the XPD shows worse behaviour at some time during the day with cancellation than without cancellation. The best procedure would be to adjust the cancellation at time-points A and B to a maximum XPD (fig. 5.15) and take the mean of the adjustments. A and

B are usually also the extrema in the XPD diagram, so it is easy to detect the time-points for adjustment. For the optimal adjustment, the XPD will give two equal minima during a day.

Usually phase and gain can not be adjusted independently. Then the best procedure will be to adjust the cancellation system at time-points X or Y (between the minimum and maximum of the uncancelled XPD-graph, fig. 5.15). At one of these time points the XPD should be maximized by adjusting amplitude and phase. When this goal is reached, the gain should be somewhat decreased to obtain higher minima of the diurnal pattern.

5.5 Preprocessing conclusions

Preprocessing is performed to remove the predictable influence of the measurement system in beacon measurements. This can improve data quality considerably both for copolar and crosspolar measurements, if useful templates can be derived. The uncertainty in the obtained data is mainly limited by unpredictable errors and the quality of templates. Bias removal should only be performed if errors due to the template uncertainty are smaller than the predictable system errors. Thus in practice template quality should be evaluated together with performing preprocessing. A method has been given to perform this evaluation.

In copolar measurements, radiometer measurements in the 20 to 30 GHz range are required to determine the clear-sky reference levels for attenuation measurements. Using radiometer measurements atmospheric attenuation of beacon signals may be derived with an uncertainty of 0.2 dB. During clear-sky conditions the attenuation derived from radiometer measurements has better accuracy.

Cancellation of crosspolarization due to the groundstation or satellite is essential to obtain accurate crosspolar data. The various cancellation methods are evaluated for typical system conditions. Especially during little atmospheric depolarization, cancellation improvement is significant. The errors due to correction limitations in the XPD and DPH are smaller than ±1.0 dB and ±6 degrees respectively. For the B1 beacon, matrix cancellation is compared with vector cancellation. Left matrix cancellation seems to give the best results for OLYMPUS. Measurements have been used to evaluate the template uncertainty for vector cancellation. This shows that, for little atmospheric depolarization, the accuracy in the obtained XPD and DPH depends mainly on the template uncertainty. With adaptive vector cancellation it seems feasible to obtain depolarization data (XPD and DPH) with an uncertainty of about 1.3 dB and 10° for XPD measurements up to 35 dB (B0 and B2). For OLYMPUS it was the goal to obtain XPD-data with an accuracy of ±1 dB up to a XPD of 35 dB. This seems feasible for EUT (B0 and B2) if adaptive cancellation is used. Presently it is not possible to make any valid templates for the B1 beacon.

To obtain a good estimate of the general quality of OLYMPUS data after preprocessing, data of several weeks has to be evaluated with an operational preprocessing system. Note that up to now equipment outage time and tracking problems have reduced the amount of useful data for this evaluation considerably.

Adaptive cancellation is better than fixed cancellation in general. A procedure has been given to adjust fixed cancellation for optimal performance. A combination of fixed cancellation (in hardware) and adaptive cancellation is not to be preferred at EUT as hardware cancellation limits the amount of useful data for software adaptive cancellation.

5.5 Some considerations for data analysis

The dual-polarized beacon measurements (B1) provide the opportunity to determine the complete transmission matrix of the propagation medium. Physical medium properties such as anisotropy and canting angle can be derived from the transmission matrix (see paragraph 2.5). These properties are determined by the crosspolar phasors of both polarizations and differential attenuation and phase-shift between the polarizations.

The uncertainty in obtained parameters of the transmission matrix after preprocessing may be obtained by applying the method given in the previous paragraphs. For evaluation of the accuracy of the obtained anisotropy and canting angle, the medium can be assumed to be homogeneous in practical situations. In that case the following formulae for anisotropy and inclination angle may be used to evaluate the sensitivity of data variations on the obtained physical parameters (use the assumption $t_{ll} = t_{rr}$ in appendix A).

$$\Delta = 2\tanh^{-1}\sqrt{\frac{(T_{xx}-T_{yy})^2 + (T_{xy}+T_{yx})^2}{(T_{xx}+T_{yy})^2 + (T_{xy}-T_{yx})^2}} \tag{5.24}$$

$$\phi = \frac{j}{4}\ln\left(\frac{(T_{xx}-T_{yy}) - j(T_{xy}+T_{yx})}{(T_{xx}-T_{yy}) + j(T_{xy}+T_{yx})}\right) \tag{5.25}$$

Paraboni [9] observed that the sensitivity of data variations increased for increasing XPD values. Van de Kamp [7] suggested therefore to keep a certain threshold of the XPD level, beyond which data should be excluded from analysis.

In the previous paragraphs it was shown that for considerable atmospheric depolarization, the accuracy of data after preprocessing is mainly limited by unpredictable errors such as thermal noise. If one is only interested in mean values of canting angle and anisotropy corresponding to certain conditions (rain rate, wind velocity, attenuation etc.), uncertainties are much smaller if averaging is applied to a data base of several years.

Only recently, the complete measurements of the B1 beacon are available. Event data of B1 still has to be evaluated for accuracy to obtain an estimate of the uncertainties in the transmission matrix and physical medium parameters.

6 CONCLUSIONS AND RECOMMENDATIONS

6.1 Conclusions

Obtaining accurate propagation data is complicated by the influence of the measurement system. The EUT groundstation receives two single-polarized beacons and one dual-polarized beacon of the OLYMPUS satellite. Errors in the measurements are caused by the satellite and groundstation. These can be divided into unpredictable and predictable errors. Unpredictable errors, such as noise are inevitable, but predictable errors may be removed from the data. Clear-sky measurements can provide information about the system behaviour (biases) to predict the influence (templates) during events. Removal of biases is performed by correcting measurements with a template.

Bias removal and template extraction are part of a preprocessing system. EUT measurements have been evaluated to determine the accuracy after preprocessing in practice.

For copolar measurements a reference level has to be determined. Using radiometer measurements in the 20-30 GHz range it seems feasible to obtain attenuation data with an uncertainty of 0.2 dB. The uncertainty is mainly due to unpredictable errors.

To obtain crosspolar information of the atmosphere it is essential to remove system influence, because the amount of system depolarization is comparable to atmospheric depolarization. Vector or matrix cancellation (only for dual polarized beacons) may be used to limit the predictable system influence. Vector cancellation can be realized in hard- and software. Adaptive vector cancellation (realized in software) shows better accuracy results than fixed vector cancellation (usually realized in hardware). For little atmospheric depolarization, the uncertainty in crosspolar data is mainly limited by the uncertainty of the template. Using adaptive vector cancellation for 12.5 and 30 GHz measurements, it seems feasible to obtain crosspolar data (XPD and DPH) with an uncertainty smaller than 1.3 dB and 10° for XPD measurements up to 35 dB. Crosspolar bias removal for the 20 GHz beacon is not sensible at EUT as system depolarization is smaller than the range of the receiver hardware.

A method has been given to determine the uncertainty of propagation data in practice.

6.2 Recommendations

The following points are recommended to consider in order to obtain accurate propagation data at the EUT groundstation:

- Use radiometer measurements to derive the copolar reference level for attenuation measurements.
- Use adaptive vector cancellation in software on 12.5 and 30 GHz crosspolar measurements to limit system influence on crosspolar data.

- Do not perform crosspolar bias removal for B1 beacon, because presently clears-sky measurements contain no useful system information for template extraction. The receiver hardware could be reviewed.
- Do not combine fixed cancellation (in hardware) with adaptive cancellation (in software) as hardware cancellation limits the amount of useful system information for template extraction.

To obtain a good estimation of typical data quality for Olympus, preprocessed data of several weeks has to be evaluated. This requires an operational preprocessing package. When this package is available, the following points are recommended to investigate:
- Evaluate the template procedure. Determine the distribution of the template uncertainties over a day as a function of the number of days for averaging and the time period for interpolation.
- Evaluate the changes of the diurnal behaviour.
- Build the transmission matrix for the B1-measurements and derive physical medium parameters. Evaluate the accuracy in the transmission matrix and the physical parameters.
- Evaluate the uncertainty of and the difference between radiometer procedures using radiometer measurements.

LITERATURE

[1] ESA, OPEX Olympus Propagation Experiment, HANDBOOK FOR DATA PREPROCESSING, Part 1: Theory and basic information, Issue 1, Edited by A. Mawira, 1986, Noordwijk, OPEX-11.

[2] CCIR Report 719-2, ATTENUATION BY ATMOSPHERIC GASES, Recommendations and Reports of the CCIR, ITU, Vol.5, 1986.

[3] Slobin,S.D., MICROWAVE NOISE TEMPERATURE AND ATTENUATION OF CLOUDS: STATISTICS OF THESE EFFECTS AT VARIOUS SITES INN THE UNITED STATES, ALASKA, AND HAWAII, Rad.Sc. Vol.17 (1982), No.6, p.1443-1454.

[4] CCIR Report 721-2, ATTENUATION BY HYDROMETEORS IN PARTICULAR PRECIPITATION AND OTHER ATMOSPHERIC PARTICLES, Recommendations and Reports of the CCIR, ITU, Vol.5, 1986, p.199-214.

[5] Meulemans, P.A.C.M., SYSTEM CONSIDERATIONS FOR A RECEIVING STATION BUILT FOR PROPAGATION EXPERIMENTS WITH THE OLYMPUS SATELLITE, Graduation Report, Eindhoven University of Technology, Faculty of Electr. Eng., Communications division, 1986.

[6] CCIR Report 722-2, CROSS-POLARIZATION DUE TO THE ATMOSPHERE, Recommendations and Reports of the CCIR, ITU, Vol.5, 1986, p.219-230.

[7] Kamp, M.M.J.L. van, SOFTWARE SET-UP FOR DATAPROCESSING OF DEPOLARIZATION DUE TO RAIN AND ICE CRYSTALS IN THE OLYMPUS PROJECT, Graduation report, Eindhoven University of Technology, Faculty of Electr.Eng., Communications division, 1989.

[8] Howell, R.G., CROSSPOLAR PHASE VARIATION AT 20 & 30 GHZ ON SATELLITE-EARTH PATHS, El.letters, Vol.13 (1977), p.405-6.

[9] ESA, Olympus Propagation Experiment, REQUIREMENTS FOR DATA ANALYSIS, Issue 1, Edited by A. Paraboni, 1986, Noordwijk, OPEX-12.

[10] Ippolito, L.J., PROPAGATION EFFECTS HANDBOOK FOR SATELLITE SYSTEMS DESIGN, A summary of propagation impairments on 10 to 100 GHz Satellite links with techniques for systems design, Washington: NASA, 1989, Ref. Publ.1082(04).

[11] Gelissen, P.J.W., VERGELIJKING VAN BAKENMETINGEN VAN DE OLYMPUS SATELLIET MET RADIOMETER DATA, Graduation Report, Eindhoven University of Technology, Faculty of Electr. Eng., Communications division, 1989. (in Dutch)

[12] ESA, OPEX Olympus Propagation Experiment, HANDBOOK FOR BEACON RECEIVER DESIGN, Issue 1, Edited by S.K. Barton, 1985, Noordwijk, OPEX-10.

[13] ESA, OLYMPUS IN ORBIT TESTING FINAL REPORT, Prepared by the Earth Segment Section, April 1990, Noordwijk: ESA.

[14] Pocha, J.J., AN INTRODUCTION TO MISSION DESIGN FOR GEOSTATIONARY SATELLITES, 1987, Dordrecht: Reidel.

[15] Marincic, A.S., RADIATION PROPERTIES OF MICROWAVE REFLECTOR ANTENNAS COVERED WITH A WATER FILM, IEE Proc. Vol 125, 1978, p. 933-34.

[16] Effenberger, J.A. et al, EFFECTS OF RAIN ON A RADOME'S PERFORMANCE, Microw.J., 1986, No.5, p. 261-72.

[17] CCIR, HANDBOOK ON SATELLITE COMMUNICATIONS, (Fixed-satellite service), Geneva 1985, p.224-227.

[18] COST, DER EINFLUSS DER ATMOSPHÄRE AUF DIE AUSBREITUNG ELEKTROMAGNETISCHER WELLEN AUF SATELLITE-ERDE-STRECKEN BEI FREQUENZEN ÜBER 10 GHZ, COST-Projekt 205, Schlussbericht, Brussels: EC, 1985. (in German)

[19] Ortgies, G., CORRECTION OF SATELLITE BEACON SIGNALS BY MEANS OF SIMULTANEOUSLY MEASURED CLEAR-AIR ATTENUATION WITH RADIOMETER, 5th URSI Com. Symp., Wave prop. and rem. sensing, La Londe, France, 11-15 Sept 1989, p.6.7.1-4.

[20] Thompson, P.T., SOME POINTS ON THE ACCURACY OF CROSS POLARISATION MEASUREMENTS AND THE USE OF STATIC CANCELLATION, Brit.Tel.Res.Mem. No.76R6/35, 1976.

[21] Evans, B.G. and Thompson, P.T., USE OF CANCELLATION TECHNIQUES IN MEASUREMENTS OF ATMOSPHERE CROSS-POLARIZATIONS, El.Lett., Vol.9, No.19, 1973, p.447-8.

[22] Dilworth, I.J., CROSS-POLAR CANCELLATION - A REVIEW OF EXISTING WORK, IEE Coll., Group E11, Digest No: 1985/111, p. 2/1-7.

[23] Thompson, P.T., CROSS POLARISATION CANCELLATION AND ITS USE TO IMPROVE THE ACCURACY OF PROPAGATION MEASUREMENTS, IEE Coll., Group E11, Digest No: 1985/111, p.5/1-9.

[24] Arnold, H.W. and Cox, D.C., DEPENDENCE OF DEPOLARIZATION ON INCIDENT POLARIZATION FOR 19-GHZ SATELLITE SIGNALS, B.S.T.J., Vol.57 (1978), No.9, p.3267-75.

[25] Maekawa, Y. et al, CROSS-POLARIZATION DISCRIMINATION MEASUREMENT AT THE CS-2 EXPERIMENTAL EARTH STATION, Proc. ICAP'87, Virginia, 15-19 June 1987, p.444-48.

[26] Fukuchi, H. et al, CENTIMETER WAVE PROPAGATION EXPERIMENTS USING THE BEACON SIGNALS OF CS AND BSE SATELLITES, IEEE Trans. Ant.and Prop., Vol.AP-31 (1983), No.4, p.603-13.

[27] Freeman, R.L., RADIO SYSTEMS DESIGN FOR TELECOMMUNICATIONS (1-100 GHz), 1987, New York: Wiley & Sons.

[28] Fukuchi, H. et al, IMPROVED THEORETICAL FORMULA FOR THE RELATIONSHIP BETWEEN RAIN ATTENUATION AND DEPOLARISATION, El.Lett., Vol.20 (1984), No.21, p.859-860.

[29] Fukuchi, H. et al, A THEORETICAL FORMULA FOR THE PREDICTION OF CROSS-POLARIZED SIGNAL PHASE, Trans. Ant.& Prop., Vol.33 (1985), No.9, p.997-1002.

[30] Liebe, H.J., MILLIMETER-WAVE ATTENUATION AND DELAY RATES DUE TO FOG/CLOUD CONDITIONS, IEEE Trans. Ant. & Prop, Vol.37 (1989), No.12, p.1617-1623.

Appendix A: Anisotropy and canting angle

Medium models describe a medium with parameters independent of the configuration of the experiment. Thus these parameters are very suitable for international statistical purposes. Below the procedure is given for deriving anisotropy and canting angle from the transmission matrix. For this purpose the transmission matrix is normalized to T_{xx}:

$$t_{lin} = \frac{1}{T_{xx}}.T = \begin{pmatrix} t_{xx} & t_{xy} \\ t_{yx} & t_{yy} \end{pmatrix} = \begin{pmatrix} 1 & t_{xy} \\ t_{yx} & t_{yy} \end{pmatrix} \quad \text{(A.1)}$$

Paraboni [9] proposed to derive canting angle and anisotropy from the transmission matrix in circular polarization to obtain better accuracy and uniformity for medium models. Next the processing method is given to derive real and imaginary parts of canting angle and anisotropy from (A.1).

The transmission matrix in circular polarization is given by [9]:

$$t_{rr} = ½ [(t_{xx} + t_{yy}) + j(t_{yx} - t_{xy})] \quad \text{(A.2)}$$

$$t_{ll} = ½ [(t_{xx} + t_{yy}) - j(t_{yx} - t_{xy})] \quad \text{(A.3)}$$

$$t_{rl} = ½ [(t_{xx} - t_{yy}) + j(t_{yx} + t_{xy})] \quad \text{(A.4)}$$

$$t_{lr} = ½ [(t_{xx} - t_{yy}) - j(t_{yx} + t_{xy})] \quad \text{(A.5)}$$

where:

$$t_{cir} = \begin{pmatrix} t_{rr} & t_{rl} \\ t_{lr} & t_{ll} \end{pmatrix} \quad \text{(A.6)}$$

where l stands for left-hand polarization and r for right-hand polarization. Using this matrix, anisotropy is given by [9]:

$$\Delta = \Delta A + j\Delta B = 2.\text{arctanh}\sqrt{\frac{t_{rl}.t_{lr}}{t_{ll}.t_{rr}}} \quad \text{(A.7)}$$

The inclination angle is given by [9]:

$$\phi = \phi' + j\phi'' = \frac{j}{4} \ln\left(\frac{t_{lr}.t_{ll}}{t_{rr}.t_{rl}}\right) \tag{A.8}$$

- Anisotropy:

Anisotropy is usually given with a real and imaginary part:

$$\Delta = \Delta A + j\Delta B \tag{A.9}$$

Below expressions are derived for this real and imaginary part.
The transmission matrix parameters are also described by their modulus and phase:

$$t_{rl} = |t_{rl}|\, e^{j\eta rl} \tag{A.10}$$

$$t_{rr} = |t_{rr}|\, e^{j\eta rr} \tag{A.11}$$

$$t_{lr} = |t_{lr}|\, e^{j\eta lr} \tag{A.12}$$

$$t_{ll} = |t_{ll}|\, e^{j\eta ll} \tag{A.13}$$

Now:

$$\sqrt{\frac{t_{rl}.t_{lr}}{t_{ll}.t_{rr}}} = \sqrt{\frac{|t_{rl}|\ |t_{lr}|}{|t_{ll}|\ |t_{rr}|}}\ e^{j\frac{-\eta_{ll}-\eta_{rr}+\eta_{rl}+\eta_{lr}}{2}} \tag{A.14}$$

$$= C\, e^{j\beta} \tag{A.15}$$

$$= C.\cos\beta + jC.\sin\beta \tag{A.16}$$

where:

$$C = \sqrt{\frac{|t_{rl}|\ |t_{lr}|}{|t_{ll}|\ |t_{rr}|}} \tag{A.17}$$

$$\beta = \tfrac{1}{2}(\eta_{rl} + \eta_{lr} - \eta_{ll} - \eta_{rr}) \tag{A.18}$$

The following mathematical relations are used to obtain the real and imaginary part of the anisotropy.

$$\text{arctanh}(c) = \frac{1}{2}\ln\left(\frac{1+c}{1-c}\right) \tag{A.19}$$

If $u = U e^{jv}$ (A.20)

Then for $v = 0..360°$

$$\ln(u) = \ln(U) + jv \tag{A.21}$$

The anisotropy is thus given by:

$$\Delta = \Delta A + j\Delta B \tag{A.22}$$

where:

$$\Delta A = 20\log(e).\frac{1}{2}\ln\left(\frac{1+C^2+2C.\cos\beta}{1+C^2-2C.\cos\beta}\right) \quad (dB) \tag{A.23}$$

$$\Delta B = \frac{180}{\pi}\arctan\left(\frac{2C.\sin\beta}{1-C^2}\right) \tag{A.24}$$

$[0..360°]$

• Canting angle:
Using equation (A.21) the real and imaginary part of the inclination angle are derived:

$$\phi = \phi' + j\phi'' \quad (rad) \tag{A.25}$$

where:

$$\phi' = -¼(\eta_{lr}+\eta_{ll}-\eta_{rl}-\eta_{rr}) \quad (rad) \tag{A.26}$$

$$\phi'' = ¼\ln|(t_{lr}t_{ll})/(t_{rl}t_{rr})| \quad (rad) \tag{A.27}$$

From these parameters the canting angle Φ and crosspolar unbalance CU are obtained:

$$\Phi = \phi' + \Phi_0 \qquad [-90..90°] \tag{A.28}$$

$$CU = 20\log\left|\frac{t_{tr}\cdot t_{ll}}{t_{rr}\cdot t_{rl}}\right| \quad (dB) \tag{A.29}$$

If ϕ'' is given in degrees, ϕ'' and CU are related by:

$$\phi''_{deg} = 1.65\ CU \tag{A.30}$$

Appendix B: Antenna pointing errors

In this appendix formulae are derived to determine errors in received signal levels due to a pointing error of the antenna. Consider an antenna aperture with uniform amplitude and phase. In terms of pointing errors this is the worst-case situation. For this antenna aperture the normalized electric field (in the far field) is given by [27]:

$$\frac{E(\theta)}{E(0)} = \frac{2J_1(u)}{u} \tag{B.1}$$

where:

$$u = \frac{\pi D \sin(\theta)}{\lambda} \tag{B.2}$$

D is the diameter of the antenna, θ is the angle between the desired direction and the boresight of the antenna and λ is the wavelength. The normalized electric field can be approximated by [5] ($u<5$):

$$\frac{E(\theta)}{E(0)} = 1 - \frac{1}{8}u^2 + \frac{1}{192}u^4 \tag{B.3}$$

The 3dB beamwidth can be found by defining:

$$\frac{E(\frac{1}{2}\theta_{3dB})}{E(0)} = \frac{1}{2}\sqrt{2} \tag{B.4}$$

This results in ((B.4) and (B.2)):

$$\theta_{3dB} = \frac{1.02\lambda}{D} \tag{B.5}$$

The 3dB beamwidth decreases for larger antennas. The pointing error (e) in the received signal level is given by ($u<5$):

$$e = 20\log\left(1 - \frac{1}{8}u^2 + \frac{1}{192}u^4\right) \quad (dB) \tag{B.6}$$

This formula is used to calculate the errors given in table 3.3.

In practice the antenna diagram may be approximated by a quadratic function shown in figure B.1.

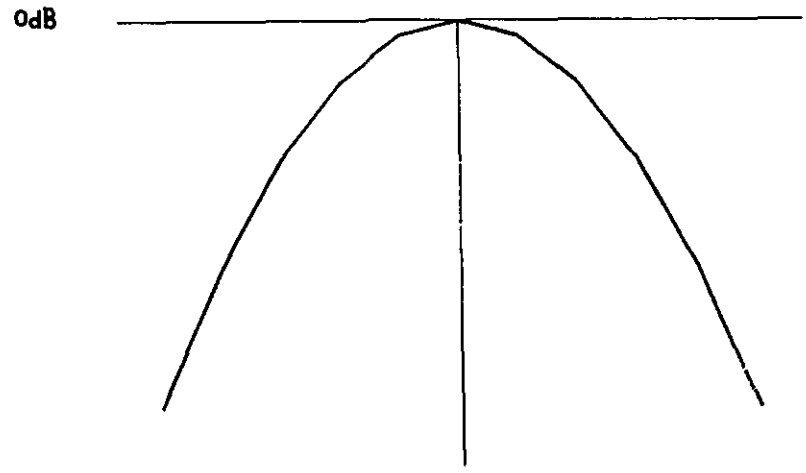

Figure B.1: Antenna diagram

The error function is thus given by:

$$e = c_\theta \, \theta^2 \qquad \text{(dB)} \tag{B.7}$$

For $\theta = \frac{1}{2}\Theta_{3dB}$ e should be -3 dB. This gives an expression for c_θ:

$$c_\theta = -\frac{12}{\Theta_{3dB}^2} \tag{B.8}$$

The signal level error for a pointing error of θ is given by:

$$e = -\frac{12\theta^2}{\Theta_{3dB}^2} \quad (dB) \tag{B.9}$$

In practice the aperture efficiency will be typically 55 to 60% for a front fed paraboloid. In that case Θ_{3dB} is given by:

$$\Theta_{3dB} \approx \frac{72\lambda}{D} \quad (°) \tag{B.10}$$

(B.9) and (B.10) are used to calculate the values of table 3.4.

Appendix C: Matrix cancellation

For the dual polarized beacon experiment matrix cancellation may be used to improve accuracy of crosspolar data. In this appendix formulae are derived for the crosspolar phasor after cancellation. The voltage tensor U is given by the matrix multiplication (2.8):

$$U = A\,T\,E \tag{C.1}$$

First order approximation (4.3):

$$U = \begin{pmatrix} A_{xx}T_{xx}E_{xx} & A_{xx}T_{xy}E_{yy}+A_{xx}T_{xx}E_{xy}+A_{xy}T_{yy}E_{yy} \\ A_{yx}T_{xx}E_{xx}+A_{yy}T_{yx}E_{xx}+A_{yy}T_{yy}E_{yx} & A_{yy}T_{yy}E_{yy} \end{pmatrix} \tag{C.2}$$

During clear-sky conditions, U_0 is given by ($T \approx I$):

$$U_0 = \begin{pmatrix} A_{xx}E_{xx} & A_{xx}E_{xy}+A_{xy}E_{yy} \\ A_{yx}E_{xx}+A_{yy}E_{yx} & A_{yy}E_{yy} \end{pmatrix} \tag{C.3}$$

The cancellation matrix is given by:

$$K = U_0^{-1} \tag{C.4}$$

in which:

$$U_0^{-1} = \frac{1}{\det}\begin{pmatrix} U_{yy0} & -U_{xy0} \\ -U_{yx0} & U_{xx0} \end{pmatrix} \tag{C.5}$$

and:

$$\det = U_{xx0}U_{yy0} - U_{yx0}U_{xy0} \approx U_{xx0}U_{yy0} \tag{C.6}$$

Using the cancellation matrix either left or right cancellation can be performed:

- Left cancellation:

$$T_L = K\,U \tag{C.7}$$

where U is the voltage matrix during an event. The first order approximation of (C.7) is given by:

$$T_L = \frac{1}{\det}\begin{pmatrix} U_{yy0}U_{xx} & U_{yy0}U_{xy}-U_{xy0}U_{yy} \\ -U_{yx0}U_{xx}+U_{xx0}U_{yx} & U_{xx0}U_{yy} \end{pmatrix} \qquad (C.8)$$

The crosspolar phasor δ_{XI} is given by:

$$\delta_{xL} = \frac{T_{yxL}}{T_{xxL}} = \frac{U_{xx0}}{U_{yy0}}\left(\frac{U_{yx}}{U_{xx}} - \frac{U_{yx0}}{U_{xx0}}\right) \qquad (C.9)$$

Using (C.2) and (C.3) δ_{XI} can be expressed in the satellite and groundstation parameters:

$$\delta_{xL} = \frac{E_{xx}}{E_{yy}}\left(\frac{T_{yx}}{T_{xx}} + \left(\frac{T_{yy}}{T_{xx}} - 1\right)\delta_x^s\right) \qquad (C.10)$$

In δ_{XL} the groundstation influence is cancelled. δ_x^s is the crosspolar phasor of the satellite.

- Right cancellation:

$$T_R = U\,K \qquad (C.11)$$

The first order approximation is given by:

$$T_R = \frac{1}{\det}\begin{pmatrix} U_{yy0}U_{xx} & U_{xx0}U_{xy}-U_{xy0}U_{xx} \\ -U_{yx0}U_{yy}+U_{yy0}U_{yx} & U_{xx0}U_{yy} \end{pmatrix} \qquad (C.12)$$

The crosspolar phasor δ_{Xr} is given by:

$$\delta_{xR} = \frac{T_{yxR}}{T_{xxR}} = \frac{U_{yx}}{U_{xx}} - \frac{U_{yy}}{U_{xx}}\frac{U_{yx0}}{U_{yy0}} \qquad (C.13)$$

Using (C.2) and (C.3), δ_{Xr} can be expressed in the satellite and groundstation parameters:

$$\delta_{xR} = \frac{A_{yy}}{A_{xx}}\frac{T_{yx}}{T_{xx}} + \left(1 - \frac{T_{yy}}{T_{xx}}\right)\delta_x^a \qquad (C.14)$$

In δ_{XR} the satellite influence is cancelled. δ_x^a is the crosspolar phasor of the groundstation. The expressions for δ_{yL} and δ_{yR} can be derived by exchanging indices in (C.10) and (C.14).

Appendix D: Differential attenuation, phase-shift and depolarization due to rain

In this appendix formulae are given to calculate errors in crosspolar discrimination measurements as a function of the attenuation caused by rain. Equations (5.16) to (5.19) show that differential attenuation, differential phase-shift and crosspolarization discrimination have to be expressed in terms of the average attenuation. Several models and raindrop-size distributions may be used, but cause only a slight difference in the numerical results and do not affect the conclusions. Here the Chu model (XPD versus CPA) and the Marshall & Palmer drop-size distribution is used. Calculations assume a zero canting angle of the medium.

- Differential attenuation

Differential attenuation is the difference in attenuation between the orthogonal polarization and the actual polarization. Differential attenuation is given by [28]:

$$\Delta A_t = p A_{av}^{q} l_{eff}^{1-q} \cos 2(\Phi - \Phi_0) \cos^2 \epsilon \exp(-0.00061 \sigma_\Phi^2) \quad \text{(dB)} \tag{D.1}$$

where:

Φ = canting angle of the medium (mean canting angle = 0°)
Φ_0 = polarization tilt angle
ϵ = elevation angle
σ_Φ = effective standard deviation of the raindrop canting angle distribution (recommended 0° [28])
l_{eff} = effective path length through rain (5.1 km for EUT groundstation [5]).
A_{av} = the average attenuation $(A_{tx}+A_{ty})/2$

p and q depend, apart from the frequency, on the rain drop-size distribution. Using the assumptions (D.1) reduces to:

$$\Delta A_t = p A_{av}^{q} l_{eff}^{1-q} \cos^2 \epsilon \cos 2\Phi_0 = k_1 A_{av}^{q} \quad \text{(dB)} \tag{D.2}$$

Table D.1 shows p- and q-values for the Marshall and Palmer drop-size distribution [28] for the Olympus beacons (Y-polarizations) together with k_1 for the EUT groundstation (ϵ = 26.7°, Φ_0 = -18.4°). Note that the attenuation for the X-polarization is greater than for the Y-polarization and thus differential attenuation for the X-polarization is negative.

- Differential phase-shift

Differential phase-shift is the difference of phase-shift in the orthogonal polarization and the actual polarization. Differential phase-shift is given by [29]:

$$\Delta \phi = \mu A_{av}^{\nu} l_{eff}^{1-\nu} \cos 2(\Phi - \Phi_0) \cos^2 \epsilon \exp(-2\sigma_\Phi^2) \quad \text{(rad)} \tag{D.3}$$

μ and ν depend apart from the frequency on the rain drop-size distribution. Using the same assumptions as for (D.1), (D.3) reduces to:

Table D.1: Differential attenuation parameters for Olympus beacons

	p	q	k_1
B0	0.157	1.27	0.065
B1	0.116	1.27	0.048
B2	0.089	1.27	0.037

$$\Delta\phi = \mu A_{av}^{\nu} l_{eff}^{1-\nu} \cos 2\Phi_0 \cos^2\epsilon = k_2 A_{av}^{\nu} \quad \text{(rad)} \tag{D.4}$$

Table D.2 shows μ- and ν-values for the Marshall and Palmer drop-size distribution [29] for the Olympus beacons (Y-polarizations) together with k_2 for the EUT groundstation. Note that the differential phase-shift for X-polarization is negative.

Table D.2: Differential phase-shift parameters for Olympus beacons

	μ	ν	k_2 (deg)
B0	0.042	1.0	1.54
B1	0.022	1.0	0.80
B2	0.0096	0.85	0.45

Figures 2.10 and 2.11 show the expected differential attenuation and phase-shift for the olympus beacons.

• Crosspolarization as a function of attenuation

Using the Chu model, the XPD is directly related to the average attenuation by [5]:

$$XPD = 11.5 - 10\log(0.5(1-\cos 4\Phi_0 \exp(-8\sigma_m^2))) + 20\log f - 40\log(\cos\epsilon) - 20\log A_{av} \pm 0.15 A_{av}\cos^2\epsilon \cos 2\Phi_0 \quad (dB) \tag{D.5}$$

(+ sign for Y- and - sign for X-polarization)

where:

σ_m = 3° (σ_m is in rad in (D.5))

A_{av} < 20 dB

11 < f < 30 GHz

For EUT conditions, equation (D.5) reduces to:

$$XPD = 17.9 + 20\log f - 20\log(A_{av}) \pm 0.048\, A_{av} \tag{D.6}$$

Figure 2.9 shows this relationship for the OLYMPUS beacons.

Equations (D.2), (D.4) and (D.6) are used in (5.16) to (5.19):

$$T_{yy}/T_{xx} = 10^{\Delta At/20}\, e^{j\Delta\phi} \qquad \text{(D.7)}$$

$$|\delta| = 10^{-XPD/20} \qquad \text{(D.8)}$$

Appendix E: Graphs for accuracy evaluation

B0

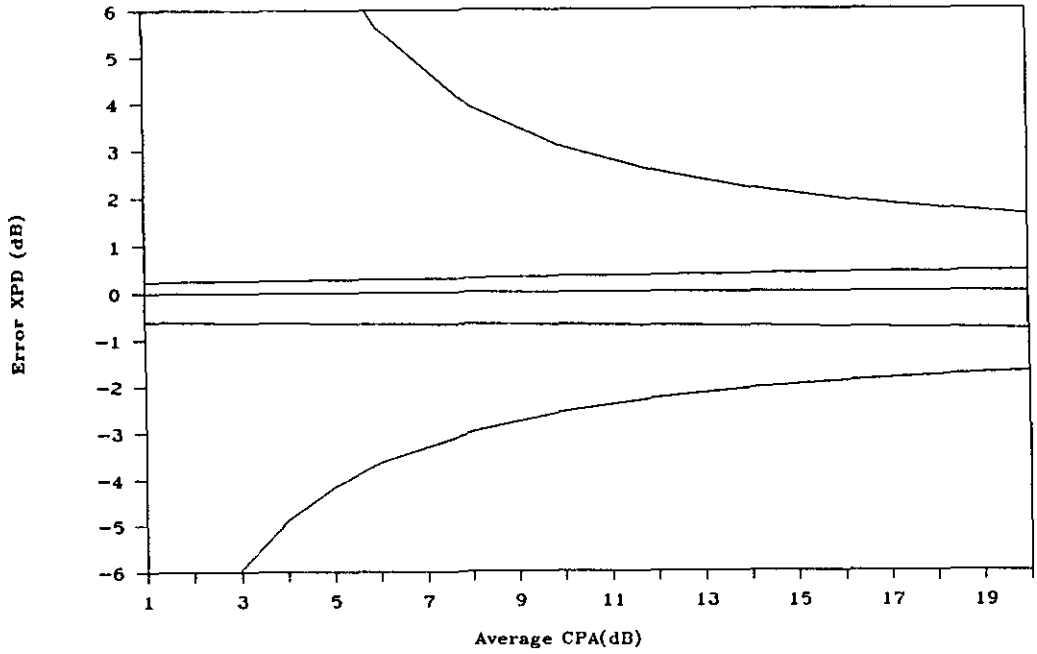

Figure E.1: Error in XPD with and without cancellation (B0)

B1,H

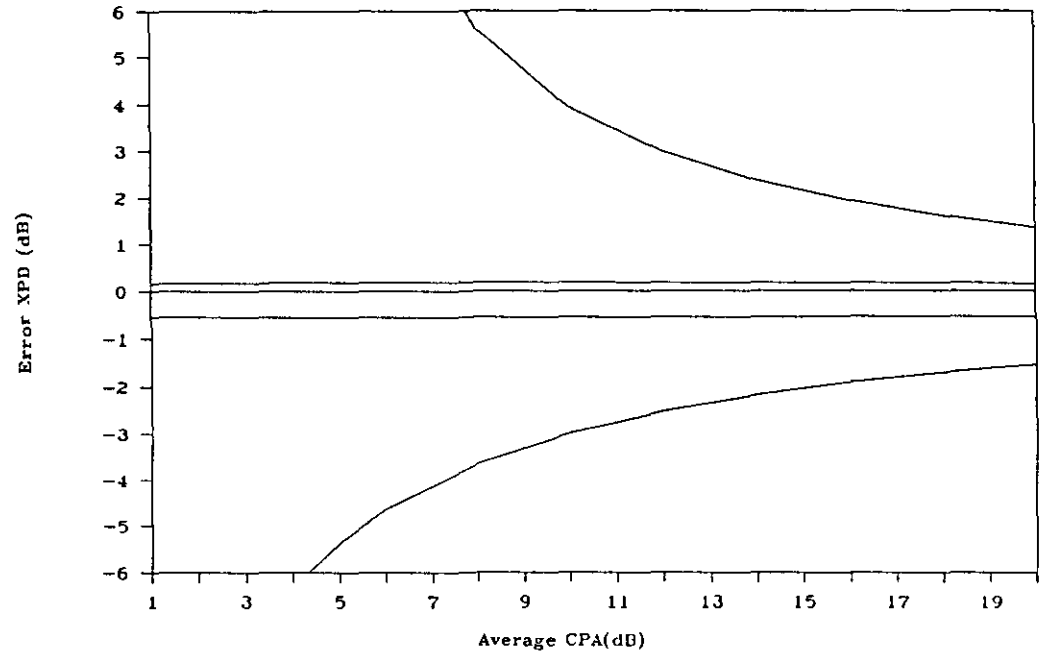

Figure E.2: Error in XPD with and without cancellation (B1,H)

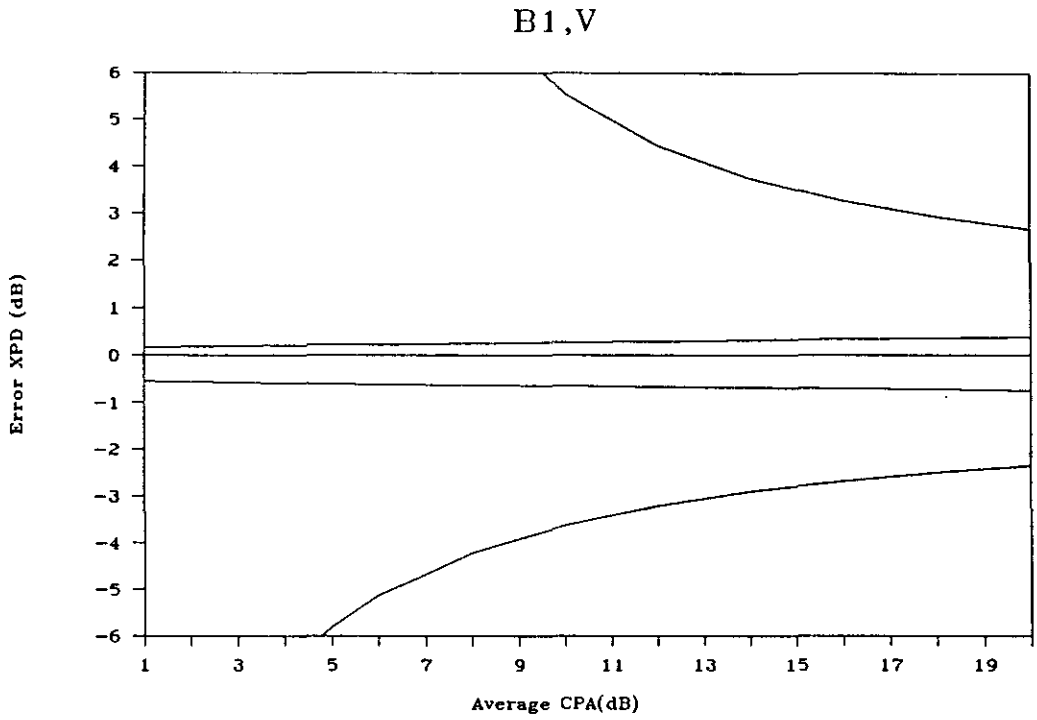

Figure E.3: Error in XPD with and without cancellation (B1,V)

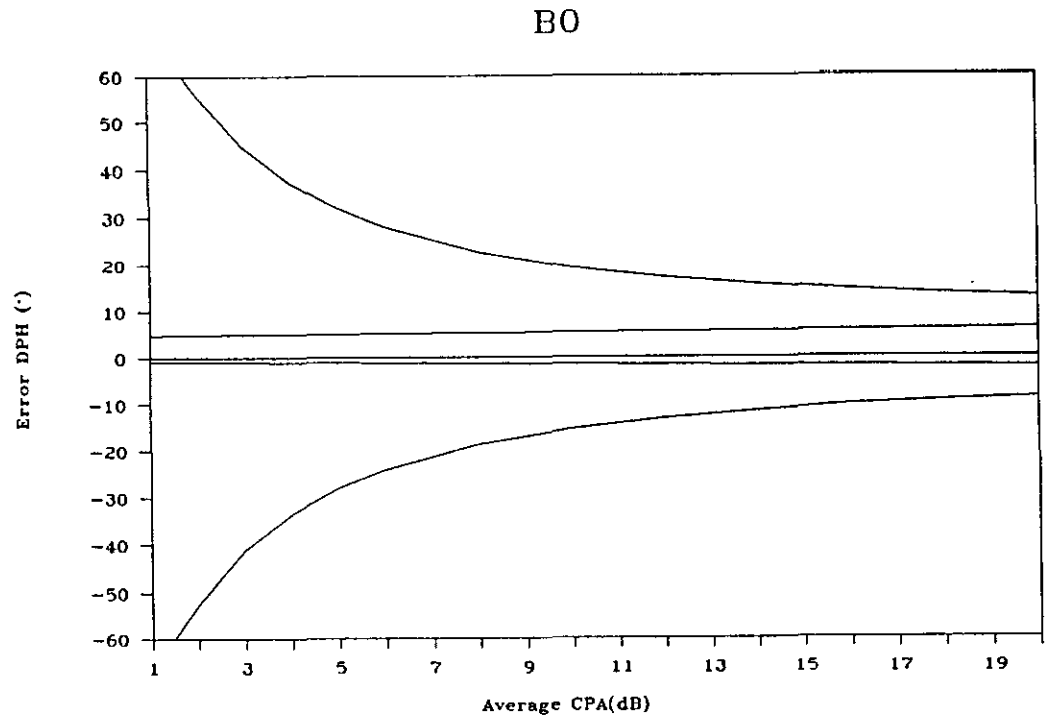

Figure E.4: Error in DPH with and without cancellation (B0)

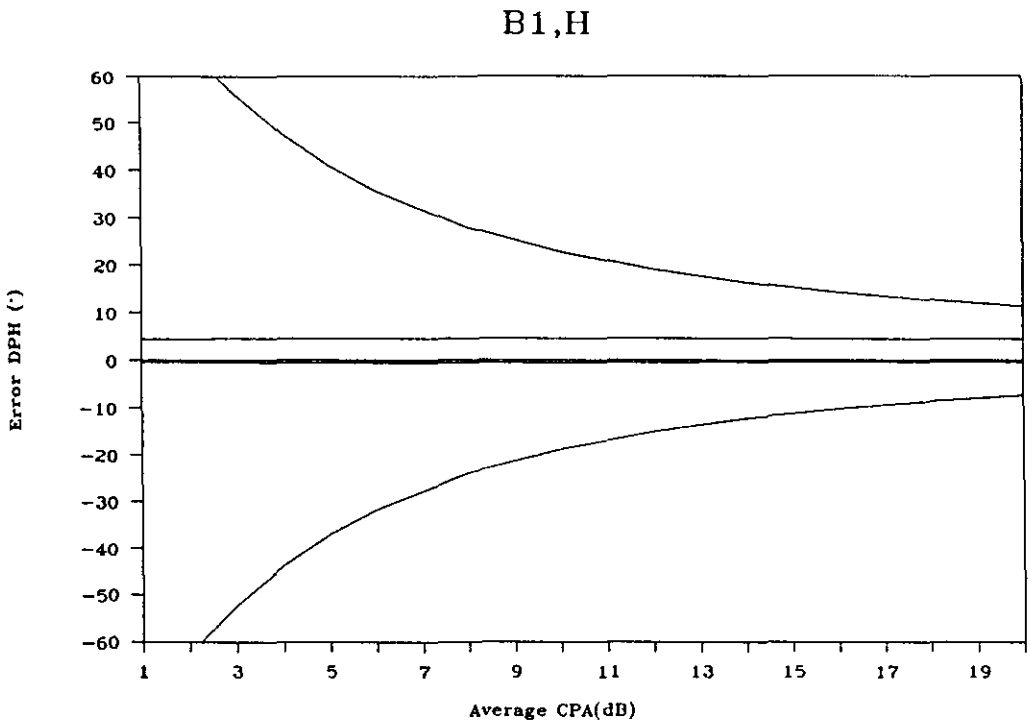

Figure E.5: Error in DPH with and without cancellation (B1,H)

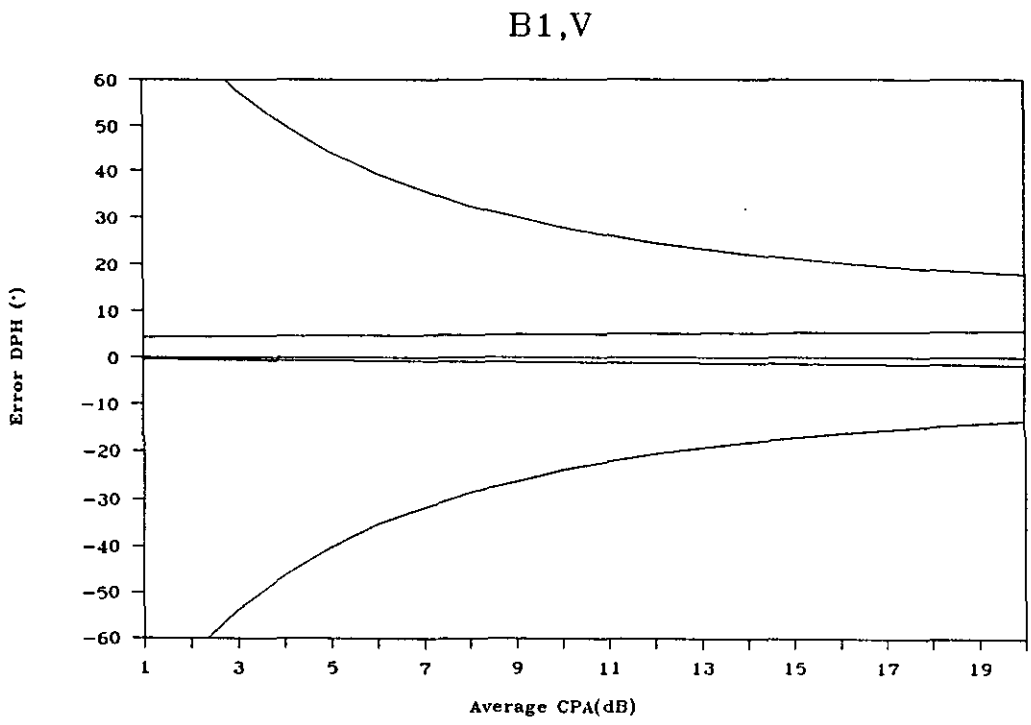

Figure E.6: Error in DPH with and without cancellation (B1,V)

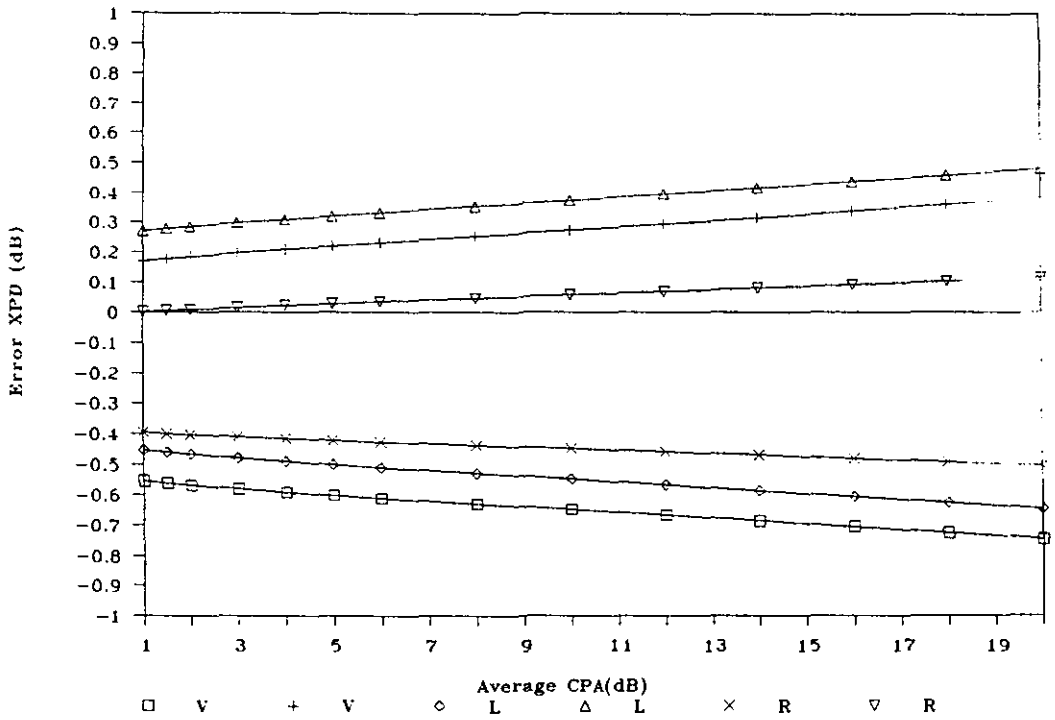

Figure E.7: Errors in XPD with various cancellation methods (B1,V)

B1,V

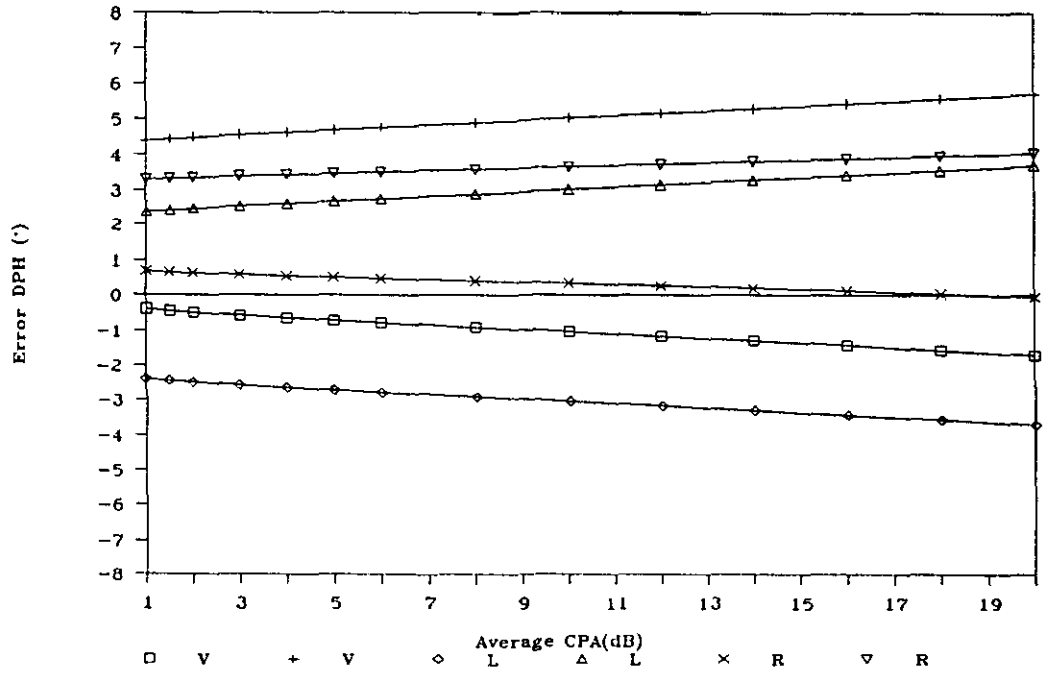

Figure E.8: Errors in DPH with various cancellation methods (B1,V)

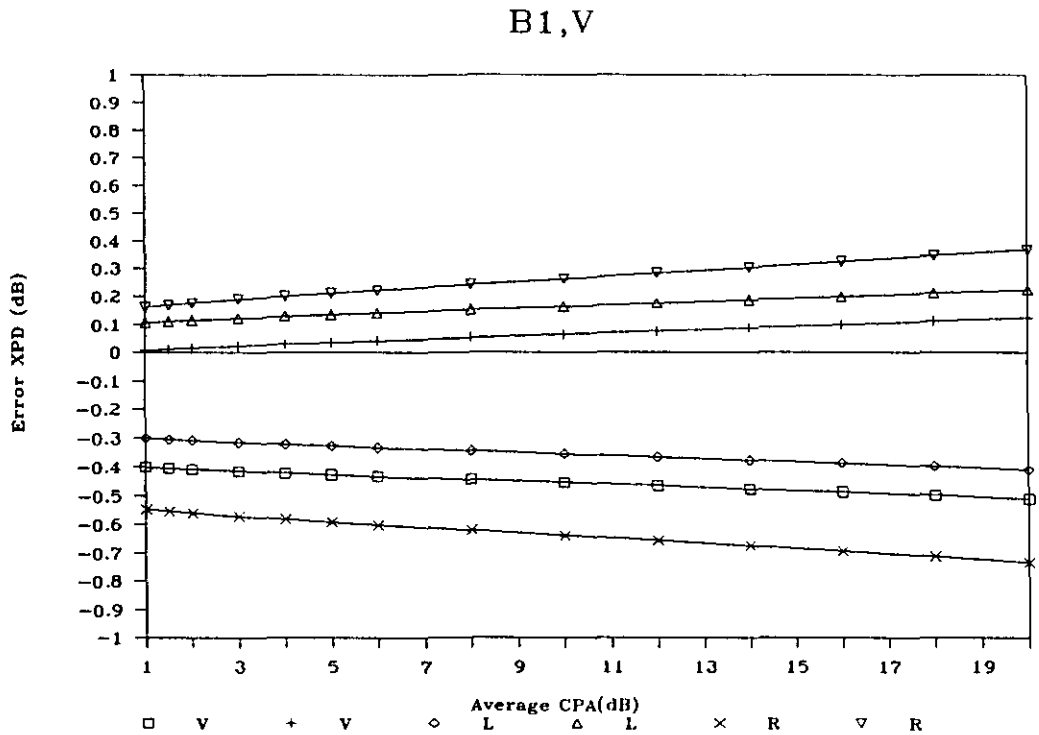

Figure E.9: Errors in XPD with various cancellation methods (B1,V system II)

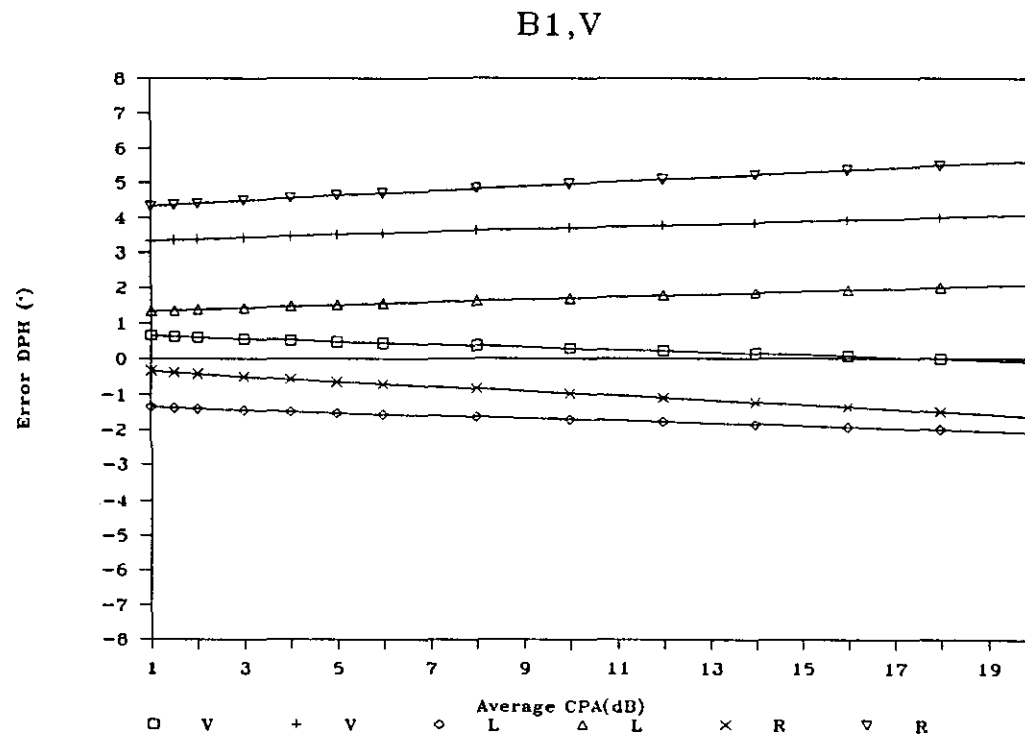

Figure E.10: Errors in DPH with various cancellation methods (B1,V system II)

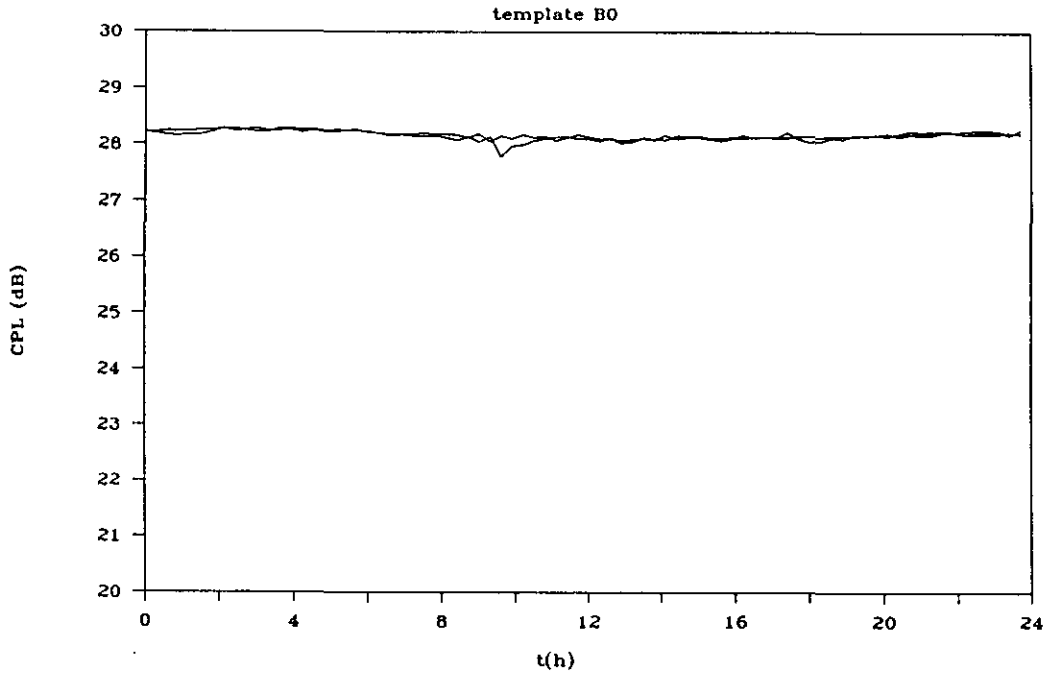

Figure E.11: Copolar level templates (B0, 06/13/90 - 06/14/90)

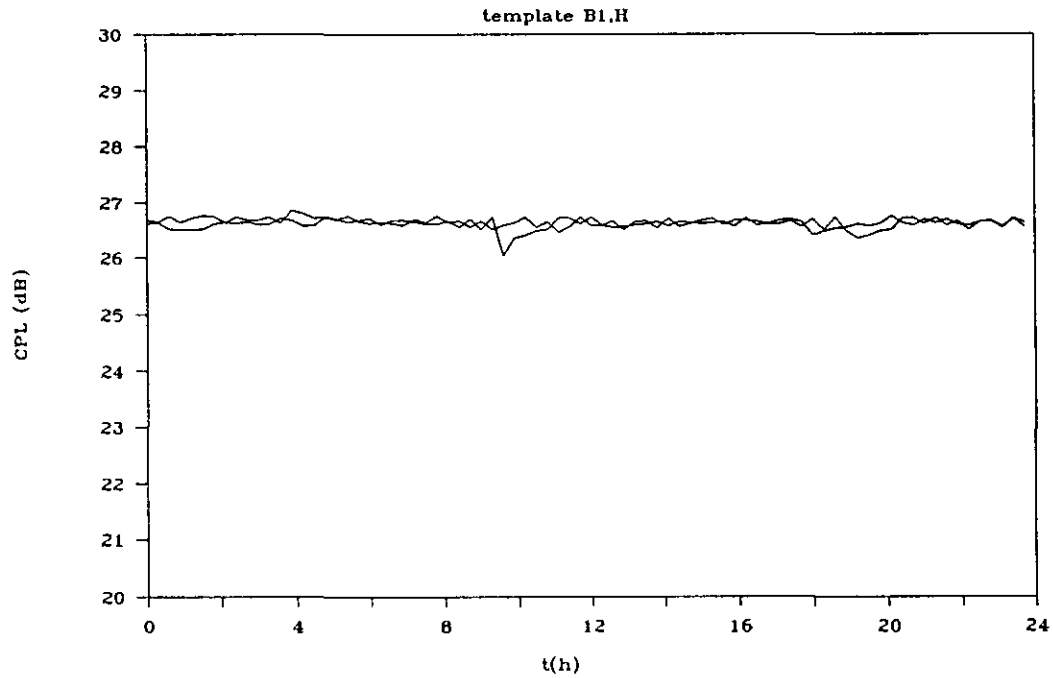

Figure E.12: Copolar level templates (B1H, 06/13/90 - 06/14/90)

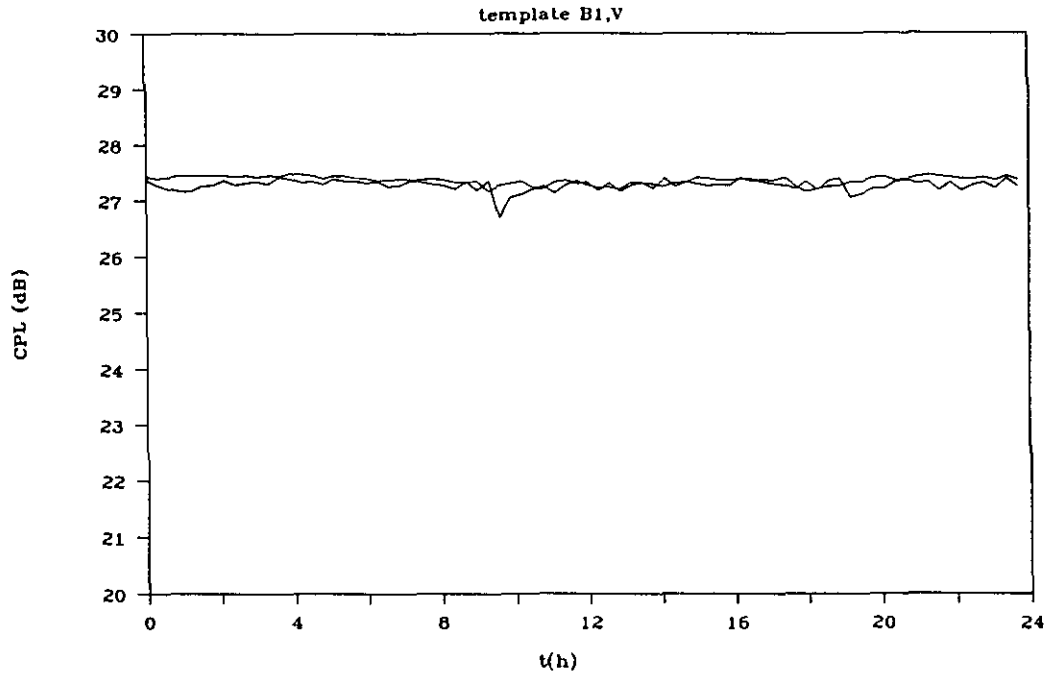

Figure E.13: Copolar level templates (B1V, 06/13/90 - 06/14/90)

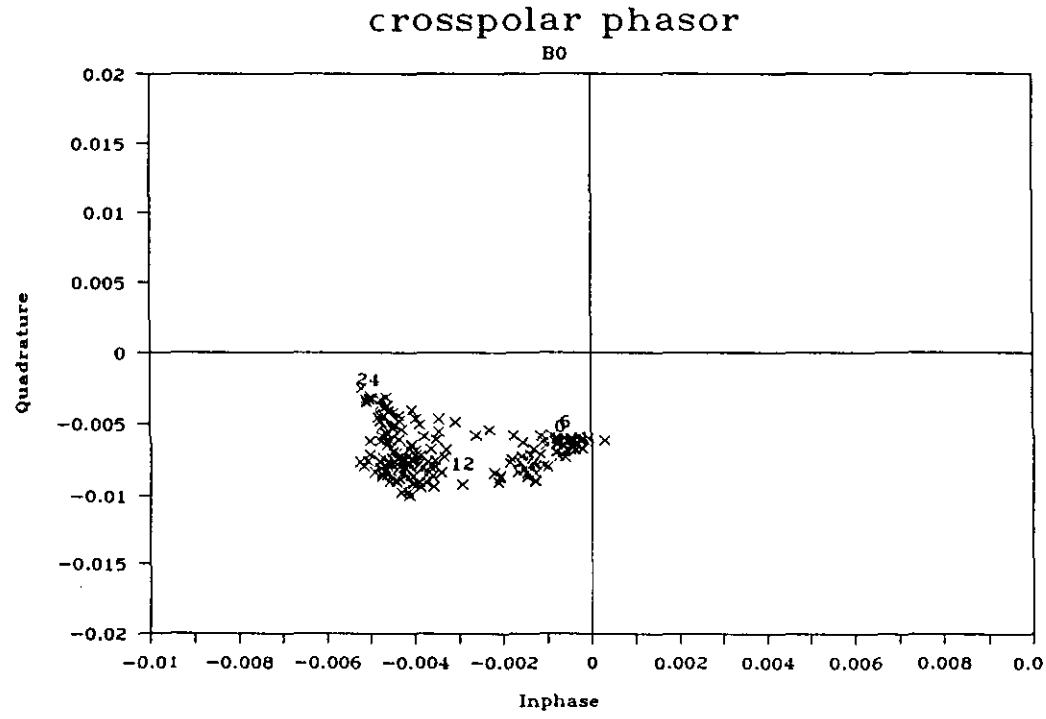

Figure E.14: Raw template of crosspolar phasor (B0, 06/13/90)

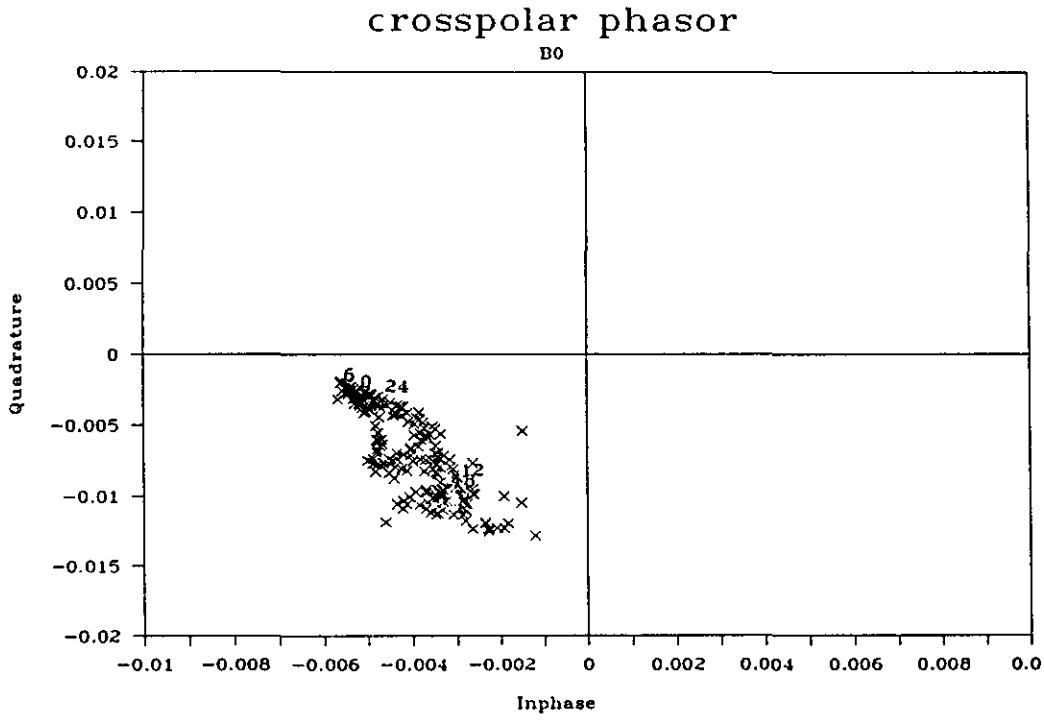

Figure E.15: Raw template of crosspolar phasor (B0, 06/14/90)

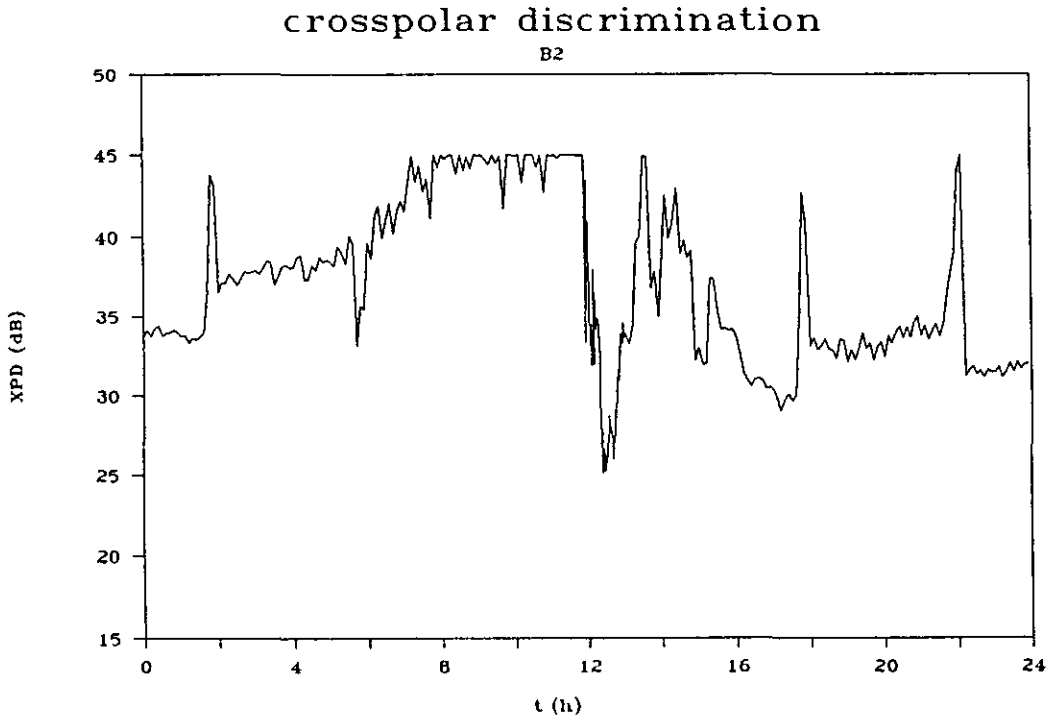

Figure E.16: XPD of B2 beacon (06/23/90)

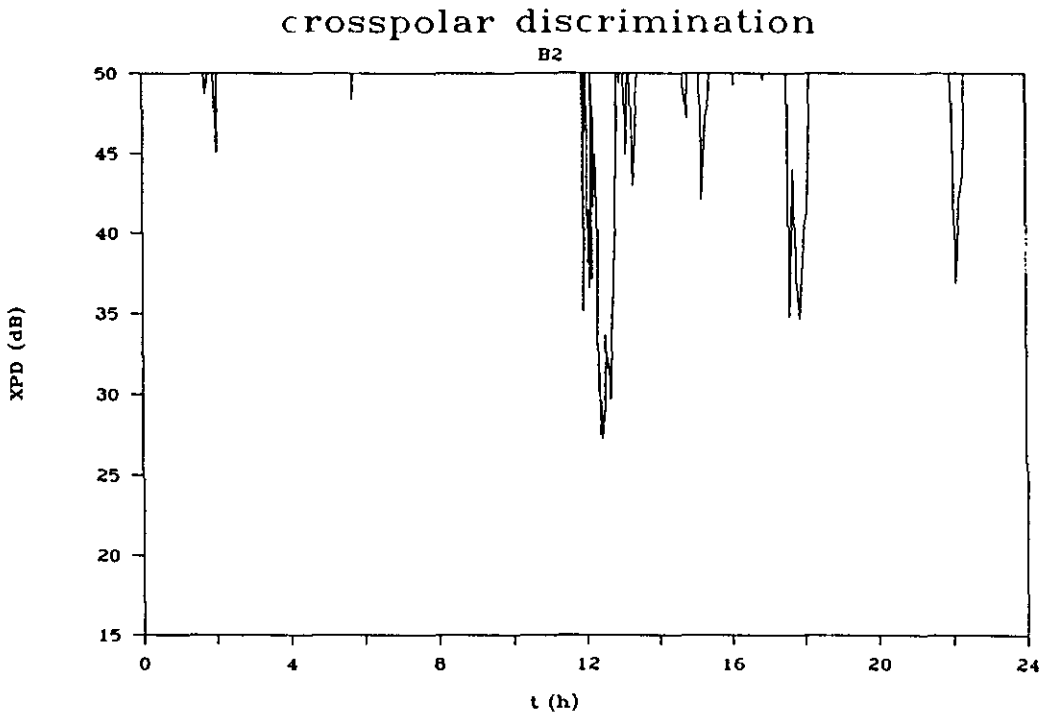

Figure E.17: XPD of B2 beacon with adaptive cancellation (06/23/90)

II

SOFTWARE SET-UP FOR DATA PREPROCESSING OF SATELLITE BEACON MEASUREMENTS

1 INTRODUCTION

During the OLYMPUS measurement campaign a large amount of propagation data will be collected at the EUT groundstation. The EUT groundstation is capable of measuring and storing 32 data channels simultaneously. These channels consist of beacon, meteorological and test measurements. The acquired data requires processing to derive graphs and information about the atmospheric propagation characteristics. The basic set-up of the EUT processing system is shown in figure 1.1.

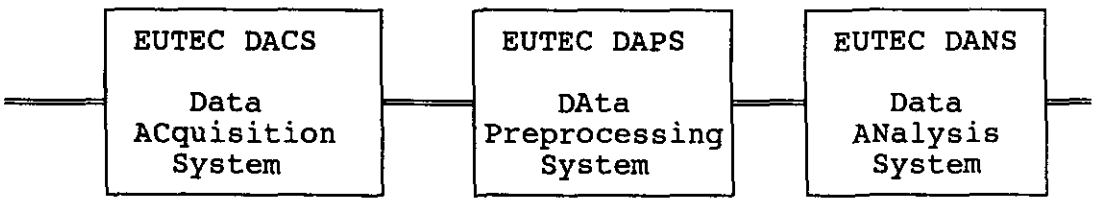

Figure 1.1: Set-up of EUT data processing system

DACS collects and stores raw data of 32 channels. In DAPS the measurement system biases are derived and removed from measurements. The output of this module has a standard event format, that can be read by the DANS to analyze propagation characteristics.

This part considers the detailed design of algorithms for the data preprocessing (DAPS). These algorithms, when implemented in software, perform the basic preprocessing of raw data. In- and output formats have been defined by Barto [1]. As of July 1990, DACS is fully operational, DAPS is under development and DANS still has to be developed. The EUTEC processing system will be used for event analysis. DAPPER (see part III) is designed to be used for statistical analysis of propagation data.

The basic flowchart of the preprocessing is given in figure 1.2.

In radiometer data processing, radiometer measurements are used to estimate attenuation at beacon frequencies. During clear-sky conditions this attenuation is used to determine reference levels for beacon attenuation measurements. In template extraction, templates are built for clear-sky periods. These templates contain information about the measurement system influence. In bias removal biases introduced by the measurements system, are removed using the templates.

Chapter 2 describes the specifications of the preprocessing system. In chapter 3,4 and 5 algorithms are derived for radiometer data processing, template extraction and bias removal respectively for EUT beacon measurements. The principles of these algorithms have been explained in part I of this report.

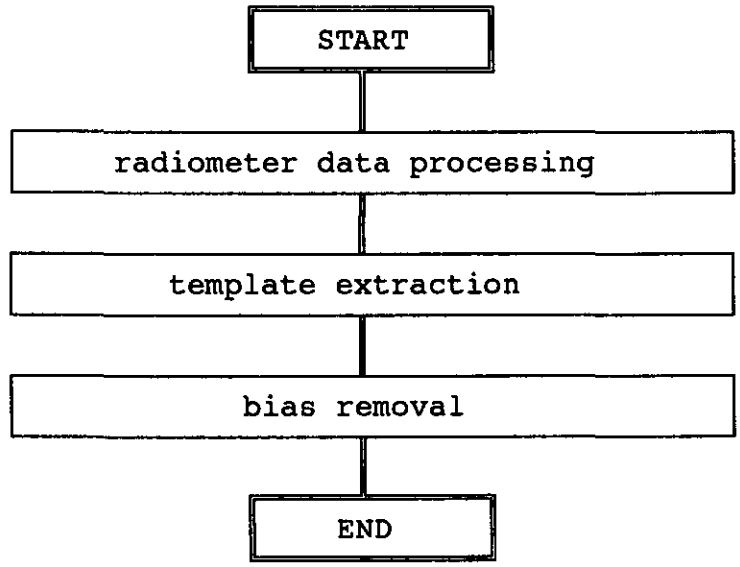

Figure 1.2: Basic flowchart of the preprocessing system

2 SPECIFICATIONS OF THE PREPROCESSING SYSTEM

• Input:

Input for DAPS is the data stored by DACS. Table 2.1 shows a list of the available measurement channels of the DACS. All the channels have a range represented by a linear 12 bit coding (0..4095). Thus for a range of 0 to 30 dB, 0 dB is represented by code 0 and 4095/4096*30 dB is represented by code 4095. Channels 0 to 7 are sampled with a frequency of 3 Hz, channels 8 to 31 with a frequency of 1 Hz.

• Output:

The output data of preprocessing is written into a standard event format [1]. In this format the amount of data is reduced during off-event periods. The standard event file consists of channels with the results of the preprocessing and auxiliary channels that have not been affected by the preprocessing. The user should choose the channels to be written to the standard event file.

• Hard- and software

The preprocessing will be implemented in TURBO-C on a MS-DOS 386 machine. This machine will be part of a network, connecting the acquisition and analysis machines.

• Status acquisition

As of July 1990 radiometer measurements (channel 13,14,15,21,24) are not yet available. Channel 25 to 29 are user defined and may be used for test purposes or to record position of the groundstation antenna and differential phase between copolar signals of different frequencies, when these measurements are available. A manual switchboard has been made to record the validity of all the 32 channels. A 32-bit word gives the status of all the channels, every channel is represented by one bit (0 = invalid, 1 = valid). This status word is stored every second.

• Requirements for preprocessing

Besides the basic function to remove system influences, preprocessing should provide means to flag data for validity and input additional text (journal). This may be done automatically using the status word information or manually. The flagging of data is essential for correct treatment in the analysis stage.

Considering these observations, the following general user requirements will have to be met by the preprocessing system:

R1. Provide a suitable data interface with DACS (raw data format) and DANS (standard event format).

R2: Provide a user-interface to the configuration of in- and output channels.

R3: Provide automatic and manual means of flagging data and making a journal.

R4: Perform preprocessing procedures, i.e. radiometer data processing, template extraction and bias-removal, correctly.

R5: Provide the opportunity to plot and print results.

R6: The output data resolution should not be smaller than the input data resolution.

During software implementation these requirements have to be worked out in detail. The following chapters will discuss the algorithms for data preprocessing.

Table 2.1: EUT data acquisition channel list (July 1, 1990)

EUTEC	CHANNEL	DEFINITION			ACQUISITION UNIT
Chn	Abbreviation	Range	Unit	Resolution factor	Explanation
0	B0VCPL_	0..30	dB	10	copolar level B0
1	B2VCPL_	0..30	dB	10	copolar level B2
2	B1HCPL_	0..30	dB	10	copolar level B1,H
3	B1VCPL_	0..30	dB	10	copolar level B1,V
4	B0VXPD_	15..45	dB	10	crosspolar discr. B0
5	B2VXPD_	15..45	dB	10	crosspolar discr. B2
6	B1HXPD_	15..45	dB	10	crosspolar discr. B1,H
7	B1VXPD_	15..45	dB	10	crosspolar discr. B1,V
8	B0VDPH_	0..360	deg	10	differential phase B0
9	B2VDPH_	0..360	deg	10	differential phase B2
10	B1HDPH_	-360..360	deg	10	differential phase B1,H
11	B1VDPH_	-360..360	deg	10	differential phase B1,V
12	B1VHPH_	-360..360	deg	10	differential phase V-H copolar B1
13	R0TANT_	0..310	K	10	radiometer at 12 GHz
14	R1TANT_	0..310	K	10	radiometer at 20 GHz
15	R2TANT_	0..310	K	10	radiometer at 30 GHz
16	M1TAMB_	311..247	K	10	dry bulb temperature
17	M2TAMB_	311..247	K	10	wet bulb temperature
18	M1RAING	0..150	mm/h	10	rain rate
19	M2RAING	0..10	mm	10	rain cumulative
20	M1PATM_	800..1100	hPa	1	atmospheric pressure
21	R1TREF_	305..315	K	10	radiometer ref. temp. 1
22	M1WINDV	0..100	m/s	10	wind velocity (speed)
23	M1WINDD	0..360	deg	10	wind velocity (direction)
24	R2TREF_	305..315	K	10	radiometer ref. temp. 2
25	UYKSPAN	0..10	V	10	user channel
26	UTEST4_	0..10	V	10	user channel
27	UTEST5_	0..10	V	10	user channel
28	UTEST6_	0..10	V	10	user channel
29	URADIOT	0..10	V	10	user channel
30	B3VXPD_	15..45	dB	10	ECS crosspolar discr.
31	B3VCPL_	0..30	dB	10	ECS copolar level

3 RADIOMETER DATA PROCESSING

3.1 Introduction

In radiometer data processing attenuation at the beacon frequencies is estimated from radiometer and meteorological measurements during clear-sky conditions. The radiometer frequencies are typically different from the beacon frequencies. The radiometer may only be used for small attenuation values as the accuracy in derived attenuation decreases with increasing attenuation values. Next the complete procedure is given to calculate the attenuation at Olympus beacon frequencies. The procedure is derived using current CCIR attenuation prediction models in the frequency area 0..50 GHz [2][3]. The method principles were recently discussed by Dintelmann [4] and Ortgies [5]. The algorithms given here, are also a reference for DAPPER preprocessing. Some extensions to the DAPPER procedures are outlined.

The flowchart of radiometer data processing is shown in figure 3.1.

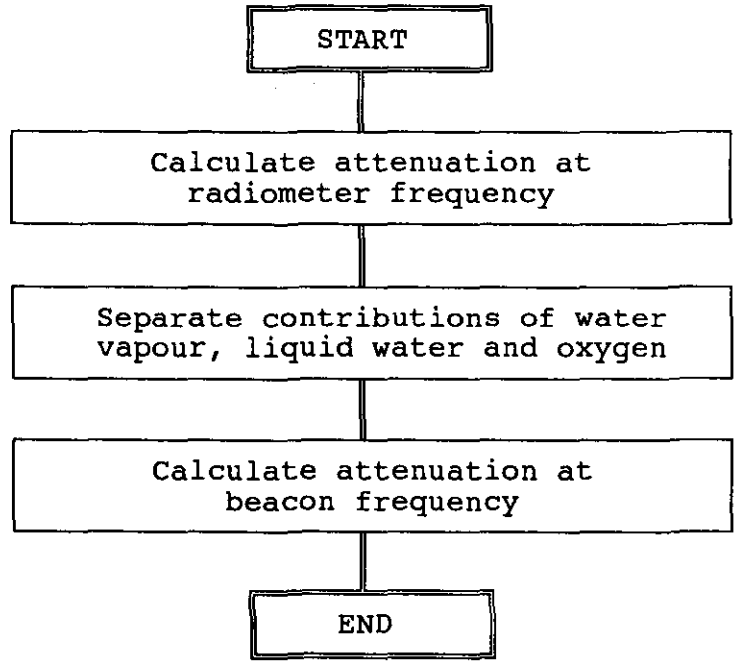

Figure 3.1: Flowchart of radiometer data processing

Attenuation due to oxygen, water vapour and liquid water are separated, because each of these contributions requires a different frequency scaling method. The attenuation on the propagation path during clear-sky conditions is given by:

$$A_t = A_v + A_l + A_o \qquad \text{(dB)} \tag{3.1}$$

where:

A_r = radiometer derived atmospheric attenuation (dB)
A_v = attenuation by water vapour (dB)
A_l = attenuation by liquid water (in clouds) (dB)
A_o = attenuation by oxygen (dB)

3.2 Atmospheric attenuation at radiometer frequency

• Purpose:
Calculate atmospheric attenuation at a radiometer frequency from the antenna noise temperature.

• Algorithm:
The formulae were derived in part 1 (2.45, 2.46).
Calculate the sky noise temperature T_s (K).

$$T_s = \frac{A_f}{h} T_a + \left(1 - \frac{A_f}{h}\right) T_g \quad (K) \tag{3.2}$$

Calculate attenuation at radiometer frequency.

$$A_r = 10 \log \left(\frac{T_m - T_c}{T_m - T_s} \right) \quad (dB) \tag{3.3}$$

• Input:
T_a = antenna noise temperature (K, RnTANT, n=0,1,2..) (variable)
T_g = ground noise temperature. In practice T_g may be approximated by the ambient temperature (K, M1TAMB) (variable)
A_f = feed loss (linear value >1) (constant).
h = antenna integration factor, part of the antenna pattern pointed to the sky (constant)
T_m = effective medium temperature (260..280 K) (constant)
T_c = cosmic noise temperature (4 K) (constant)

• Output:
A_r = attenuation at radiometer frequency (dB) (variable).

• Comments:
- A_f and h are typical parameters of the radiometer.
- T_g is the effective noise temperature of the ground, that due to reflectivity does not have to be equal to the physical temperature. Therefore it is recommended to use:

$$T_g = A_g + B_g T_e \quad (K) \tag{3.4}$$

where A_g and B_g are constants, representing a constant noise contribution and a temperature varying noise contribution. T_e is the ambient temperature (M1TAMB). This method is also used in DAPPER preprocessing (see part III).
- Equation (3.2) assumes a simple model of the radiometer antenna pattern. If the antenna pattern of a specific radiometer is known, this equation can be adapted to obtain more accurate results.
- Values of T_m and T_c may be obtained from CCIR recommendations. An alternative way to determine T_m is given by equation (2.43) in part I.

3.3 Separation of attenuation to contributions of oxygen, water vapour and liquid water.

- Purpose:

Attenuation during clear-sky conditions is caused by oxygen, water vapour and liquid water, each of them requiring different frequency scaling methods. Therefore the measured attenuation has to be separated into contributions of oxygen, water vapour and liquid water. For a specific frequency, the attenuation changes in time due to the varying amount of water vapour and liquid water on the propagation path. The contribution of oxygen can be considered constant. The amount of water vapour is represented by the integrated water vapour content (V) and the amount of liquid water is represented by the integrated liquid water content (L). In other words the separation of attenuation contributions is equivalent to the calculation of V and L, the frequency independent variables.

- Parameters for the algorithm:

Equation (3.1) is equivalent to:

$$A_r = a_r V + b_r L + c_r \qquad \text{(dB)} \tag{3.5}$$

where: a_r = coefficient for water vapour attenuation (dB)/(kg/m^2)
b_r = coefficient for liquid water attenuation (dB)/(kg/m^2)
c_r = oxygen attenuation (dB)
V = integrated water vapour content (kg/m^2)
L = integrated liquid water content (kg/m^2)

The subscript 'r' indicates that radiometer frequencies are considered. Using CCIR attenuation prediction models, equations for a_r, b_r and c_r can be derived. This will provide the opportunity to calculate a parameter set (a_r, b_r, c_r) for every radiometer frequency.

a: coefficient for contribution of water vapour

V is the integrated water vapour content on the propagation path. Thus V is given by:

$$V = \int_0^d \rho_v \, dr \sim \frac{\rho_v \, h_{vo}}{\sin(\epsilon)} \quad (kg/m^2) \tag{3.6}$$

for $\rho_v < 12$ g/m^3 at 15°C,1013 hPa

where h_{vo} is the equivalent height of water vapour (2.2 km).

The attenuation caused by water vapour is given by (Part 1, (2.17)):

$$A_v = \frac{h_v \gamma_v}{\sin(\epsilon)} = aV \quad (dB) \tag{3.7}$$

Thus a is given by:

$$a = \left(0.067 + \frac{3}{(f-22.3)^2 + 7.3}\right) f^2 \, 10^{-4} \left(1 + \frac{1.36}{(f-22.3)^2 + 3}\right) cr_1 \tag{3.8}$$

where cr_1 is the temperature correction factor.

$$cr_1 = 1 - 0.01(Te-288) \tag{3.9}$$

V can be predicted from meteorological measurements, such as relative humidity or water vapour density. The EUT groundstation measures dry and wet bulb temperatures. These can be converted to relative humidity or water vapour density.

The saturated water vapour pressure at temperature T_i is approximated by [6]:

$$e_{si} = 5.86.10^5.T_i^{-5}.10^{20-\frac{2950}{T_i}} \quad (Pa) \tag{3.10}$$

$e_{s,i}$ is calculated for i=dry and i=wet. Now the atmospheric water vapour pressure e is given by [7]:

$$e = e_{s,wet} - H.P.(T_{dry} - T_{wet}) \quad (Pa) \tag{3.11}$$

where:

T_{dry} = dry bulb temperature (K)
T_{wet} = wet bulb temperature (K)
H = 6.62 10^{-4} $K^{-1}Pa^{-1}$ if the water on wet bulb is liquid
H = 5.70 10^{-4} $K^{-1}Pa^{-1}$ if the water on wet bulb is solid (ice)
P = atmospheric pressure (Pa)

The water vapour density is given by [6]:

$$\rho_v = 2.167\ e/T_{dry} \quad (g/m^3) \tag{3.12}$$

and the relative humidity RH (RH<100%) is given by:

$$RH = e/e_{s,dry}*100 \quad (\%) \tag{3.13}$$

If RH is measured directly, ρ_v can be derived from RH and the ambient temperature T_e.

$$\rho_v = RH\ 1.27.10^4\ T_e^{-6}\ 10^{\left(20 - \frac{2950}{T_e}\right)} \quad (g/m^3) \tag{3.14}$$

b: coefficient for contribution of liquid water (in clouds)

L is the integrated liquid water content on the propagation path:

$$L = \int_0^d \rho_l\ dr \approx \rho_l . h_l \quad (kg/m^2) \tag{3.15}$$

The attenuation contribution of liquid water is given in Part 1, (2.23) and (2.24).

$$A_l = h_l\ K_l\ \rho_l \quad (dB) \tag{3.16}$$

Thus b is given by:

$$b = 5.60.10^{-4}\ f^2\ 10^{0.0122(291\ -\ T_l)} \quad (dB)/(kg/m^2) \tag{3.17}$$

where

h_l = effective path length through clouds (km)
ρ_l = average liquid water density of the clouds (g/m^3)
T_l = effective temperature of the clouds (≈ 273 K)

If T_l is taken to be 0°C, b is given by:

$$b = 9.28.10^{-4}\ f^2 \quad (dB)/(kg/m^2)) \tag{3.18}$$

For L no prediction formulae are available because h_l and ρ_l depend strongly on the size and characteristics of the clouds.

c: contribution of oxygen

c is equal to the attenuation caused by oxygen on the propagation path (Part 1, (2.17)):

$$c = \frac{\gamma_0 h_0 \, e^{-h_s/h_0}}{\sin(\epsilon)} . cr_2 \quad (dB) \tag{3.19}$$

where:

$$\gamma_0 = \left(7.19.10^{-3} + \frac{6.09}{f^2 + 0.227} + \frac{4.81}{(f - 57)^2 + 1.50} \right) f^2 .10^{-3} \quad (dB/km) \tag{3.20}$$

$$cr_2 = 1 - 0.006(T_e - 288) \tag{3.21}$$

γ_0 = specific oxygen attenuation (dB/km)
h_0 = equivalent height for oxygen (6 km)
h_s = height above sea level (km)
cr_2 = temperature correction factor
Te = environment temperature (K)

• Comments:
- Figure 2 shows the graphs for a,b and c for $0<f<50$ GHz for the EUT conditions (ϵ = 26.7°, hs = 17m, Te = 15°C, Tl = 0°C).
- a,b and c require quite some floating point calculation, so it is preferable to consider these parameters constant for a specific frequency. In that case temperature correction may be done on the constant a,b and c at 15°C. Thus a set of a,b,c for every radiometer frequency can be supplied.
- The formulae for a, b and c, can be used to calculate coefficients for use in DAPPER (see part III). Note that in DAPPER no temperature correction is performed.

• Algorithm:
V and L can be solved from a set of linear equations. The following cases can be distinguished:
- measurements at two or more radiometer frequencies
- measurements at one radiometer frequency
- no radiometer measurements

- Measurements at two or more radiometer frequencies:
If radiometer measurements are present at the beacon frequencies, the attenuation at beacon frequencies is already known. In practice the radiometer frequency may be close but is never equal to the beacon frequency. V and L calculation require at least radiometer measurements at 2 different frequencies. When radiometer measurements are present at 3 or more frequencies, the two highest frequencies should be chosen [4].

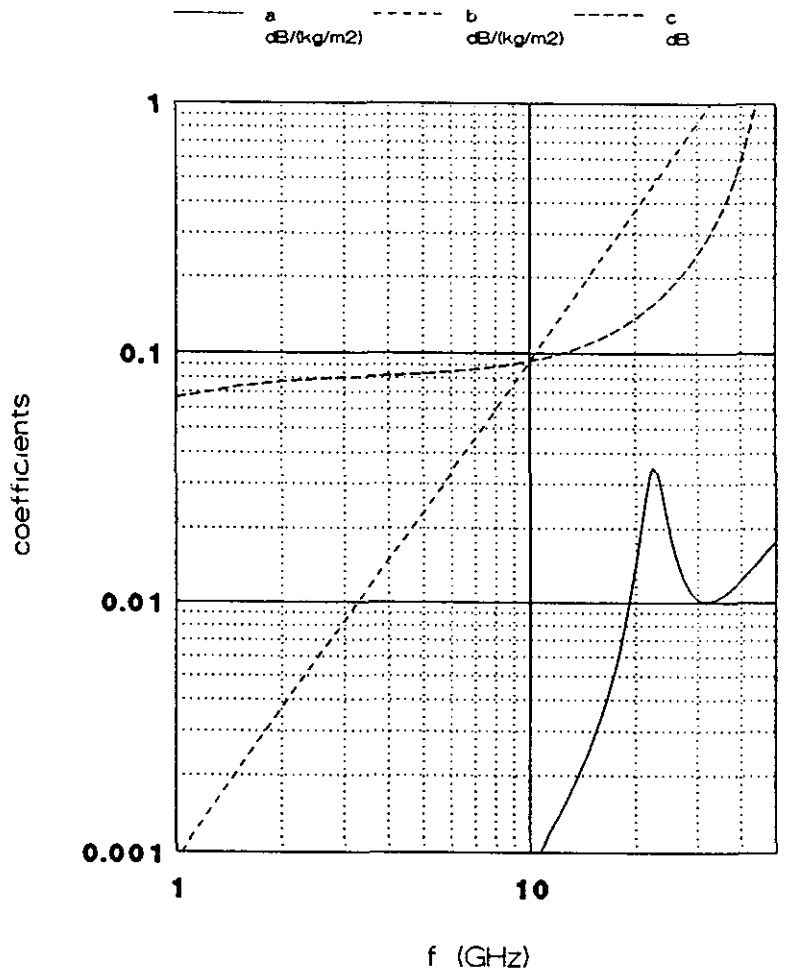

Figure 3.2 Coefficients of atmospheric attenuation

Using measurements at two different frequencies the following linear equation pair has to be solved:

$$A_{r1} = a_{r1}V + b_{r1}L + c_{r1} \quad (dB)$$
$$A_{r2} = a_{r2}V + b_{r2}L + c_{r2} \quad (dB) \qquad (3.22)$$

where A_{r1} and A_{r2} are the attenuation at the two radiometer frequencies.

Integrated liquid water content (L):

$$L = \frac{A_{r2} - (A_{r1} - c_{r1})\frac{a_{r2}}{a_{r1}} - c_{r2}}{b_{r2} - b_{r1}\frac{a_{r2}}{a_{r1}}} \quad (kg/m^2) \tag{3.23}$$

Integrated water vapour content (V):

$$V = \frac{A_{r1} - b_{r1}L - c_{r1}}{a_{r1}} \quad (kg/m^2) \tag{3.24}$$

- Measurements at one radiometer frequency:

V can be predicted from meteorological measurements. L is solved from the remaining attenuation measurement.

$$L = (A_{r1} - a_{r1}V - c_{r1})/b_{r1} \quad (kg/m^2) \tag{3.25}$$

- No radiometer measurements:

V can be predicted from meteorological measurements, but L can not be predicted. The only assumption that can be made is:

$$L = 0 \tag{3.26}$$

This method should only be used when cloud attenuation is negligible. This requires means of cloud detection.

- Input:

A_{rn} = attenuation at radiometer frequency (dB, n=1,2..) (variable)
a_{rn} = coefficient for the attenuation of water vapour (dB/(kg/m^2),n=1,2..) (constant)
b_{rn} = coefficient for the attenuation of liquid water (dB/(kg/m^2),n=1,2..) (constant)
c_{rn} = coefficient for the attenuation of oxygen (dB, n=1,2..) (constant)
T_e = ambient temperature (≈T_{dry}) (K, M1TAMB) (variable)
T_l = effective cloud temperature (K) (constant)
T_{dry} = dry bulb temperature (K, M1TAMB) (variable)
T_{wet} = wet bulb temperature (K, M2TAMB) (variable)
P = atmospheric pressure (Pa, M1PATM) (variable)
H = constant for conversion of dry and wet bulb temperature to water vapour pressure (Pa/K) (constant)

• Output:
V = integrated water vapour content (kg/m^2) (variable)
L = integrated liquid water content (kg/m^2) (variable)

• Comments:
- The user has to calculate a,b,c for every radiometer frequency.
- The user should be able to choose the method for solving V and L.
- If radiometer measurements at more than two frequencies are available, other methods using all measurements may be used to solve V and L.

3.4 Attenuation at beacon frequencies

• Purpose:
Calculate attenuation at beacon frequencies by frequency scaling of the individual contributions of water vapour, liquid water and oxygen.

• Algorithm:
Calculate a set of a, b and c for the beacon frequencies. Table 1 gives the values of a,b and c for the OLYMPUS beacon frequencies and EUT conditions (ϵ = 26.7°, hs = 17m, Te = 15°C, Tl = 0° C). The attenuation at a beacon frequency is calculated by:

$$A_{Bi} = a_{Bi}V + b_{Bi}L + c_{Bi} \quad \text{(dB)} \qquad (3.27)$$
$$i = 0,1,2$$

where A_{Bi} is the attenuation at beacon Bi.

Table 3.1: Atmospheric attenuation coefficients for OLYMPUS at EUT groundstation

Coefficients Beacon	a (dB/(kg/m^2))	b (dB/(kg/m^2))	c (dB)
B0	0.0015	0.14	0.10
B1	0.012	0.36	0.14
B2	0.010	0.82	0.24

• Input:
V = integrated water vapour content (kg/m^2) (variable)
L = integrated liquid water content (kg/m^2) (variable)
a_{Bi} = coefficient for the attenuation of water vapour (dB/(kg/m^2), n=1,2..) (constant)
b_{Bi} = coefficient for the attenuation of liquid water (dB/(kg/m^2), n=1,2..) (constant)
c_{Bi} = coefficient for the attenuation of oxygen (dB, n=1,2..) (constant)

• Output:
A_{Bi} = attenuation at beacon frequency (dB, n=1,2..) (variable)

• Comments:

- A_{Bi} is not corrected for the temperature. This may be done equivalent to paragraph 3.2. If temperature correction is not applied here, this should also be left out in deriving V and L. Then the temperature dependence of a_{Bi} will go to V and only c_{Bi} will cause a small error in A_{Bi}.
- In DAPPER preprocessing (see part III), the user has to input the values of table 3.1. Note that the default parameter set in DAPPER is only valid for an elevation angle of 90° (zenith).

4 TEMPLATE EXTRACTION

4.1 Introduction

In template extraction, templates are derived, that incorporate the predictable influence of the measurement system in both copolar and crosspolar measurements. This influence has a low frequency behaviour. Typically a template value changes only every 15 minutes. Templates are derived from averaging measured values during clear-sky conditions. Different bias removal methods require different templates:

- copolar level templates for copolar bias removal
- crosspolar phasor templates for vector cancellation
- matrix templates for matrix cancellation

The flowdiagram of template extraction is shown in figure 4.1

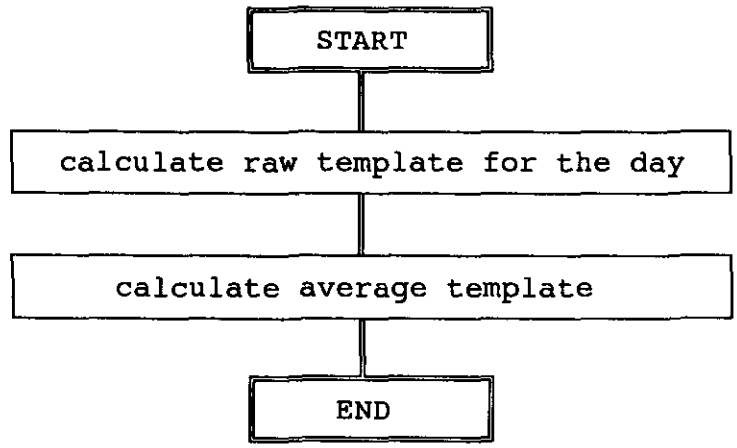

Figure 4.1: Flowchart of template extraction

First a raw template is derived for the clear-sky period of the actual day. Then by averaging over several days an average template for the day is derived. Every raw template is assumed to have a certain diurnal behaviour. During a non-clear-sky period raw template points are not available and a gap appears in the template. This gap can be filled with template points using linear interpolation, if the gap is not too large.

The following paragraphs give the procedures to derive template values from EUT measurements during clear-sky conditions. Then the algorithms are given to derive raw and average templates.

4.2 Copolar level

- Purpose:

Calculate copolar level values suitable to build raw templates.

• Algorithm:

The measured copolar level during clear-sky is corrected for the atmospheric attenuation derived from radiometer measurements:

$$CPL = CPL_{meas} + A_{Bi} \quad (dB) \quad (4.1)$$
$$i = 0,1,2$$

• Input:

CPL_{meas} = measured copolar level (dB, B0VCPL, B1HCPL, B1VCPL, B2VCPL) (variable)

A_{Bi} = attenuation at beacon frequency Bi (dB, i=0,1,2) (variable)

• Output:

CPL = copolar level for a beacon suitable to build templates (dB) (variable)

• Comments:

- Templates for copolar phase differences are directly derived from copolar phase measurements (B1VHPH)

4.3 Crosspolar phasor

• Purpose:

Derive crosspolar phasor values from EUT measurements for vector cancellation. This phasor has an inphase and quadrature component:

$$\delta = I_\delta + jQ_\delta \quad (4.2)$$

• Algorithm:

The crosspolar phasor is a linear parameter and can be derived from EUT measurements.

$$I_\delta = 10^{-XPD/20} \cos(DPH) \quad (4.3)$$

$$Q_\delta = 10^{-XPD/20} \sin(DPH) \quad (4.4)$$

• Input:

XPD = measured crosspolar discrimination (dB, B0VXPD, B1HXPD, B1VXPD, B2VXPD)

DPH = measured differential phase between crosspolar and copolar signal (°, B0VDPH, B1HDPH, B1VDPH, B2VDPH)

• Output:

I_δ = inphase component of the crosspolar phasor

Q_δ = quadrature component of the crosspolar phasor

• Comments:
- A standard groundstation according to OPEX measures inphase and quadrature components of the beacon signals. The algorithm for these measurements is given in appendix A. This algorithm has been implemented by the developers of DAPPER.

4.4 Matrix

• Purpose:
Build a receive matrix from EUT measurements. This is only applicable for the dual polarized beacon (B1).

• Algorithm:
Calculate parameters of receive matrix from EUT measurements. The matrix is given by:

$$U=\begin{pmatrix} I_{xx}+jQ_{xx} & I_{xy}+jQ_{xy} \\ I_{yx}+jQ_{yx} & I_{yy}+jQ_{yy} \end{pmatrix} \tag{4.5}$$

If the xx signal is considered to be the phase-reference (Q_{xx} = 0), the parameters are given by:

$$I_{xx} = 10^{HCPL/20}.10^{-MAX/20} \tag{4.6}$$

$$Q_{xx} = 0 \tag{4.7}$$

$$I_{yx} = I_{xx}.10^{-HXPD/20}.\cos(HDPH) \tag{4.8}$$

$$Q_{yx} = I_{xx}.10^{-HXPD/20}.\sin(HDPH) \tag{4.9}$$

$$I_{yy} = 10^{VCPL/20}.\cos(VHPH).10^{-MAX/20} \tag{4.10}$$

$$Q_{yy} = 10^{VCPL/20}.\sin(VHPH).10^{-MAX/20} \tag{4.11}$$

$$I_{xy} = 10^{VCPL/20-VXPD/20}.\cos(VDPH+VHPH).10^{-MAX/20} \tag{4.12}$$

$$Q_{xy} = 10^{VCPL/20-VXPD/20}.\sin(VDPH+VHPH).10^{-MAX/20} \tag{4.13}$$

• Input:
HCPL = copolar level of horizontal polarization (dB, B1HCPL) (variable)
HXPD = crosspolar discrimination of horizontal polarization (dB, B1HXPD) (variable)
HDPH = phase difference between cross- and copolar signal of horizontal polarization (°, B1HDPH) (variable)
VCPL = copolar level of vertical polarization (dB, B1VCPL) (variable)
VXPD = crosspolar discrimination of vertical polarization (dB, B1VXPD) (variable)

VDPH = phase difference between cross- and copolar signal of vertical polarization (°, B1VDPH) (variable)
VHPH = phase difference between copolar signals of vertical and horizontal polarization (°, B1VHPH) (variable)
MAX = range maximum of copolar level (dB) (constant)

- Output:

U = receive matrix with 8 parameters (linear values) (variable)

4.5 Raw and average templates

- Purpose:

Build raw and average templates for the parameters derived in paragraph 4.2 to 4.4. Raw template points are calculated by averaging clear-sky parameter values for a certain time. Average templates are calculated by averaging raw templates over several days. Templates are always derived for a period of one day.

- Algorithm:

A raw template point is calculated every 15 minutes by averaging over a number of seconds around the 15 minute timestamp (97 points per day). The template has the value of a template point for the whole period of 15 minutes. Consider z to be a parameter suitable for building templates.

$$z_{rtempl} = \frac{\sum_{1}^{M} z}{M} \tag{4.14}$$

z_{rtempl} is the raw template for parameter z. If a gap appears in the template, this gap can be linearly interpolated if the gap time is smaller than a defined time period T_{def}.

The average template is calculated by averaging raw template points (of the same timestamp) over a user defined number of days (N). If a template point of a day is not valid, this point should not be used in the averaging process.

$$z_{atempl} = \frac{\sum_{1}^{N} z_{rtempl}}{N} \tag{4.15}$$

- Input:

z = parameter suitable to build templates (see paragraph 4.2 to 4.4) (variable)
T = number of seconds to average for calculating raw templates points (typically 60 s) (constant)
N = number of days to average for calculating average templates (constant)
T_{def} = maximum number of seconds of a gap that can be interpolated (s) (constant)

- Output:

z_{rtempl} = raw template of a parameter for one day (variable)

z_{atempl} = average template of a parameter for one day (variable)

- Comments:

- T determines the frequency content of the raw template and thus how unpredictable errors may deteriorate the raw template.
- N determines how fast the average template adapts to changes in the diurnal behaviour. If the diurnal behaviour changes rapidly, the system behaviour is not easily predictable and N should be kept small (1 to 2 days).
- The interpolation procedure may be adapted if linear interpolation is not appropriate
- The uncertainty in the average template can be calculated from the standard deviation of template points of the same timestamp of the used raw templates
- The user should choose T, N and T_{def} and experiment with several values. It is not yet known how they will influence the templates and bias removal in practice.

5 BIAS REMOVAL

5.1 Introduction

In bias removal the predictable influence of the measurement system is removed from copolar and crosspolar measurements. Bias removal uses average templates built by template extraction. Three methods can be distinguished:
- copolar bias removal
- crosspolar vector bias removal
- crosspolar matrix bias removal

For bias removal the same parameters have to be derived from EUT measurements as in template extraction. Procedures are given in chapter 4.

5.2 Copolar bias removal

• Purpose:
Determine atmospheric attenuation and phase-shift.

• Algorithm:
Correct measured copolar level with copolar level template:

$$CPA = CPL_{templ} - CPL_{meas} \quad (5.1)$$

Correct measured copolar phase with copolar phase template:

$$CPH = CPH_{meas} - CPH_{templ} \quad (5.2)$$

• Input:
CPL_{templ} = template of copolar level for a certain beacon (dB) (variable)
CPL_{meas} = measured copolar level (dB, B0VCPL, B1HCPL, B1VCPL, B2VCPL) (variable)
CPH_{templ} = template of copolar phase shift (°, B1VHPH) (variable)
CPH_{meas} = measured copolar phase shift (°, B1VHPH) (variable)

• Output:
CPA = atmospheric attenuation for a certain beacon (dB, B0VCPA, B1HCPA, B1VCPA, B2VCPA) (variable)
CPH = atmospheric phase shift (°, B1VHPH)

5.3 Crosspolar vector correction

• Purpose:
Determine atmospheric crosspolarization using vector cancellation.

• Algorithm:
Correct the measured crosspolar phasor with the template crosspolar phasor:

$$\delta_{corr} = \delta_{meas} - \delta_{templ} \tag{5.3}$$

As δ has an inphase and quadrature component this can be implemented as:

$$I_{\delta corr} = I_{\delta meas} - I_{\delta templ} \tag{5.4}$$

$$Q_{\delta corr} = Q_{\delta meas} - Q_{\delta templ} \tag{5.5}$$

The crosspolar discrimination and phase is calculated from the corrected crosspolar phasor δ_{corr}.

$$XPD_{corr} = -10\log(I_{\delta corr}^2 + Q_{\delta corr}^2) \quad \text{(dB)} \tag{5.6}$$

$$DPH_{corr} = \text{arctg}(Q_{\delta corr}/I_{\delta corr}) \tag{5.7}$$

$$(0..360°)$$

• Input:
$I_{\delta templ}$ = inphase component of template crosspolar phasor (variable)
$Q_{\delta templ}$ = quadrature component of template crosspolar phasor (variable)
$I_{\delta meas}$ = inphase component of measured crosspolar phasor (variable)
$Q_{\delta meas}$ = quadrature component of measured crosspolar phasor (variable)

• Output:
$I_{\delta corr}$ = inphase component of corrected crosspolar phasor (variable)
$Q_{\delta corr}$ = quadrature component of corrected crosspolar phasor (variable)
XPD_{corr} = crosspolar discrimination after correction (dB, B0VXPD, B1HXPD, B1VXPD, B2VXPD) (variable)
DPH_{corr} = phase of crosspolar phasor after correction (°, B0VDPH, B1HDPH, B1VDPH, B2VDPH) (variable)

• Comments:
- The user may choose to perform matrix cancellation for the dual-polarized beacon B1. In that case vector cancellation is not performed for the B1 beacon.
- A standard groundstation according to OPEX measures inphase and quadrature components of the beacon signals. The algorithm for these measurements is given in appendix A. This algorithm has been implemented by the developers of DAPPER.

5.4 Crosspolar matrix correction

• Purpose:
Determine atmospheric crosspolarization using matrix cancellation. This is only applicable for dual polarized beacons (OLYMPUS B1).

- Algorithm:

Calculate the cancellation matrix K.

$$K = U_{templ}^{-1} \tag{5.8}$$

where U_{templ} is the template matrix derived from during clear-sky conditions. For a 2 by 2 matrix the inverse can easily be calculated:

$$U_{templ}^{-1} = \frac{1}{det}\begin{pmatrix} I_{yytempl}+jQ_{yytempl} & -I_{xytempl}-jQ_{xytempl} \\ -I_{yxtempl}-jQ_{yxtempl} & I_{xxtempl}+jQ_{xxtempl} \end{pmatrix} \tag{5.9}$$

where det is the determinant of U_{templ}.

The corrected matrix is calculated by performing either left or right cancellation (matrix multiplications):

Left cancellation (groundstation correction):

$$T_{corr} = K\, U_{meas} \tag{5.10}$$

Right cancellation (satellite correction):

$$T_{corr} = U_{meas}\, K \tag{5.11}$$

T_{corr} is a matrix with 8 parameters:

$$T_{corr} = \begin{pmatrix} I_{xxcorr}+jQ_{xxcorr} & I_{xycorr}+jQ_{xycorr} \\ I_{yxcorr}+jQ_{yxcorr} & I_{yycorr}+jQ_{yycorr} \end{pmatrix} \tag{5.12}$$

From this matrix the corrected XPD and phase are derived for both beacon polarizations:

$$XPD_{xcorr} = 10\log\left(\frac{I_{xxcorr}^2 + Q_{xxcorr}^2}{I_{yxcorr}^2 + Q_{yxcorr}^2}\right) \quad (dB) \tag{5.13}$$

$$DPH_{xcorr} = \text{arctg}(Q_{yxcorr}/I_{yxcorr}) - \text{arctg}(Q_{xxcorr}/I_{xxcorr}) \tag{5.14}$$

$$(0..360°)$$

The y-polarization values are derived by interchanging the indices in (5.13) and (5.14).

- Input:

U_{templ} = template matrix (variable)

U_{meas} = measured receive matrix (variable)

● Output:

T_{corr} = corrected transmission matrix (variable)

XPD_{xcorr} = crosspolar discrimination for horizontal polarization after correction (dB, B1HXPD) (variable)

XPD_{ycorr} = crosspolar discrimination for vertical polarization after correction (dB, B1VXPD) (variable)

DPH_{xcorr} = phase of crosspolar phasor for horizontal polarization after correction (°, B1HDPH) (variable)

DPH_{xcorr} = phase of crosspolar phasor for vertical polarization after correction (°, B1VDPH) (variable)

● Comments:

- The user should be able to choose either the left or right cancellation method.

6 CONCLUSIONS AND RECOMMENDATIONS

6.1 Conclusions

The EUT groundstation is capable of receiving all the beacons transmitted by the OLYMPUS satellite. Algorithms have been developed to perform the preprocessing of the beacon measurements for the EUT groundstation configuration. In preprocessing, the measurements are corrected for the influence of the satellite and groundstation and converted to a format, suitable for data analysis. Preprocessing consists basically of three processing stages that affect the raw measurement values:

- Radiometer data processing:

Using radiometer measurements at either no, 1, 2 or more frequencies, atmospheric attenuation can be calculated at the beacon frequencies. During clear-sky this provides the opportunity to determine the reference level for attenuation measurements. If no or only one radiometer frequency is available, information about the humidity has to be supplied.

- Template extraction:

From clear-sky measurements the system behaviour may be determined. The diurnal behaviour is represented by templates of one day. The uncertainty in templates can be calculated from the variation of the diurnal behaviour.

- Bias removal:

The measurement system bias is removed using appropriate methods for bias removal. The bias removal procedures make use of the templates derived in template extraction. For crosspolar measurements, procedures for vector and matrix cancellation are given.

The algorithms have yet to be implemented in software together with some general procedures to interface with the user. These algorithms are in principle compatible with the algorithms implemented in DAPPER preprocessing. Some have actually been used by the developers of DAPPER.

Limitations of the methods should not be disregarded. The most important are:
- The measurement system is assumed to have some kind of diurnal behaviour. Due to unpredictable errors, this behaviour may be deteriorated, so that bias removal does not improve the accuracy of the results.
- The method to calculate attenuation from radiometer antenna noise measurements may not be very accurate. This could be improved by adapting the formulae for a know antenna pattern of a radiometer.

6.2 Recommendations

During the implementation of the algorithms, it is recommended to consider:
- providing a suitable user interface to inspect results

- providing the user with the opportunity to choose the methods he wants to use. This makes it possible to compare methods and compare the EUT preprocessing system with other preprocessing systems.
- keeping the internal data resolution sufficiently high.
- calculating the accuracy of preprocessing results, due to the uncertainty in templates.

The EUT preprocessing system can be used to evaluate preprocessing algorithms in practice and to compare with DAPPER preprocessing. After this initial phase, preprocessing of propagation data should be carried out with a fixed procedure, to obtain data for analysis with constant quality.

LITERATURE

[1] Barto, R., SOFTWARE VOOR HET OLYMPUS DATA SYSTEEM, Graduation Report, Eindhoven University of Technology, Faculty of Electr. Eng., Communications division, 1990.(in Dutch)

[2] CCIR Report 719-2, ATTENUATION BY ATMOSPHERIC GASES, Recommendations and Reports of the CCIR, ITU, Vol.5, 1986.

[3] CCIR Report 721-2, ATTENUATION BY HYDROMETEORS IN PARTICULAR PRECIPITATION AND OTHER ATMOSPHERIC PARTICLES, Recommendations and Reports of the CCIR, ITU, Vol.5, 1986, p.199-214.

[4] Ortgies, G., CORRECTION OF SATELLITE BEACON SIGNALS BY MEANS OF SIMULTANEOUSLY MEASURED CLEAR-AIR ATTENUATION WITH RADIOMETER, 5th URSI Com. Symp., Wave prop. and rem. sensing, La Londe, France, 11-15 Sept 1989, p.6.7.1-4.

[5] Dintelmann, F., LOW-ATTENUATION STATISTICS FOR 30-GHz EARTH TEMRINALS, 5th URSI Com. Symp., Wave prop. and rem. sensing, La Londe, France, 11-15 Sept 1989, p.6.5.1-4.

[6] Ippolito, L.J., PROPAGATION EFFECTS HANDBOOK FOR SATELLITE SYSTEMS DESIGN, A summary of propagation impairments on 10 to 100 GHz Satellite links with techniques for systems design, Washington: NASA, 1989, Ref. Publ.1082(04).

[7] BETRIEBSANLEITUNG ASPIRATIONS PSYCHROMETER NACH ASSMANN, Göttingen, 1976.

Appendix A: Crosspolar template extraction and bias removal in DAPPER

Template Extraction - Single polarized beacon

Vector normalisation of the XPL - template

General

$$(2.1) \qquad \delta = \frac{I_x + j\,Q_x}{I_c + j\,Q_c}$$

where

$$(2.2) \qquad I_\delta = \frac{I_x I_c + Q_x Q_c}{I_c^{\,2} + Q_c^{\,2}}$$

$$(2.3) \qquad Q_\delta = \frac{Q_x I_c - I_x Q_c}{I_c^{\,2} + Q_c^{\,2}}$$

δ ... normalized vector (to copolar)

I_δ, Q_δ ... inphase and quadrature components of 'δ';

Crosspolar average template (single polarized beacon)

$$(2.3) \qquad I_{\delta\,templ} = \frac{\sum_{1}^{n} I_\delta}{n}$$

$$(2.4) \qquad Q_{\delta\,templ} = \frac{\sum_{1}^{n} Q_\delta}{n}$$

$I_{\delta templ}$, $Q_{\delta templ}$	...	average template values
n	...	number of raw templates to be used; (user defined !)
δ_{templ}	...	Template vector for correction of crosspolar single polarized beacon components

(2.5) $$\delta_{templ} = I_{\delta templ} + j\, Q_{\delta templ}$$

Bias Removal

Vektor correction of crosspolar single polarized signals :

(3.1) $$\delta_{corr} = \delta_{meas} - \delta_{templ}$$

(3.2) $$\delta_{corr} = (I\delta x + j\, Q\delta x) - (I\delta templ + j\, Q\delta templ)$$

(3.3) $$I_{\delta corr} = \frac{Ix\,meas \cdot Ic\,meas + Qx\,meas \cdot Qc\,meas}{Ic\,meas^{2} + Qc\,meas^{2}} - I\delta templ$$

(3.4) $$Q_{\delta corr} = \frac{Qx\,meas \cdot Ic\,meas - Ix\,meas \cdot Qc\,meas}{Ic\,meas^{2} + Qc\,meas^{2}} - Q\delta templ$$

δtempl	...	averaged template (normalized)
δmeas	...	measured XP-vector (normalized)
Iδcorr,Qδcorr	...	corrected components of crosspolar signal
Icmeas, Qcmeas Ixmeas, Qxmeas	...	measured co- and crosspolar beacon components

(3.5) $$XPD_{corr} = -10 \log (I\delta corr^{2} + Q\delta corr^{2}) \quad [dB]$$

(3.6) $$arg\,(XPD_{corr}) = arctg \left(\frac{Q\delta corr}{I\delta corr} \right) \quad [deg]$$

XPDcorr	...	corrected crosspolar discrimination
arg(XPDcorr)	...	differential phase (co-and crosspolar)

Note : This method (developed by TU Eindhoven) will be used only for single polarized beacons !

Matrix correction of dual polarized beacon signals (crosspolar)

Multipliaction from left :

(3.7) $$\mathbf{T} = (\mathbf{M}_{templ})^{-1} . \mathbf{E}_m$$

Multiplication from right :

(3.8) $$\mathbf{T} = \mathbf{E}_m . (\mathbf{M}_{templ})^{-1}$$

$\mathbf{T}$	...	Transfer matrix
$\mathbf{M}_{templ}$	...	Template matrix (clear sky values)
$\mathbf{E}_m$	...	Matrix of measured values

(3.9) $$\mathbf{T} = \begin{vmatrix} I_{chcorr} + j\,Q_{chcorr} & I_{xvcorr} + j\,Q_{xvcorr} \\ I_{xhcorr} + j\,Q_{xhcorr} & I_{cvcorr} + j\,Q_{cvcorr} \end{vmatrix}$$

By replacing the index 'corr' with 'templ' or 'meas' (ie. $I_{chtempl}$ or I_{chmeas}, etc.) the 'M_{templ}' and the 'E_m'- matrices respectively, will be obtained !

(3.10) $$XPD_{hcorr} = 10 \log \left(\frac{I_{chcorr}^{\,2} + Q_{chcorr}^{\,2}}{I_{xhcorr}^{\,2} + Q_{xhcorr}^{\,2}} \right) \quad [dB]$$

(3.11) $$XPD_{vcorr} = 10 \log \left(\frac{I_{cvcorr}^{\,2} + Q_{cvcorr}^{\,2}}{I_{xvcorr}^{\,2} + Q_{xvcorr}^{\,2}} \right) \quad [dB]$$

(3.12) $$arg\left(XPD_{hcorr}\right) = arctg\left(\frac{Q_{xhcorr}}{I_{xhcorr}}\right) - arctg\left(\frac{Q_{chcorr}}{I_{chcorr}}\right) \quad [deg]$$

range : 0 - 360°

(3.13) $$arg\left(XPD_{vcorr}\right) = arctg\left(\frac{Q_{xvcorr}}{I_{xvcorr}}\right) - arctg\left(\frac{Q_{cvcorr}}{I_{cvcorr}}\right) \quad [deg]$$

range : 0 - 360°

Note : The matrix will be used only for the correction of crosspolar components of the dual polarized beacon !

III

SET-UP AND TESTS OF DAPPER PREPROCESSING

1 INTRODUCTION

Members of the OPEX (Olympus Propagation EXperiment) will operate groundstations in many parts of Europe to receive beacon signals of the OLYMPUS propagation payload. Standardization of procedures for data treatment by the individual experimenters is important to assure compatibility, comparability and to be able to collect data into a common data base.

The software system DAPPER (Data Analysis and Preprocessing for Propagation Effects Research) is designed to establish an agreed standard at least in Europe for propagation data processing. The data treatment consists of data preprocessing, a station dependent part, and data analysis, a station independent part. The software development is done by Siemens-PSE/IAS in Austria under contract by ESA (European Space Agency). As of July 1990 both systems are still under development. April 1990 a prototype of the preprocessing was supplied to EUT for evaluation, as EUT was the first ground station ready to use this software with real data. July 1990 an improved prototype of preprocessing was supplied to EUT.

This part considers operating the DAPPER preprocessing system. First a short overview is given of the preprocessing functions. In chapter 3 the set-up is described to use DAPPER at the EUT groundstation. Chapter 4 discusses tests of the first prototype with real EUT data. In chapter 5 some first results of preprocessing are presented, using the second prototype.

2 OVERVIEW OF DAPPER PREPROCESSING

The main objective of the standardized data preprocessing is to achieve 'cleaned' data suitable for analysis. Figure 2.1 shows the building blocks of DAPPER preprocessing.

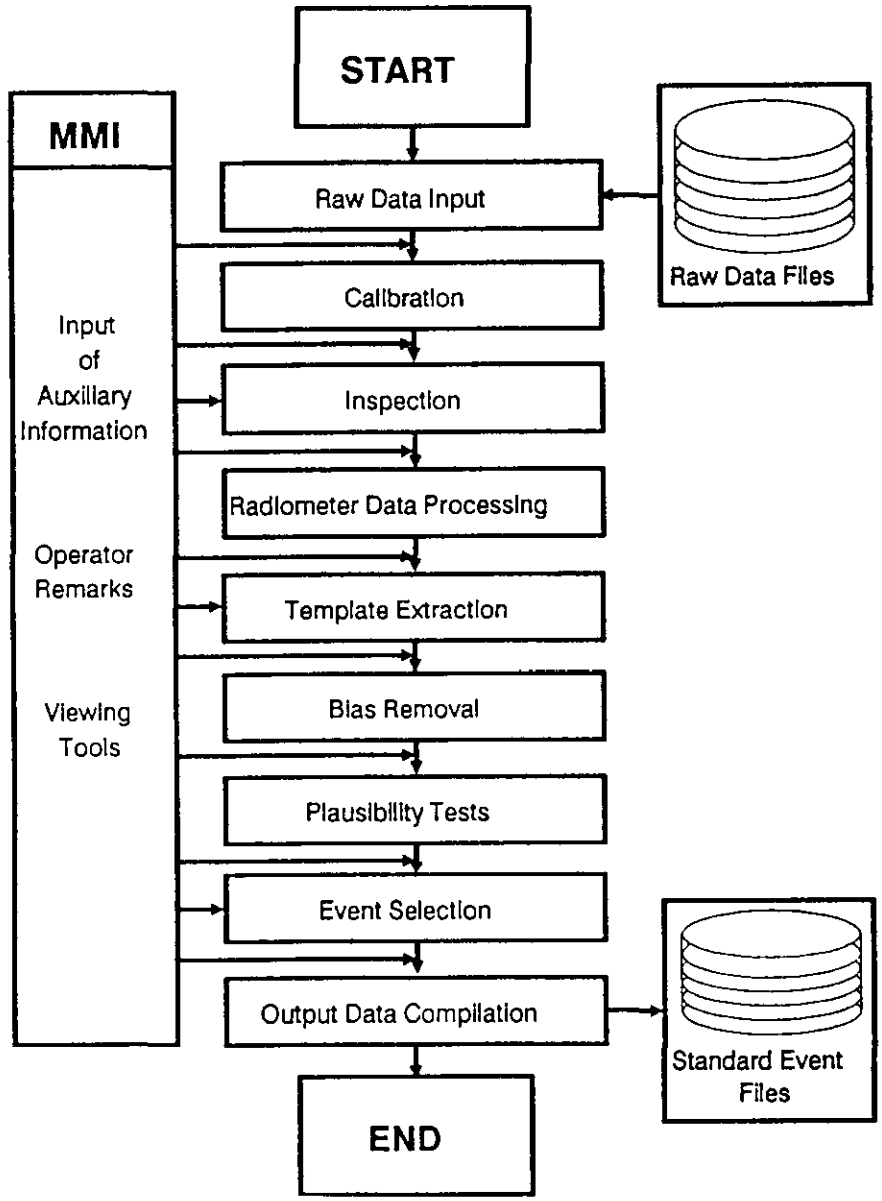

Figure 2.1: DAPPER preprocessing functions

The following functions are performed:

- Raw data input: Raw data files are read and converted to an internal data structure. An initial quality test is performed using status word information and performing consistency checks.
- Calibration: Raw data values are converted into physical values.
- Inspection: The user inspects data and can change data quality flags.

- Radiometer data processing: Radiometer noise measurements are converted to attenuation at radiometer and beacon frequencies.
- Template extraction: Clear-sky templates for periods of a day are derived from the beacon signals, showing the influence of the measurement system.
- Bias removal: Biases, introduced by the measurement system, are removed from the data.
- Plausibility tests: The data is checked to detect physical impossible behaviour.
- Event selection: Event periods are chosen semi-automatically.
- Output data compilation: Clean propagation data, user defined data and the journal file are stored in a standard event format.

Further tools to display and edit data and text information are supplied:
- Text editor
- Graphic editor

OPEX has defined a standard list of about 40 measurement channels that are supported by DAPPER. These channels have standard abbreviations [1]. Additional channels have to be defined as user channels. Standard channels consist of:
- beacon channels
- radiometer channels
- meteorological channels
- antenna channels
- status and time channels

Usually every experimenter has his own data acquisition system set up, with his own data base structure. A user of DAPPER has to convert his data format to the RDIF (Raw Data Input Format) of DAPPER. Subsequently DAPPER has to be configured for the groundstation measurements. The next chapter describes the set up procedure to use DAPPER at a groundstation (EUT groundstation).

3 SET-UP OF PREPROCESSING

3.1 Introduction

DAPPER software is designed for use at any OLYMPUS ground station. At a specific groundstation measurement data have to be converted to a format compatible with DAPPER and DAPPER has to be configured for the groundstation measurements. The following steps in the software set-up may be distinguished:
- conversion of data to DAPPER Raw Data Input Format
- define input channel reference table
- define status word reference table
- define output channel reference table
- define calibration curves
- determine default parameters to use in preprocessing

The target hardware system is a 386 machine running on SCO UNIX system V/386 release 3.2.0. This machine was present at EUT.

In the following paragraphs the set-up is given for the EUT groundstation. Detailed information about the routines to configure DAPPER can be found in the Software User's Manual Preprocessing Software [2]. The tables are given in the same format as in the Software Transfer Document [6].

3.2 Conversion to DAPPER

The file structure and data channels of EUT acquisition output are different from DAPPER input. A conversion module has to be developed. The EUT channels were listed in part II, Table 2.1. These are not all according to the standard OPEX channels [1]. Standard preprocessing is only performed on the standard OPEX channels. Consequently the conversion module has two functions:
- convert to Raw Data Input Format
- convert to standard OPEX channels

The conversion to the Raw Data Input Format is described by Barto [3]. The procedures to convert to the standard OPEX channels will be given here. Two types of inconsistencies occur between the EUT channel list and the OPEX channel list:
- EUT beacon channels are copolar level, crosspolar discrimination and differential phase. OPEX beacon channels are defined by the inphase and quadrature components of the beacon signals,
- EUT channels for the humidity are dry and wet bulb temperature. Standard OPEX channels are the relative humidity or water vapour density.

These inconsistencies require conversion of beacon channels and bulb temperatures. For DAPPER input, 37 channels are defined (Table 3.1). The abbreviations used are according to the DAPPER standards [2].

• Conversion of beacon channels

DAPPER requires linear Inphase and quadrature components of the beacon signals. EUT measures the copolar level, crosspolar discrimination and differential phase. The inphase and quadrature components will all be normalized to the maximum value of the copolar inphase component. Copolar and crosspolar signals are thus given by (beacon B0 and B2):

copolar signal: Ic + jQc (3.1)

crosspolar signal: Ix + jQx (3.2)

The measured voltage matrix for the B1 beacon is given by:

$$U=\begin{pmatrix} I_{xx}+jQ_{xx} & I_{xy}+jQ_{xy} \\ I_{yx}+jQ_{yx} & I_{yy}+jQ_{yy} \end{pmatrix} \quad (3.3)$$

As the phase of the copolar signal is arbitrary, Qc and Qxx are chosen to be 0. The following formulae are used in the conversion:

B0 and B2 beacon signal:

$$Ic = 10^{CPL/20}.10^{-MAX/20} \quad (3.4)$$

$$Qc = 0 \quad (3.5)$$

$$Ix = Ic.10^{-XPD/20}.\cos(DPH) \quad (3.6)$$

$$Qx = Ic.10^{-XPD/20}.\sin(DPH) \quad (3.7)$$

B1 beacon signal:

$$I_{xx} = 10^{HCPL/20}.10^{-MAX/20} \quad (3.8)$$

$$Q_{xx} = 0 \quad (3.9)$$

$$I_{yx} = I_{xx}.10^{-HXPD/20}.\cos(HDPH) \quad (3.10)$$

$$Q_{yx} = I_{xx}.10^{-HXPD/20}.\sin(HDPH) \quad (3.11)$$

$$I_{yy} = 10^{VCPL/20}.\cos(VHPH).10^{-MAX/20} \quad (3.12)$$

$$Q_{yy} = 10^{VCPL/20}.\sin(VHPH).10^{-MAX/20} \quad (3.13)$$

$$I_{xy} = 10^{VCPL/20-VXPD/20}.\cos(VDPH+VHPH).10^{-MAX/20} \quad (3.14)$$

$$Q_{xy} = 10^{VCPL/20-VXPD/20}.\sin(VDPH+VHPH).10^{-MAX/20} \quad (3.15)$$

Input:
CPL = copolar level (dB, B0VCPL, B2VCPL) (variable)
XPD = crosspolar discrimination (dB, B0VXPD, B2VXPD) (variable)
DPH = differential phase (°, B0VDPH, B2VDPH) (variable)
HCPL = copolar level of horizontal polarization (dB, B1HCPL) (variable)
HXPD = crosspolar discrimination of horizontal polarization (dB, B1HXPD) (variable)
HDPH = phase difference between cross- and copolar signal of horizontal polarization (°, B1HDPH) (variable)
VCPL = copolar level of vertical polarization (dB, B1VCPL) (variable)
VXPD = crosspolar discrimination of vertical polarization (dB, B1VXPD) (variable)
VDPH = phase difference between cross- and copolar signal of vertical polarization (°, B1VDPH) (variable)
VHPH = phase difference between copolar signals of vertical and horizontal polarization (°, B1VHPH) (variable)
MAX = maximum range of copolar level (30 dB) (constant)

Output:
I_c = inphase component of copolar beacon signal (B0VCPIN, B2VCPIN)
Q_c = quadrature component of copolar beacon signal (B0VCPQU, B2VCPQU)
I_x = inphase component of crosspolar beacon signal (B0VXPIN, B2VXPIN)
Q_x = quadrature component of crosspolar beacon signal (B0VXPQU, B2VXPQU)
I_{xx} = inphase component of copolar beacon signal horizontal polarization (B1HCPIN)
Q_{xx} = quadrature component of copolar beacon signal horizontal polarization (B1HCPQU)
I_{yx} = inphase component of crosspolar beacon signal horizontal polarization (B1HXPIN)
Q_{yx} = quadrature component of crosspolar beacon signal horizontal polarization (B1HXPQU)
I_{yy} = inphase component of copolar beacon signal vertical polarization (B1VCPIN)
Q_{yy} = quadrature component of copolar beacon signal vertical polarization (B1VCPQU)
I_{xy} = inphase component of crosspolar beacon signal vertical polarization (B1VXPIN)
Q_{xy} = quadrature component of crosspolar beacon signal vertical polarization (B1VXPQU)

Comments:
- Due to floating point calculations some accuracy may be lost. Results of the conversion are stored over the maximum integer range (-32767..32767), so that decrease of accuracy due to the quantization after conversion is negligible

• Humidity

For radiometer data processing relative humidity together with ambient temperature or the water vapour density is needed. Using this data it is possible to perform radiometer data processing in DAPPER even without radiometer data. The relative humidity can be calculated from dry (T_{dry}) and wet (T_{wet}) bulb temperatures of the psychrometer and from atmospheric pressure (P) using the following equations (see part II, 3.3).

The saturated water vapour pressure $e_{s,i}$ at temperature T_i is approximated by [4]:

$$e_{si} = 5.86.10^5.T_i^{-5}.10^{20-\frac{2950}{T_i}} \quad (Pa) \tag{3.16}$$

$e_{s,i}$ is calculated for i=dry and i=wet. Now the atmospheric water vapour pressure e is given by [5]:

$$e = e_{s,wet} - H.P.(T_{dry} - T_{wet}) \quad (Pa) \tag{3.17}$$

where:

T_{dry} = dry bulb temperature (K)
T_{wet} = wet bulb temperature (K)
$H = 6.62\ 10^{-4}\ K^{-1}Pa^{-1}$ if the water on wet bulb is liquid
$H = 5.70\ 10^{-4}\ K^{-1}Pa^{-1}$ if the water on wet bulb is solid (ice)
P = atmospheric pressure (Pa)

The water vapour density ρ_v is given by [4]:

$$\rho_v = 2.167\ e/T_{dry} \quad (g/m^3) \tag{3.18}$$

and the relative humidity RH (RH<100%) is given by:

$$RH = e/e_{s,dry}*100 \quad (\%) \tag{3.19}$$

Either ρ_v or RH can be chosen for DAPPER input. Here both ρ and RH are calculated to test radiometer data processing in DAPPER.

Input:
T_{dry} = dry bulb temperature (K, M1TAMB) (variable)
T_{wet} = wet bulb temperature (K, M2TAMB) (variable)
P = atmospheric pressure (Pa, M1PATM) (variable)
H = psychrometer constant ($K^{-1}Pa^{-1}$, constant)

Output:
ρ_v = water vapour density (g/m^3, M1RHO) (variable)
RH = relative humidity (%, M1RLHUM) (variable)

Comments:
- To keep accuracy, the maximum integer range is chosen for the output values.
- The following channels may be added to the input channel list, when these measurements are available:
  - standard deviation of copolar level
  - antenna pointing
  - antenna tracking error

Table 3.1: DAPPER input channels (July 1, 1990)

EUT	CHANNEL	DESCRIPTION		OLYMPUS	OPEX CHANNEL STANDARDS
Chn	Abbreviation	Range	Unit	Sample range	Description
0	B0VCPIN	-1..1	_	-32767..32767	inphase copolar level B0,V
1	B2VCPIN	-1..1	_	-32767..32767	inphase copolar level B2,V
2	B1HCPIN	-1..1	_	-32767..32767	inphase copolar level B1,H
3	B1VCPIN	-1..1	_	-32767..32767	inphase copolar level B1,V
4	B0VCPQU	-1..1	_	-32767..32767	quadrature copolar B0,V
5	B2VCPQU	-1..1	_	-32767..32767	quadrature copolar B2,V
6	B1HCPQU	-1..1	_	-32767..32767	quadrature copolar B1,H
7	B1VCPQU	-1..1	_	-32767..32767	quadrature copolar B1,V
8	B0VXPIN	-0.17783..0.17783	_	-32767..32767	inphase crosspolar B0,V
9	B2VXPIN	-0.17783..0.17783	_	-32767..32767	inphase crosspolar B2,V
10	B1HXPIN	-0.17783..0.17783	_	-32767..32767	inphase crosspolar B1,H
11	B1VXPIN	-0.17783..0.17783	_	-32767..32767	inphase crosspolar B1,V
12	B0VXPQU	-0.17783..0.17783	_	-32767..32767	quadrature crosspolar B0,V
13	R0TANT_	0..310	K	0..4096	radiometer at 12 GHz
14	R1TANT_	0..310	K	0..4096	radiometer at 20 GHz
15	R2TANT_	0..310	K	0..4096	radiometer at 30 GHz
16	M1TAMB_	311..247	K	0..4096	dry bulb temperature
17	M2TAMB_	311..247	K	0..4096	wet bulb temperature
18	M1RAING	0..150	mm/h	0..4096	rain rate
19	M2RAING	0..10	mm	0..4096	rain cumulative
20	M1PATM_	800..1100	hPa	0..4096	atmospheric pressure
21	R1TREF_	305..315	K	0..4096	radiometer ref. temp. 1
22	M1WINDV	0..100	m/s	0..4096	wind velocity (speed)
23	M1WINDD	0..360	deg	0..4096	wind velocity (direction)
24	R2TREF_	305..315	K	0..4096	radiometer ref. temp. 2
25	UYKSPAN	0..10	V	0..4096	user channel
26	UTEST4_	0..10	V	0..4096	user channel
27	UTEST5_	0..10	V	0..4096	user channel
28	UTEST6_	0..10	V	0..4096	user channel
29	URADIOT	0..10	V	0..4096	user channel
30	B3VXPD_	15..45	dB	0..4096	ECS crosspolar discrimination
31	B3VCPL_	0..30	dB	0..4096	ECS copolar level
32	B2VXPQU	-0.17783..0.17783	_	-32767..32767	quadrature crosspolar B2,V
33	B1HXPQU	-0.17783..0.17783	_	-32767..32767	quadrature crosspolar B1,H
34	B1VXPQU	-0.17783..0.17783	_	-32767..32767	quadrature crosspolar B1,V
35	M1RHO__	0..50	g/m^3	0..32767	water vapour density
36	M1RLHUM	0..100	%	0..32767	relative humidity

3.3 Input Channel Reference Table

The input channel reference table contains all the information concerning the input channels. For every channel the following information has to be supplied:

user's channel number	:	channel number (0..999)
abbreviation	:	(standard) abbreviation (8 characters)
internal channel code	:	S (for OPEX channel, else 'U')
full channel name	:	full name for output purposes
measurement range min	:	minimum range of raw data input
measurement range max	:	maximum range of raw data input
calibration method	:	method for calibration (0,1,2,3), 1 uses a calibration file
calibration file name	:	name of the calibration file (6 characters)
conversion factor	:	output resolution factor of calibration
unit	:	unit of the channel
sample interval	:	(1,10,60 seconds)

A raw data input file is recognized by its system acquisition code ('0000' for EUT groundstation). Appendix A1 gives the ICRT for the input channel list (table 3.1). Whenever a channel description changes, the ICRT has to be changed.

3.4 Status Word Reference Table

The SWRT describes the meaning and effects of status words. EUT uses 2 status words of 16 bits, every bit representing the validity of one EUT channel (channel 0..31). An invalid EUT channel can affect more OPEX channels because of the conversion. The user has to define the following entries for every possible condition:

Status Word Number	:	0 or 1
Status Word abbreviation	:	e.g. STATUS0_ (8 characters)
Code	:	16 bits code e.g. xxxxx1xxxxxxxxx0 (x = don't care)
Channel abbreviation	:	abbreviation of channel affected (8 characters)
Flag number	:	0,1,2,3,4
Status Report Text	:	e.g. invalid raw B0VCPA

Appendix A2 gives the status word entries for the EUT channels (acquisition code '0000').

3.5 Output Channel Reference Table

The OCRT describes the output channels created by data preprocessing. These channels are transferred to the standard event file. The following fields are defined:

user's channel number	:	channel number (0..999)
abbreviation	:	(standard) abbreviation (8 characters)
channel standard	:	S (for standard processing, else 'P')
internal channel code	:	S (for OPEX channel, else 'U')
full channel name	:	e.g. copolar level B0
conversion factor	:	resolution of channel
unit	:	e.g. dB
sample interval	:	(1,10,60)

Appendix A3 gives the OCRT for the EUT groundstation (acquisition code '0000').

3.6 Calibration curves

Calibration curves are used to define the relation between raw data values and physical values. In the ICRT a calibration file is connected to an input channel. The definition of a calibration curve consists of two parts:
- define the in- and output specifications
- define the relation between in- and output values. This can be done by entering separate points or by entering parameters of an equation. Usually a linear equation is defined:

$$y = A + B\,x \tag{3.20}$$

where x is the input value and y is the output value. A and B are defined by the user.

For every linear calibration curve the following entries have to be defined:

Begin of validity	:	e.g. 900501000000
X unit	:	unit of raw data value
X conversion factor	:	resolution factor of input (has to be 1)
Y unit	:	unit of output value
Y conversion factor	:	resolution factor of calibration output
X-minimum	:	minimum x-range calibration curve
X-maximum	:	maximum x-range calibration curve
Y-minimum	:	minimum y-range calibration curve
Y-maximum	:	maximum y-range calibration curve
A, B	:	equation parameters

Appendix A4 gives the parameters of the calibration curves for the EUT groundstation.

Comments:
- The X conversion factor has to be 1 to operate DAPPER correctly
- The unit of X is not important if calibration is performed.
- The Y conversion factor is the same conversion factor as defined in the ICRT.
- The Y conversion factor determines the resolution of the calibration. The calibrated channels are used in preprocessing components so this resolution should be sufficiently high to assure that no accuracy is lost in the preprocessing. Here the resolution factor will be chosen about 10 times the resolution factor of the standard OPEX channels [1].

3.7 Parameter list

DAPPER asks the user to input parameters at several preprocessing stages. In order to perform standard preprocessing, a default parameter list should be used during the process. The following parameters have to input by the user:

RAW DATA INPUT

- Maximum difference between two consecutive samples of a channel.
This number is used to detect abnormal jumps (spikes) for flagging.

CALIBRATION

- Number of samples for averaging a channel.
For each channel out of the ICRT having the calibration method 2 or 3, the number of data points used to calculate the mean value is to be entered.

INSPECTION

RADIOMETER DATA PROCESSING

- For every radiometer:

h	:	antenna pattern integration factor
Ag, Bg	:	model constants for estimation of ground temperature
Tm	:	effective medium temperature (K)
Tc	:	cosmic noise temperature (K)
a_r	:	coefficient for water vapour attenuation
b_r	:	coefficient for liquid water attenuation
c_r	:	coefficient for oxygen attenuation

- If no or only one radiometer frequency is available:

s	:	scale length for water vapour attenuation (km)

- For every beacon:

a_B	:	coefficient for water vapour attenuation
b_B	:	coefficient for liquid water attenuation
c_B	:	coefficient for oxygen attenuation

Comments:
- In the prototype of DAPPER, July 1990, it is not yet possible to input the a,b and c parameters for the radiometer frequencies, and it is assumed that the radiometer frequencies are at the beacon frequencies ($a_r = a_B$, $b_r = b_B$, $c_r = c_B$). This will be changed in future.

- The user has to determine the parameters for his groundstation configuration. Note that the parameters c and s depend on the elevation angle. Equations to calculate s, a, b and c were given in part II of this report (part II, chapter 3).

TEMPLATE EXTRACTION

number of seconds for averaging	:	number of seconds used to calculate one raw template point (60..180)
number of previous raw templates	:	number of previous raw template used for averaging
missing points per day	:	maximum number of invalid raw template points to create a valid raw template file.
abbreviation of total attenuation channel	:	channel used to determine clear-sky period automatically
threshold for total attenuation channel	:	threshold for clear-sky attenuation

BIAS REMOVAL

Matrix multiplication from left or right (L/R)		choose either left or right matrix cancellation for crosspolar correction for B1

PLAUSIBILITY TESTS

For every test:

Parameter subset	:	test set to determine impossible physical behaviour

EVENT SELECTION

For every automatic event selection:

parameter abbreviation	:	abbreviation of channel used to detect events
threshold	:	threshold for that channel
evaluation hint	:	indicating if event is found below (b) or above (a) threshold

OUTPUT DATA COMPILATION

country code	:	e.g. NL
groundstation code	:	e.g. EUT
longitude	:	longitude of groundstation (°)
latitude	:	latitude of groundstation (°)
altitude	:	altitude of groundstation (m)
tilt angle	:	tilt angle (°)
operator name	:	e.g. Van de Berg

Appendix A5 gives a suitable default parameter list for DAPPER to be used at EUT groundstation.

4 TEST OF PREPROCESSING

4.1 Introduction

DAPPER is a standard software system for processing and analysis of propagation measurements, developed by SIEMENS for the OLYMPUS propagation experiment (OPEX). A prototype was supplied to the EUT Olympus group at the OPEX conference, ESTEC, Noordwijk in March 1990. Most preprocessing functions are available in this prototype. This chapter gives comments on this prototype of DAPPER and hints for the user in addition to the DAPPER software users manual [1]. Realistic input data of the EUT groundstation is used to test the DAPPER procedures. The Detailed Design Documents of Preprocessing were used to understand the preprocessing software procedures and to verify the preprocessing algorithms [7] [8] [9] [10] [11] [12] [13] [14] [15] [16] [17] [18] [19].

4.2 General functions

4.2.1 Installation and start

DAPPER is initially developed for the UNIX operating system running on a 386 machine. Below the installation procedure to run DAPPER is given on SCO UNIX System V/386, release 3.2.0.

- installation — Install mouse and streams (parts of SCO UNIX): mkdev mouse, mkdev streams.
  Install X-Sight (Graphics server).
  Install DAPPER.

The DAPPER system is now ready to run. DAPPER software uses the following disk structure:

directory	contents
DAPPER = /usr/bin/proto3	executable files of DAPPER
HOME = /usr/proto3	working directory DAPPER, defaults parameters
HOME/rawdat	raw data files
HOME/data	internal signal files: temporary data
HOME/system	configuration, history, status
HOME/cali	calibration files
HOME/templ	raw and average templates
HOME/status	status and auxiliary reports
HOME/replay	replay files
HOME/sef	standard event files

DAPPER uses the X-server for graphics capabilities. X-Sight is started on a UNIX user by the command:

$ *X*

and terminated by the key combination Alt-PrtSc (Sys Rq).

- hints -The mouse does not function properly with X-Sight. This can be solved by moving the mouse when starting up X-Sight. This will slow down the X-initialisation and will catch the mouse.

DAPPER preprocessing is started on another UNIX user by the command:

$ *prep*

Change back to the X-server to get the graphics display of DAPPER.

4.2.2 Initialization

After a system breakdown or a fatal error, the user may want to initialise DAPPER. Otherwise the fatal error 'History file does not confirm with system status file' occurs. The following procedure should be used to establish the initialisation.

$ *cd $HOME/data*
$ *rm **
$ *cd $HOME/system*
$ *rm Prep_H**
$ *$DAPPER/sys*
$ *$DAPPER/history*
STATUS EINGEBEN: *E*
$ *cd*
$ *prep*

Old temporary data files are removed and new history and system status files are created. DAPPER will go to its initial status. This should not be done during processing.

4.2.3 Configuration

DAPPER is configured for a groundstation with reference tables: input channel (ICRT), status word (SWRT) and output channel reference table (OCRT). Tables are created and edited using a tool outside DAPPER:

$ *$DAPPER/Table*

This tool deals with all tables. Changing tables takes a lot of time and effort, as every channel has to be described separately. A channel can only be changed by entering a complete new channel description.

ICRT:
In the ICRT all raw data input channels have to be defined. In this table channels are connected to calibration files. The names of the channels should have 8 characters and preferably be standard. The calibration module won't find the channels if shorter names are used.
Changing the ICRT table after raw data input does not affect the processed data. An AICRT table is created for the actual processed data. This table can be changed by copying the new ICRT table to the AICRT table.

SWRT:
Status words are defined.

OCRT:
Output channels are defined. Channels such as attenuation (e.g. B0VCPA), created by DAPPER have to be defined in the OCRT, in order to generate output in radiometer data processing, template extraction and bias-removal correctly.

4.2.4 Calibration files

Calibration files describe the relation between raw data samples (integer type) and measurement values (double type). Creating and editing of calibration files can be performed in the graphic editor, selecting calibration curves mode.

The definition of calibration file header is not completely clear. Below an interpretation is given:

Begin of validity	e.g. 900501000000
X unit	e.g. V
X conversion factor (x_conv)	conversion factor to scale (integer type) raw data values to realistic (double type) values.
Y unit	unit out of ICRT
Y conversion factor (y_conv)	conversion factor out of ICRT
X-minimum (x_min)	minimum x-range graph, x_min/x_conv has to be less or equal than minimum value in ICRT.
X-maximum (x_max)	maximum x-range graph, x_max/x_conv has to be greater or equal than maximum value in ICRT
Y-minimum (x_min)	minimum value y-range graph
Y-maximum (x_max)	maximum value y-range graph

The conversion factors scale input (x_int) and output integer (y_int) values to realistic values (x_real and y_real). x and y values in the calibration curve are realistic values. Thus a linear calibration curve can be described by:

$$x\_int = x\_real * x\_conv$$
$$y\_int = y\_real * y\_conv$$

$$y\_real = A + B*x\_real$$

where: $x\_min < x\_real < x\_max$
$y\_min < y\_real < y\_max$

A, B are equation parameters.

- hints
  - All necessary calibration files have to be defined with a start date smaller than the raw data input stream.
  - The parameters of a calibration file can only be changed when defining a new calibration file or the same with a higher index.
  - Channels using the same calibration file should have the same conversion factors and units.
  - Equation parameters E and G will go out of range if x becomes negative. E and G have to be made very large to (>1e5) to overcome this problem. All other parameters have to be chosen to keep the integer y-values smaller than 23767.
  - Conversion factor and unit for y have to be the same as in the ICRT
  - y_conv determines the quantization accuracy of the calibrated data. If the minimum number of required quantization steps is 1000 then the condition y_conv*(y_max - y_min) > 1000 should be valid.
  - The number of calculated values in the look-up table: nr_steps = (y-max - y-min)*20.
  - Equation parameters are input using fixed notation. For small and big numbers this gives a problem. Change the output range to solve this problem.

- errors
  - Different values in ICRT and calibration file cause fatal errors during calibration ('cannot create lookup table').
  - Some channels will appear not to be configured if names with a length smaller than 8 characters are used.
  - x,y values seem not to be remembered after input in graphic editor.
  - calibration crashes if x_conv > 1. It is recommended to choose x_conv=1.
  - If y_int goes out of range calibration will be incorrect. Thus y-real * y-conv < 32767 should be valid for all y_real.
  - Creation of a look-up table will fail if (y-max - y-min)> 1638.

4.2.5 General comments

Time performance:
The DAPPER preprocessing system is rather slow. Below an estimation is given of the time-consumption for preprocessing 3 days of raw data (37 channels and 2 status words, 1 Hz data) on a 386 ACER with a 33 MHz clockrate.

Raw data input (no abnormal jumps):	70 minutes
Calibration (x_conv,y_conv=1):	95 minutes
Inspection:	20 minutes
Radiometer data processing:	10 minutes
Template extraction:	8 minutes (part 1)
	7 minutes (graphic editor)
	50 minutes (part 2)
Bias-removal (no matrix cancellation):	20 minutes
Plausibility test:	15 minutes
Event selection:	15 minutes
Output data compilation:	30 minutes
TOTAL time:	340 minutes
	(5 hours, 40 minutes)

Most of the time, the user is waiting for the completion of a module. The estimation is rather minimal, as abnormal jumps and a higher output resolution will increase process time.

Disk space:
Processing of 3 days of data (37 channels of 1 Hz) requires 170 Mb total harddisk space. The size of the HOME/data directory grows enormously during processing.

Units:
DAPPER asks values for several parameters without giving any definition and any unit indication. The definition can be part of the help function, but the unit of the parameter should be given on the screen together with the symbol name.

Standard procedure:
The user cannot choose what methods to use in several preprocessing stages. the system checks data channels and chooses a method automatically. In some functions this prevents the user doing odd things, but in other functions this causes incorrect restrictions.

Errors:
When errors occur in a preprocessing component, the process has to be started over at the beginning of the component. This is not time-efficient. DAPPER should give the user hints or ask the user to edit the parameter or table, that caused the error.

4.3 Preprocessing functions

4.3.1 Raw data input

Raw data is read in and prepared for further preprocessing functions. Internal signal files with data quality flags are created.

- hints -Raw data files (i.e. 900515_01.rda) can be edited by the program rd_edit outside DAPPER.
  -All channels of the raw data input stream have to be defined in the ICRT tables.
  -A jump threshold has to be given to detect invalid periods. Setting a low margin will increase the time for performing raw data input significantly (Abnormal jumps will occur). 10% of the maximum range of the channel is a suitable value.

- errors -It is not possible to change the time period of a whole day.
  -A system breakdown occurs when trying to process parts of a day. The system detects overlapping of data at the last time record. The date/time error function does not work properly.

4.3.2 Calibration

The 'Internal Signal Files' produced by the Raw Data Input are further processed by applying different calibration methods. If calibration files are used, look-up tables are created.

- hints -Before calibration can be done, all specified calibration files in the ICRT have to be present. Otherwise the fatal error 'Wrong amount of ICRT files' will occur.
  -If conversion factor in ICRT is not equal to the conversion factor y of the calibration file fatal error 'cannot create look-up table' occurs.
  -System breakdown occurs if calibration files are inconsistent with ICRT specifications.

- errors -Calibration will produce wrong calibrated data values if another value than y_conv = 1 is used.
  -The out of range of certain parameters and output values is not checked properly.

4.3.3 Inspection

The user may inspect the calibrated data and change data quality flags.

Uncalibrated and calibrated channels can be displayed.

- error -The uncalibrated channels seem to be displayed as x_int/y_conv. The calibrated channels seem to be displayed as y_real*y_conv. For both types realistic values should be displayed (x_real, y_real).

4.3.4 Radiometer data processing

Radiometer data processing calculates the attenuation at beacon frequencies from sky noise measurements. Depending on the number of radiometer channels in the ICRT, this module asks to give the names of radiometers channels and parameters for calculation. Using either 0, 1 or 2 radiometers, the attenuation at beacon frequencies is calculated (e.g. B0TOTATP, B1TOTATP, B2TOTATP).

- hints -In case the number of radiometers is smaller than 2, the relative humidity and ambient temperature or water vapour density is used to calculate the water vapour content. If both are present, the use of relative humidity and ambient temperature have higher priority.
  -If radiometer channels are present, DAPPER uses these and assumes these are at beacon frequencies. DAPPER does not ask additional parameters if another radiometer frequency is used (i.e. R3TANT_). By supplying radiometer channels with a non-standard name, the use of invalid channels can be avoided.

- error -If a radiometer channel is invalid, the user should be able to use another radiometer processing method. The method is chosen automatically, according to the presence of channels.
  -It is not possible to use radiometer measurements at another frequency than the beacon frequency.
  -DAPPER does not warn that the value of some parameters depends on the elevation angle.
  -The radiometer data processing procedure does not produce correct results. The algorithms derived in the DDD [13] are not correct.

4.3.5 Template extraction

This component generates template files, that are the basis of the bias-removal.
Part 1:
Determine the clear-sky period for template extraction with a threshold for attenuation calculated from radiometer measurements (BnTOTATP). For each of the copolar channels, copolar levels are generated. Afterwards the clear-sky period may be changed manually in the graphic editor.
Part 2:
Calculate raw and average templates for CPA, CPH, XPIN and XPQU channels. Radiometer attenuation (BnTOTATP) is used to derive CPA templates. CPA templates seem to be copolar level templates (CPL) with radiometer correction. A template point is calculated every 15 minutes. Valid templates of previous days have to be present. It is not possible to create templates without enough previous templates.

- hints -Use 97 missing template points to make any raw template valid. This avoids the error: too few useful templates available. This procedure does not work always, so try again.

- errors -The tool, to create raw templates, is not present.
  -Processing data is not possible without enough previous raw templates or when days are missing.

4.3.6 Bias removal

Bias removal removes influence of the equipment in the measurements. Average templates are used to perform the bias removal of copolar and crosspolar channels.

- errors -Templates of B1 are searched in the wrong path.
  -For dual-polarized beacons left or right matrix cancellation has to be chosen. Matrix cancellation does not work (system break-down). Rename B1 channels, so DAPPER does not recognize these as a dual-polarized beacon. Now the other bias-removal functions may be tested.
  -The shape of the output signals seem to be correct, but values are not.

- hints The corrected files are produced (Bn?CPA_B.Chn, Bn?CPH_B.Chn, Bn?XPD_B.Chn, Bn?XPH_B.Chn, Bn?CPMVB.Chn). These have to be configured in the OCRT table.

4.3.7 Plausibility tests

This component determines physical impossibilities of signal behaviour. Output is written into the status report.

- hints - Use spaces to clear a field
- errors - Adding a test causes a system breakdown.

4.3.8 Event Selection

In event selection event and off-event periods are automatically assigned.

This process is completed in two parts:
Part 1: automatic event selection using threshold for event channels.
Part 2: alter length of event period manually.

4.3.9 Output compilation

The results of the whole preprocessing are written in the Standard Event File (SEF) format. All channels described in the OCRT are transferred to SEF file.

- error -Not all temporary files are removed after completion of this component.

4.3.10 Errors in the algorithms

Several preprocessing algorithms used in the DAPPER prototype are incorrect. This was noticed by analyzing the detailed design documents and DAPPER preprocessing annex [20]. The algorithms were compared with the algorithms derived for the EUT groundstation (Part II). Differences have been discussed with the DAPPER developers and ESA. Some algorithms will be corrected in DAPPER. These corrections concern the following parts of DAPPER preprocessing:

- Radiometer data processing:
- The user chooses the radiometer method
- Solve V and L from a set of linear equations.
- Radiometer coefficients for attenuation.

- Template extraction
- Derive crosspolar templates for single polarized beacons.
- Calculate uncertainty in templates

- Bias removal
- Perform crosspolar bias removal for single polarized beacons.

4.4 Conclusions

The DAPPER preprocessing prototype is tested and evaluated. A lot of functional and numerical errors occur during processing. As a whole the preprocessing system seems to be too time-consuming for the user. It is not possible to evaluate the performance of the preprocessing functions on typical propagation measurements, as the numerical output of this prototype is useless.

These test results were discussed with the developers at the interim meeting of the OPEX Small User's Group in Vienna, 5-6 July 1990.

5 RESULTS OF PREPROCESSING

5.1 Introduction

At the interim meeting of the Small User's Group of OPEX on July 5 and 6 1990, the progress of the developement of DAPPER was discussed. At the meeting Siemens supplied the EUT with a new prototype of preprocessing for testing. In this chapter some output is discussed, that is obtained with this second prototype using realistic data from EUT groundstation. The data of June 13 and 23, 1990, was also used for evaluation of template quality in part I. The output may be compared with graphs in Part I.

Figure 5.1 shows the main menu of DAPPER preprocessing after performing the first six modules. The modules that have been performed have a darker colour. The main preprocessing routines will be discussed on the basis of screen pictures as the print/plot module does not work yet. The displayed input-channel names are explained in table 3.1.

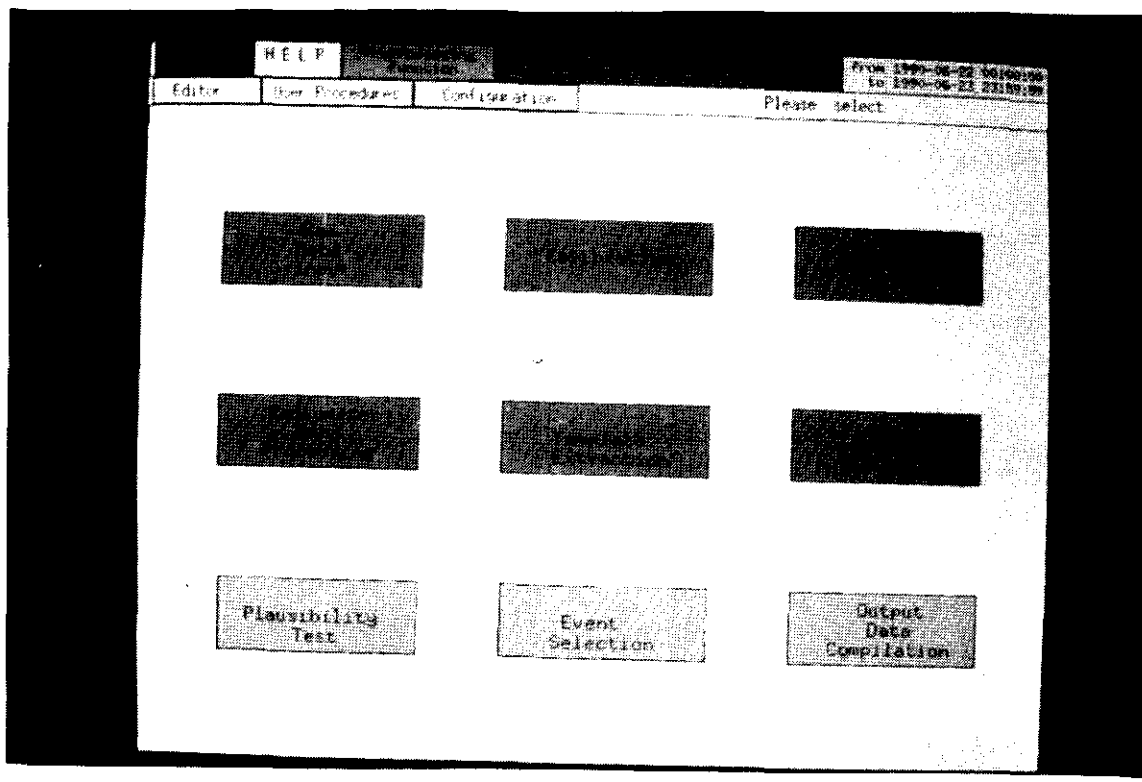

Figure 5.1: Main menu of DAPPER preprocessing

5.2 Copolar measurements

Preprocessing for copolar attenuation measurements consists of:
- Radiometer data processing.
- Template extraction.
- Bias removal.

Preprocessing results are discussed for the data of June 23, that contained some events.

• Radiometer data processing

No radiometer measurements were available at the EUT, so in the radiometer processing the relative humidity and the ambient temperature are used to estimate the beacon attenuation. Figure 5.2 shows the results of radiometer data processing for beacon B2. The background colour indicates the clear-sky and non-clear-sky periods; it is darker (blue) for the clear-sky periods. The output channels of radiometer data processing have the extension P, M1VAP__P is the integrated water vapour content and B2TOTATP is the derived attenuation for beacon B2.

The procedure calculates the integrated water vapour content (V) and integrated liquid water content (L) and determines the attenuation at beacon frequencies. Values of V and attenuation are reasonable. L (not shown) is 0, according to the assumptions of the used method. During the main event the relative humidity increases and temperature drops, so the water vapour density only changes slightly. This is shown in figure 5.2. Thus the behaviour of V seems to be in agreement with theory.

To check other radiometer processing methods, radiometer data channels have been filled with data derived from beacon attenuation measurements. The results were in agreement with the basic procedures. However V and L are limited to positive values, which is a false restriction. When V or L are smaller than zero, they are set to zero and corresponding data is flagged invalid.

• Template extraction

Figure 5.3 shows two template channels. R900623 is the raw template for the copolar level of B2, A900623 is the average template for the copolar level of B2. Template values only change every 15 minutes as expected. The raw template is derived from B2VCPA_T, the copolar level after radiometer correction. Raw template values are in agreement with B2VCPA_T.

The average template is derived using raw templates of this day and two previous days. It seems that the current raw template is also used during the events. Event periods have been declared non-clear-sky in the template extraction, so during these periods the raw template of the day should not be used to derive average templates.

• Bias removal

The average template is used to derive the attenuation channel for B2, B2VCPA_B. This channel is an output channel of the bias removal module. The results show that using the average template, attenuation sometimes will be smaller than zero, due to wrong template values. To obtain correct attenuation values during events, the user can declare the whole raw template of this day invalid and only use templates of previous clear-sky days. Besides these errors, B2VCPA_B shows the typical behaviour of an attenuation channel after bias removal. Using the time zoom function, figure 5.4 gives a closer look at the corrected copolar level, the attenuation and rain rate during the event periods.

5.3 Crosspolar measurements

Preprocessing crosspolar measurements basically consists of:
- Template extraction.
- Bias removal.

Preprocessing results are discussed for data of June 13. The date has been changed for DAPPER to June 22 to have clear-sky measurements for the bias removal during the events of June 23. Real EUT data of June 22 was not complete.

• Template extraction

Figure 5.5 shows the inphase and quadrature templates of the crosspolar phasor for B2. The first channel is the inphase template B2VXPDI, the second channel is the quadrature template B2VXPDQ. the data can be compared with the graph of the crosspolar phasor in figure 5.12 of part I. The values of the templates seem to be a factor 60 too small. This is probably due to the use of a wrong conversion factor for these channels. The shape of the channels is in agreement with the variation of the crosspolar phasor in figure 5.12 of Part I.

• Bias removal

The third channel shows the XPD after adaptive vector cancellation (B2VXPD_B). The template values were too small, so the cancellation does not really improve the crosspolar performance. The XPD is almost identical to the one shown in figure 5.14 of part I without any cancellation. Performing bias removal with matrix cancellation for B1 causes system errors.

5.4 Conclusions

Some output of DAPPER preprocessing is obtained with realistic data. Errors in the procedures have been discovered:
- The calculation of the integrated water vapour content and the integrated liquid water content is limited to positive values.
- The extraction of average templates uses also raw template points of non-clear-sky periods.
- The inphase and quadrature templates of the crosspolar phasor have wrong conversion factors.

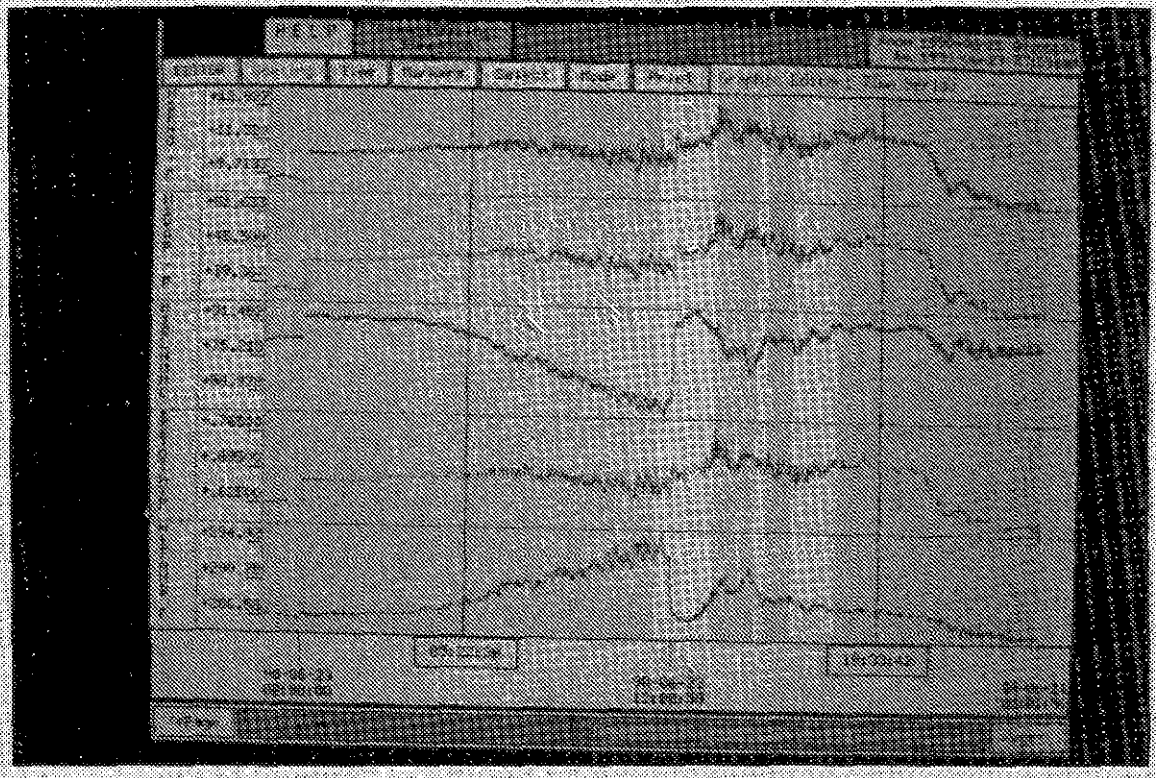

Figure 5.2: Results of radiometer data processing

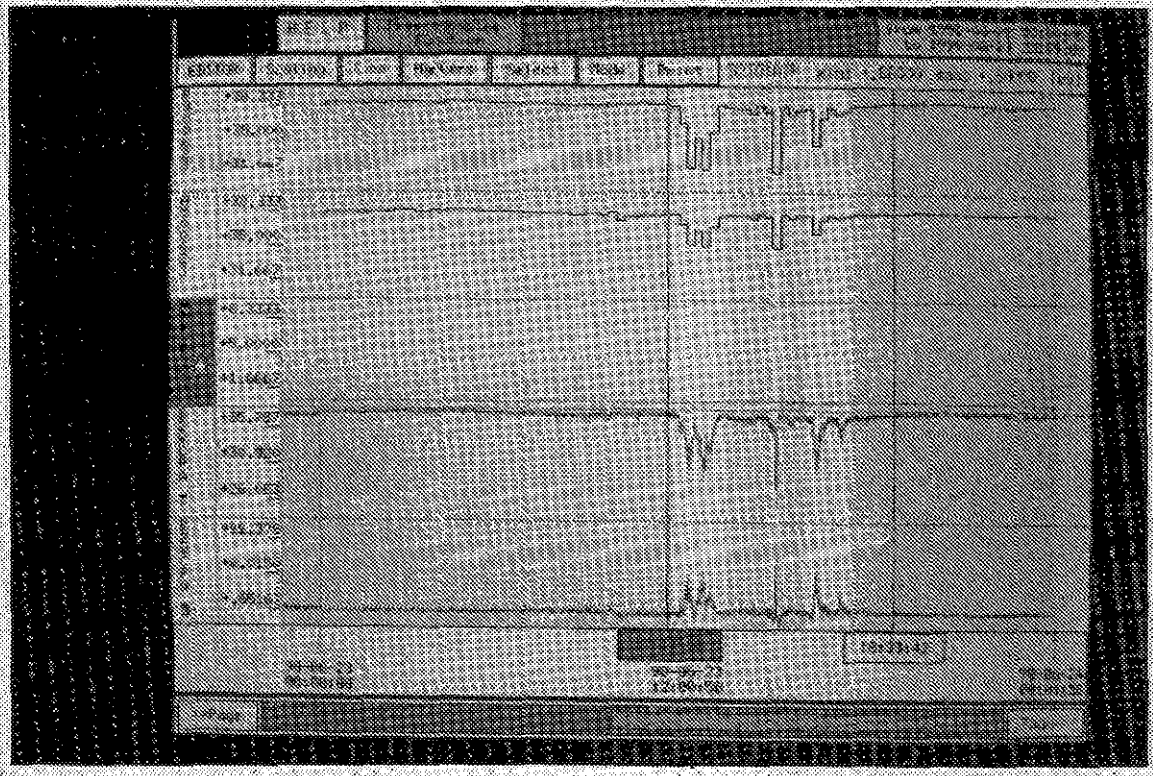

Figure 5.3: Results of template extraction and bias removal for copolar measurements

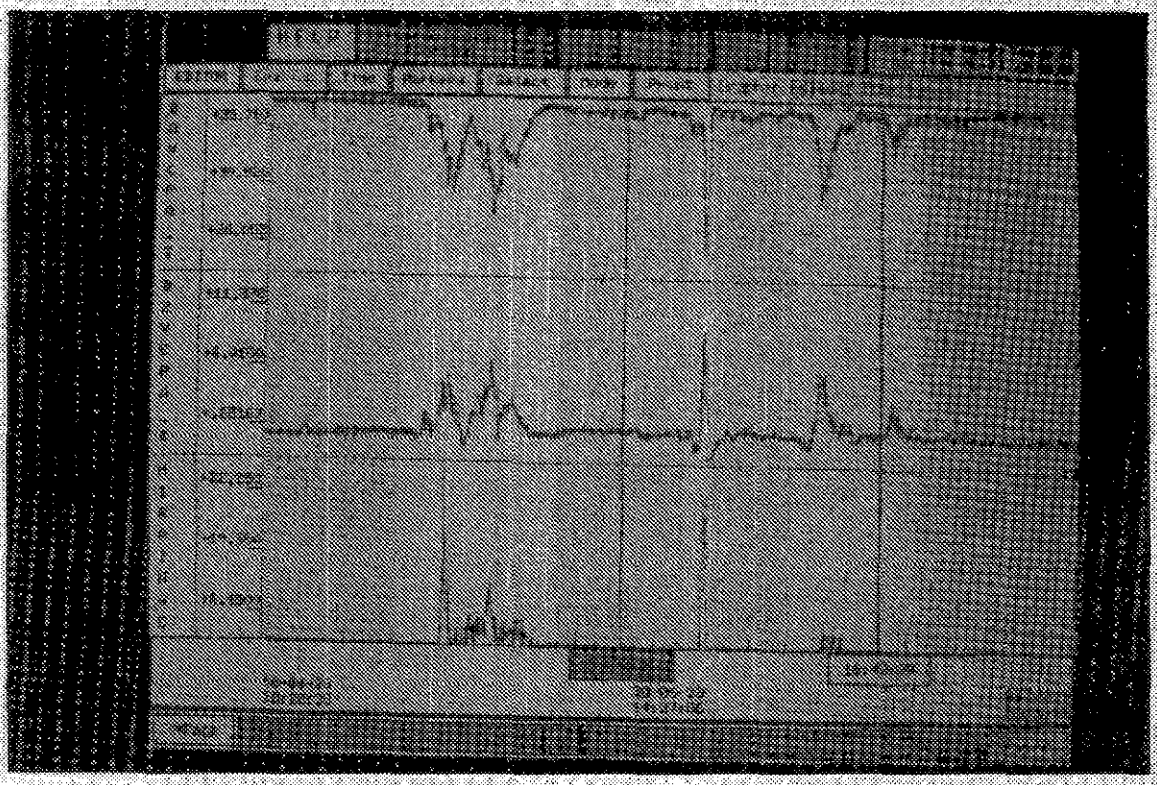

Figure 5.4: Copolar behaviour during events

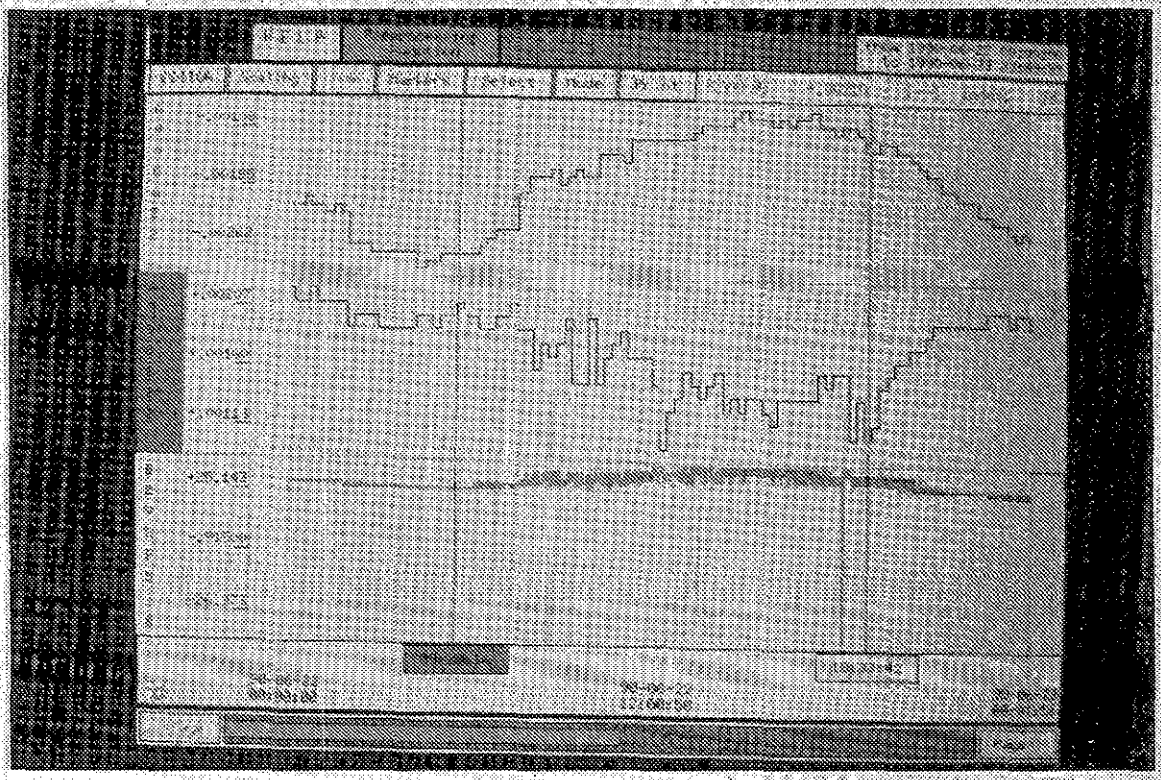

Figure 5.5: Template extraction and bias removal for crosspolar measurements

6 CONCLUSIONS AND RECOMMENDATIONS

6.1 Conclusions

DAPPER is a standard data processing software system to perform preprocessing and analysis of propagation measurement data. It has been especially designed for the OLYMPUS propagation project to be used throughout Europe. A prototype of the preprocessing was supplied to the EUT groundstation for testing the software system and the standard preprocessing procedures.

A conversion program was developed to convert the EUT channels in an EUT format to OPEX channels in a raw data input format. The DAPPER system was set up for the EUT groundstation. Tests of the preprocessing system showed, that still a lot of problems have to be fixed in the software system and preprocessing algorithms. The test results were discussed with the developers. An improved prototype of preprocessing was supplied to EUT to get some reasonable preprocessing output.

6.2 Recommendations

The effects of the DAPPER preprocessing procedures on realistic propagation data has not been tested thoroughly. This is a requirement to come to some conclusions on the quality of data after preprocessing. However these tests are only feasible when the procedures in the software are correct and the system operates without problems.

The following tests will have to be performed on realistic data of a several weeks:
- determine the quality difference between the methods for radiometer data processing.
- create templates of typical clear-sky days and determine the variation in diurnal behaviour.
- determine the influence of the number of raw templates on the quality of the derived average template
- determine the quality of templates with periods of interpolation
- determine the practical uncertainty in the obtained average templates.
- perform bias removal for several periods with events. Determine the improvement of accuracy using bias removal.
- compare the results of bias removal using different methods for the dual polarized beacon.
- determine the influence of unpredictable errors, such as spikes and tracking errors, on the quality of the preprocessing output.

LITERATURE

[1] Siemens-PSE/CSR Ltd/IAS, USER'S REQUIREMENT DOCUMENT, Part 1 Data Preprocessing Software, European Space Agency Report, Final version 1.0, November 1988, Austria: Siemens AG.

[2] Siemens-PSE/IAS, DAPPER, SOFTWARE USER'S MANUAL PREPROCESSING SOFTWARE, European Space Agency Report, Draft version 0.1, March 1990, Austria: Siemens AG.

[3] Barto, R., SOFTWARE VOOR HET OLYMPUS DATA SYSTEEM, Graduation Report, Eindhoven University of Technology, Faculty of Electr. Eng., Communications division, 1990.*(in Dutch)*

[4] Ippolito, L.J., PROPAGATION EFFECTS HANDBOOK FOR SATELLITE SYSTEMS DESIGN, A summary of propagation impairments on 10 to 100 GHz Satellite links with techniques for systems design, Washington: NASA, 1989, Ref. Publ.1082(04).

[5] BETRIEBSANLEITUNG ASPIRATIONS PSYCHROMETER NACH ASSMANN, Göttingen, 1976.

[6] Siemens-PSE/IAS, DAPPER, SOFTWARE TRANSFER DOCUMENT, European Space Agency Report, Draft version 0.1, April 1990, Austria: Siemens AG.

[7] Siemens-PSE/IAS, DAPPER, DETAILED DESIGN DOCUMENT PART 2, Detailed Design Specification of the Common Modules, European Space Agency Report, Draft version 0.3, November 1989, Austria: Siemens AG.

[8] Siemens-PSE/IAS, DAPPER, DETAILED DESIGN DOCUMENT PART 2 PDL ANNEX, Detailed Design Specification of the Common Modules, European Space Agency Report, Draft version 0.2, October 1989, Austria: Siemens AG.

[9] Siemens-PSE/IAS, DAPPER, DETAILED DESIGN DOCUMENT PART 2 SRC ANNEX, Detailed Design Specification of the Common Modules, European Space Agency Report, Draft version 0.3, November 1989, Austria: Siemens AG.

[10] Siemens-PSE/IAS, DAPPER, DETAILED DESIGN DOCUMENT PART 3.1 PREPROCESSING SOFTWARE, Detailed Design Specification of the Main Module, European Space Agency Report, Draft version 0.3, November 1989, Austria: Siemens AG.

[11] Siemens-PSE/IAS, DAPPER, DETAILED DESIGN DOCUMENT PART 3.2 PREPROCESSING SOFTWARE, Detailed Design Specification of the Raw Data Input

Module, European Space Agency Report, Draft version 0.3, November 1989, Austria: Siemens AG.

[12] Siemens-PSE/IAS, DAPPER, DETAILED DESIGN DOCUMENT PART 3.3 PREPROCESSING SOFTWARE, Detailed Design Specification of the Calibration Module, European Space Agency Report, Draft version 0.3, November 1989, Austria: Siemens AG.

[13] Siemens-PSE/IAS, DAPPER, DETAILED DESIGN DOCUMENT PART 3.4 PREPROCESSING SOFTWARE, Detailed Design Specification of the Radiometer Data Processing Module, European Space Agency Report, Draft version 0.3, November 1989, Austria: Siemens AG.

[14] Siemens-PSE/IAS, DAPPER, DETAILED DESIGN DOCUMENT PART 3.5 PREPROCESSING SOFTWARE, Detailed Design Specification of the Template Extraction Module, European Space Agency Report, Draft version 0.3, November 1989, Austria: Siemens AG.

[15] Siemens-PSE/IAS, DAPPER, DETAILED DESIGN DOCUMENT PART 3.6 PREPROCESSING SOFTWARE, Detailed Design Specification of the Bias Removal Module, European Space Agency Report, Draft version 0.3, November 1989, Austria: Siemens AG.

[16] Siemens-PSE/IAS, DAPPER, DETAILED DESIGN DOCUMENT PART 3.7 PREPROCESSING SOFTWARE, Detailed Design Specification of the Plausibility Test Module, European Space Agency Report, Draft version 0.3, November 1989, Austria: Siemens AG.

[17] Siemens-PSE/IAS, DAPPER, DETAILED DESIGN DOCUMENT PART 3.8 PREPROCESSING SOFTWARE, Detailed Design Specification of the Event Selection Module, European Space Agency Report, Draft version 0.3, November 1989, Austria: Siemens AG.

[18] Siemens-PSE/IAS, DAPPER, DETAILED DESIGN DOCUMENT PART 3.9 PREPROCESSING SOFTWARE, Detailed Design Specification of the Output Data Compilation Module, European Space Agency Report, Draft version 0.3, November 1989, Austria: Siemens AG.

[19] Siemens-PSE/IAS, DAPPER, DETAILED DESIGN DOCUMENT PART 3.11 PREPROCESSING SOFTWARE, Detailed Design Specification of the Configuration Module, European Space Agency Report, Draft version 0.3, November 1989, Austria: Siemens AG.

[20] Siemens-PSE/IAS, DAPPER, SOFTWARE USER'S MANUAL PREPROCESSING SOFTWARE, ANNEX, European Space Agency Report, Draft version 0.2, April 1990, Austria: Siemens AG.

Appendix A: Dapper configuration

A.1 Input Channel Reference Table

ICRT "0000" for EUT groundstation, valid since May 6, 1990

Comments:
- The ICRT has been defined according to the input channel list.
- Conversion factors are chosen to assure resolution of calibration is about 10 times the desired resolution by OPEX for the channels that are processed by DAPPER.

user's channel number : 0
abbreviation : B0VCPIN_
internal channel code : S
full channel name : B0 inphase component copolar
measurement range min :-32767
measurement range max:32767
calibration method : 1
calibration file name : bcolin
conversion factor : 100
unit :
sample interval : 1

user's channel number : 1
abbreviation : B2VCPIN_
internal channel code : S
full channel name : B2 inphase component copolar
measurement range min.:-32767
measurement range max.:32767
calibration method : 1
calibration file name : bcolin
conversion factor : 100
unit :
sample interval : 1

user's channel number : 2
abbreviation : B1HCPIN_
internal channel code : S
full channel name : B1,H inphase component copolar
measurement range min.:-32767
measurement range max.:32767
calibration method : 1
calibration file name : bcolin
conversion factor : 100
unit :
sample interval : 1

user's channel number : 3
abbreviation : B1VCPIN_
internal channel code : S
full channel name : B1,V inphase component copolar
measurement range min.:-32767
measurement range max.:32767
calibration method : 1
calibration file name : bcolin
conversion factor : 100
unit :
sample interval : 1

user's channel number : 4
abbreviation : B0VCPQU_
internal channel code : S
full channel name : B0 quadrature component copolar
measurement range min.:-32767
measurement range max.:32767
calibration method : 1
calibration file name : bcolin
conversion factor : 100
unit :
sample interval : 1

user's channel number : 5
abbreviation : B2VCPQU_
internal channel code : S
full channel name : B2 quadrature component copolar
measurement range min.:-32767
measurement range max.:32767
calibration method : 1
calibration file name : bcolin
conversion factor : 100
unit :
sample interval : 1

user's channel number : 6
abbreviation : B1HCPQU_
internal channel code : S
full channel name : B1 quadrature component copolar horizontal
measurement range min.:-32767
measurement range max.:32767
calibration method : 1
calibration file name : bcolin
conversion factor : 100
unit :
sample interval : 1

user's channel number : 7
abbreviation : B1VCPQU_
internal channel code : S
full channel name : B0 quadrature component copolar vertical
measurement range min.:-32767
measurement range max.:32767
calibration method : 1
calibration file name : bcolin
conversion factor : 100
unit :
sample interval : 1

user's channel number : 8
abbreviation : B0VXPIN_
internal channel code : S
full channel name : B0 inphase component crosspolar
measurement range min.:-32767
measurement range max.:32767

calibration method : 1
calibration file name : bcrlin
conversion factor : 1000
unit :
sample interval : 1

user's channel number : 9
abbreviation : B2VXPIN_
internal channel code : S
full channel name : B2 inphase component crosspolar
measurement range min.:-32767
measurement range max.:32767
calibration method : 1
calibration file name : bcrlin
conversion factor : 1000
unit :
sample interval : 1

user's channel number : 10
abbreviation : B1HXPIN_
internal channel code : S
full channel name : B1 inphase component crosspolar horizontal
measurement range min.:-32767
measurement range max.:32767
calibration method : 1
calibration file name : bcrlin
conversion factor : 1000
unit :
sample interval : 1

user's channel number : 11
abbreviation : B1VXPIN_
internal channel code : S
full channel name : B0 inphase component crosspolar vertical
measurement range min.:-32767
measurement range max.:32767
calibration method : 1
calibration file name : bcrlin
conversion factor : 1000
unit :
sample interval : 1

user's channel number : 12
abbreviation : B0VXPQU_
internal channel code : S
full channel name : B0 quadrature component crosspolar
measurement range min.:-32767
measurement range max.:32767
calibration method : 1
calibration file name : bcrlin
conversion factor : 1000
unit :
sample interval : 1

user's channel number : 13
abbreviation : R0TANT__
internal channel code : S
full channel name : 12 GHz antenne noise temperature
measurement range min.:0
measurement range max.:4096
calibration method : 1
calibration file name : rcpacl
conversion factor : 10
unit : K
sample interval : 1

user's channel number : 14
abbreviation : R1TANT__
internal channel code : S
full channel name : 20 GHz antenne noise temperature
measurement range min.:0
measurement range max.:4096
calibration method : 1
calibration file name : rcpacl
conversion factor : 10
unit : K
sample interval : 1

user's channel number : 15
abbreviation : R2TANT__
internal channel code : S
full channel name : 30 GHz antenne noise temperature
measurement range min.:0
measurement range max.:4096
calibration method : 1
calibration file name : rcpacl
conversion factor : 10
unit : K
sample interval : 1

user's channel number : 16
abbreviation : M1TAMB__
internal channel code : S
full channel name : dry bulb temperature
measurement range min.:0
measurement range max.:4096
calibration method : 1
calibration file name : mtambc
conversion factor : 10
unit : K
sample interval : 1

user's channel number : 17
abbreviation : M2TAMB__
internal channel code : S
full channel name : wet bulb temperature
measurement range min.:0
measurement range max.:4096
calibration method : 1
calibration file name : mtambc
conversion factor : 10
unit : K
sample interval : 1

user's channel number : 18
abbreviation : M1RAING_
internal channel code : S
full channel name : rain rate
measurement range min.:0
measurement range max.:4096
calibration method : 1
calibration file name : mrain1
conversion factor : 10
unit : mm/h
sample interval : 1

user's channel number : 19
abbreviation : M2RAING_
internal channel code : S
full channel name : rain cumulative
measurement range min.:0

measurement range max.:4096
calibration method : 1
calibration file name : mrain2
conversion factor : 100
unit : mm
sample interval : 1

user's channel number : 20
abbreviation : M1PATM__
internal channel code : S
full channel name : atmospheric pressure
measurement range min.:0
measurement range max.:4096
calibration method : 1
calibration file name : mpatmc
conversion factor : 10
unit : hPa
sample interval : 1

user's channel number : 21
abbreviation : R1TREF__
internal channel code : S
full channel name : radiometer reference temperature 1
measurement range min.:0
measurement range max.:4096
calibration method : 1
calibration file name : mtrefc
conversion factor : 100
unit : K
sample interval : 1

user's channel number : 22
abbreviation : M1WINDV_
internal channel code : S
full channel name : wind velocity
measurement range min.:0
measurement range max.:4096
calibration method : 1
calibration file name : mvelcl
conversion factor : 10
unit : m/sec
sample interval : 1

user's channel number : 23
abbreviation : M1WINDD_
internal channel code : S
full channel name : wind direction
measurement range min.:0
measurement range max.:4096
calibration method : 1
calibration file name : mdircl
conversion factor : 10
unit : deg
sample interval : 1

user's channel number : 24
abbreviation : R2TREF__
internal channel code : S
full channel name : radiometer reference temperature 2
measurement range min.:0
measurement range max.:4096
calibration method : 1
calibration file name : mtrefc
conversion factor : 100
unit : K
sample interval : 1

user's channel number : 25
abbreviation : UYKSPAN_
internal channel code : U
full channel name : yk-span
measurement range min.:0
measurement range max.:4096
calibration method : 1
calibration file name : muserc
conversion factor : 100
unit : V
sample interval : 1

user's channel number : 26
abbreviation : UTEST4__
internal channel code : U
full channel name : test 4
measurement range min.:0
measurement range max.:4096
calibration method : 1
calibration file name : muserc
conversion factor : 100
unit : V
sample interval : 1

user's channel number : 27
abbreviation : UTEST5__
internal channel code : U
full channel name : test 5
measurement range min.:0
measurement range max.:4096
calibration method : 1
calibration file name : muserc
conversion factor : 100
unit : V
sample interval : 1

user's channel number : 28
abbreviation : UTEST6__
internal channel code : U
full channel name : test 6
measurement range min.:0
measurement range max.:4096
calibration method : 1
calibration file name : muserc
conversion factor : 100
unit : V
sample interval : 1

user's channel number : 29
abbreviation : URADIOT_
internal channel code : U
full channel name : radiotest
measurement range min.:0
measurement range max.:4096
calibration method : 1
calibration file name : muserc
conversion factor : 100
unit : V
sample interval : 1

user's channel number : 30
abbreviation : UB3VXPD__

internal channel code : U
full channel name : B0 crosspolar discrimination ECS
measurement range min.:0
measurement range max.:4096
calibration method : 1
calibration file name : bxpdcl
conversion factor : 10
unit : dB
sample interval : 1

user's channel number : 31
abbreviation : UB3VCPA__
internal channel code : U
full channel name : B0 copolar level ECS
measurement range min.:0
measurement range max.:4096
calibration method : 1
calibration file name : bcpacl
conversion factor : 10
unit : dB
sample interval : 1

user's channel number : 32
abbreviation : B2VXPQU_
internal channel code : S
full channel name : B2 quadrature component crosspolar
measurement range min.:-32767
measurement range max.:32767
calibration method : 1
calibration file name : bcrlin
conversion factor : 1000
unit :
sample interval : 1

user's channel number : 33
abbreviation : B1HXPQU_
internal channel code : S
full channel name : B1 quadrature comp. crosspolar horizontal
measurement range min.:-32767
measurement range max.:32767
calibration method : 1
calibration file name : bcrlin
conversion factor : 1000
unit :
sample interval : 1

user's channel number : 34
abbreviation : B1VXPQU_
internal channel code : S
full channel name : B1 quadrature comp. crosspolar vertical
measurement range min.:-32767
measurement range max.:32767
calibration method : 1
calibration file name : bcrlin
conversion factor : 1000
unit :
sample interval : 1

user's channel number : 35
abbreviation : M1RHO___
internal channel code : S
full channel name : water vapor density
measurement range min.:0
measurement range max.:32767
calibration method : 1
calibration file name : mrhocl
conversion factor : 100
unit : g/m3
sample interval : 1

user's channel number : 36
abbreviation : M1RLHUM_
internal channel code : S
full channel name : relative humidity
measurement range min.:0
measurement range max.:32767
calibration method : 1
calibration file name : mrlhum
conversion factor : 100
unit : %
sample interval : 1

A.2 Status Word Reference Table

SWRT '0000' valid since May 6, 1990

Comments:
- Every status word bit represents a channel: (0 = invalid,1 = valid).
- Two status words are used, indicating validity of 32 EUT channels (converted to 37 OPEX channels):

STATUS0_

1) Status Word Number :0
Status Word abbreviation :STATUS0_
Code :xxxxxxxxxxxxxxx0
Channel abbreviation :B0VCPIN_
Flag number :4
Status Report Text :Invalid raw B0VCPA

2) Status Word Number :0
Status Word abbreviation :STATUS0_
Code :xxxxxxxxxxxxxx0
Channel abbreviation :B0VXPIN_
Flag number :4
Status Report Text :Invalid raw B0VCPA

3) Status Word Number :0
Status Word abbreviation :STATUS0_
Code :xxxxxxxxxxxxxx0
Channel abbreviation :B0VXPQU_
Flag number :4
Status Report Text :Invalid raw B0VCPA

4) Status Word Number :0
Status Word abbreviation :STATUS0_
Code :xxxxxxxxxxxxx0x
Channel abbreviation :B2VCPIN_
Flag number :4
Status Report Text :Invalid raw B2VCPA

5) Status Word Number :0
Status Word abbreviation :STATUS0_
Code :xxxxxxxxxxxxx0x
Channel abbreviation :B2VXPIN_
Flag number :4
Status Report Text :Invalid raw B2VCPA

6) Status Word Number :0
Status Word abbreviation :STATUS0_
Code :xxxxxxxxxxxxx0x
Channel abbreviation :B2VXPQU_
Flag number :4
Status Report Text :Invalid raw B2VCPA

7) Status Word Number :0
Status Word abbreviation :STATUS0_
Code :xxxxxxxxxxxx0xx
Channel abbreviation :B1HCPIN_
Flag number :4
Status Report Text :Invalid raw B1HCPA

8) Status Word Number :0
Status Word abbreviation :STATUS0_
Code :xxxxxxxxxxxx0xx
Channel abbreviation :B1HXPIN_
Flag number :4
Status Report Text :Invalid raw B1HCPA

9) Status Word Number :0
Status Word abbreviation :STATUS0_
Code :xxxxxxxxxxxx0xx
Channel abbreviation :B1HXPQU_
Flag number :4
Status Report Text :Invalid raw B1HCPA

10) Status Word Number :0
Status Word abbreviation :STATUS0_
Code :xxxxxxxxxxx0xxx
Channel abbreviation :B1VCPIN_
Flag number :4
Status Report Text :Invalid raw B1VCPA

11) Status Word Number :0
Status Word abbreviation :STATUS0_
Code :xxxxxxxxxxx0xxx
Channel abbreviation :B1VCPQU_
Flag number :4
Status Report Text :Invalid raw B1VCPA

12) Status Word Number :0
Status Word abbreviation :STATUS0_
Code :xxxxxxxxxxx0xxx
Channel abbreviation :B1VXPIN_
Flag number :4
Status Report Text :Invalid raw B1VCPA

13) Status Word Number :0
Status Word abbreviation :STATUS0_
Code :xxxxxxxxxxx0xxx
Channel abbreviation :B1VXPQU_
Flag number :4
Status Report Text :Invalid raw B1VCPA

14) Status Word Number :0
Status Word abbreviation :STATUS0_
Code :xxxxxxxxxx0xxxx
Channel abbreviation :B0VXPIN_
Flag number :4
Status Report Text :Invalid raw B0VXPD

14) Status Word Number :0
Status Word abbreviation :STATUS0_
Code :xxxxxxxxxx0xxxx
Channel abbreviation :B0VXPQU_
Flag number :4
Status Report Text :Invalid raw B0VXPD

15) Status Word Number :0
Status Word abbreviation :STATUS0_
Code :xxxxxxxxx0xxxxx

Channel abbreviation :B2VXPIN_
Flag number :4
Status Report Text :Invalid raw B2VXPD

16) Status Word Number :0
Status Word abbreviation :STATUS0_
Code :xxxxxxxxxx0xxxxx
Channel abbreviation :B2VXPQU_
Flag number :4
Status Report Text :Invalid raw B2VXPD

17) Status Word Number :0
Status Word abbreviation :STATUS0_
Code :xxxxxxxxx0xxxxxx
Channel abbreviation :B1HXPIN_
Flag number :4
Status Report Text :Invalid raw B1HXPD

18) Status Word Number :0
Status Word abbreviation :STATUS0_
Code :xxxxxxxxx0xxxxxx
Channel abbreviation :B1HXPQU_
Flag number :4
Status Report Text :Invalid raw B1HXPD

19) Status Word Number :0
Status Word abbreviation :STATUS0_
Code :xxxxxxxx0xxxxxxx
Channel abbreviation :B1VXPIN_
Flag number :4
Status Report Text :Invalid raw B1VXPD

20) Status Word Number :0
Status Word abbreviation :STATUS0_
Code :xxxxxxxx0xxxxxxx
Channel abbreviation :B1VXPIN_
Flag number :4
Status Report Text :Invalid raw B1VXPD

21) Status Word Number :0
Status Word abbreviation :STATUS0_
Code :xxxxxxx0xxxxxxxx
Channel abbreviation :B0VXPIN_
Flag number :4
Status Report Text :Invalid raw B0VDPH

22) Status Word Number :0
Status Word abbreviation :STATUS0_
Code :xxxxxxx0xxxxxxxx
Channel abbreviation :B0VXPQU_
Flag number :4
Status Report Text :Invalid raw B0VDPH

23) Status Word Number :0
Status Word abbreviation :STATUS0_
Code :xxxxxx0xxxxxxxxx
Channel abbreviation :B2VXPIN_
Flag number :4
Status Report Text :Invalid raw B2VDPH

24) Status Word Number :0
Status Word abbreviation :STATUS0_
Code :xxxxxx0xxxxxxxxx
Channel abbreviation :B2VXPQU_
Flag number :4
Status Report Text :Invalid raw B2VDPH

25) Status Word Number :0
Status Word abbreviation :STATUS0_
Code :xxxxx0xxxxxxxxx
Channel abbreviation :B1HXPIN_
Flag number :4
Status Report Text :Invalid raw B1HDPH

26) Status Word Number :0
Status Word abbreviation :STATUS0_
Code :xxxxx0xxxxxxxxx
Channel abbreviation :B1HXPQU_
Flag number :4
Status Report Text :Invalid raw B1HDPH

27) Status Word Number :0
Status Word abbreviation :STATUS0_
Code :xxxx0xxxxxxxxxx
Channel abbreviation :B1VXPIN_
Flag number :4
Status Report Text :Invalid raw B1VDPH

28) Status Word Number :0
Status Word abbreviation :STATUS0_
Code :xxxx0xxxxxxxxxx
Channel abbreviation :B1VXPQU_
Flag number :4
Status Report Text :Invalid raw B1VDPH

29) Status Word Number :0
Status Word abbreviation :STATUS0_
Code :xxx0xxxxxxxxxxx
Channel abbreviation :B1VCPIN_
Flag number :4
Status Report Text :Invalid raw B1VHPH

30) Status Word Number :0
Status Word abbreviation :STATUS0_
Code :xxx0xxxxxxxxxxx
Channel abbreviation :B1VCPQU_
Flag number :4
Status Report Text :Invalid raw B1VHPH

31) Status Word Number :0
Status Word abbreviation :STATUS0_
Code :xxx0xxxxxxxxxxx
Channel abbreviation :B1VXPIN_
Flag number :4
Status Report Text :Invalid raw B1VHPH

32) Status Word Number :0
Status Word abbreviation :STATUS0_
Code :xxx0xxxxxxxxxxx
Channel abbreviation :B1VXPQU_
Flag number :4
Status Report Text :Invalid raw B1VHPH

33) Status Word Number :0
Status Word abbreviation :STATUS0_
Code :xx0xxxxxxxxxxxx
Channel abbreviation :R0TANT__
Flag number :4
Status Report Text :Invalid raw R0TANT

34) Status Word Number :0
Status Word abbreviation :STATUS0_
Code :x0xxxxxxxxxxxxxx
Channel abbreviation :R1TANT__
Flag number :4
Status Report Text :Invalid raw R1TANT

35) Status Word Number :0
Status Word abbreviation :STATUS0_
Code :0xxxxxxxxxxxxxx
Channel abbreviation :R2TANT__
Flag number :4
Status Report Text :Invalid raw R2TANT

STATUS1_

36) Status Word Number :1
Status Word abbreviation :STATUS1_
Code :xxxxxxxxxxxxxx0
Channel abbreviation :M1TAMB__
Flag number :4
Status Report Text :Invalid raw M1TAMB

37) Status Word Number :1
Status Word abbreviation :STATUS1_
Code :xxxxxxxxxxxxxx0
Channel abbreviation :M1RHO___
Flag number :4
Status Report Text :Invalid raw M1TAMB

38) Status Word Number :1
Status Word abbreviation :STATUS1_
Code :xxxxxxxxxxxxxx0
Channel abbreviation :M1RLHUM_
Flag number :4
Status Report Text :Invalid raw M1TAMB

39) Status Word Number :1
Status Word abbreviation :STATUS1_
Code :xxxxxxxxxxxxxx0x
Channel abbreviation :M2TAMB__
Flag number :4
Status Report Text :Invalid raw M2TAMB

40) Status Word Number :1
Status Word abbreviation :STATUS1_
Code :xxxxxxxxxxxxxx0x
Channel abbreviation :M1RHO___
Flag number :4
Status Report Text :Invalid raw M2TAMB

41) Status Word Number :1
Status Word abbreviation :STATUS1_
Code :xxxxxxxxxxxxxx0x
Channel abbreviation :M1RLHUM_
Flag number :4
Status Report Text :Invalid raw M2TAMB

42) Status Word Number :1
Status Word abbreviation :STATUS1_
Code :xxxxxxxxxxxxx0xx
Channel abbreviation :M1RAING_
Flag number :4
Status Report Text :Invalid raw M1RAING

43) Status Word Number :1
Status Word abbreviation :STATUS1_
Code :xxxxxxxxxxx0xxx
Channel abbreviation :M2RAING_
Flag number :4
Status Report Text :Invalid raw M1RAING

44) Status Word Number :1
Status Word abbreviation :STATUS1_
Code :xxxxxxxxxx0xxxx
Channel abbreviation :M1PATM__
Flag number :4
Status Report Text :Invalid raw M1PATM

45) Status Word Number :1
Status Word abbreviation :STATUS1_
Code :xxxxxxxxxx0xxxx
Channel abbreviation :M1RHO___
Flag number :4
Status Report Text :Invalid raw M1PATM

46) Status Word Number :1
Status Word abbreviation :STATUS1_
Code :xxxxxxxxxx0xxxx
Channel abbreviation :M1RLHUM_
Flag number :4
Status Report Text :Invalid raw M1PATM

47) Status Word Number :1
Status Word abbreviation :STATUS1_
Code :xxxxxxxxx0xxxxx
Channel abbreviation :R1TREF__
Flag number :4
Status Report Text :Invalid raw R1TREF

48) Status Word Number :1
Status Word abbreviation :STATUS1_
Code :xxxxxxxx0xxxxxx
Channel abbreviation :M1WINDV_
Flag number :4
Status Report Text :Invalid raw M1WINDV

49) Status Word Number :1
Status Word abbreviation :STATUS1_
Code :xxxxxxx0xxxxxxx
Channel abbreviation :M1WINDD_
Flag number :4
Status Report Text :Invalid raw M1WINDD

50) Status Word Number :1
Status Word abbreviation :STATUS1_
Code :xxxxxx0xxxxxxx
Channel abbreviation :R2TREF__
Flag number :4
Status Report Text :Invalid raw R2TREF

51) Status Word Number :1
Status Word abbreviation :STATUS1_
Code :xxxxx0xxxxxxxx
Channel abbreviation :UYKSPAN_
Flag number :4
Status Report Text :Invalid raw UYKSPAN

52) Status Word Number :1
Status Word abbreviation :STATUS1_

Code :xxxxx0xxxxxxxxx
Channel abbreviation :UTEST4__
Flag number :4
Status Report Text :Invalid raw UTEST4

53) Status Word Number :1
Status Word abbreviation :STATUS1_
Code :xxxx0xxxxxxxxxx
Channel abbreviation :UTEST5__
Flag number :4
Status Report Text :Invalid raw UTEST5

54) Status Word Number :1
Status Word abbreviation :STATUS1_
Code :xxx0xxxxxxxxxxx
Channel abbreviation :UTEST6__
Flag number :4
Status Report Text :Invalid raw UTEST6

55) Status Word Number :1
Status Word abbreviation :STATUS1_
Code :xx0xxxxxxxxxxxx
Channel abbreviation :URADIOT_
Flag number :4
Status Report Text :Invalid raw URADIOT

56) Status Word Number :1
Status Word abbreviation :STATUS1_
Code :x0xxxxxxxxxxxxx
Channel abbreviation :UB3VXPD_
Flag number :4
Status Report Text :Invalid raw B3VXPD

57) Status Word Number :1
Status Word abbreviation :STATUS1_
Code :0xxxxxxxxxxxxxx
Channel abbreviation :UB3VCPA_
Flag number :4
Status Report Text :Invalid raw B3VCPA

A.3 Output Channel Reference Table

OCRT "0000" for EUT groundstation, valid since May 6, 1990

Comments:
- The conversion factor is chosen to assure that resolution of channels used processed by DAPPER is about 10 times higher than the required resolution.

user's channel number	:0
abbreviation	:B0VCPA__
channel standard	:S
internal channel code	:S
full channel name	:copolar level B0
conversion factor	:100
unit	:dB
sample interval	:1

user's channel number	:1
abbreviation	:B0VCPMV_
channel standard	:S
internal channel code	:S
full channel name	:mean copolar level B0
conversion factor	:100
unit	:dB
sample interval	:1

user's channel number	:2
abbreviation	:B0VCPH__
channel standard	:S
internal channel code	:S
full channel name	:copolar phase B0
conversion factor	:10
unit	:deg
sample interval	:1

user's channel number	:3
abbreviation	:B0VXPD__
channel standard	:S
internal channel code	:S
full channel name	:copolar discrimination B0
conversion factor	:100
unit	:dB
sample interval	:1

user's channel number	:4
abbreviation	:B0VDPH__
channel standard	:S
internal channel code	:S
full channel name	:differential phase B0
conversion factor	:10
unit	:deg
sample interval	:1

user's channel number	:5
abbreviation	:B1HCPA__
channel standard	:S
internal channel code	:S
full channel name	:copolar level B1,H
conversion factor	:100
unit	:dB
sample interval	:1

user's channel number	:6
abbreviation	:B1HCPMV_
channel standard	:S
internal channel code	:S
full channel name	:mean copolar level B1,H
conversion factor	:100
unit	:dB
sample interval	:1

user's channel number	:7
abbreviation	:B1HCPH__
channel standard	:S
internal channel code	:S
full channel name	:copolar phase B1,H
conversion factor	:10
unit	:deg
sample interval	:1

user's channel number	:8
abbreviation	:B1HXPD__
channel standard	:S
internal channel code	:S
full channel name	:copolar discrimination B1,H
conversion factor	:100
unit	:dB
sample interval	:1

user's channel number	:9
abbreviation	:B1HDPH__
channel standard	:S
internal channel code	:S
full channel name	:differential phase B1,H
conversion factor	:10
unit	:deg
sample interval	:1

user's channel number	:10
abbreviation	:B1VCPA__
channel standard	:S
internal channel code	:S
full channel name	:copolar level B1,V
conversion factor	:100
unit	:dB
sample interval	:1

user's channel number	:11
abbreviation	:B1VCPMV_
channel standard	:S
internal channel code	:S
full channel name	:mean copolar level B1,V
conversion factor	:100
unit	:dB
sample interval	:1

user's channel number	:12
abbreviation	:B1VCPH__

channel standard :S
internal channel code :S
full channel name :copolar phase B1,V
conversion factor :10
unit :deg
sample interval :1

user's channel number :13
abbreviation :B1VXPD__
channel standard :S
internal channel code :S
full channel name :copolar discrimination B1,V
conversion factor :100
unit :dB
sample interval :1

user's channel number :14
abbreviation :B1VDPH__
channel standard :S
internal channel code :S
full channel name :differential phase B1,V
conversion factor :10
unit :deg
sample interval :1

user's channel number :15
abbreviation :B1DCPA__
channel standard :S
internal channel code :S
full channel name :Differential attenuation B1
conversion factor :100
unit :dB
sample interval :1

user's channel number :16
abbreviation :B1VHPH__
channel standard :S
internal channel code :S
full channel name :Diff. Phase B1
conversion factor :10
unit :deg
sample interval :1

user's channel number :17
abbreviation :B2VCPA__
channel standard :S
internal channel code :S
full channel name :copolar level B2
conversion factor :100
unit :dB
sample interval :1

user's channel number :18
abbreviation :B2VCPMV_
channel standard :S
internal channel code :S
full channel name :mean copolar level B2
conversion factor :100
unit :dB
sample interval :1

user's channel number :19
abbreviation :B2VCPH__
channel standard :S
internal channel code :S
full channel name :copolar phase B2
conversion factor :10
unit :deg
sample interval :1

user's channel number :20
abbreviation :B2VXPD__
channel standard :S
internal channel code :S
full channel name :copolar discrimination B2
conversion factor :100
unit :dB
sample interval :1

user's channel number :21
abbreviation :B2VDPH__
channel standard :S
internal channel code :S
full channel name :differential phase B2
conversion factor :10
unit :deg
sample interval :1

user's channel number :22
abbreviation :B0TOTAT_
channel standard :S
internal channel code :S
full channel name :total attenuation B0
conversion factor :100
unit :dB
sample interval :1

user's channel number :23
abbreviation :B1TOTAT_
channel standard :S
internal channel code :S
full channel name :total attenuation B1
conversion factor :100
unit :dB
sample interval :1

user's channel number :24
abbreviation :B2TOTAT_
channel standard :S
internal channel code :S
full channel name :total attenuation B2
conversion factor :100
unit :dB
sample interval :1

user's channel number :25
abbreviation :M1TAMB__
channel standard :S
internal channel code :S
full channel name :ambient temperature
conversion factor :10
unit :K
sample interval :1

user's channel number :26
abbreviation :M1RAING_
channel standard :S
internal channel code :S
full channel name :rain rate
conversion factor :10

unit :mm/h
sample interval :1

user's channel number :27
abbreviation :M2RAING_
channel standard :S
internal channel code :S
full channel name :rain cumulative
conversion factor :100
unit :mm
sample interval :1

user's channel number :28
abbreviation :M1PATM__
channel standard :S
internal channel code :S
full channel name :atmospheric pressure
conversion factor :10
unit :hPa
sample interval :1

user's channel number :29
abbreviation :M1WINDV_
channel standard :S
internal channel code :S
full channel name :wind velocity (speed)
conversion factor :10
unit :m/s
sample interval :1

user's channel number :30
abbreviation :M1WINDD_
channel standard :S
internal channel code :S
full channel name :wind velocity (direction)
conversion factor :10
unit :deg
sample interval :1

user's channel number :31
abbreviation :M1RHO___
channel standard :S
internal channel code :S
full channel name :water vapor density
conversion factor :100
unit :g/m3
sample interval :1

user's channel number :32
abbreviation :M1RLHUM_
channel standard :S
internal channel code :S
full channel name :relative humidity
conversion factor :100
unit :%
sample interval :1

user's channel number :33
abbreviation :M1LIQU__
channel standard :S
internal channel code :S
full channel name :total liquid water content
conversion factor :100
unit :kg/m2
sample interval :1

user's channel number :34
abbreviation :M1VAP___
channel standard :S
internal channel code :S
full channel name :total water vapour content
conversion factor :100
unit :kg/m2
sample interval :1

A.4 Calibration files

Every Raw Data Input Channel with a calibration method 1,2 or 3 requires a calibration file for calibration.

Calibration files are valid since 900507000000

x-axis:
- The range of the x-axis for every calibration curve is the same as defined in the ICRT '0000'. The conversion factor is always 1.

calibration file	range
bcolin, bcrlin	:- 32767..32767
mtambc, rcpacl, mrain1, mrain2, mpatmc, mtrefc, mvelcl, mdircl, muserc, bxpdcl,	
bcpacl	:0..4096
mrhocl, mrlhum	:0..32767

y-axis:
- The range of the y-axis is different for each curve. The range should be greater than the output range of the equation.
- For the beacon channel the output-range of the equation is chosen 100 times the range in the input channel list. Otherwise it was not possible to input the equation parameters with enough accuracy. The y-conversion factor and the y-unit should have the same values as in the ICRT '0000' for a channel using that calibration curve.

All calibration curves listed below are stored in calibration files as an equation with parameters A and B.

bcolin

unit for y	:_
conversion factor for y	:100
minimum value for y	:-100
maximum value for y	:100
equation parameter A	:0
equation parameter B	:0.003052

bcrlin

unit for y	:_
conversion factor for y	:1000
minimum value for y	:-20
maximum value for y	:20
equation parameter A	:0
equation parameter B	:0.0005427

mtambc

unit for y	:K
conversion factor for y	:10
minimum value for y	:245
maximum value for y	:315
equation parameter A	:311.15
equation parameter B	:-0.01563

rcpacl

unit for y	:K
conversion factor for y	:10
minimum value for y	:0
maximum value for y	:310
equation parameter A	:0
equation parameter B	:0.07568

mrain1

unit for y	:mm/h
conversion factor for y	:10
minimum value for y	:0
maximum value for y	:150
equation parameter A	:0
equation parameter B	:0.03662

mrain2

unit for y	:mm
conversion factor for y	:100
minimum value for y	:0
maximum value for y	:10
equation parameter A	:0
equation parameter B	:0.002441

mpatmc

unit for y	:hPa
conversion factor for y	:10
minimum value for y	:800
maximum value for y	:1100
equation parameter A	:800

equation parameter B :0.07324

mtrefc
unit for y :K
conversion factor for y :100
minimum value for y :305
maximum value for y :315
equation parameter A :305
equation parameter B :0.002441

mvelcl
unit for y :m/s
conversion factor for y :10
minimum value for y :0
maximum value for y :100
equation parameter A :0
equation parameter B :0.02441

mdircl
unit for y :deg
conversion factor for y :10
minimum value for y :0
maximum value for y :360
equation parameter A :0
equation parameter B :0.08789

muserc
unit for y :V
conversion factor for y :100
minimum value for y :0
maximum value for y :10
equation parameter A :0
equation parameter B :0.002441

bxpdcl
unit for y :dB
conversion factor for y :10
minimum value for y :15
maximum value for y :45
equation parameter A :15
equation parameter B :0.007324

bcpacl
unit for y :dB
conversion factor for y :10
minimum value for y :0
maximum value for y :30
equation parameter A :0
equation parameter B :0.007324

mrhocl
unit for y :g/m3
conversion factor for y :100
minimum value for y :0
maximum value for y :50
equation parameter A :0
equation parameter B :0.001526

mrlhum
unit for y :%
conversion factor for y :100
minimum value for y :0
maximum value for y :100
equation parameter A :0
equation parameter B :0.003052

A.5 Parameter list

Default parameter list for EUT conditions.

RAW DATA INPUT

For all channels having:
range -32767..32767, 10000 is entered as jump check;
range 0..4095, 1000 is entered as jump check.
range 0..32767, 10000 is entered as jump check.

CALIBRATION

-

INSPECTION

-

RADIOMETER DATA PROCESSING

Radiometer measurements are not yet available. The following parameters are recommended until detailed specifications of the radiometer are known.

h = 0.95
Ag = 0
Bg = 1.00
Tm = 270 K
Tc = 4.0 K

s = 4.9 km (ϵ = 26.7°)

a_f, b_f and c_f parameters have to be calculated for the radiometer frequencies. They can not be entered in DAPPER yet. The radiometer frequencies at Eindhoven will be close (within a few 100 MHz) to the beacon frequencies, so using the same coefficients of the beacon frequencies for the radiometer frequencies will not cause too large errors.

Table 1 gives the a_B, b_B and c_B parameters for the OLYMPUS beacons (ϵ = 26.7°, hs = 17m, Te = 15°C, Tl = 0°C).

Table 1: Atmospheric attenuation coefficients for EUT conditions

Coefficients Beacon	a_B (dB/(kg/m^2))	b_B (dB/(kg/m^2))	c_B (dB)
B0	0.0015	0.14	0.10
B1	0.012	0.36	0.14
B2	0.010	0.82	0.24

TEMPLATE EXTRACTION

number of seconds for averaging:	60
number of previous raw templates:	2
missing points per day:	30
abbreviation of total attenuation channel:	B2TOTAT
threshold for total attenuation channel:	1.0 dB

BIAS REMOVAL

Matrix multiplication from left or right (L/R)	L

PLAUSIBILITY TESTS

No parameter subset

EVENT SELECTION

parameter abbreviation:	B2TOTATP
threshold:	1.0 dB
evaluation hint:	a

OUTPUT DATA COMPILATION

country code:	NL
groundstation code:	EUT
longitude:	-5.487 ° W
latitude:	51.448 ° N
altitude:	17 m
tilt angle:	-18.4 °
operator name:	Van de Berg

ISSN 0167-9708
Coden: TEUEDE

(222) Jóźwiak, L.
THE FULL-DECOMPOSITION OF SEQUENTIAL MACHINES WITH THE SEPARATE REALIZATION OF THE NEXT-STATE AND OUTPUT FUNCTIONS.
EUT Report 89-E-222. 1989. ISBN 90-6144-222-2

(223) Jóźwiak, L.
THE BIT FULL-DECOMPOSITION OF SEQUENTIAL MACHINES.
EUT Report 89-E-223. 1989. ISBN 90-6144-223-0

(224) Book of abstracts of the first Benelux-Japan Workshop on Information and Communication Theory, Eindhoven, The Netherlands, 3-5 September 1989.
Ed. by Han Vinck.
EUT Report 89-E-224. 1989. ISBN 90-6144-224-9

(225) Hoeijmakers, M.J.
A POSSIBILITY TO INCORPORATE SATURATION IN THE SIMPLE, GLOBAL MODEL OF A SYNCHRONOUS MACHINE WITH RECTIFIER.
EUT Report 89-E-225. 1989. ISBN 90-6144-225-7

(226) Dahiya, R.P. and E.M. van Veldhuizen, W.R. Rutgers, L.H.Th. Rietjens
EXPERIMENTS ON INITIAL BEHAVIOUR OF CORONA GENERATED WITH ELECTRICAL PULSES SUPERIMPOSED ON DC BIAS.
EUT Report 89-E-226. 1989. ISBN 90-6144-226-5

(227) Bastings, R.H.A.
TOWARD THE DEVELOPMENT OF AN INTELLIGENT ALARM SYSTEM IN ANESTHESIA.
EUT Report 89-E-227. 1989. ISBN 90-6144-227-3

(228) Hekker, J.J.
COMPUTER ANIMATED GRAPHICS AS A TEACHING TOOL FOR THE ANESTHESIA MACHINE SIMULATOR.
EUT Report 89-E-228. 1989. ISBN 90-6144-228-1

(229) Oostrom, J.H.M. van
INTELLIGENT ALARMS IN ANESTHESIA: An implementation.
EUT Report 89-E-229. 1989. ISBN 90-6144-229-X

(230) Winter, M.R.M.
DESIGN OF A UNIVERSAL PROTOCOL SUBSYSTEM ARCHITECTURE: Specification of functions and services.
EUT Report 89-E-230. 1989. ISBN 90-6144-230-3

(231) Schemmann, M.F.C. and H.C. Heyker, J.J.M. Kwaspen, Th.G. van de Roer
MOUNTING AND DC TO 18 GHz CHARACTERISATION OF DOUBLE BARRIER RESONANT TUNNELING DEVICES.
EUT Report 89-E-231. 1989. ISBN 90-6144-231-1

(232) Sarma, A.D. and M.H.A.J. Herben
DATA ACQUISITION AND SIGNAL PROCESSING/ANALYSIS OF SCINTILLATION EVENTS FOR THE OLYMPUS PROPAGATION EXPERIMENT.
EUT Report 89-E-232. 1989. ISBN 90-6144-232-X

(233) Nederstigt, J.A.
DESIGN AND IMPLEMENTATION OF A SECOND PROTOTYPE OF THE INTELLIGENT ALARM SYSTEM IN ANESTHESIA.
EUT Report 90-E-233. 1990. ISBN 90-6144-233-8

(234) Philippens, E.H.J.
DESIGNING DEBUGGING TOOLS FOR SIMPLEXYS EXPERT SYSTEMS.
EUT Report 90-E-234. 1990. ISBN 90-6144-234-6

(235) Heffels, J.J.M.
A PATIENT SIMULATOR FOR ANESTHESIA TRAINING: A mechanical lung model and a physiological software model.
EUT Report 90-E-235. 1990. ISBN 90-6144-235-4

(236) Lammers, J.O.
KNOWLEDGE BASED ADAPTIVE BLOOD PRESSURE CONTROL: A Simplexys expert system application.
EUT Report 90-E-236. 1990. ISBN 90-6144-236-2

(237) Ren Qingchang
PREDICTION ERROR METHOD FOR IDENTIFICATION OF A HEAT EXCHANGER.
EUT Report 90-E-237. 1990. ISBN 90-6144-237-0

Eindhoven University of Technology Research Reports
Faculty of Electrical Engineering

ISSN 0167-9708
Coden: TEUEDE

(238) Lammers, J.O.
THE USE OF PETRI NET THEORY FOR SIMPLEXYS EXPERT SYSTEMS PROTOCOL CHECKING.
EUT Report 90-E-238. 1990. ISBN 90-6144-238-9

(239) Wang, X.
PRELIMINARY INVESTIGATIONS ON TACTILE PERCEPTION OF GRAPHICAL PATTERNS.
EUT Report 90-E-239. 1990. ISBN 90-6144-239-7

(240) Lutgens, J.M.A.
KNOWLEDGE BASE CORRECTNESS CHECKING FOR SIMPLEXYS EXPERT SYSTEMS.
EUT Eeport 90-E-240. 1990. ISBN 90-6144-240-0

(241) Brinker, A.C. den
A MEMBRANE MODEL FOR SPATIOTEMPORAL COUPLING.
EUT Report 90-E-241. 1990. ISBN 90-6144-241-9

(242) Demarteau, J.I.M. and H.C. Heyker, J.J.M. Kwaspen, Th.G. van de Roer
MICROWAVE NOISE MEASUREMENTS ON DOUBLE BARRIER RESONANT TUNNELING DIODES.
EUT Report 90-E-242. 1990. ISBN 90-6144-242-7

(243) Massee, P. and H.A.L.M. de Graaf, W.J.M. Balemans, H.G. Knoopers, H.H.J. ten Kate
PREDESIGN OF AN EXPERIMENTAL (5-10 MWt) DISK MHD FACILITY AND PROSPECTS OF COMMERCIAL (1000 MWt) MHD/STEAM SYSTEMS.
EUT Report 90-E-243. 1990. ISBN 90-6144-243-5

(244) Klompstra, Martin and Ton van den Boom, Ad Damen
A COMPARISON OF CLASSICAL AND MODERN CONTROLLER DESIGN: A case study.
EUT Report 90-E-244. 1990. ISBN 90-6144-244-3

(245) Berg, P.H.G. van de
ON THE ACCURACY OF RADIOWAVE PROPAGATION MEASUREMENTS: Olympus propagation experiment.
EUT Report 90-E-245. 1990. ISBN 90-6144-245-1